A NEW THERAPEUTIC TARGET TO FACILITATE RADIOIODINE TREATMENT OF BREAST CANCER

by

VIKKI LOUISE POOLE

A thesis submitted to
The University of Birmingham
for the degree of
DOCTOR OF PHILOSOPHY

Centre for Endocrinology, Diabetes and Metabolism,
Institute of Metabolism and Systems Research
University of Birmingham
February 2017

Abstract

The development of new therapeutic strategies for breast cancer is urgently needed. Exploitation of radioiodide uptake by the overexpressed sodium iodide symporter (NIS) has been widely proposed as a novel therapeutic strategy. However, radioiodide uptake is insufficient for tumour destruction. The proto-oncogene PBF binds NIS and inhibits its plasma membrane retention, thereby repressing critical radioiodide uptake in thyroid cancer. This thesis demonstrated that PBF, also upregulated in breast cancer, similarly repressed NIS in breast cancer cells, where phosphorylation of PBF at Y174 was key to NIS interaction and could be disrupted via treatment with the Src inhibitor dasatinib. Mutation of a predicted Src consensus sequence (EEN/AAA170-172AAA) abrogated pY174 PBF and radioiodide uptake repression. In the presence of dasatinib-resistant Src (T341I), dasatinib no longer rescued PBF repression of NIS, indicating that Src specifically mediates PBF phosphorylation. Inhibition of *N*-myristoylation also significantly increased radioiodide uptake. Combined Src and myristoylation inhibition induced a ~70% increase of radioiodide uptake in the absence of PBF overexpression. Thus, disrupting Src phosphorylation of PBF by targeted mutagenesis and Src kinase inhibition reveal radioiodide uptake into breast cancer cells can be significantly enhanced through therapeutic approaches focused on Src:PBF:NIS and myristoylation, making radioiodide treatment of breast cancer potentially viable.

Dedication

For My Loving Parents–

Sue and Andy Poole

Thank you for your continual love and support

Without it I would never have got this far

Acknowledgements

Thank you to my three fantastic supervisors, Prof Chris McCabe, Dr Vicki Smith and Dr Kristien Boelaert for all their encouragement, guidance and support. Thank you Chris for knowing when to give me free reign in the lab and when to stop me and pull me back in. Vicki, thank you for all the times I have approached you with failed experiments or confusing Westerns and you took time to sit, go through them all with me and curse at those darn Western gods - sorry I never did manage that Madras though.

Thank you to all the fellow McCabers, past and present, without your continual support, smiles and inspiration I would have never made it through the past three years – Alice Fletcher, Becky Thompson, Waraporn, Gavin Ryan, Martin Read, Neil Sharma and Rachel Watkins. A special mention to my fellow MRes colleagues, these three years would not have been the same without you and I am eternally grateful to have met such great friends to share the PhD journey with. Thank you to everyone on the CEDAM floor for all the support and joy shared, from the random lunchtime conversations to scientific advice, it wouldn't have been the same without you.

Thank you to the MRC and the University of Birmingham for funding this PhD, without this financial support, the research presented here would have not been possible. Thank to the Breast Cancer Campaign for the donation of matched tissue and the University of Dundee Drug Discovery for their collaboration and gifting of the NMT inhibitor compounds.

On a more personal level, thank you to all my friends and family for their ongoing support and love - particularly my wonderful parents who have supported me both at my best and at my worst. A special thanks to my fantastic partner, David Cartwright, who has kept sane and supported me through both the good and bad times –I don't think I would have managed final year and writing without you there beside me.

Table of Contents

List of Figures

List of Tables

List of Abbreviations

°C	Degrees centigrade
^{123}I	Radioactive iodide 123
^{124}I	Radioactive iodide 124
^{125}I	Radioactive iodine 125
^{131}I	Radioactive iodide 131
ab	Antibody
AF	Activation function
AKT	Protein kinase B
ALL	Acute lymphoblastic leukaemia
AML	Acute myeloid leukaemia
AMV	Avian myeloblastosis virus
ANOVA	Analysis of variance
APC	AC133+ progenitor cells
APS	Ammonium persulphate
AQP4	Aquaporin 4
ATP	Adenosine triphosphate
ATM	Ataxia telangiectasia mutated
ATR	Ataxia telangiectasia and Rad3-related
ATRA	All-*trans* retinoic acid
BCA	Bicinchoninic acid
BLAST	Basic Local Alignment Search Tool
BMI	Body mass index
bp	Base pair
BRCA	Breast cancer (gene)
BrdU	Bromodeoxyuridine
BrdU-POD	Bromodeoxyuridine-peroxidase
BSA	Bovine serum albumin
cAMP	Cyclic adenosine monophosphate
CAS	Crk-associated substrate
CCD	Charge-coupled device
cDNA	Complementary deoxyribonucleic acid
CHK2	Checkpoint kinase 2
CML	Chronic Myeloid Leukaemia
CMV	Cytomegalovirus
Co-IP	Co-immunoprecipitation assay
COS-7	CV-1 origin, SV40 7
COSMIC	Catalogue of Somatic Mutations in Cancer
Cox2	Prostaglandin-endoperoxide synthase 2
cpm	Counts per minute
CREB	cAMP response element-binding
CSK	C-src tyrosine kinase
cT	Cycle threshold value
DCIS	Ductal carcinoma *in situ*
Dex	Dexamethasone
DIT	Diiodotyrosine
DMSO	Dimethyl sulfoxide
DNA	Deoxyribonucleic acid
E1	Oestrone
E2	Oestradiol
E3	Oestriol
EDTA	Ethylene diamine tetraacetic acid
EGF	Epidermal growth factor
EGFR	Epidermal growth factor receptor
EGTA	Ethylene glycol tetraacetic acid
ER	Oestrogen receptor
ERE	Oestrogen response element
ERα	Oestrogen receptor alpha
ERβ	Oestrogen receptor beta
FAK	Focal adhesion kinase

FAM	6-carboxy-fluorsciein
FBS	Foetal bovine serum
FDA	Food and Drug Administration
FGF	Fibroblast growth factor
FRET	Fluorescence resonance energy transfer
FRTL-5	Fischer rat thyroid cell line 5
FTC	Follicular thyroid carcinoma
GAS	γ-interferon activation sequence
GFP	Green fluorescent protein
GST	Glutathione S-transferase
GTP	Guanosine triphosphate
HA	Haemagglutinin
hCG	Human chorionic gonadotropin
HBSS	Hank's balanced salt solution
HER2	Human epidermal growth factor receptor 2
hNIS	Human sodium iodide symporter
hr	Hour
HRP	Horseradish peroxidise
HRT	Hormone replacement therapy
HSP90	Heat shock protein 90
I^-	Iodide
I_2	Iodine
IARC	International Agency for Research on Cancer
IC_{50}	Half maximal inhibitory concentration
ID	Inhibitory domain
IDC	Invasive ductal carcinoma
IF	Immunofluorescence
IGF	Insulin-like growth factor
Ig	Immunoglobulin
IHC	Immunohistochemistry
ILC	Invasive lobular carcinoma
IP	Intraperitoneal
IRS	Insulin receptor substrate
JAK	Janus Kinase
kDa	Kilodalton
LARG	Leukaemia-associated RhoA guanine exchange factor
LB	Luria broth
LBD	Ligand-binding domain
LCIS	Lobular carcinoma *in situ*
LRP16	Lipoprotein receptor-related protein 16
M	Molar
mA	Milliamp
MAPK	Mitogen-activated protein kinase
MAPKK3B	MAPK Kinase 3B
MCF-7	Michigan Cancer Foundation-7
MCT8	Monocarboxylate transporter 8
MDM2	Mouse double minute 2 homolog
MEM	Minimum essential medium
MetAP	Methionylaminopeptdiase
mg	Milligram
min	Minute
MIT	Monoiodotyrosine
ml	Millilitre
mM	Millimolar
MMTV-PyVT	Murine mammary tumor virus Polyoma virus middle T antigen
MRI	Magnetic resonance imaging
mRNA	Messenger ribonucleic acid
MSC	Mesenchymal stem cell
MUC1	Mucin 1
Na^+/K^+ ATPase	Sodium/potassium ATPase
NCS	Newborn calf serum
ND	Not detected
NES	Nuclear export signal
ng	Nanogram

NIS	Sodium iodide symporter
NLoS	Nucleolar localisation signal
NLS	Nuclear localisation signal
nM	Nanomolar
NMT	*N*-myristoyltransferase
NMTi	*N*-myristoyltransferase inhibitor
NST	No special type
NUE	NIS upstream enhancer
ORF	Open reading frame
PI3K	Phosphoinositide 3-kinase
PBF	PTTG binding factor
PBS	Phosphate buffered saline
pcDNA	Plasmid control deoxyribose nucleic acid
PCR	Polymerase chain reaction
PDGF	Platelet-derived growth factor
PDZ	Post synaptic density protein-drosophila disc large tumour suppressor-zonula occludens-1 protein
PFU	Plaque forming units
PKA	Protein kinase A
PKC	Protein kinase C
PLA	Proximity ligation assay
PP1	1-(1,1-Dimethylethyl)-1-(4-methylphenyl)-1*H*-pyrazolo[3,4-*d*]pyrimidin-4-amine
PR	Progesterone receptor
PRE	Progesterone response element
PSA	Prostate-specific antigen
PSI	Plexin-semaphorin-intergrin
PTC	Papilliary thyroid cancer
PTEN	Phosphatase and tensin homolog
PTTG	Pituitary tumor transforming gene
PVDF	Polyvinylidene difluoride
PyMT	Polyoma virus medium T
qRT-PCR	Quantitative real time polymerase chain reaction
RA	Retinoic acid
RAR	Retinoic acid receptor
RARE	Retinoic acid response element
rcf	Relative centrifugal force
RET	Rearranged during transfection
RFP	Red fluorescent protein
RIPA	Radioimmunoprecipitation assay
RISC	RNA-induced silencing complex
RNA	Ribonucleic acid
ROS	Reactive oxygen species
rpm	Revolutions per minute
RXR	Retinoid X receptor
SDS	Sodium dodedecyl sulphate
SDS-PAGE	SDS –polyacrylamide gel electrophoresis
sec	Second
SEM	Standard error of the mean
SERM	Selective oestrogen response modulators
SFK	Src Family Kinase
SFM	Serum free media
SH2	Src homology 2
SH3	Src homology 3
shRNA	Small hairpin ribonucleic acid
siRNA	Short interfering ribonucleic acid
SLC5A5	Solute carrier family 5 member 5
SPECT	Single photon emission computer tomography
SPIO	Superparamagentic iron oxide
STAT	Signal transducer and activator of transcription
STK11	Serine/threonine kinase 11
SUMO	Small ubiquitin-like modifier

SV40	Simian virus 40
T_3	Triiodothyronine
T_4	Thyroxine
TAMRA	6-carboxylate-tetramethyl-rhodamine
TATA	Thymine-adenine-thymine-adenine
TBS	Tris-buffered saline
TBST	Tris-buffered saline with Tween
TCGA	The Cancer Genome Atlas
TEMED	Tetramethylethylenediamine
Tg	Thyroglobulin
TKI	Tyrosine-kinase inhibitor
TMA	Tissue microarray
TN	Triple negative
TNM	Tumour-node-metastasis
TSH	Thyroid stimulating hormone
TSHR	Thyroid stimulating hormone receptor
TU/ml	Transducing units per millilitre
U/l	Units per litre
USF	Upstream stimulating factor
UT	Untransfected
v/v	Volume to volume ratio
VEGF	Vascular endothelial growth factor
VeO	Vehicle only
VO	Empty Vector
WNT11	Wingless/integrated 11
WT	Wildtype
µCi	MicroCurie
µg	Microgram
µl	Microlitre
µM	Micromolar
ZAP-70	Zeta-chain-associated protein kinase 70

CHAPTER 1 – GENERAL INTRODUCTION

1.1 Breast cancer

Breast cancer is the second most common cancer worldwide, and is the leading cause of cancer-related death in women. The global burden of breast cancer is greater than that of all other cancers and the rate of incidence is steadily increasing (Jemal et al., 2010). Based on current incidence projections, 3.2 million new cases of breast cancer will be diagnosed each year by 2050 (Hortobagyi et al., 2005). In the UK, around 55,000 people are diagnosed with breast cancer each year (Cancer Research UK, 2015). In order to understand the pathology and risk factors of this multi-faceted disease, it is important to first cover the biology and anatomy of the normal breast.

1.1.1 The normal breast

Breasts are comprised of glandular tissue and under hormonal control produce milk for the purpose of feeding infants. Along with the brain and lungs, breasts are one of the only organs that are not fully developed at birth and undergo multiple changes throughout life (Russo and Russo, 1987). The adult human breast sits atop the anterior chest wall and is composed of layers of different types of tissue, predominantly adipose and glandular tissue (Guinebretiere et al., 2005).

The glandular tissue is made up of a network of ducts that transport milk from lobules to the nipple (Figure 1-1). Lobules are functional units located at the end of ducts that synthesise milk. Each lobule consists of around 20 smaller structures known as acini. Acini have a layer of epithelial cells that line the lumen that synthesise and secrete milk into the terminal duct, surrounded by an external layer of myoepithelial cells. The duct network is composed of 15-20 larger ducts which divide into smaller ducts creating a ductal tree. Like acini, the ductal lumen is lined with a single layer of epithelial cells surrounded by an

external layer of myoepithelial cells. These myoepithelial cells have the ability to contract which narrows the ductal lumen facilitating the transport of milk. The ducts and lobules are surrounded by connective tissue composed of blood and lymphatic vessels, nerves, adipose and fibrous tissue (Guinebretiere et al., 2005).

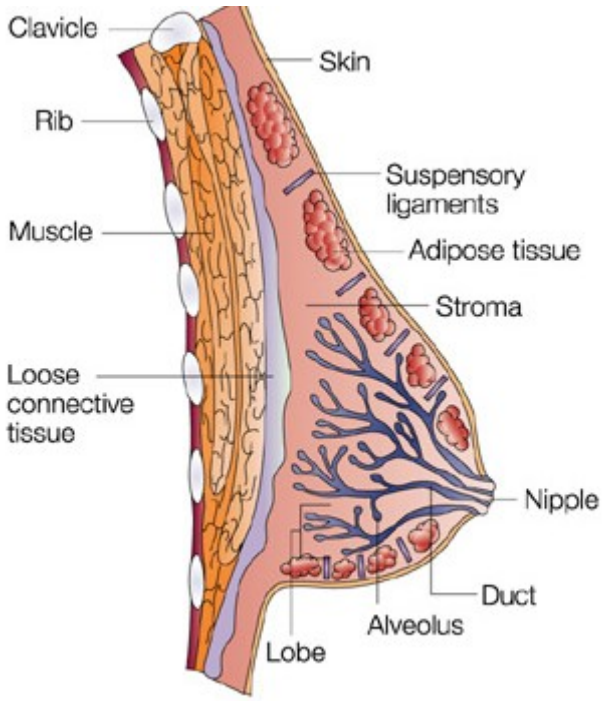

Figure 1-1. Anatomy of the breast. Each mammary gland contains 15–20 lobes, each lobe containing a series of branched ducts that drain into the nipple. Taken from Ali and Coombes, 2002.

1.1.2 Pathology of breast cancer

Breast cancer is a heterogeneous disease that can be divided into a number of subtypes dependent on pathology, location, receptor status and gene signatures. There are two major subdivisions of breast cancer based on pathology alone, carcinoma *in situ* and invasive carcinoma.

1.1.2.1 Carcinoma in situ

There are two major forms of carcinoma *in situ*; ductal (DCIS) and lobular (LCIS) carcinoma *in situ*. Both involve the growth of abnormal cells that follow the existing regional architecture (Guinebretiere et al., 2005).

LCIS was first described in 1941 (Foote and Stewart, 1941) and accounts for approximately 15% of *in situ* breast cancers. It is difficult to detect, as it is not associated with calcification and often does not display any mammographic abnormalities (Sonnenfeld et al., 1991), so is usually discovered after coincidental surgery (Guinebretiere et al., 2005). It is often multifocal and bilateral with women commonly being diagnosed between the ages of 40 and 50, and fewer than 10% of patients being post-menopausal (Fulford et al., 2004). A high frequency of LCIS diagnoses are characterised by the loss of heterozygosity on chromosome 16q at the site of the gene that encodes the cell adhesion molecule E-cadherin (Berx et al., 1995).

As DCIS is difficult to detect at the pre-symptomatic stage it was considered rare, and patients were generally diagnosed upon presenting with nipple discharge or a palpable tumour (Contesso and Petit, 1979). However due to the availability of advanced screening technologies, DCIS diagnoses now account for more than 15-25% of breast cancers (Van Cleef et al., 2014), the most common mammographic indicator being an isolated cluster of microcalcifications (Guinebretiere et al., 2005). The majority of DCIS are unilateral, with the tumour confined to one quadrant of the breast, but larger lesions may be multi-centred. Many clinicians consider DCIS to be pre-malignant, as over time the tumours can progress to invasive ductal carcinoma (Buerger et al., 1999; Giardina et al., 2003; Wellings and Jensen, 1973). DCIS patients tend to be diagnosed later in life than those that develop LCIS, with

most DCIS patients being post-menopausal. In DCIS patients disease prognosis is relatively good, with an overall 10 year mortality rate of between 1-2% (Allegra et al., 2009; Van Cleef et al., 2014).

1.1.2.2 Invasive carcinoma

Similar to carcinomas *in situ*, there are two major forms of invasive carcinomas; invasive ductal carcinoma (IDC) and invasive lobular carcinoma (ILC).

IDC (also referred to as invasive carcinoma of no special type (NST)) accounts for approximately 55% of all breast carcinomas (Eheman et al., 2009) and can occur in both pre- and post-menopausal women (Guinebretiere et al., 2005). IDC can arise from DCIS (Sinn and Kreipe, 2013) and the tumours are devoid of characteristics seen in other breast cancers (Eheman et al., 2009).

ILC is less common than IDC, accounting for only 10-15% of breast carcinomas (Guinebretiere et al., 2005) and as the nomenclature suggests the tumours originate from terminal areas of lobules within breasts (Ogbagabriel et al., 2005). The disease can occur in both pre- and post-menopausal women and is associated with a relatively poor prognosis (Guinebretiere et al., 2005). The tumours are often multifocal within the breast, presenting as singly dispersed cells which lack E-cadherin, a trait shared by LCIS tumours (Wahed et al., 2002).

1.1.3 Risk Factors for breast cancer

1.1.3.1 Gender and Age

In the UK, of the 55,000 people that are diagnosed each year with breast cancer, the vast majority are women, with only around 400 being male. As with many carcinomas, the

incidence of breast cancer increases with age, with the chance of developing the disease doubling approximately every ten years until menopause, at which point the rate of increase significantly slows (McPherson et al., 2000) (Figure 1-2). In the UK between 2010 and 2012, 80% of breast cancer cases were diagnosed in females over the age of 50. The high number of cases diagnosed in women in their 50s may partly be explained by the age women are first offered a mammogram in the UK (Cancer Research UK, 2015).

Until the age of 50 there is a similar incidence of oestrogen receptor positive and negative carcinomas (discussed further in section 1.1.4.3). After 50, oestrogen negative tumour rates decrease while oestrogen receptor positive tumour diagnoses continue to slowly increase (Benson et al., 2009).

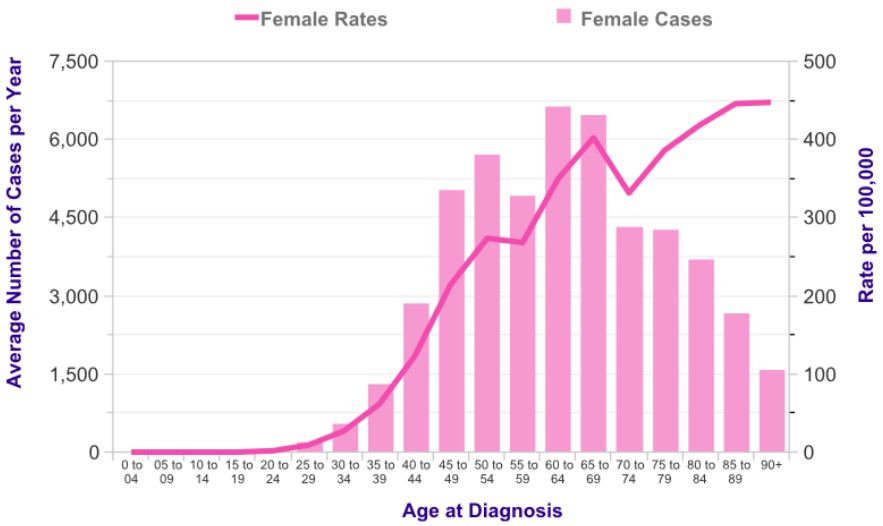

Figure 1-2. Incidence of breast cancer in the UK by age. Average number of new breast cancer cases per year and age-specific incidence rates per 100,000 the UK female population. Taken from Cancer Research UK, http://www.cancerresearchuk.org/content/ breast-cancer-incidence-statistics#heading-One, Accessed Jan 2016.

1.1.3.2 Age at menarche and menopause

Women who experience menarche at an early age (< 12 years old) have a significantly higher chance of developing breast cancer, as this increases overall lifetime exposure to the

hormonal milieu associated with regular menstrual cycles. Breast cancer risk is reduced by about 10% for every two years there is a delay in the onset of menstruation (Kelsey et al., 1993).

Women who have a late menopause also have a dramatically increased risk of developing breast cancer (Collaborative Group on Hormonal Factors in Breast, 2012; Kelsey et al., 1993) with those who have a natural menopause at the age of 45 having half the breast cancer risk of those who do not undergo menopause until the age of 55. A bilateral oophorectomy before the age of 35 decreases the risk of developing breast cancer by 60% compared with women who go through natural menopause (McPherson et al., 2000).

1.1.3.3 Age at first full-term pregnancy

In addition to early menarche and late menopause, nulliparity and late age at first birth have both been identified to increase the incidence of breast cancer in women. The risk of breast cancer in women who have their first child in their 20s is half that of women who have a baby over the age of 30, though only full-term pregnancies are linked with a reduced breast cancer risk (Choudhury et al., 2013; Kelsey et al., 1993). Interestingly, nulliparous women have a lower chance of developing breast cancer than women who have their first child over the age of 35, and having a second child at an early age can further reduce the risk of developing breast cancer (McPherson et al., 2000).

1.1.3.4 Family History

As many as 10% of breast cancer incidences in Western countries have been attributed to genetic predisposition to the disease. Breast cancer susceptibility is generally inherited in an autosomal manner with limited penetrance. The risk of developing breast cancer is

increased if a first degree female relative has developed breast cancer, up to as much as nine-fold if the disease was bilateral and pre-menopausal (McPherson et al., 2000).

The best characterised indicators of genetic predisposition are mutations within the genes BRCA1 and BRCA2, which are located on the long arms of chromosomes 17 and 13 respectively. BRCA1/2 are tumour suppressors with roles in DNA repair mechanisms, the disruption of which can lead to genomic instability and therefore an increased risk of cancer. BRCA1/2 mutations account for approximately 75% of hereditary breast cancer cases (McPherson et al., 2000). Inherited mutations in other genes that have been associated with breast cancer include ATM, TP53, CHEK2, PTEN and STK11, although their contribution to disease incidence is minimal compared with that of BRCA1/2 (Benson et al., 2009).

1.1.3.5 Lifestyle

As well as factors beyond the control of the individual, diet, exercise and weight can influence the risk of developing breast cancer, as is indeed the case with many cancers. Both pre- and post-menopausal women who are physically active have a 30-40% lower risk of developing breast cancer compared with sedentary women (Thune and Furberg, 2001), with as little as 2-3 hours of moderate intensity exercise a week being associated with a 40-50% reduction in breast cancer risk (Holick et al., 2008; Holmes et al., 2005).

Associations have been identified between body mass index (BMI) and breast cancer risk in relation to menopausal status. In post-menopausal women, an association between being overweight (defined as a BMI of 25 to 29.9 kg/m^2) or obese (BMI of 30 kg/m^2 or greater) and increased breast cancer incidence has been found in many studies (Eliassen et al., 2006; Lahmann et al., 2004; Renehan et al., 2008). There have been conflicting reports regarding the effect of BMI on breast cancer risk in pre-menopausal women. One large

cohort study reported that increased BMI in pre-menopausal women actually decreases breast cancer risk (Reeves et al., 2007). Conversely, another study identified a positive correlation between BMI and breast cancer risk in the Asian population (Cheraghi et al., 2012) and abdominal obesity has been linked with pre-menopausal cancer risk (Harvie et al., 2003). Obesity has also been associated with increased tumour diameter, decreased survival and increased lymph node involvement (Berclaz et al., 2004; Cleveland et al., 2007).

Populations with high fat diets exhibit an increased incidence of breast cancer (Key et al., 2003) and it has been shown that a reduction of the proportion of dietary fat can decrease breast cancer risk by up to 8% (Prentice et al., 2006). Smoking and alcohol intake are also implicated as risk factors for breast cancer development (Ferrini et al., 2015; Key et al., 2003).

1.1.3.6 Hormone Replacement Therapy (HRT)

Long-term use of combined oestrogen-progestogen hormone replacement therapy (HRT) has been classified by the International Agency for Research on Cancer (IARC) as a cause of breast cancer (Ritte et al., 2012) and an estimated 3% of UK breast cancer cases have been linked to HRT use (Parkin, 2011). The risk of developing breast cancer decreases 5 years after cessation of HRT. Although there is no correlation between HRT use and breast cancer mortality, HRT can reduce the sensitivity and specificity of breast cancer screening by increasing breast density and thus reducing the chance of early detection (McPherson et al., 2000).

1.1.4 Hormones and Hormone Receptors

As evidenced by the major risk factors discussed above, there is substantial evidence of a link between breast cancer and female sex hormones. This association is further supported by HRT

being classified as a cause of breast cancer. Early menarche and late menopause result in the woman being exposed to a higher number of menstrual cycles, thus a prolonged exposure to cycles of oestrogen and progesterone. Oestrogen and progesterone cycles have a stimulatory effect on breast epithelium and can induce differentiation of immature ducts into terminal end buds (Cork et al., 2008)(the roles of prolactin and oxytocin are discussed in sections 1.2.3 and 1.2.4.1). Pregnancy reduces the cumulative exposure to oestrogen and causes lobules to further differentiate. Undifferentiated epithelial lobular cells from nulliparous women have been observed to be more susceptible to transformation than differentiated cells in parous women (Russo et al., 2005).

Further to the role hormones play in the development of breast cancer, the disease is split into different subtypes based on the presence or absence of hormone receptors. The key hormone receptors in breast cancer classification are the oestrogen (ER), progesterone (PR) and epidermal growth factor 2 (ERBB2/HER2) receptors.

1.1.4.1 Oestrogen

Oestrogens have an essential role in the development of the female sex organs and secondary sex characteristics such as the regulation of the menstrual cycle and reproduction (Travis and Key, 2003). There are 3 major forms of oestrogen; oestrone (E1), oestradiol (E2) and oestriol (E3). E2, also known as 17-β-estradiol, is the most biologically active and potent form of oestrogen. The biological effects of oestrogens are dictated by circulating concentrations and differential rates of intracellular conversion of the molecules to derivatives. In pre-menopausal women, oestradiol is the predominant form of circulating oestrogen, which is secreted by the ovaries in monthly cycles. Post-menopause, peripheral tissues such as adipose tissue become the major source of oestrogen, secreting oestrone produced from androgen precursors (Cleary and Grossmann, 2009).

Much of the evidence for the link between oestrogen and breast cancer comes from retrospective observational studies that have found circulating and excreted levels to be associated with risk for the disease. Post-menopausal women who have a relatively high serum level of oestrogen have been reported to have a two-fold risk of breast cancer compared with women with lower serum levels (Key et al., 2002). Though there are conflicting reports, some associations have been made between breast cancer risk and polymorphisms in genes involved in oestrogen synthesis, such as *CYP17, CYP19* and *HSD17B1* (Dunning et al., 1999; Feigelson et al., 2001).

1.1.4.2 Oestrogen Receptor

Oestrogens mediate cellular effects by binding to the intracellular nuclear receptors oestrogen receptor (ER) alpha (ERα) and beta (ERβ). Of the two oestrogen receptors, ERα was the first to be identified with ERβ remaining undiscovered until the late 90s (Kuiper et al., 1996). The ERα gene is over 140kb and is located on chromosome 6q25.1, encoding a 595 amino acid protein, whereas the human ERβ gene is ~61.2kb and located on chromosome 14q23.2, spanning 8 exons and producing a 530 amino acid protein. Both forms contain autonomous domains with specific roles including ligand-binding (E), a hinge region (D), DNA-binding (C) and transactivation domains (A/B)(Figure 1-3). The DNA-binding domain is highly conserved between the two isoforms, only differing by two amino acids (Ruff et al., 2000).

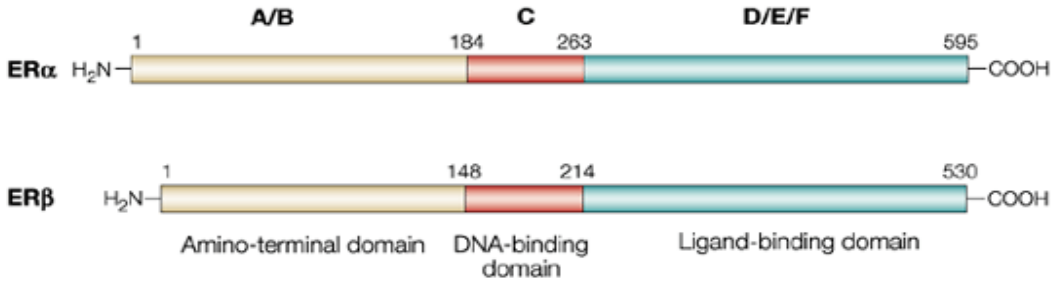

Figure 1-3. Comparison of the structures of ERα and ERβ. Both human oestrogen receptors — ERα and ERβ — share structural domains (A–F). From a functional perspective, ERs can be divided into three parts — the amino-terminal or A/B domain, the DNA-binding or C domain, and the ligand-binding or E domain. The F domain is involved in distinguishing between oestrogen agonists and antagonists. Taken from Behl, 2002.

In the classical pathway, oestrogens bind to ligand-binding domains in region E inducing the migration of the receptor from the cytosol to the nucleus. Here the receptors form stable homo- (ERα/α or ERβ/β) or hetero- (ERα/β) dimers. The activated dimers then interact with the oestrogen response elements (ERE) of target genes. Interaction between the dimers and ERE induces dissociation of co-repressor proteins and the recruitment of coactivators leading to chromatin remodelling and target gene transcription (Chen et al., 2008). Genes heavily regulated by the EREs include the progesterone receptor and vitellogenins. Other pathways include the interaction of ERs with transcription factors such as AP1 (Jakacka et al., 2001) and SP1 (Porter et al., 1997) rather than direct binding to DNA. Oestrogens also have non-genomic effects on cells and have been shown to induce an increase in intracellular calcium and nitric oxide leading to activation of pathways including mitogen-activated protein kinase (MAPK) and phosphoinositide 3-kinase (PI3K) (Chen et al., 2008).

In normal mammary tissue, ERβ is the predominant form of ER, with expression in both luminal and myoepithelial cells (Speirs et al., 2002). Though ERβ knockout mice

undergo normal mammary gland development there are subtle differences associated with decreased differentiation and increased proliferation in the alveoli of lactating mammary glands dependent on age of the mice (Forster et al., 2002; Palmieri et al., 2002).

1.1.4.3 Oestrogen in breast cancer

The carcinogenic effect of oestrogen is said to be executed via three mechanisms. Oestrogen is capable of promoting cellular proliferation and survival via ER through the genomic and non-genomic mechanisms outlined in 1.1.4.2 (Figure 1-4). There are an ever increasing number of molecules being identified to be under the regulation of EREs. Two examples include LRP16 and WNT11. E2 stimulates LRP16 expression, a protein that can interfere with the transcription of E-cadherin, subsequently increasing the invasiveness of the breast cancer (Han et al., 2008). E2 also induces WNT11 expression via ER which increases the resistance of cells to apoptosis (Lin et al., 2007; Vendrell et al., 2007).

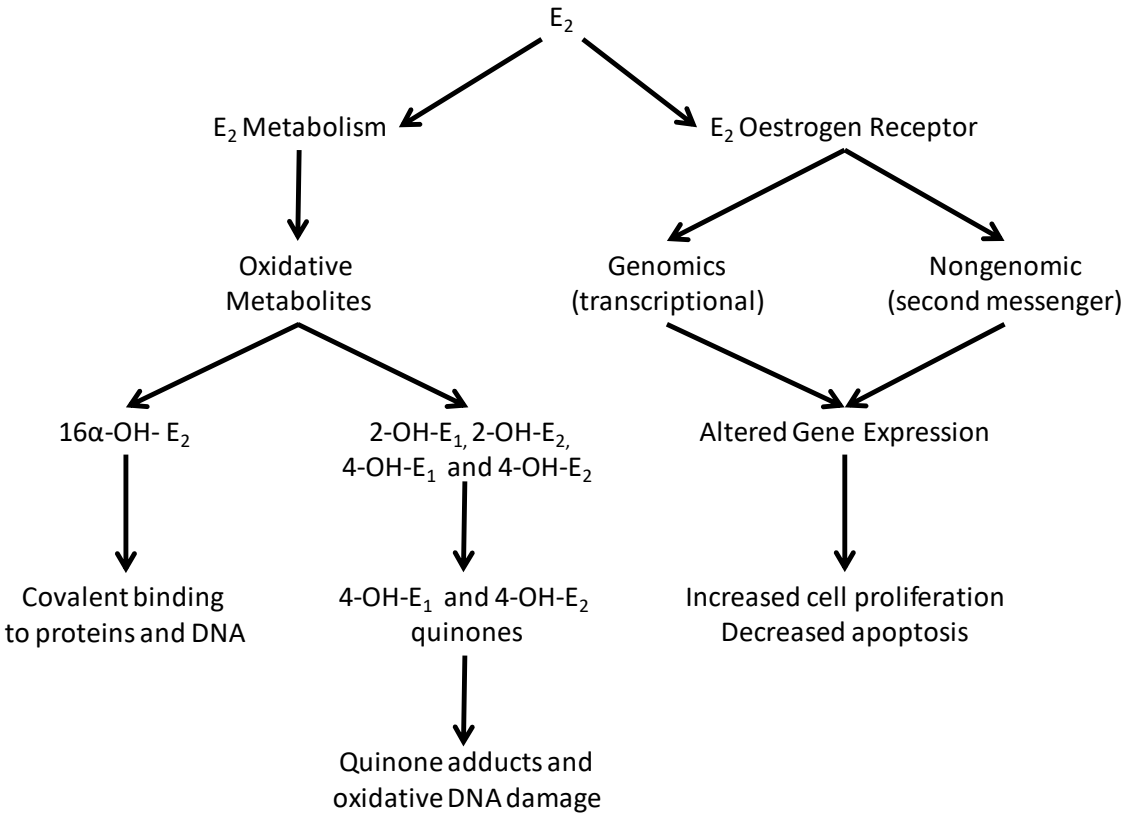

Figure 1-4. Pathways for oestrogen-induced carcinogenesis. The complementary pathways contribute to the carcinogenicity of oestrogen and to the initiation, promotion, or progression of breast cancer. Adapted from Yager and Davidson, 2006.

Oestrogen can also promote cellular proliferation via ER-independent mechanisms as witnessed in ER-negative breast cancer cells. In ER-negative MDA-MB-231 cells, treatment with oestrogen induced the rapid phosphorylation of AKT at Ser473 leading to protein activation along with stimulation of protein kinase C (PKC), resulting in increased cell proliferation (Chen et al., 2008).

In addition to these downstream effects, many oestrogen metabolites are thought to be carcinogenic and have been observed to have direct genotoxic effects (Figure 1-4)(Cavalieri and Rogan, 2016; Yager and Davidson, 2006).

1.1.4.4 Progesterone

Progesterone is an endogenous steroid and progestogen sex hormone that is essential in the regulation of the menstrual cycle, pregnancy and embryogenesis. The hormone is also essential for normal breast development during puberty, lactation and breastfeeding. Progesterone is heavily prescribed, often alongside oestrogen, as contraception or HRT. It mediates its cellular effects through interaction with the progesterone receptors (PR) (Lange and Yee, 2008).

1.1.4.5 Progesterone Receptor

The progesterone receptor (PR) is vital for female reproductive activities, as evidenced by knockout PR mice displaying pleiotropic reproductive abnormalities (Lydon et al., 1995). There are two major isoforms of the PR - PR-A and PR-B - both of which belong to the nuclear hormone receptor family. Both isoforms are expressed from a single gene, with transcription of each being regulated by different promoters and the initiation of translation at two different AUG codons (Kastner et al., 1990). PR-A and PR-B are comprised of autonomous domains including several transactivation domains (A/B), a DNA-binding domain (C), a hinge region (D) containing a nuclear localisation signal and a ligand-binding domain (E).

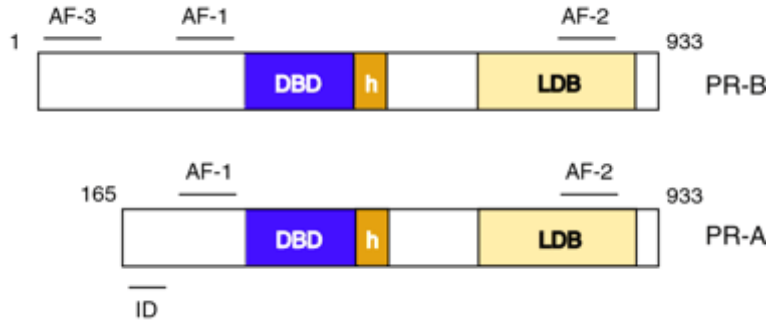

Figure 1-5. Structure of PR variants. Domain organization of the human PR-A and -B isoforms. h*, hinge region;* LDB*, ligand-binding domain;* ID*, inhibitory domain. The numbers denote the positions of amino acids for each isoform. AF-1, -2, and -3 are transcription activation domains. Taken from Li and O'Malley, 2003.*

Upon progesterone binding to PR, the receptor undergoes a conformational change inducing nuclear translocation, dimerisation and interaction with progesterone response elements (PRE) in the promoter regions of target genes. As with ER, the binding of PR to PRE leads to the dissociation of co-repressors and the recruitment of co-activators to form a productive transcription initiation complex at the promoter of the target gene. PRs can also be activated in a ligand-independent manner by cell-permeable agents that increase intracellular kinase activity (Conneely and Lydon, 2000). Target genes of PR are involved in a wide array of cellular activities including cell signalling, proliferation, apoptosis and metabolism of lipids and steroids (Cork et al., 2008).

1.1.4.6 Progesterone in breast cancer

The cited effects of progesterone on breast cancer remain largely controversial. There have been some suggestions that progesterone combined with oestrogen in HRT increases the risk of breast cancer more so than therapies containing oestrogen alone (Cork et al., 2008). However, progesterone has also been reported to be protective against breast cancer risk as it can inhibit enzymes involved in E2 formation in breast cancer cells and stimulate the

activity of enzymes converting oestrogens to less biologically active forms, thus inhibiting promotion of breast cancer via oestrogen (Pasqualini, 2007). In rats, it was observed that a combination treatment of progesterone and tamoxifen could inhibit the oestrogen-induced tumour formation more effectively than single reagent therapies (Mohammed et al., 2015). As the different forms of progestogens also have different affinities for PR-A and -B, it may be the case that progesterone can have both synergistic and antagonistic effects on the oestrogen pathways (Kenemans and Bosman, 2003).

1.1.4.7 HER2

Human epidermal growth factor receptor 2 (HER2), also referred to as NEU or ERBB2, is an orphan receptor that is amplified in many breast cancers. It is a proto-oncogene located on chromosome 17q12 that encodes for a 1255 amino acid transmembrane glycoprotein (Rubin and Yarden, 2001). Like other members of the HER family it is comprised of a cysteine-rich extracellular ligand binding site, a transmembrane domain and an intracellular region that has tyrosine kinase catalytic activity. Although HER2 does not have a ligand, all other HER variants are activated by ligand binding, leading to dimerisation and transphosphorylation (Moasser, 2007). HER2 is often the dimerisation partner of choice for other HER family members, as it is always in an open conformation having its dimerisation domains exposed. To add to this, HER2 has the strongest catalytic kinase activity giving HER2 heterodimers the strongest signalling activity (Graus-Porta et al., 1997).

In breast cancer, HER2 is the dominant tyrosine kinase receptor, being amplified in 20% of cases (Slamon et al., 1987). A variant of HER2 lacking the extracellular p95 domain is present in up to 30% of human breast tumours with HER2 overexpression (Molina et al.,

2002). This mutated form is constitutively active and resistant to drugs targeted at HER2 (Scaltriti et al., 2007).

1.1.4.8 Receptor Status

Breast cancer can be further subdivided into categories based on the expression of ER, PR and HER2 within the tumour. The table below describes the subcategories of breast cancer dependent on receptor status and their prevalence (Table 1-1). The differential expression of these receptors can determine the treatment a patient receives for their specific form of the disease.

Subtype	ER Status	HER2 Status	PR Status	Prevalence
Basal-like (Triple Negative)	-	-	-	15-20%
Luminal A	+	-	+	40%
Luminal B	+	+	+	20%
HER2 amplified	-	+	-	10-15%

Table 1-1. Breast cancer subtypes. The subdivisions of breast cancer dependent on receptor status and their prevalence. Adapted from Carey et al., 2006.

1.1.5 Treatments

There are four major strategies for the treatment and management of patients with breast cancer - surgery, chemotherapy, radiotherapy and hormone treatment. A combined approach using several of these methods is usually employed. After diagnosis of the disease, it is important to gauge disease stage and receptor status as these factors can dictate treatment plans. Disease staging is determined based on the tumour size, lymph node involvement and presence of metastases (Moulder and Hortobagyi, 2008).

1.1.5.1 Surgery

Surgical resection of the disease involves removing the primary tumour and any involved lymph nodes. Traditionally, even localised breast cancer was treated with a radical mastectomy and axillary lymph node dissection. However more recently it has been reported that lumpectomy followed by radiation therapy (breast-conserving surgery) is equally effective with similar rates of local recurrence and overall survival (Clarke et al., 2005). A double mastectomy may be performed if a young patient presents with a known BRCA mutation, with the aim of removing the primary cancer and reducing the risk of a second cancer incidence.

1.1.5.2 Chemotherapy

Chemotherapy is frequently used in patients with breast cancer to palliate symptoms and reduce the risk of recurrence. Chemotherapy may be used prior to surgery with the hope of shrinking the tumour but is more commonly used after surgery to kill residual cancer cells. Adjuvant chemotherapy reduces the risk of death by 25% and the risk of distant metastasis by 18% (Rossi et al., 2015). Drugs are usually administered in a combination of two or three, with the most common class of drugs for breast cancer treatment being anthracyclines including doxorubin and epirubin. These compounds inhibit DNA synthesis by intercalating between base pairs and topoisomerase II which blocks transcription and replication (Pommier et al., 2010). Though chemotherapy can be an effective treatment, patients often experience a plethora of side effects and resistance to therapy can arise.

1.1.5.3 Radiotherapy

The role of radiotherapy in the treatment of breast cancer has a long and controversial history with the first clinical trial into its use as a treatment for breast cancer beginning in

1949 (Paterson and Russel, 1959). Although radiotherapy decreases risk of a local relapse by 70%, the reduction in relapse rates does not translate into a reduction in mortality (Cuzick, 2005). This disparity may be due to the detrimental effect radiotherapy has on the immune system (Stjernsward, 1974). More recent data have suggested that radiotherapy used following breast-conserving surgery has a positive effect on overall survival (Vinh-Hung and Verschraegen, 2004).

1.1.5.4 Hormone Therapy

There are a variety of hormone treatments available to patients dependent on their receptor status. For the 70% of breast cancer patients that have ER-positive tumours, selective oestrogen response modulators (SERM) can be used. These are a group of compounds that have a similar chemical structure to oestrogens and are capable of binding to the ER (Moulder and Hortobagyi, 2008). Tamoxifen is the most publicised SERM, and is recommended for the treatment of both pre- and post-menopausal women (Jordan, 1993). In the US it has also been approved by the FDA for the prevention of breast cancer in women at high risk of developing the disease. Tamoxifen competitively inhibits the action of oestrogen by binding to the ER itself. In the same manner as oestrogen, tamoxifen causes dimerisation of the receptors which then bind to discrete EREs in target genes. However when oestrogen binds to the ER, both activation function (AF) domains, AF-1 and AF-2, are activated, yet when tamoxifen binds only AF-1 is activated (Figure 1-6). The inactivity of AF-2 attenuates transcription and coactivator binding, resulting in inhibition of the G_1 phase of the cell cycle and slower cell proliferation (Figure 1-6) (Howell et al., 2000). Though tamoxifen is generally well tolerated, there are side effects and patients can develop resistance, particularly those with amplified HER2 (Clemons et al., 2002).

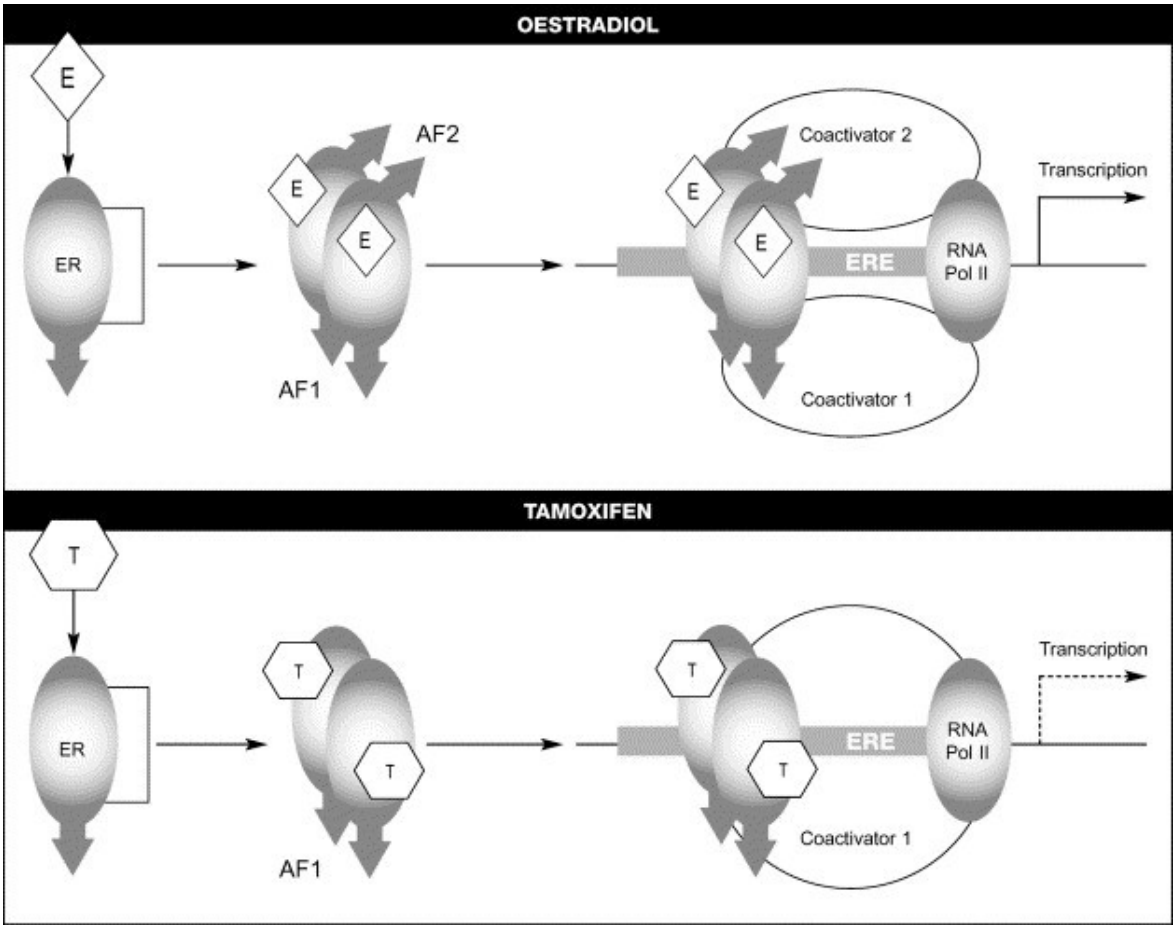

Figure 1-6. Mode of action of oestrogen and tamoxifen. The top panel illustrates the mechanism by which oestradiol can activate transcription of target genes. The bottom panel demonstrates the effect tamoxifen has on binding to ER. Taken from Clemons et al., 2002.

Trastuzumab (Herceptin) is a recombinant monoclonal antibody targeted to the extracellular domain of HER2 for patients that have amplified HER2. Trastuzumab decreases signalling via several mechanisms including prevention of HER2 dimerisation, inhibition of extracellular domain shedding, immune activation and increased degradation of HER2 (Valabrega et al., 2007). The addition of trastuzamab to chemotherapy reduced recurrence by half and mortality by a third in women with HER2 positive breast cancer (Romond et al., 2005).

1.1.6 New Treatments Required

Although there are a variety of treatments available for breast cancer patients, it is still the leading cause of cancer-related death in women and thus still remains a formidable issue. The heterogeneity of the disease observed at both intra- and inter-tumoural level continues to make the disease challenging to treat. This is particularly true for patients with metastatic triple negative disease, where there are reduced treatment options. Resistance to chemotherapy and hormone therapies can also arise, rendering the drugs ineffective. Side effects can also cause patients discomfort and reduce their quality of life, as well as increasing the risk of chronic illnesses such as chemo-induced acute myeloid leukaemia (AML).

Currently used in the management and diagnostic imaging of thyroid disorders, the inherent ability of breast cells to take up iodide opens the possibility for a potential alternative treatment for breast cancer via radioiodide therapy. Although utilisation of radioiodide treatment for breast cancer has been proposed previously, further understanding into the regulation and post-translational modifications are required before it can be translated from bench to bedside.

1.2 Sodium Iodide Symporter (NIS)

1.2.1 Identification and Structure

The sodium iodide symporter (NIS) is a large integral plasma membrane glycoprotein (Figure 1-7), the primary role of which is transporting iodide (I^-) into cells. NIS is primarily expressed in the thyroid but has also been described to have roles in the salivary glands, gastric mucosa and lactating mammary glands (discussed in section 1.2.3). The ability of the thyroid to accumulate iodide was reported as early as 1896 (Baumann, 1896), although molecular information on NIS was not available until the rat gene was cloned in 1996 (Dai et al., 1996). Human NIS, also referred to as solute carrier family 5 member 5 (SLC5A5), was cloned a year later and was found to share 84% homology and 92% similarity to rat NIS (Smanik et al., 1997). Located on chromosome 19p13.11, the human NIS gene comprises 15 exons interrupted by 14 introns and encodes a 643 amino acid protein (Smanik et al., 1997). The protein consists of thirteen transmembrane domains, an extracellular N-terminal and a cytosolic C-terminal tail (Figure 1-7). Several phosphorylation sites have been identified *in vivo* along with three N-linked glycosylation sites at positions 225, 485 and 497 (Levy et al., 1998; Vadysirisack et al., 2007) (Figure 1-7). Mutation of all three glycosylation sites reduced NIS function by approximately 50%, suggesting that although important for maximum NIS function, glycosylation is not essential (Levy et al., 1998).

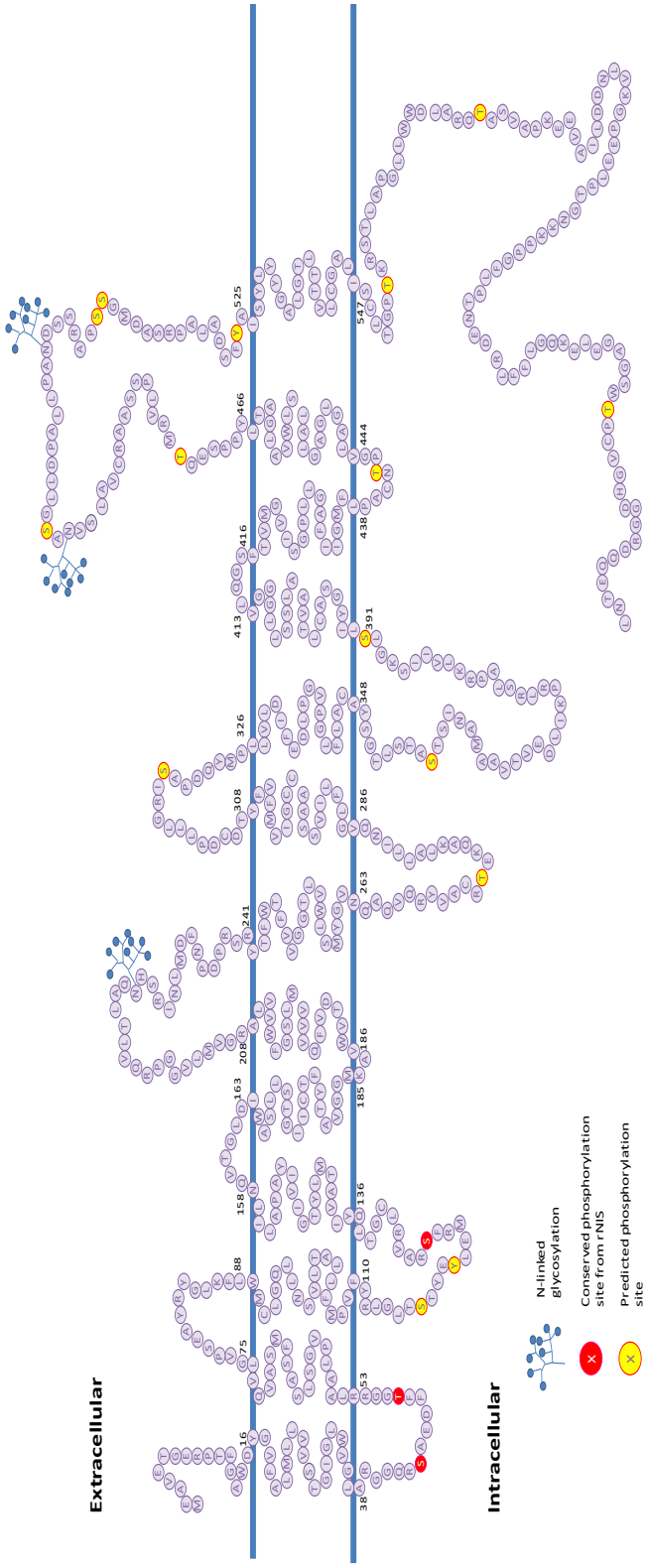

Figure 1-7. Secondary structure of hNIS. The secondary structure of human NIS with 13 transmembrane domains as predicted by UniProt (http://www.uniprot.org/uniprot/Q92911). NIS is glycosylated at Asn225, Asn485 and Asn497, all found on hydrophilic extracellular loops. Red amino acids are conserved residues that have been observed to be phosphorylated in rat NIS, while amino acids in yellow are those predicted to be phosphorylated by NetPhos2.0.

1.2.2 NIS in the thyroid

1.2.2.1 Function

The primary function of the thyroid is to produce the iodine-containing hormones triiodothyronine (T_3) and thyroxine (T_4). The concentration of iodide within thyroid follicular cells is 20-50 times greater than the extracellular concentration, so iodide cannot passively diffuse into cells. NIS takes advantage of the inverse sodium ion (Na^+) electrochemical gradient, maintained by the Na^+/K^+-ATPase, to couple the transport of one I^- anion and two Na^+ cations across the basolateral membrane into thyroid follicular epithelial cells. The NIS-mediated transport of I^- into thyroid follicular cells is the rate-limiting step of T_3 and T_4 biosynthesis (Spitzweg et al., 2001).

Once within cells, I^- is transported across the apical membrane of cells into the follicular lumen where it is organified by thyroid peroxidase. Organification involves the oxidation and subsequent incorporation of iodine into tyrosine residues in thyroglobulin molecules. Iodide can be incorporated into tyrosine residues producing either monoiodotyrosine (MIT) or diiodotyrosine (DIT). Thyroglobulin is later digested in lysosomes releasing MIT and DIT with the hormone being produced dependent on the coupling reaction - T_4 is formed from the coupling of two DIT molecules whereas T_3 is a combination of DIT and MIT.

1.2.2.2 Regulation

The main proximal promoter region of human NIS is located between -478 and -389 relative to the translation start codon, and contains both a TATA box (AATAAAT) and a GC box (CCCGCCCC) (Ryu et al., 1998). A putative ERE (5' CG-GGTCA-CCG-CCGACT-CC 3') was also identified 9bp upstream of the TATA box element (Alotaibi et al., 2006). Along with an important enhancer region at -2504 to -2260, a NIS upstream enhancer (NUE) was

identified between -9348 and -9054 (Ohno et al., 1999). The activity of the NUE has been observed to be specific to thyroid cells whereas the proximal promoter is functional in a variety of cell-lines (Schmitt et al., 2002; Taki et al., 2002).

In the thyroid, NIS expression is primarily regulated by thyroid stimulating hormone (TSH) (Kogai et al., 1997). When TSH binds to its receptor (TSHR), a G protein-coupled receptor adenylate cyclase becomes activated (Kogai et al., 2006) generating intracellular cyclic adenosine monophosphate (cAMP). This increase in cAMP activates transcription factors including the cAMP response element-binding protein (CREB) and Pax8 (Poleev et al., 1997). NIS transcription is subsequently induced by the binding of Pax8 and CREB to the NUE (Ohno et al., 1999).

TSH not only regulates transcription of NIS in the thyroid, but also plays a key role in the post-translational regulation of NIS. Withdrawal of TSH for 5 days in FRTL-5 cells abolished radioiodide uptake and decreased membrane vesicle expression of NIS by 50% (Riedel et al., 2001). The presence of TSH in thyroid cells can modulate NIS stability, increasing the half-life of NIS by up to 40%. TSH also regulates the subcellular distribution of NIS (Riedel et al., 2001). In the presence of TSH, NIS is primarily located at the basolateral membrane. However, NIS expression at the plasma membrane was observed to decrease over time following TSH withdrawal from cells. Phosphorylation of NIS has been observed *in vivo,* and phosphopeptide mapping revealed a marked change in NIS phosphorylation in the presence and absence of TSH. There were five phosphopeptides detected in the presence of TSH which reduced to three after TSH withdrawal. However, the precise sites, mechanism and importance of NIS phosphorylation remain unknown (Riedel et al., 2001).

The concentration of iodide within thyroid follicles also plays a role in NIS regulation. In response to critically high levels of iodide, the organification process is inhibited by an autoregulatory phenomenon known as the acute Wolf-Chaikoff effect. This mechanism protects the thyroid from high doses of iodide whilst maintaining an adequate supply for thyroid hormone synthesis (Wolff et al., 1949). Although the mechanism for the acute Wolff-Chaikoff effect is still not fully understood, there is evidence to suggest that the generation of thyroid peroxidase inhibitors such as intrathyroidal iodolactones, iodoaldehydes and iodolipids contribute to the decreased synthesis of thyroid hormones (Leung and Braverman, 2014). The Wolf-Chaikoff effect has been observed to be transient lasting approximately 24 hours and thyroid hormone production resumes after adaptation (Wolff et al., 1949). This adaptation has been associated with decreased expression of NIS in thyroid follicular cells (Eng et al., 1999).

It has been demonstrated that high levels of I^- can downregulate NIS mRNA in both dog (Uyttersprot et al., 1997) and rat thyroid (Eng et al., 1999). However a later study in FRTL-5 cells observed no change in NIS mRNA but did identify a reduction in NIS protein at high I^- concentrations, suggesting a post-transcriptional effect (Eng et al., 2001). In the PCCl3 rat thyroid follicular cell line, excess iodide resulted in increased Akt phosphorylation and PI3K activity. Additionally, use of specific PI3K and Akt inhibitors abolished the I^- inhibitory effect on NIS function (Serrano-Nascimento et al., 2014). Increased iodide has also been observed to increase cellular reactive oxygen species (ROS) inhibiting NIS function at the cell surface through post-translational mechanisms (Arriagada et al., 2015).

1.2.2.3 NIS in thyroid disease

The natural ability of the thyroid to take up iodide is central to the diagnosis and treatment of thyroid diseases such as hyperthyroidism, Graves' Disease and thyroid cancer. This mechanism has been exploited for the treatment of thyroid disease for over 70 years with radioiodide being used to treat thyroid carcinoma as early as the 1940s (Hertz and Roberts, 1942; Seidlin et al., 1946). A large proportion (68-80%) of thyroid cancers and their metastases retain the ability to accumulate iodide with functional NIS expression (Castro et al., 2001). This uptake has allowed ablation of malignant tissue using the β-emitting radioiodide-131 (^{131}I) and nuclear imaging of the disease using radioiodide 123, 124 and 125 (^{123}I, ^{124}I and ^{125}I)(Spitzweg et al., 2001).

Although ^{131}I has a place as a therapeutic treatment for thyroid cancer it also represents a significant public health hazard. It has been widely implicated in many of the detrimental effects associated with open-air atomic bomb testing in the 1950s, the Chernobyl disaster in 1986, and the Fukushima explosion of 2011. One of the major products from the nuclear fission of both uranium and plutonium is ^{131}I. This isotope of iodide decays through beta decay and is notable for causing mutation and death in cells that it penetrates and other cells up to several millimetres away (the 'Bystander Effect'). In nuclear fallout, the doses of radioiodide received from nuclear contamination are much lower than the high doses used therapeutically to kill diseased cells. These lower doses are not sufficient to induce cell death but are capable of initiating mutations that may then drive cell transformation and tumourigenesis.

1.2.3 NIS expression in the lactating breast

While iodide accumulation in the thyroid is important for the production of thyroid hormones, it is also vital that breastfeeding mothers accumulate iodide in their milk. Iodide is an essential constituent of breast milk as infants that receive deficient levels of iodide are at an increased risk of mortality and impaired neurological development (Cao et al., 1994; DeLong et al., 1997).

The ability of mothers to accumulate iodide in their milk was observed as early as 1952 (Honour et al., 1952) but NIS was not identified as the transporter responsible until nearly 50 years later (Cho et al., 2000; Tazebay et al., 2000). Alveolar cells display distinct functional NIS expression in the basolateral plasma membrane (Cho et al., 2000). Rat lactating mammary gland NIS is only ~75kDa in size which is smaller than the 100kDa form observed in rat thyroid. However the difference in size can be attributed to differences in glycosylation as both the rat mammary gland and thyroidal NIS have an unglycosylated form of NIS of ~50kDa (Tazebay et al., 2000). Although unglycosylated forms of NIS are still functional, they are observed to have a reduced activity compared to fully glycosylated mature NIS (Levy et al., 1998).

NIS expression in mammary glands is under different regulation to that in the thyroid, with expression solely being induced towards the end of gestation and throughout suckling. However within 24 hours of weaning, NIS expression is significantly reduced (Tazebay et al., 2000). Investigation into regulation of mammary gland NIS has focused on the potential roles of hormones heavily involved in lactation such as oxytocin and prolactin (discussed in 1.2.4.1).

Treatment of mice with oxytocin increased both the expression of NIS in mammary tissue and accumulation of radioiodide within milk (Tazebay et al., 2000). This was also confirmed in rats, where an antagonist of oxytocin decreased radioiodide uptake compared with control treated animals (Cho et al., 2000). The role of prolactin in NIS expression is not as clear cut and has produced varying results in different studies. Mice treated with prolactin alone and in combination with oxytocin did not display altered iodide accumulation in their milk, nor was NIS expression induced. However, rats treated with prolactin displayed increased NIS mRNA levels and use of bromocriptine, a potent inhibitor of prolactin release from the pituitary gland, decreased radioiodide uptake in rat mammary glands (Cho et al., 2000). Despite this, it is clear that oxytocin and prolactin do not act synergistically. Prolactin is documented to have an inhibitory effect on steroidogenesis (Dorrington and Gore-Langton, 1981), which has been suggested to decrease oestrogen levels below a threshold level, subsequently preventing NIS induction by concomitantly administered oxytocin. The combination of oestrogen, prolactin and oxytocin (in the absence of progesterone) led to the highest levels of mammary gland NIS expression in ovariectomised mice. This combination of hormones closely resembles relative hormonal levels in mice and rats during lactation (Tazebay, 2000).

1.2.4 NIS in breast cancer

Breast carcinomas have been documented to possess the ability to take up radioiodide for over 40 years. Initial studies established that breast tumour biopsies were capable of taking up more radioiodide than their normal counterparts (Eskin et al., 1974) with subsequent murine experiments replicating these findings (Thorpe, 1976). However it was not until the new millennium that expression of NIS was identified in breast cancer

with NIS mRNA being detected in 6 out of 7 human tumours (Kilbane et al., 2000) and the presence of NIS protein confirmed by immunohistochemistry (IHC) (Tazebay et al., 2000). Although none of the of the normal breast samples showed any IHC staining for NIS, 87% of the breast carcinoma samples were reported positive for NIS expression (Tazebay et al., 2000). Expression of NIS did not differentiate between tumour type with tumours such as invasive carcinoma and ductal carcinoma *in situ* having similar NIS levels (Tazebay et al., 2000; Wapnir et al., 2003). Initial studies did not indicate any correlation between NIS expression and the expression of TSHR, ER or PR in breast cancer (Oh et al., 2005), however a more recent study has identified an association between ER and NIS expression (Chatterjee et al., 2013).

Despite many tumours having NIS expression, only those with the highest NIS levels have measurable functional NIS, with only 17% of NIS positive tumours being capable of ^{99m}Tc-pertechnetate uptake (Moon et al., 2001). A subsequent study found 2/8 (25%) NIS expressing tumours had detectable ^{123}I uptake (Wapnir et al., 2004). The disparity between radioiodide uptake and NIS expression levels has resulted in the hypothesis that NIS may be aberrantly localised within breast cancer cells. In the lactating breast, NIS was primarily located along the basolateral membrane of epithelial cells whereas in breast cancer cells a mixture of cell surface and intracellular staining has been reported (Tazebay et al., 2000). This was confirmed by a later study where only 27% of NIS expressing breast cancers had staining for NIS at the plasma membrane (Beyer et al., 2009).

To establish if NIS expression correlated with any genes heavily associated with breast cancer, 14 different genetically engineered mouse models of breast cancer were

investigated. Those that stained strongly for NIS expression included mice expressing the oncogene PyMT, HER2, the hCG subunit and Cox-2 within murine mammary glands. hCG and Cox-2 can induce cAMP whilst PyMT, HER2 and Cox-2 are capable of activating the PI3K pathway (Knostman et al., 2004). Increased levels of cAMP have previously been described to induce NIS expression in the thyroid (Section 1.2.2.2) (Ohno et al., 1999) and PI3K levels have been observed to positively correlate with NIS expression in breast tumours (Knostman et al., 2007). Investigation into the individual pathways in MCF-7 cells showed elevated cAMP levels increased NIS promoter activity and mRNA levels but did not alter radioiodide uptake, whereas PI3K activation increased both expression of NIS protein and radioiodide uptake (Knostman et al., 2004). Further studies revealed that although PI3K activation increases NIS expression, it leads to expression of an underglycosylated form of NIS with disrupted cell surface trafficking (Knostman et al., 2007).

Along with primary breast tumours, the use of radioiodide has been proposed for locating, monitoring and treating metastases. Whilst metastases may not retain NIS expression, with only 33% of metastases having detectable expression in one study (Wapnir et al., 2004), a study of 28 brain metastases from primary breast tumours reported that 75% of the tumours were NIS positive and only 24% of these tumours had plasma membrane staining for NIS (Renier et al., 2010). Of the 21 metastases that had NIS expression, all were ER and PR negative with a mixture of positive and negative HER2 staining. Currently patients with brain metastases have to rely solely on surgery and/or external radiation due to the impermeability of the blood brain barrier to chemotherapy

reagents, so the potential for just under 20% of brain metastases to be treated with radioiodide therapy would be revolutionary (Renier et al., 2010).

1.2.4.1 NIS regulation in breast cancer

As discussed in section 1.2.2.2, NIS expression in the thyroid is under the regulation of TSH; however, TSH has no effect on NIS expression in breast cancer. To be able to exploit NIS for therapeutic use it is important to understand its regulation in breast cells.

As oxytocin and prolactin regulate NIS expression in the lactating breast it was logical to investigate their role in breast cancer. In 3D histocultures of breast tumours, treatment with oxytocin and prolactin individually induced NIS mRNA expression in a dose-dependent manner. However, as within the lactating breast a combination of the two hormones was not capable of further inducing NIS expression (Cho et al., 2000). The majority of breast cancers (50-90%) express the oxytocin receptor (Bussolati et al., 1996; Ito et al., 1996; Sapino et al., 1998) and it is hypothesised that induction of NIS via oxytocin acts in a similar manner to TSH stimulation in thyrocytes. The oxytocin receptor is a G protein-coupled receptor which activates the G_s-cAMP-protein kinase A (PKA) pathway (Olins and Bremel, 1984)(Figure 1-8). Prolactin is known to increase the expression of genes containing γ-interferon activation sequences (GAS) in their promoter regions, through the activation of the Jak2/STAT5 cascade in breast cells (Burdon et al., 1994) (Figure 1-8). A GAS sequence was subsequently identified within the NIS proximal promoter (Cho et al., 2000). Further studies have produced conflicting results in MCF-7 cells, with one failing to identify any induction of NIS expression after prolactin treatment (Kogai et al., 2005), whereas another observed increased NIS mRNA and iodide-trapping post-prolactin treatment (Arturi et al., 2005).

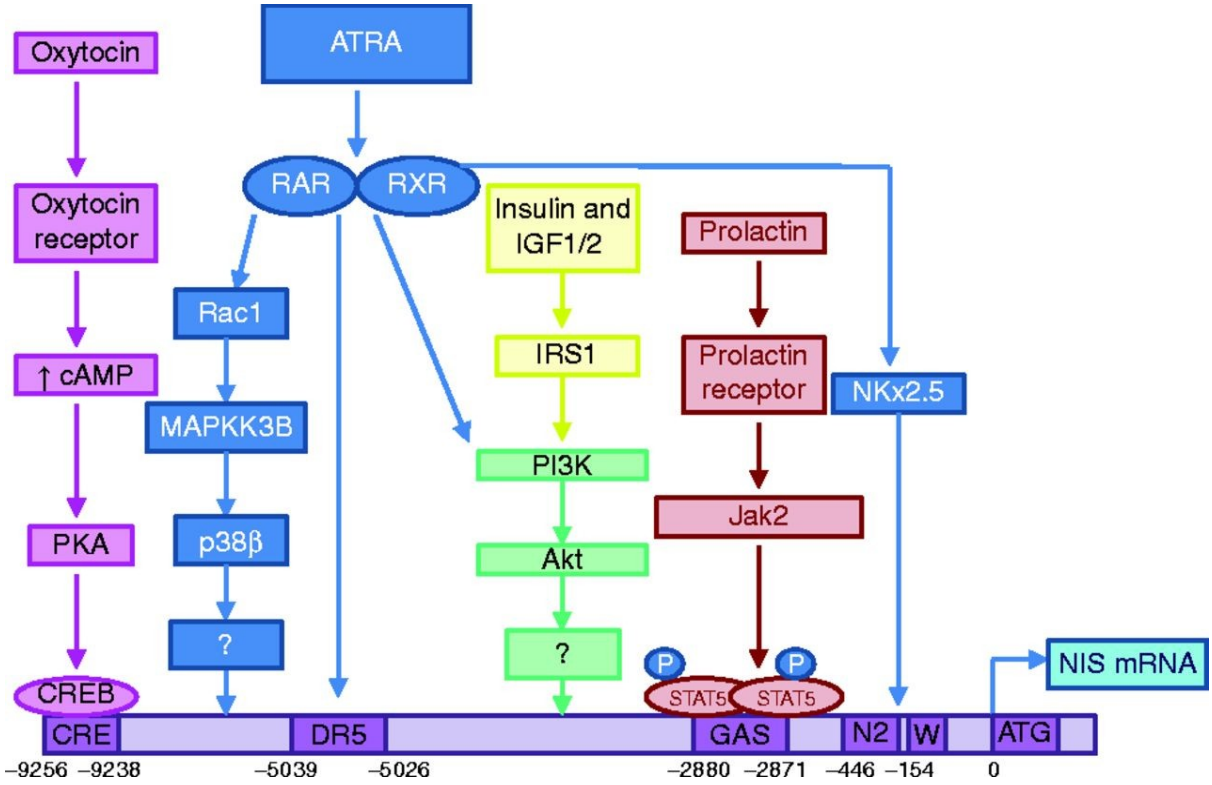

Figure 1-8. NIS transcriptional regulation in breast cancer. A schematic displaying the different mechanisms by which NIS expression can be induced in breast cancer. Akt - Protein kinase B, cAMP - Cyclic adenosine monophosphate, CRB - cAMP response element-binding,GAS - γ-interferon activation sequence, IGF - Insulin-like growth factor, IRS1 - Insulin receptor substrate, JAK - Janus Kinase, MAPKK3B - Mitogen-activated protein kinase Kinase 3B, PI3K - phosphoinositide 3-kinase, PKA - Protein kinase A, RAR - Retinoic acid receptor, RXR - Retinoid X receptor, STAT5 - Signal transducer and activator of transcription 5. Taken from Poole and McCabe, 2015.

Insulin and insulin-like growth factors (IGF) 1/2 have also been implicated in regulating NIS expression in breast cancer. Treatment with insulin and IGF1/2 stimulated both NIS mRNA and protein expression in MCF-7 cells and increased ^{125}I uptake (Arturi et al., 2005). Ligand-activated IGF-1 receptor is known to act on the insulin receptor substrate-1 (IRS-1), which leads to activation of the PI3K pathway (Dupont and Le Roith, 2001) and has previously been associated with NIS expression in breast cancer cells (Section 1.2.4) (Figure 1-8).

Retinoids are well documented to be useful for the treatment of a variety of neoplasms (reviewed in (Connolly et al., 2013)) with the use of systemic retinoids being approved by the FDA for the treatment of cutaneous T cell lymphoma (Duvic et al., 2001) and acute promyelocytic leukaemia (APL) (Tallman et al., 1997). Treatment of MCF-7 cells with all *trans*-retinoic acid (ATRA) increased ^{125}I uptake in a dose-dependent manner that could be inhibited by the potent NIS inhibitor potassium perchlorate, indicating specific NIS-mediated uptake (Kogai et al., 2000). Treatment with ATRA not only increased NIS mRNA and protein expression in MCF-7 cells, it also reduced colony formation in the presence of ^{131}I suggesting radioiodide in combination with ATRA may be a viable breast cancer treatment. MCF-12A cells (derived from normal breast tissue) and ER-negative MDA-MB-231 cells did not display such a marked response to ATRA, with MDA-MB-231 cells only having slight induction of NIS protein expression and neither cell-line displaying altered radioiodide uptake (Kogai et al., 2000). A major disparity between the two cancer cell-lines is that MCF-7 cells are known to express both the retinoic acid receptor (RAR) and retinoid X receptor (RXR) whereas MDA-MB-231 are considered RA 'resistant' due to decreased expression of RARα and RARβ compared with MCF-7 cells (Liu et al., 1996). Further to this, responsiveness to ATRA was later positively correlated with expression of ERα in breast cancer cells, with both ERα and RARα being required for NIS induction (Alotaibi et al., 2006).

To establish whether systemic retinoids would be useful *in vivo*, mice bearing MCF-7 xenograft tumours were assessed for NIS expression and activity. Mice that were treated with an ATRA slow-release pellet for five days prior to treatment with ^{125}I displayed increased NIS expression and accumulated almost 15 times more radioiodide

than control treated mice. In a murine model of breast cancer (murine mammary tumor virus-polyoma virus middle T antigen (MMTV-PyVT)-transgenic mice), treatment with ATRA doubled radioiodide accumulation (Kogai et al., 2004).

Dexamethasone (Dex) has been identified to synergistically increase both NIS expression and radioiodide uptake when used in conjunction with ATRA in MCF-7 cells. Dex treatment alone only slightly induced NIS mRNA levels, but when used in combination with ATRA there was a ~70-fold increase in NIS mRNA. Additionally, Dex was observed to increase the stability of NIS mRNA (Kogai et al., 2005). Further studies confirmed the synergistic effect of ATRA and Dex with MCF-7 cells treated with the combination displaying reduced cell survival compared with cells treated with ATRA alone after treatment with ^{131}I (Unterholzner et al., 2006).

In cells, ATRA and other retinoids bind to RAR which leads to homodimerisation or heterodimerisation with RXR. These heterodimers then go on to bind to retinoic acid response elements (RAREs) on target genes stimulating transcription (Figure 1-8). Although the NIS promoter in MCF-7 cells does not contain any putative full RAREs, it does contain several DR-2 element sequences with typical half-sites between the first and thirteenth intron. Initial studies identified these DR-2 sites to be unresponsive to ATRA (Kogai et al., 2008), although a subsequent study reported binding of RARα to the intronic DR-2 elements 30 minutes after MCF-7 cells were treated with ATRA (Alotaibi et al., 2010), suggesting a potential role in NIS induction (Kogai and Brent, 2012). A DR-5 element located within in promoter region of NIS was discovered to be responsive to ATRA in MCF-7 cells (Kogai et al., 2008) (Figure 1-8). Although these half-sites have been reported to be active in human cells *in vitro*, introns of murine NIS do not contain DR-2 or

DR-5 elements yet ATRA is still capable of inducing NIS expression in transgenic mice models (Kogai et al., 2004), suggesting non-traditional mechanisms of transduction may be apparent.

Following treatment with ATRA, a homeobox protein, Nkx-2.5 is induced in MCF-7 cells (Figure 1-8) (Dentice et al., 2004). It has been suggested that Nkx-2.5 is crucial for the induction of NIS with ATRA since mutations in Nkx-2.5 significantly reduce radioiodide uptake (Dentice et al., 2004). To further identify proteins involved in ATRA's induction of NIS expression, a range of inhibitors were utilised to identify critical pathways. Among the proteins identified to be important were the IGF receptor, PI3K, AKT and p38 mitogen-activated protein kinase (MAPK) (Kogai et al., 2008). It is well documented that natural retinoids can stimulate IGF receptors (Kang et al., 1997) and that activated RAR/RXR heterodimers can interact with IRS-1 (del Rincon et al., 2003). It is also hypothesised that activated heterodimers interact with IRS-1, which leads to activation of the PI3K pathway inducing NIS expression (Kogai et al., 2008) (Figure 1-8). A subunit of PI3K, p85, has also been observed to directly interact with activated RAR/RXR heterodimers with inhibition and silencing of the p85 subunit resulting in reduced NIS expression after ATRA treatment (Ohashi et al., 2009).

The MAPK signalling pathway has also been associated with ATRA's induction of NIS with activated RAR/RXR heterodimers being observed to stimulate the p38-Rac1 pathway (Alsayed et al., 2001) (Figure 1-8). Inhibition of p38 reduced both basal NIS expression and induction after ATRA treatment in MCF-7 cells (Kogai et al., 2008). Silencing and inhibition of Rac1, MAPK kinase 3B (MAPKK3B) and p38β revealed all three were critical for full induction of NIS by ATRA in MCF-7 cells. It has been hypothesised

that in breast cancer cells, ATRA activated RAR/RXR heterodimers interact with the small GTPase Rac-1 resulting in MAPKK3B phosphorylation of p38. The phosphorylation of p38 leads to the induction of NIS transcription through unknown factors (Kogai et al., 2012) (Figure 1-8).

Although prolactin, oxytocin and ATRA can be utilised to boost endogenous NIS expression within breast cancer cells, their mechanisms of action are not fully elucidated and the complications of systemic treatment, such as toxicity, still exist. Thus, there have been multiple efforts to increase NIS levels and radioiodide uptake using exogenous NIS.

1.2.4.2 NIS gene therapy in breast cancer

There have been several methods utilised in attempts to exogenously boost NIS expression, including retro-, adeno- and oncolytic-viral expression. The first technique employed to exogenously express NIS was retroviral delivery with ^{131}I uptake being sufficient to kill murine and human tumour cells in xenograft models (Mandell et al., 1999). To establish whether pre-existing tumours could benefit from exogenous expression of NIS, murine xenograft MCF-7 and SiHa (cells originating from a cervical carcinoma) tumours were directly injected with NIS adenovirus. Directly injected tumours were capable of accumulating 25 times more radioiodide than their control counterparts. However, there was no difference in tumour size between control and NIS transduced cells after treatment with ^{131}I. It was hypothesised that this disparity between uptake and cell death was due to the length of time that cells retain radioiodide being too short to sufficiently inhibit cell growth and ablate tumour cells (Boland et al., 2000). In adenovirally-transduced MCF-7 cells with NIS under the expression of the CMV promoter, retinoic acid was capable of further increasing radioiodide uptake in a similar manner to

cells endogenously expressing NIS (Lim et al., 2007). The CMV promoter is known to contain RAREs within its sequence (Angulo et al., 1996) which can be bound by activated endogenous RAR/RXRs (Titcomb et al., 1994).

Another approach to increasing NIS expression is to exogenously express NIS within cells under the control of cell-type specific promoters. In a prostate cancer study, LNCaP prostate cancer cells were stably transfected with NIS under the regulation of the prostate-specific antigen (PSA) promoter and used to generate xenograft models. After an intraperitoneal (IP) injection of 3 mCi ^{131}I, there was a significant reduction in tumour size compared with control tumours (Spitzweg et al., 2000). Similar to PSA, in breast cancer cells the MUC1 promoter has also been investigated. MUC1, a glycoprotein usually found in haematopoietic cells, is expressed in approximately 90% of breast cancers and is associated with poor survival and increased metastasis (Gendler, 2001). In MUC1-positive breast cancer T47D cells, adenoviral transduction of NIS led to a 58-fold increase in radioiodide uptake. In comparison, MDA-MB-231 cells that are MUC1-negative displayed no increase in radioiodide uptake after transduction. Studies *in vivo* using T47D murine xenograft tumours that were injected at multiple sites with adenoviral NIS under the MUC1 promoter displayed an 83% reduction in tumour size after IP treatment with ^{131}I, while tumours injected with control adenovirus continued to increase in size (Dwyer et al., 2005). The oestrogen receptor promoter and the human telomerase reverse transcriptase promoter have also been successfully used in breast cancer cells resulting in increased ^{131}I uptake and inhibited tumour growth after adenoviral transduction of NIS (Riesco-Eizaguirre et al., 2011).

Oncolytic viruses have also been employed as a method to deliver NIS to tumour cells. Murine xenograft tumours that were injected with GLV-h153, an oncolytic vaccinia virus carrying human NIS, had increased visualisation with ^{124}I compared with control tumours. Further to this, virally injected tumours displayed a significant reduction in tumour growth after treatment with ^{131}I (Gholami et al., 2014).

Although NIS gene therapy appears effective, an efficient and optimal method of delivery of the gene to the tumour site has not yet been established. Superparamagnetic iron oxide (SPIO)-labelled AC133+ progenitor cells (APCs) that had been adenovirally-transduced with human NIS increased ^{99m}Tc uptake in mice with MDA-MB-231 xenograft tumours. MRI and single photon emission computer tomography (SPECT) showed that although the labelled APCs had been injected intravenously, there was a large accumulation of the cells at the site of the tumour (Rad et al., 2009). Due to the fact that mesenchymal stem cells (MSCs) have been well-documented to migrate to tumour sites *in vivo*, they have been hypothesised to be an efficient delivery mechanism for gene therapy (Dwyer et al., 2010; Spaeth et al., 2008). Intravenous injection of MSCs adenovirally-transduced with NIS increased the levels of ^{99m}Tc detected at the site of the MDA-MB-231 murine xenograft tumours using SPECT. Not only did this form of delivery increase the levels of ^{99m}Tc detected, there was also an increase in retention with ^{99m}Tc remaining detectable at the tumour site after 14 days. Expression of NIS was confirmed within tumour cells and compared with control mice there was a significant reduction in tumour size after treatment with ^{131}I (Dwyer et al., 2011).

1.2.5 Binding partners of NIS

Only three putative binding partners of NIS have been reported; pituitary tumor-transforming gene (PTTG)-binding factor (PBF) (Smith et al., 2009) (discussed in 1.4), heat-shock protein 90 (HSP90) (Marsee et al., 2004) and leukemia-associated RhoA guanine exchange factor (LARG) (Lacoste et al., 2012).

HSP90 was initially identified as a novel RET/PTC1-interacting protein, a rearranged form of the RET tyrosine kinase seen in 10-20% of papillary thyroid cancers. It has been observed to indirectly associate with NIS, with inhibition of hsp90 resulting in an increase in radioiodide uptake with NIS expression levels remaining unchanged. It has been hypothesised that hsp90 may function as a chaperone protein for NIS (Marsee et al., 2004).

LARG is a guanine nucleotide exchange factor for the RhoA GTPase that has been implicated in many cellular roles including cell adhesion and reorganisation of the cytoskeleton. LARG is capable of binding NIS directly through its N-terminal PDZ domain in multiple cancer cell-lines, including breast. The interaction between LARG and NIS leads to the activation of RhoA, which facilitates cell migration and invasion. The interaction between NIS and LARG was found to occur intracellularly, suggesting that the aberrant localisation of NIS within cancer cells may increase migration of these cells. This correlates with the observation that NIS is localised at the leading edge of metastatic breast cancer cells (Lacoste et al., 2012).

1.3 Pituitary Tumor-Transforming Gene-Binding Factor (PBF)

1.3.1 Structure

The pituitary tumor-transforming gene-binding factor, hereafter referred to as PBF (also known as PTTG1IP) gene is located on chromosome 21 at 21q22.3. The human PBF gene consists of 6 exons spanning 24kb and encodes a 180 amino acid protein with a predicted molecular mass of 22kDa (Chien and Pei, 2000). Although PBF shares no significant homology with other human proteins, it is highly conserved among a range of species (73% homology to mouse, 60% to chicken and 52% to zebrafish) (Yaspo et al., 1998) implying it has evolutionary importance.

Initial protein prediction studies suggested that PBF was a cell surface glycoprotein due to the presence of a potential *N*-terminal signal peptide, a transmembrane domain and an endocytosis motif (Yaspo et al., 1998). The presence of a plexin-semaphorin-integrin (PSI) domain between residues 40 - 95 supports the theory that PBF is a cell surface protein as PSI domains are usually located extracellularly, being involved in cellular signalling and protein-protein interaction (Bork et al., 1999). However the presence of a bipartite nuclear localisation signal (Chien and Pei, 2000) and the detection of a nucleolus signal and nuclear export signal using appropriate prediction software (La Cour et al., 2004; Scott et al., 2010) suggest that PBF may also have a role in the nucleus/nucleolus.

PBF is a poorly studied protein but is predicted to contain sites for post-translational modifications such as phosphorylation, SUMOylation and *N*- and *O*-

glycosylation (Chien and Pei, 2000). Phosphorylation prediction software identified Y174 as a phosphotyrosine site (discussed in 1.4.3) with S85, S126, S132 and T10 as potential phosphoserine/threonine sites (Figure 1-9). Small Ubiquitin-Like Modifier (SUMO) proteins covalently bind to many proteins altering their cellular function; prediction software (Zhao et al., 2014) has located the presence of a potential SUMOylation site at lysine 169 (Figure 1-9). PBF contains five potential glycosylation sites for *N*-linked and *O*-linked oligosaccharides (Chien and Pei, 2000) with asparagine residues 45 and 54 both fulfilling criteria for *N*-terminal glycosylation (Rao and Bernd, 2010) (Figure 1-9).

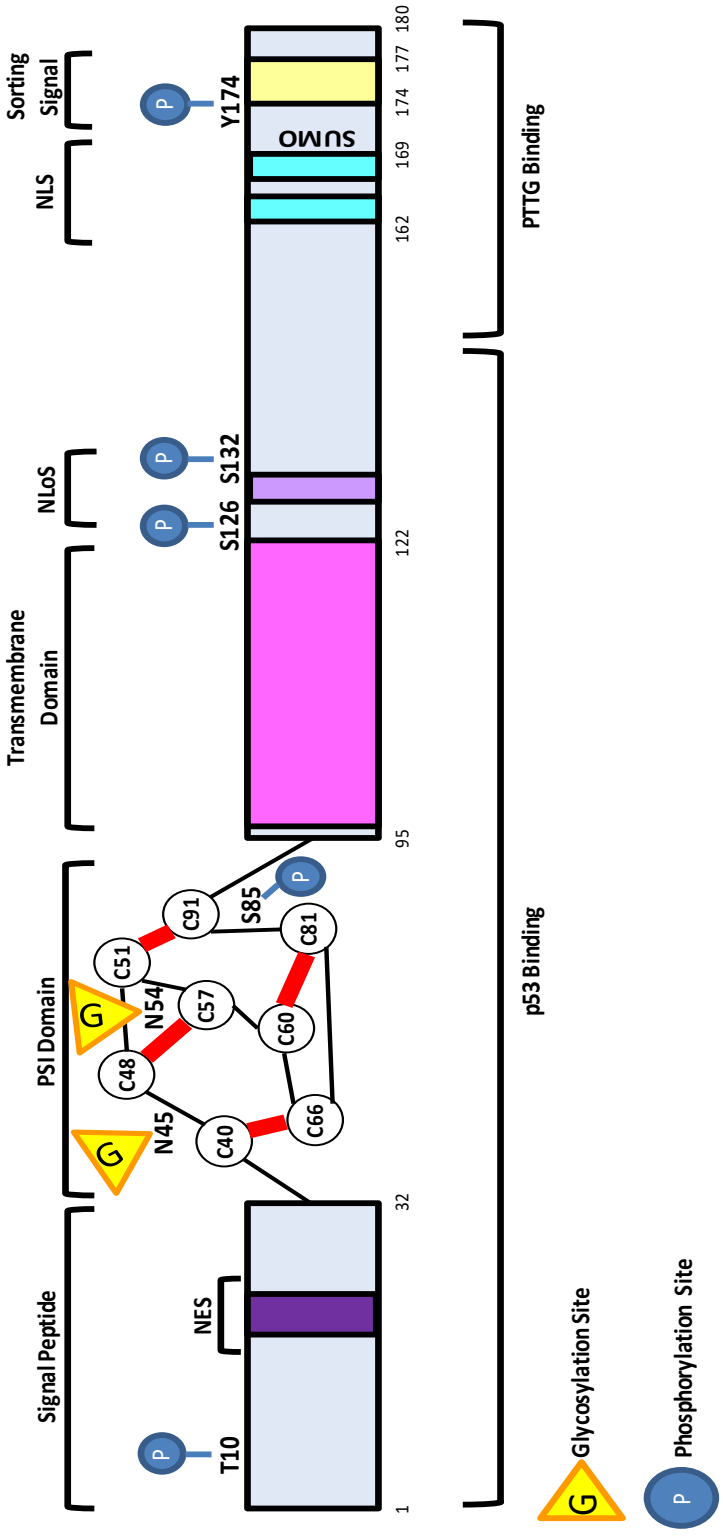

Figure 1-9. A schematic diagram of the structure of PBF. PBF contains a putative N-terminal signal peptide, a PSI domain, a transmembrane domain and an intracellular C-terminal region. The PSI domain is cysteine rich containing multiple disulphide bonds represented by red lines. The C-terminal region contains a nuclear localisation signal (NLS) and a tyrosine based sorting signal. P represents a phosphorylation site and G a glycosylation site.NES = nuclear export signal, NLoS = nucleolar localisation signal.

1.3.2 PBF Expression

PBF is ubiquitously expressed in normal tissues, with Northern blot analysis revealing PBF mRNA expression in tissues such as the stomach, spleen, testis, colon and thyroid (Chien and Pei, 2000; Stratford et al., 2005; Yaspo et al., 1998). PBF was first implicated in tumourigenesis when it was found to be overexpressed in pituitary tumours compared with normal pituitary tissue (McCabe et al., 2003). Subsequently the upregulation of PBF mRNA and protein was detected in well-differentiated thyroid carcinomas, including papillary thyroid cancer (PTC) and follicular thyroid carcinoma (FTC), with a significant association with early tumour recurrence (Stratford et al., 2005). Further investigations have observed PBF upregulation in a wide array of cancers including colon (Read et al., 2014b) and breast (Watkins et al., 2010).

1.3.3 PBF Identification and Interaction with PTTG

PBF was first identified through its interaction with pituitary tumor-transforming gene (PTTG)(Chien and Pei, 2000). PTTG is a multifunctional human securin that has roles in cell transformation (Pei and Melmed, 1997), control of mitosis (Zou et al., 1999), DNA repair (Romero et al., 2001), gene regulation (Zhang et al., 1999b) and foetal development (Boelaert et al., 2003). First identified due to its high expression in pituitary tumours compared with normal pituitary tissue (Pei and Melmed, 1997), PTTG has since been reported to be overexpressed in a variety of tumours, such as thyroid (Heaney et al., 2001), breast (Solbach et al., 2004) and colorectal (Heaney et al., 2000) cancer, where high expression correlates with poor prognosis (Heaney et al., 2000; McCabe et al., 2003; Zhang et al., 1999a). The PTTG protein is comprised of 202 amino acids and has been

demonstrated to have potent transforming ability both *in vitro* and *in vivo* (Pei and Melmed, 1997).

The interaction between PBF and PTTG was identified through a yeast two-hybrid screen with binding confirmed using GST-pulldown (Chien and Pei, 2000). Deletion studies have shown that the 30 C-terminal amino acids of PBF interact with PTTG within a domain located between amino acids 123 and 154. PBF facilitates the translocation of PTTG into the nucleus and is required for PTTG activation of fibroblast growth factor 2 (FGF-2) (Chien and Pei, 2000). Subsequently levels of PTTG and PBF were found to correlate in pituitary adenomas (McCabe et al., 2003) and thyroid carcinomas (Stratford et al., 2005). Overexpression of PTTG was observed to increase PBF mRNA expression *in vitro* (Stratford et al., 2005) although neither EGFR nor TGF-α affected PBF expression despite causing an increase in PTTG levels (Vlotides et al., 2006).

Recently a bitransgenic mouse model has been created with thyroid-specific expression of PTTG and PBF (Bi-Tg). Phenotypically Bi-Tg mice displayed enlarged thyroids and an increased number of hyperplastic lesions compared with wild-type (WT), PBF-Tg and PTTG-Tg mice. The expression of both PBF and PTTG led to genetic instability and the induction of the tumour suppressor protein p53. Approximately 30 genes involved with DNA damage repair were also downregulated compared with WT mice. These findings suggest that both PBF and PTTG may accelerate cancer initiation and progression with fundamental roles in interrupting DNA damage pathways and increasing genetic instability (Read et al., 2016).

1.3.4 PBF in thyroid cancer

Thus far, PBF has primarily been studied within the context of thyroid cancer, with PBF mRNA expression being 3.3-fold higher in a cohort of differentiated thyroid cancers compared with normal thyroid tissue. Within this disease PBF upregulation has been correlated with unfavourable clinical parameters such as age, early recurrence, distant metastases at diagnosis, tumour multicentricity, tumour, node, and metastasis (TNM) stage and disease-specific mortality (Figure 1-10)(Hsueh et al., 2013; Stratford et al., 2005).

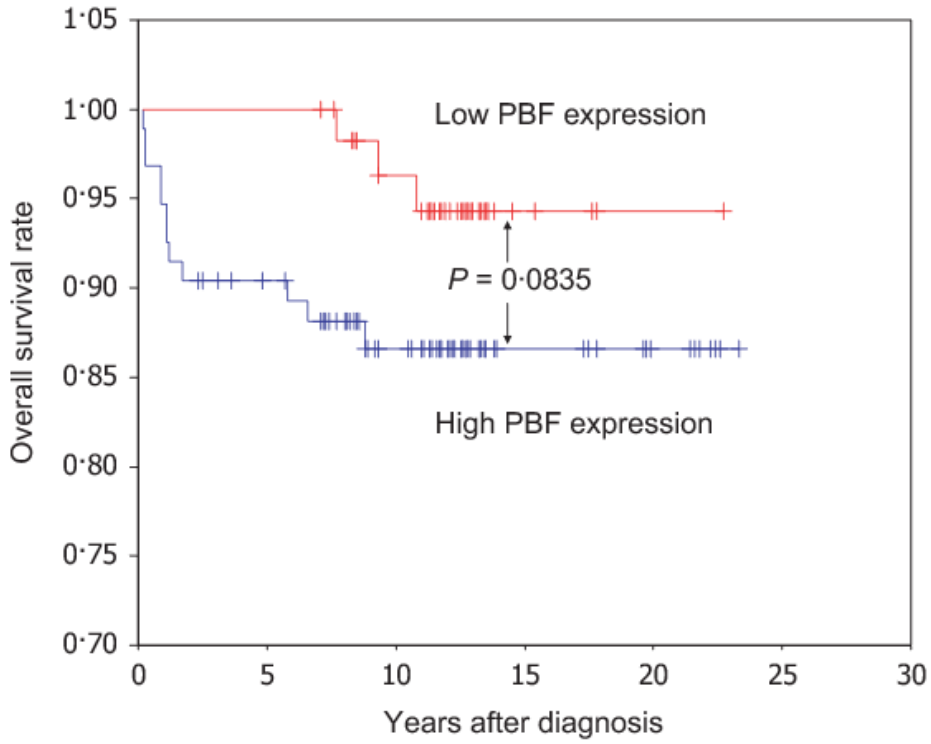

Figure 1-10. PBF overexpression is associated with disease-specific mortality. There is a significant association between high PBF expression and decreased disease specific survival rates by Kaplan–Meier analysis (P=0.0835). Taken from Hsueh et al. 2013.

Though PBF upregulation is associated with thyroid cancer, no mutations in PBF have so far been identified within thyroid cancers. The entire coding region of PBF was

initially sequenced in 24 thyroid tumours and no mutations were detected (Stratford et al., 2005). Subsequently, no PBF mutations were reported in the 507 papillary thyroid tumours that were sequenced as part of The Cancer Genome Atlas (TCGA) study (TCGA, 2016). Similar large-scale sequencing studies have identified 27 PBF mutations in a variety of other human cancers, with 18 missense substitutions, 5 synonymous substitutions, 2 in-frame deletions and 2 in-frame insertions. However, the detection of PBF mutations in only 27 out of the 29,052 tumour samples sequenced to date suggests that it is a very rare event (COSMIC Database, 2016a).

PBF has been observed to have transforming ability both *in vitro* and *in vivo*. In a fibroblast cell line (NIH3T3) stably transfected with PBF, there was a 12-fold increase in colony formation compared with vector-only transfected cells. These stably expressing cell lines were subsequently injected into nude mice. Mice injected with the PBF over-expressing cells developed aggressive high grade invasive carcinomas (Stratford et al., 2005).

To further investigate the specific role of PBF in thyroid disease, a transgenic mouse model was generated. These mice overexpressed hemagglutinin (HA) tagged PBF (PBF-HA) specifically in the thyroid gland (PBF-Tg mice). To ensure that PBF expression was achieved only within the thyroid, PBF was inserted under the control of the thyroglobulin promoter. Although there was no tumour induction in mice aged up to 18 months, all PBF-Tg mice had significantly enlarged thyroids compared with their WT counterparts. PBF-Tg thyroid glands were 1.7 times heavier by 7 weeks and 3.2 times heavier by 52 weeks compared with WT littermates. The enlarged thyroids had significantly increased numbers of macrofollicular and hyperplastic lesions suggesting PBF

upregulation affects the structural development of the thyroid. PBF-Tg mice also displayed altered thyroid hormone secretion with increased intra-thyroidal T_3 and T_4 levels compared with WT mice (Smith et al., 2012). Within PBF-Tg thyroids, there was increased expression of phosphorylated AKT (p-AKT), cyclin D1 and thyroid-stimulating hormone receptor (TSHR) (Read et al., 2011).

PBF has recently been discovered to have roles in DNA damage repair and genetic instability, and has been identified to be a negative regulator of the tumour suppressor protein p53 in both thyroid (Read et al., 2014a) and colorectal cancer (Read et al., 2014b). PBF has also been observed to interact with the DNA repair enzyme ATR, suggesting PBF may have an impact on p53-independent DNA damage repair mechanisms (unpublished observations from the McCabe Group, Birmingham, UK).

1.3.5 PBF in breast cancer

Though PBF has mainly been studied in the context of thyroid disease, there is an interest in PBF within the breast cancer field. Whereas PBF is minimally expressed within normal breast tissue it has been found to be strongly expressed in breast tumours. In a study of 6 normal breast specimens and 20 TMA specimens, PBF mRNA was not detected in any of the normal samples whereas in 18 breast cancer specimens PBF was detected with a mean ΔCt of ~8 to 10 (Watkins et al., 2010) (Figure 1-11A). Immunohistochemistry confirmed that normal breast samples had absent or low expression of PBF protein in contrast to strong expression in epithelial cells of all tumour types and grades of breast cancer assessed (Watkins et al., 2010) (Figure 1-11B). Though PBF expression was strong in all tumour types, there was a particularly significant correlation between ERα and PBF

expression (Watkins et al., 2010). An independent study with a larger cohort later confirmed the correlation between PBF and ER expression (Xiang et al., 2012).

This correlation between PBF and ERα sparked further investigation into their relationship. PBF was observed to be regulated by oestrogen with PBF mRNA and protein expression being induced in ERα-positive MCF-7 breast cancer cells after 48 hour treatment with diethylstilbestrol and 17β-estradiol (Watkins et al., 2010). Analysis of the human PBF promoter revealed that the region from -399 to -292 relative to the start codon was replete with putative ERE. This polymorphic region contains a variable number of tandem repeats of an 18-nucleotide sequence housing an ERE half-site (gcccctcGGTCAcgcctc). A greater number of repeats in the promoter correlated with higher levels of PBF mRNA in breast specimens. Of three normal tissues successfully analysed all were homozygous for three repeats whereas the 27 tumour samples successfully analysed were either homozygous for three repeats or heterozygous for three and five repeats. These EREs were found to be oestrogen-responsive with ERα directly binding to the promoter region of PBF (Watkins et al., 2010).

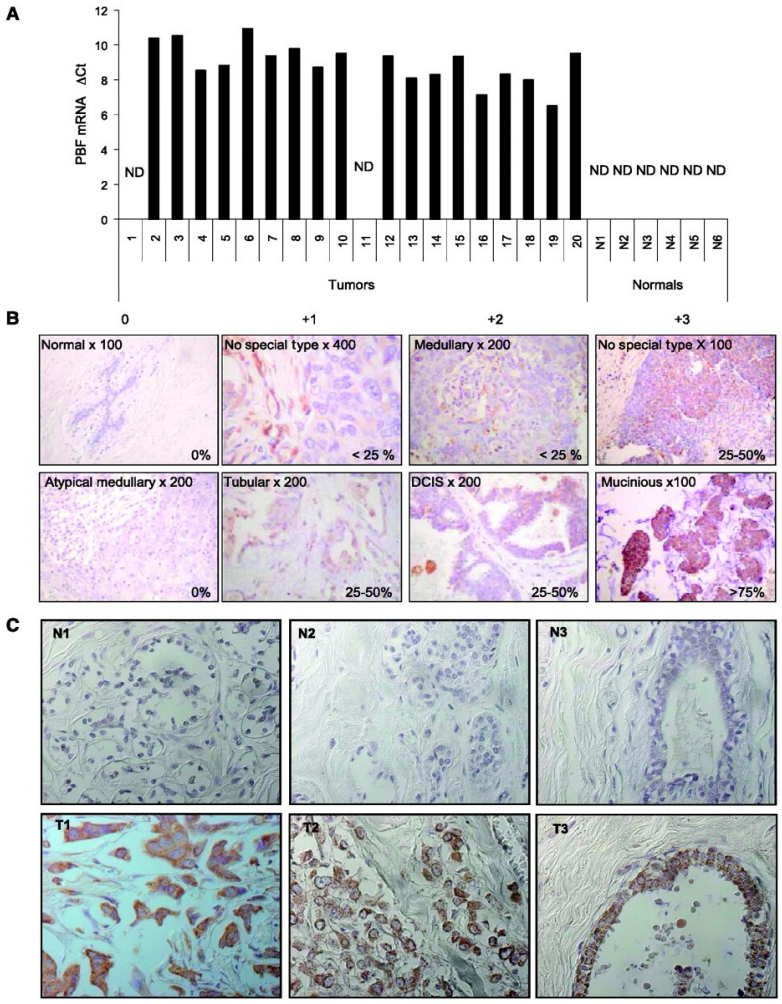

Figure 1-11. Expression of PBF in normal and cancerous breast tissue. (A) Expression of PBF mRNA relative to 18s mRNA (ΔCt values) in 20 TMA samples of breast tumours compared with normal breast. ND, not detected after 40 cycles of PCR. (B) Representative immunohistochemical examination of PBF staining in one normal breast sample and seven tumour samples from TMA sections. Columns 1 to 4 represent the different staining intensities observed from 0 (absent) to +3 (intense). Values in the bottom right-hand corners indicate the percentage of PBF expression observed in the whole section, with original magnifications annotated next to tumour type. (C) Representative immunohistochemical examination of PBF staining in three normal breast samples (N1–N3; US BioMax; ×40 original magnification) and three tumour samples from TMA sections. T1, Grade I; T2, Grade II; T3, Grade III; all ×40 original magnification. Taken from Watkins et al.2010.

The exact function of PBF within cell transformation and breast cancer is yet to be elucidated, although it has been observed to increase cell invasion in MCF-7 cells. MCF-7 cells transfected with PBF displayed a 2.5-fold increase in cell invasion compared with

empty vector transfected cells *in vitro* (Watkins et al., 2010). Though treatment with oestrogen is well-documented to induce invasion in MCF-7 cells (Thompson et al., 1988), it was unable to do so in cells lacking PBF expression suggesting that PBF plays a role in mediating the induction of invasion by oestrogen (Watkins et al., 2010). PBF was subsequently found to be a secreted protein, with mutational studies confirming the need for PBF to be secreted to induce cell invasion (Watkins et al., 2010).

1.3.6 PBF and Cell Motility

Tandem mass spectrometry identified cortactin as a putative binding partner of PBF (Watkins et al., 2016). Cortactin is a scaffold protein that is essential to the assembly of individual actin filaments into branched structures, thus having a major influence on the ability of cells to migrate and invade. Overexpression of cortactin has been associated with increased cellular motility and invasion (Kirkbride et al., 2011).

PBF and cortactin were confirmed to bind *in vitro* with PBF further increasing the ability of cortactin-expressing cells to migrate and invade. PBF and cortactin were shown to co-localise within invading cells in both invadopodia actin puncta and surrounding podosome-like adhesion rings. Knockdown of PBF decreased the ability of cortactin to induce cell invasion and migration. Further to this, abrogation of PBF phosphorylation at Y174 also decreased cell migration and disrupted the binding affinity of PBF and cortactin (Watkins et al., 2016). With PBF and cortactin both being dysregulated in multiple tumour types, PBF may be a potential target for decreasing tumour metastasis through inhibition of its interaction with cortactin.

1.4 PBF and NIS

As briefly mentioned earlier, PBF and NIS can interact within thyroid carcinoma cells with PBF being shown to potently repress iodide uptake. Primary cells originating from the thyroids of PBF-Tg mice (discussed in 1.3.4) were assessed for their ability to take up radioiodide compared with cells from WT mice. Thyroid cells from PBF-Tg were capable of approximately 70% less radioiodide uptake compared with their WT mice counterparts. Use of siRNAs targeting PBF rescued radioiodide uptake in cells from PBF-Tg mice. These findings were subsequently confirmed in human primary thyrocytes where endogenous PBF knockdown increased radioiodide uptake (Read et al., 2011). There are two known mechanisms for PBF's repression of NIS: transcriptional and post-translational.

1.4.1 PBF repression of NIS transcription

In vitro overexpression of PBF in primary human thyrocytes decreased NIS mRNA expression by 95% (Boelaert et al., 2007). PBF was observed to repress NIS mRNA expression through interactions with both the NIS proximal promoter and the NUE in FRTL-5 cells. Further investigation in primary human thyrocytes confirmed PBF repression of NIS through the NUE, although proximal promoter activity was unaffected by the presence of PBF. Mutational studies revealed that PBF's repression of the NUE relies on the presence of an upstream stimulating factor 1 (USF1)-binding site (Boelaert et al., 2007) located within the PAX8 consensus sequence in the NUE (Lin et al., 2004). Specific deletion of the PAX8 site while maintaining the USF1 site also prevented PBF repression of NIS and even resulted in a 28% increase in NUE activity (Boelaert et al., 2007).

Knockdown of PBF also increased NIS mRNA expression in the human primary thyrocytes (Read et al., 2011).

1.4.2 Effect of PBF on NIS subcellular localisation

Along with influencing NIS expression, PBF can modulate the subcellular localisation of NIS. PBF and NIS have been shown to co-localise in FRTL-5 and COS-7 cells, particularly within intracellular vesicles (Smith et al., 2009). GST-pulldown and coimmunoprecipitation experiments confirmed that NIS and PBF bind *in vitro* (Figure 1-12A). Immunofluorescence studies revealed that not only did PBF and NIS co-localise, PBF overexpression was able to alter the subcellular localisation of NIS (Figure 1-12B). Exogenous NIS localised predominantly at the plasma membrane with partial staining in intracellular vesicles (Figure 1-12B(i)). However when PBF was co-transfected into cells alongside NIS, there was increased NIS staining within vesicles and a reduction in plasma membrane staining (Figure 1-12B(ii)). Cell surface biotinylation studies confirmed a reduction of plasma membrane NIS in the presence of PBF overexpression. Within intracellular vesicles PBF and NIS both co-localised with CD63 (Smith et al., 2009), a tetraspanin with known links to clathrin-dependent trafficking (Berditchevski and Odintsova, 2007), having a similar staining pattern to late endosomes. This reduction in plasma membrane NIS correlated with a reduction in radioiodide uptake *in vitro*. Mutational studies revealed the 30 C-terminal amino acids of PBF were important for its interaction with NIS and localisation within clathrin-coated vesicles (Smith et al., 2009). In a similar manner, PBF modulates the subcellular localisation of monocarboxylate transporter 8 (MCT8) impacting on thyroid hormone transport (Smith et al., 2012).

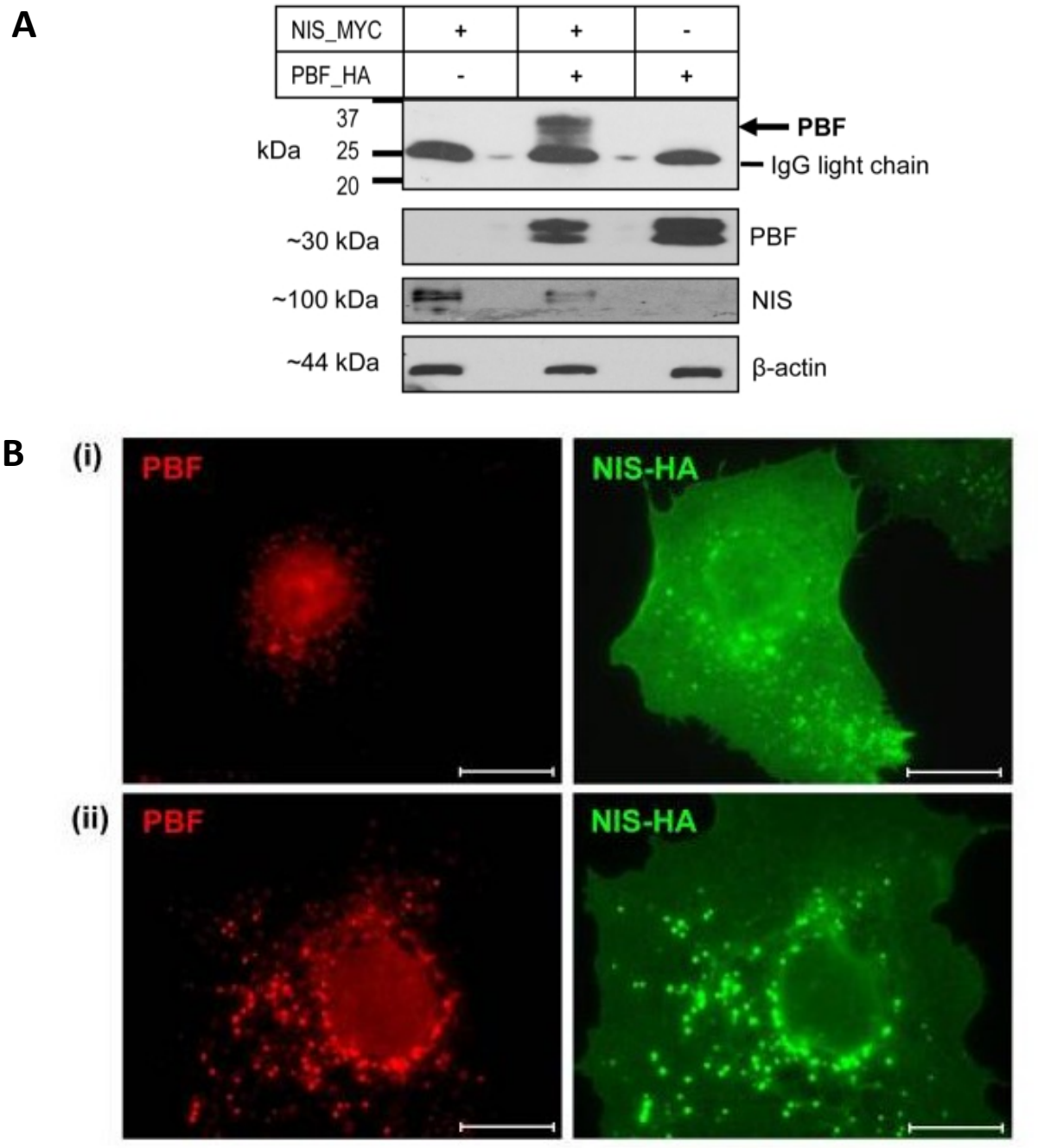

Figure 1-12. PBF binds to and alters the subcellular localisation of NIS. (A) Coimmunoprecipitation assays in COS-7 cells transfected with NIS-MYC and empty vector (VO), PBF-HA and empty vector (VO), or NIS-MYC and PBF-HA. A band corresponding to PBF (arrowed) was observed at approximately 30 kDa when NIS-MYC and PBF-HA were cotransfected. Total cell lysate was assessed for expression of NIS-MYC, PBF-HA and β-actin in each sample. (B) (i) Immunofluorescent detection of NIS-HA and endogenous PBF in cells transfected with NIS-HA and empty vector (VO) control. (ii) Immunofluorescent detection of exogenous NIS-HA and PBF. Scale bars: 20 µM. Taken from Smith et al., 2009.

1.4.3 Discovery and Importance of pY174 PBF

PBF contains a tyrosine-based sorting signal between Y174-F177 (Smith et al., 2013), with the amino acid sequence obeying the YXXΦ motif (Y for tyrosine, X for any residue and Φ for a large hydrophobic residue) witnessed in many endocytosed proteins (Bonifacino and Dell'Angelica, 1999). The lead tyrosine in PBF's motif (Y174) was predicted to be phosphorylated, thus it was proposed that phosphorylation of this residue may regulate PBF localisation. The use of an antibody specific to pY174 PBF confirmed that the residue was phosphorylated, with a Y174A mutant form of PBF not being detected by the antibody (Smith et al., 2013). pY174 PBF was observed to co-localise with NIS in a variety of cell-lines, primarily at the plasma membrane with some intracellular staining. The Y174A PBF mutant was retained in the plasma membrane of cells and did not colocalise intracellularly with NIS. Co-immunopreciptation assays confirmed reduced binding between NIS and Y174A PBF.

Tandem mass spectrometry was used in multiple cell-lines to elucidate tyrosine kinases that might be responsible for phosphorylating PBF. Several members of the Src Family Kinase (SFK) family including Lyn (data not published) and Src were identified (Smith et al., 2013). Binding between PBF and Src was confirmed in HeLa cells with exogenous expression of Src increasing pY174 PBF levels without altering total PBF levels in several thyroid cell-lines. Treatment with PP1, a potent SFK inhibitor (discussed in 5.1.2.1), decreased pY174 PBF levels *in vitro* in both transformed thyroid cell-lines and primary human thyrocytes (Figure 1-13A). PP1 treatment decreased the interaction between PBF and NIS as determined by proximity ligation assays (PLA) and restored PBF's repression of radioiodide uptake in TPC-1 cells and primary thyrocytes (Figure 1-13B).

These findings are significant as they suggest that the interaction between NIS and PBF in thyroid cancer is reliant on the phosphorylation of PBF at Y174 (Smith et al., 2013).

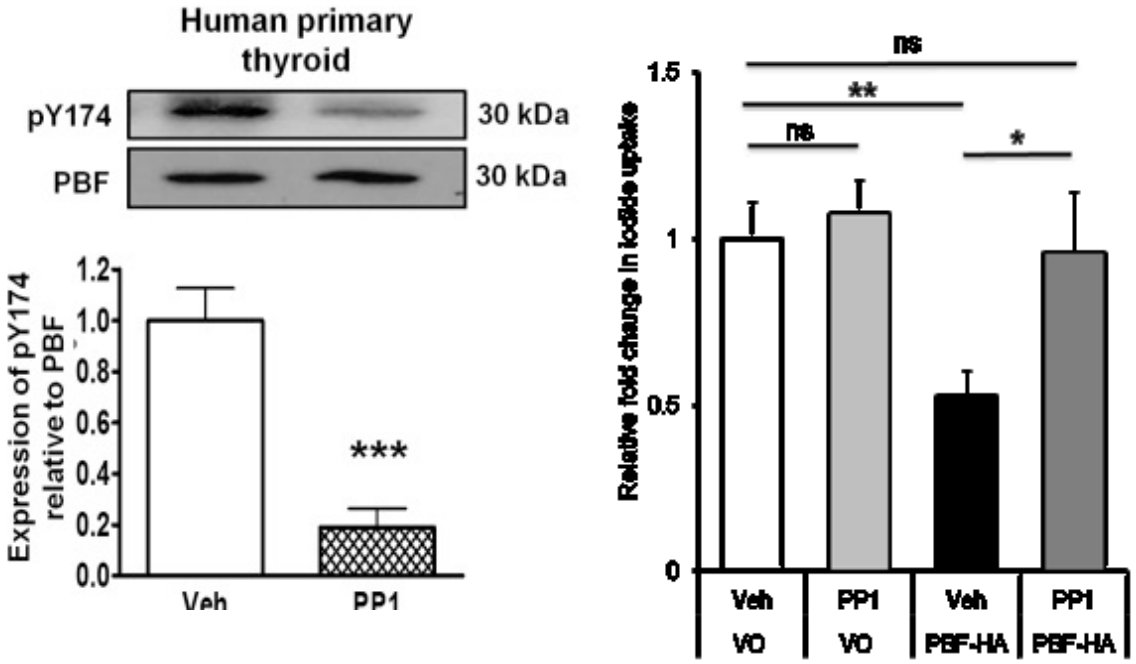

*Figure 1-13. PP1 inhibits PBF phosphorylation and restores radioiodide uptake in primary thyrocytes. (A) Endogenous pY174 PBF in human primary thyroid cultures treated with 2 µM PP1 for 30 minutes. (B) Human primary thyroid cells were transfected with empty vector (VO) or PBF-HA and treated with vehicle (Veh = DMSO) or PP1 (2 µM) for 24 hours prior to the measurement of ^{125}I uptake. ns = not significant.***=p <0 .001. **= p <0 .01. *=p <0.05.Taken from Smith et al., 2013.*

1.5 Hypothesis and Aims

Radioiodide therapy is a central treatment for patients diagnosed with thyroid cancer. However, many differentiated tumours are challenging to treat due to their decreased NIS expression and functionality. Patients affected by this reduction often have poorer outcomes than patients for whom the treatment is effective. PBF is overexpressed in many thyroid cancers repressing radioiodide uptake via transcriptional and post-translational mechanisms. PBF is capable of binding to and altering the subcellular

localisation of NIS, rendering the transporter inactive due to its aberrant localisation. The phosphorylation of PBF at Y174 is critical for this interaction between NIS and PBF with abrogation of phosphorylation restoring radioiodide uptake in thyroid cancer cells.

With NIS expression being upregulated in around 80% of breast cancers, it has widely been hypothesised that radioiodide therapy may be an effective treatment for many breast cancer patients. However, in a similar manner to thyroid cancer, NIS is aberrantly localised intracellularly rather than at the plasma membrane. With PBF also known to be upregulated in breast cancer, the hypothesis of this thesis is that PBF represses radioiodide uptake in breast cancer by altering the subcellular localisation of NIS in a similar manner to that observed in thyroid cancer. Further to this, it is proposed that Src-mediated phosphorylation of PBF at Y174 is integral to the interaction with NIS and that the utilisation of drugs to inhibit PBF phosphorylation will significantly enhance radioiodide uptake in breast cancer cells. If the interaction can be overcome in the manner hypothesised it may enable the use of ^{131}I as a therapeutic option for breast cancer.

The main aims of this thesis are to:-

1. determine whether NIS expression and function are repressed by PBF in breast cancer.
2. assess the phosphorylation of PBF at Y174 and its effect on NIS repression in breast cancer
3. determine whether the inhibition of PBF phosphorylation can restore plasma membrane localisation of NIS and radioiodide uptake in breast cancer cells.

4. identify drugs that most potently inhibit PBF phosphorylation and maximise radioiodide uptake in breast cancer cells.

CHAPTER 2 – MATERIALS AND METHODS

Unless otherwise stated, all reagents described were obtained from Sigma-Aldrich (Poole, Dorset, UK)

Additional materials and methods can be located within each chapter.

2.1 Cell Culture

2.1.1 Cell lines

MCF-7 (Michigan Cancer Foundation-7) cells were obtained from the European Collection of Cell Cultures (supplied by Sigma). MCF-7 cells originated from a pleural effusion in a 69 year-old Caucasian female with a primary invasive breast ductal carcinoma in 1973 (Soule et al., 1973). They can be classified into the luminal A subcategory, as the cells are positive for both ER and PR (Levenson and Jordan, 1997) but do not have HER2 amplification (Benz et al., 1992).

MDA-MB-231 cells were obtained from the American Type Culture Collection (Virginia, USA). MDA-MB-231 cells are derived from a pleural effusion metastasis of an adenocarcinoma in a 51 year-old Caucasian female in the 1970s. The cells fall into the triple negative subcategory of breast cancer having no amplification of HER2 nor expression of ER and PR.

Both cell lines were purchased fresh from cell culture collections at the beginning of this project and underwent ploidy and STR cell line authentication profiling every 18 months to confirm cell line identity (electropherograms not shown)(DDC Medical).

2.1.2 Cell culture

Both cell lines were routinely cultured in RPMI 1640 medium (Life Technologies Ltd, Paisley, UK) supplemented with 10% (v/v) heat-inactivated foetal bovine serum (FBS), penicillin (10^5 U/l) and streptomycin (100 mg/l) (Invitrogen, Paisley, UK). Cells were passaged biweekly and incubated at 37^{o}C and 5% CO_2 in humidified conditions.

2.1.3 Cell splitting and seeding

Cells were briefly washed in phosphate-buffered saline (PBS) before incubation at 37˚C for 5 minutes in 0.125% trypsin-EDTA (Life Technologies). Trypsin was neutralised using complete media, with 20% of the suspension being transferred to a new T75 with fresh medium to maintain the cell line. Remaining cells were counted using a FastRead Counting Slide (Immune Systems Ltd) before being seeded at a density appropriate for the experiment.

2.2 Transfection and transduction

2.2.1 Plasmids

Overexpression of protein was achieved through transfection with mammalian expression vectors containing the complete coding sequence for the gene of interest. For transient transfection the pcDNA3.1 (+) vector (Invitrogen) was utilised whereas for stable transfection the vector pCI-neo (Promega, Madison, WI, USA) was used. Both plasmids contained full-length cDNA under the cytomegalovirus (CMV) promoter and sites for antibiotic resistance.

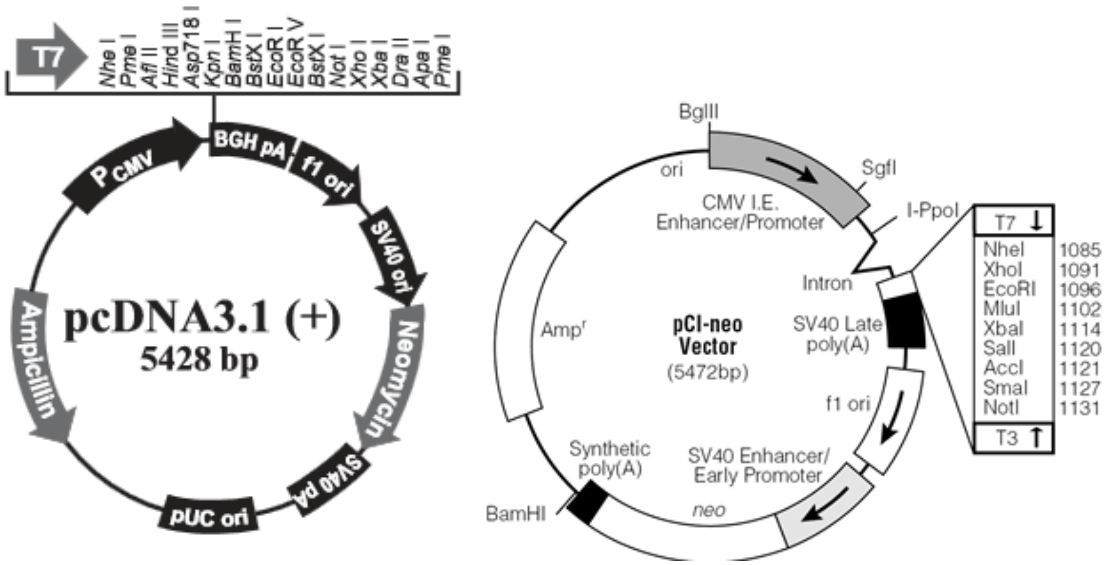

Figure 2-1. Schematics of pcDNA3.1 (+) and pCI-neo vectors. pcDNA3.1 (+) schematic taken from Invitrogen website and the pCI-neo schematic taken from the Promega website. Both vectors contain CMV promoters, ampicillin bacterial resistance gene and a neomycin resistance gene.

2.2.2 Plasmid Preparation

2.2.2.1 Bacterial Transformation

Transformation was carried out using Subcloning Efficiency™ DH5α™ Competent *E.Coli* cells (Invitrogen) according to the manufacturer's instructions. Plasmid DNA (10ng) was combined with 50µl of DH5α Cells and incubated for 30 minutes on ice. The bacterial cells were then heat shocked at 42°C for 20 seconds to increase the permeability of the cell membranes. The cells were incubated on ice for a further 2 minutes before 950µl of Luria Broth (LB) was added and the suspension incubated for 1 hour at 37°C with shaking. Bacterial cells were pelleted by centrifugation at 13,000rpm and the supernatant discarded. The cells were resuspended in remaining supernatant (~50µl) and was plated on LB-Agar (1% Agar) plates containing carbenicillin (100µg/ml) and incubated at 37°C for 16 hours.

Bacterial colonies that grew on LB-carbenicillin (100µg/ml) plates were deemed to have been transformed and single colonies were to inoculate 5ml of LB broth containing carbenicillin (100µg/ml) and incubated at 37°C for 8 hours with shaking at 200rpm.

2.2.2.2 DNA Amplification

Amplification of the plasmid was performed using the GenElute™ HP Plasmid Maxiprep kit (Sigma) according to the manufacturer's instructions. The DH5-α bacterial suspension from 2.2.2.1 was added to 150ml LB broth containing carbenicillin (100µg/ml) cultured overnight at 37°C in an orbital shaker. After incubation, 270µl of glycerol was combined with 1.53ml of the bacterial suspension in LB broth to create a glycerol stock which can be stored long-term at -80°C and used to re-amplify DNA as required. The remaining suspension was centrifuged at 5000 x g for 10 minutes and the supernatant was discarded. The bacterial pellet was thoroughly re-suspended in 12ml Resuspension Solution, followed by the addition of 12ml Lysis Solution. The mixture was inverted eight times and left to stand for 5 minutes. The lysis was terminated by the addition of chilled 12ml Neutralisation Solution. 9ml of Binding Solution was added to the suspension which after mixing was immediately transferred to the barrel of a filter syringe and incubated at room temperature for 5 minutes. During this time, a spin column was prepared by centrifuging 12ml Column Preparation through it at 3000 x g for 2 minutes. The eluate was discarded and the DNA suspension filtered through the syringe into the spin column before being centrifuged at 3000 x g for 2 minutes. The column was then washed in two stages, initially with 12ml of Column Wash Solution 1 with centrifuging at 3000 x g for 1 minute followed by 12ml of Column Wash Solution 2 with centrifugation for 5 minutes at 3000 x g. The DNA was then eluted from the column using 3ml nuclease free water and

centrifuging at 1000 x g for 5 minutes. Plasmid DNA was quantified using the NanoDrop© ND-1000 Spectrophotometer (NanoDrop) and sequenced as detailed in 4.2.5.

2.2.2.3 Sequencing

To sequence the plasmid DNA, 300ng of DNA was combined with 3.2pmol of the forward (T7 short or T7) or reverse (BGH reverse primer or T3) primer and made up to 10µl with nuclease free water (Table 2-2). Plasmid to profile sequencing was performed by the functional genomics department at the University of Birmingham.

Plasmid	**Sequencing Primer**	**Sequence**
pcDNA3.1 (+)	T7 Short	**5'** AATACGACTCACTATAG **3'**
	BGH Reverse	**5'** TAGAAGGCACAGTCGAGG **3'**
pCI-neo	T7	**5'** TAATACGACTCACTATAGG **3'**
	T3	**5'** AATTAACCCTCACTAAAGG **3'**

Table 2-1. Primers used for sequencing cDNA within pcDNA3.1 (+) and pCI-neo plasmids.

2.2.3 Transient plasmid transfection

Transfection was performed using TransIT®-LT1 Transfection Reagent (Geneflow, Staffordshire, UK) at a 3:1 ratio with the DNA plasmid. Cells were seeded 18 hours prior to transfection. Plasmid DNA was combined with OPTI-MEM medium and incubated for 5 minutes before the addition of TransIT®-LT1. The mixture was further incubated for 25-30 minutes before the appropriate volume (shown in Table 2-2) was added to cells.

Vessel	Number of cells seeded per flask/well	Plasmid DNA (µg/condition)	Volume of transfection solution added (µl)
T75	1,000,000	15	1500
T25	350,000	5	500
6 well plate	150,000	2	200
12 well plate	75,000	1	100
24 well plate	32,500	0.5	50

Table 2-2. Amount of plasmid DNA used in transient transfection dependent on cell number.

2.2.4 Stable plasmid transfection

Prior to stable transfection, a kill curve was performed to determine the concentration of Geneticin (G418) (Sigma-Aldrich) required to kill all untransfected cells that do not have any endogenous resistance to G418. A range of doses from 0.5 to 5mg/ml in complete medium was utilised and both MCF-7 and MDA-MB-231 cells required 1mg/ml G418 for 100% cell death within 10-14 days.

Cells were transfected as described in 2.2.3 but pCI-neo vectors were utilised in place of the pcDNA3.1 (+) vectors. After transfection, both transfected and untransfected control cells were subjected to 14 days in medium containing a pre-determined concentration of 1mg/ml G418. Once the control untransfected cells had died, the stable transfected cells were maintained as described in 2.1 with the addition of 1mg/ml G418 in the cell media.

Stability of stable cell-lines was checked on a monthly basis by performing qRT-PCR to ensure the stables cell-lines maintained increased expression of their transfected vectors.

2.2.5 Lentiviral stable transduction

To stably express NIS within cell lines lentiviral particles containing the NIS gene (precision LentiORF SLC5A5 (w/o Stop Codon) particles) were purchased (Dharmacon, GE Healthcare, Buckinghamshire, UK) along with Precision LentiORF RFP Positive Control particles (Dharmacon). The viral particles contain plasmid DNA containing ampicillin and blasticidin resistance genes, a CMV promoter, an IRES element and a multiple cloning site. The NIS particles contained the complete coding sequence for full-length human NIS within the multiple cloning site whereas the control particles contained red fluorescent protein (RFP) gene within this site (Figure 2-2). Prior to lentiviral transduction, a blasticidin kill curve was performed to determine the concentration of blasticidin required to kill all cells without resistance genes.

Relative lentiviral transduction efficiency was determined using Precision LentiORF RFP Positive Control particles (Dharmacon). Cells were seeded in 96 well plates (1000 per well) for 24 hours prior to transduction. Cell medium was removed and replaced with 45µl Opti-MEM serum free medium (SFM) before 5µl viral mixture was added to each well. The viral mixture contained 80µg/ml polybrene (8µg/ml final concentration) (Sigma) and viral particles at varying concentrations from $4.45x10^7$ – $5.69x10^2$ transducing units (TU)/ml in SFM. Cells expressing GFP were counted and relative transduction efficiency calculated. For MCF-7 cells $6.5x10^5$ TU/ml was the optimum concentration of particles whereas MDA-MB-231 cells only required $2.2x10^5$ TU/ml for efficient transduction.

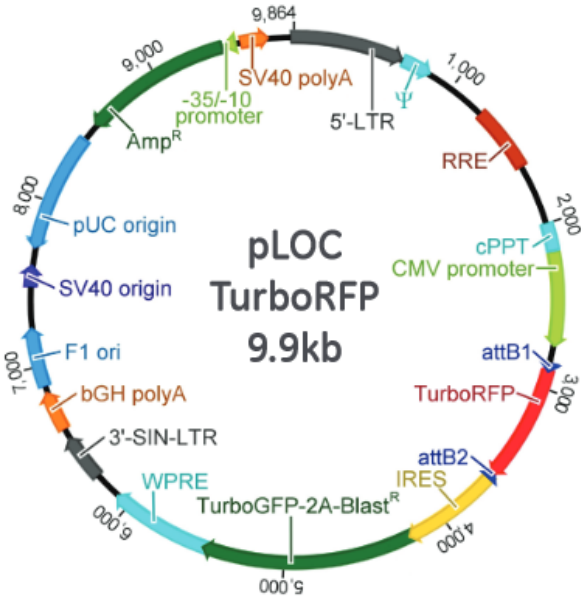

Figure 2-2. Schematic of the plasmid DNA within RFP-control particles. This schematic shows the plasmid that is contained within Precision LentiORF RFP Positive Control particles. Precision LentiORF SLC5A5 (w/o Stop Codon) particles contain human NIS cDNA in place of the TurboRFP cDNA. Diagram was taken from the Dharmacon website (http://dharmacon.gelifesciences.com/uploadedFiles/Resources/precision-lentiorf-manual.pdf).

Once transduction efficiency had been calculated, cells were transduced for long-term culture. Cells were seeded into 96 well plates (1000 cells per well) and incubated for 24 hours before medium was replaced with 45µl SFM. Viral mixtures containing polybrene and either RFP-control particles or NIS particles at the pre-determined concentrations in SFM were prepared and 5µl was added into each well. Cells were then incubated for 6 hours before 50µl complete medium was added. Medium was replaced after 24 hours and then again 48 hours later with the addition of blasticidin. Cells were maintained in medium supplemented with blasticidin for all future cultures.

Following successful transduction the cells were kindly single-cell sorted by Dr Matt MacKenzie (University of Birmingham, UK) using Summit (v6.2.3.15613) on a

Beckman Coulter Moflo Astrios EQ™. Control RFP cells were gated for strong expression of RFP and GFP whereas cells transduced with NIS lentiviral particles were sorted on GFP expression alone (Figure 2-3). Single cell colonies with strong and medium expression of sorting genes were selected and grown from a single cell in a 96 well plate. Cells were maintained in medium containing blasticidin throughout. Colonies utilised for the majority of experiments were clone 1 and 2, selected on the basis of consistent cell growth, cell survival, NIS and PBF expression and high levels of radioiodide uptake. Radioiodide uptake experiments were performed on a fortnightly basis to ensure the NIS transduced cell-lines maintained functional NIS overexpression, with qRT-PCR being performed bimonthly to ensure increased NIS mRNA expression.

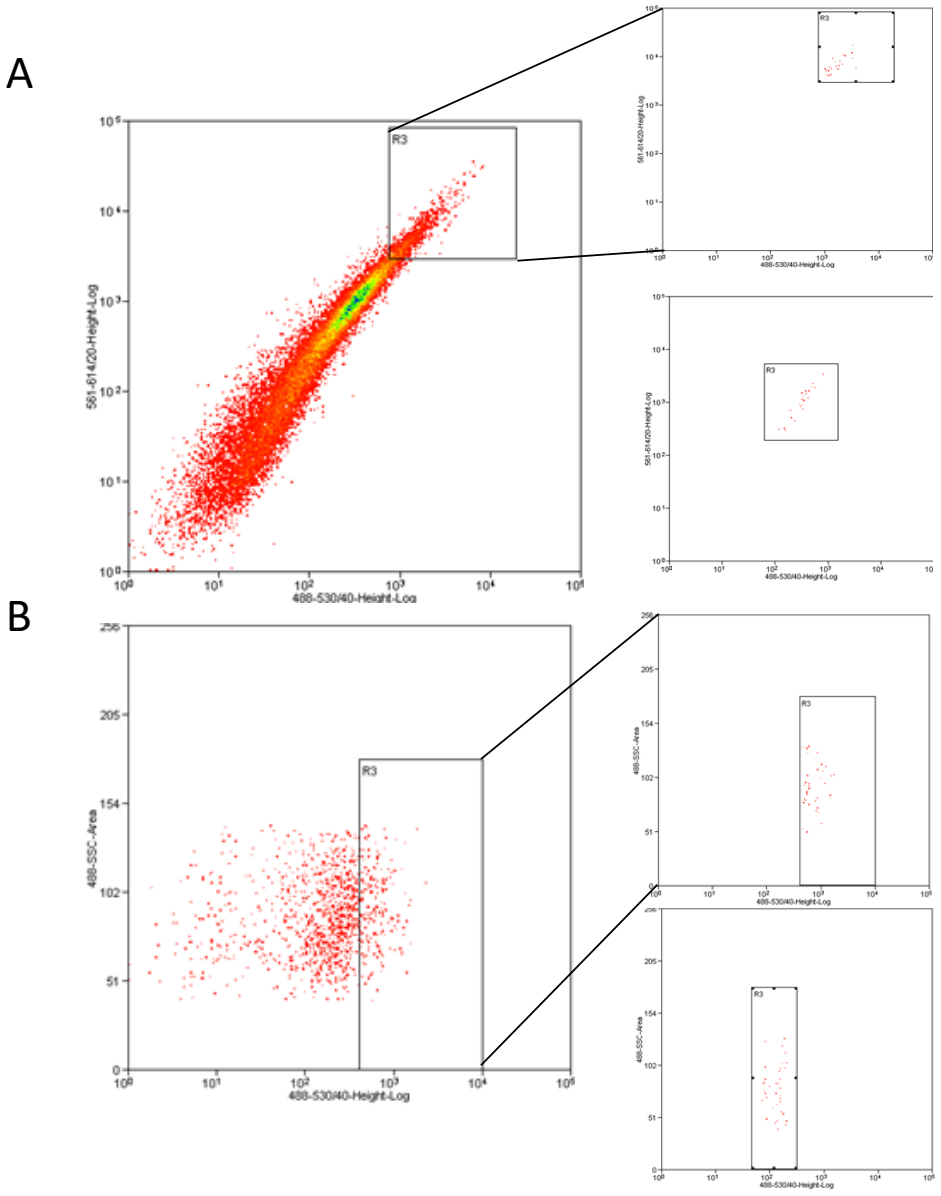

Figure 2-3. Gating for lentiviral single cell sorting. (A) The gating for the RFP control lentiviral MDA-MB-231 cells with GFP expression on the x axis and RFP expression on the y axis. Cells were then selected for high expression or intermediate expression of both as shown in the right-hand panel. (B) The gating for NIS lentiviral MDA-MB-231 cells with GFP expression on the x axis. Cells were then selected for high expression or intermediate expression of both as shown in the right-hand panel.

2.3 Western blotting

2.3.1 Protein extraction and quantification

Forty-eight hours post-transfection, cells were washed with PBS and then lysed in radioimmunoprecipitation assay (RIPA) buffer (50 mM Tris-HCl, pH 7.4, 150 mM NaCl, 1% v/v Igepal CA-630, 6 mM sodium deoxycholate, 1mM EDTA) containing 60 µl/ml protease inhibitor cocktail (Sigma) and phosphatase inhibitor cocktails 2 and 3 (1% v/v)(Sigma). To aid lysis, cells were subjected to a freeze-thaw cycle at -20°C for a minimum of 20 minutes before cell plates were scraped and lysate suspension transferred into microcentrifuge tubes. Lysates were then sonicated for 3x30 seconds on medium setting (200W) (Bioruptor Standard, Diagenode, Liège, Belgium) and centrifuged for 10 minutes at 13,000rpm to pellet cell debris.

A bicinchoninic acid (BCA) colourimetric assay (Thermo scientific, Pittsburgh, PA) was utilised to determine protein concentration. Protein standards comprised of bovine serum albumin (BSA) in RIPA buffer were prepared at concentrations ranging from 0-5 mg/ml. Both lysates and standards were measured in duplicate with 4 µl being combined with 80µl of BCA reagent (78.4µl Reagent A and 1.6µl Reagent B). After a 30 minute incubation at 37°C, the absorbance was measured at 560nm using a Victor^3 1420 Multilabel Counter (Perkin Elmer, Waltham, MA, USA). A standard curve was then produced which could be used to determine lysate protein concentration.

2.3.2 Western blotting

Protein lysates (10-60 µg) were denatured at 37˚C for 30 minutes in 5x Laemmli buffer (250mM Tris-HCl pH 6.8, 10% SDS, 0.02% bromophenol blue, 50% glycerol, 12.5% β-mercaptoethanol). Resolving gels (375mM Tris (from 1.5M pH 8.8 stock), 12% acrylamide (from 30% (w/v) acrylamide:0.8% (w/v) bis-acrylamide stock (Geneflow)), 3.5mM SDS, 0.1% (v/v) tetramethylethylenediamine (TEMED) (Sigma), 4.4mM ammonium persulphate (APS)) were made and any loose acrylamide cleared from wells. Denatured protein samples were loaded onto the gel along with a well of 4µl of protein ladder (BLUeye pre stained protein ladder, Geneflow). Proteins were then separated by SDS-Polyacrylamide gel electrophoresis (SDS-PAGE) in running buffer (24.8mM Tris, 192mM glycine, 3.47 mM SDS) initially at 70 V but later increased to 140 V.

Proteins were transferred to activated polyvinylidene fluoride membranes (PVDF) (Fisher) at 360mA for 1 hour 20 minutes in transfer buffer (25mM Tris, 192mM glycine, 20% methanol). Following transfer the membranes were blocked in 5% non-fat milk (Marvel dried milk powder, Premier Foods Group Ltd, London) in Tris-Buffered Saline with Tween (TBST)(20mM Tris, 137mM NaCl, 0.025% v/v Tween 80) for 1 hour at room temperature. The membranes were then incubated with primary antibodies (Table 2-3) in 5% non-fat milk in TBST overnight at 4°C. After three washes in TBST, blots were incubated for 1 hour at room temperature, with the appropriate horseradish peroxidise-conjugated secondary antibody (Dako, Denmark). After three further washes, SuperSignal West Pico Chemiluminescent Substrate (Thermo Scientific) or Pierce ECL 2 (Thermo Scientific) chemiluminescence detection systems were used to visualise the bands on Kodak film for 5 seconds to 60 minutes. Scanning densitometry was carried out to

determine quantifiable differences in protein expression (ImageJ software, http://imagej.nih.gov/ij/).

2.4 Fluorescence immunocytochemistry

Glass coverslips were washed in ethanol and sterile PBS and placed into 6 well plates before cells were seeded on top of them. Forty-eight hours after transfection, cells were washed briefly in PBS before being fixed using 800µl of fixing solution (0.1 M phosphate buffer (pH 7.4) containing 2% paraformaldehyde, 2% glucose and 0.2% sodium azide) for 20 minutes at room temperature. Three subsequent washes in PBS were performed before cells were permeabilised in chilled methanol for 10 minutes. Cells were further washed in PBS, before blocking in 10% newborn calf serum (NCS) diluted in PBS at room temperature for 30 minutes. Primary antibodies (Table 2-3) were diluted to the desired concentrations in 1% BSA in PBS and added to cells for 1 hour at room temperature. Further washes in PBS were carried out before cells were incubated for an hour at room temperature with secondary antibodies in 1% BSA, 1% NCS in PBS. Secondary antibodies were as follows: Alexa-Fluor 488-conjugated goat anti-mouse IgG and Alexa-Fluor-594-conjugated goat anti-rabbit IgG (Invitrogen), both used at 1:250 along with Hoechst 33342 stain (Sigma-Aldrich) for nuclei (1:1000). After rinsing in PBS, the coverslips were mounted onto slides using Fluorescent Mounting Solution (Dako) and stored at 4°C. Cells were visualised on Zeiss Axioplan fluorescent microscope (Zeiss, Oberkochen, Germany) using 10x, 20x 40x or 100x objectives.

2.5 RNA extraction and Reverse Transcription

2.5.1 RNA extraction

Total RNA was extracted from cells using TRI Reagent® RNA Isolation Reagent (Sigma-Aldrich) to perform a single step acid guanidinium phenol-chloroform extraction. Cells in 6 well plates were harvested with 500µl TRI Reagent/well. Following the manufacturer's protocol, the samples were then thoroughly mixed with chloroform (200µl/ml TRI reagent) (Sigma-Aldrich) and incubated for 15 minutes at room temperature. To separate the samples into three phases they were centrifuged for 15 minutes at 12,000 g at 4°C. The top aqueous layer, containing the RNA, was transferred to fresh microcentrifuge tubes and incubated with isopropanol (500µl/ml TRI reagent) (Sigma-Aldrich) for 10 minutes at room temperature before further centrifugation for 10 minutes at 12,000 g at 4°C. The supernatant was then discarded and the pellet washed with 75% ethanol (1ml/ml Tri-reagent). The samples were vortexed and centrifuged for a further 5 minutes at 7,500 g at 4°C. The supernatant was again discarded and the pellet left to air-dry at room temperature for 10 minutes. Once dry, the pellet was re-suspended in 30µl of nuclease free water and stored at -80°C. RNA concentration was determined by measuring absorbance at a wavelength of 260nm on a NanoDrop ND-1000 Spectrophotometer (NanoDrop Products, Wilmington, DE, USA).

2.5.2 Reverse Transcription

RNA (500ng) was diluted in nuclease free water to a volume of 5µl and incubated at 70°C for 10 minutes. The RNA was then combined with reagents from the Reverse Transcription System (Promega) to give a 10µl total volume. Each reaction consisted of

2µl 25mM $MgCl_2$, 1µl RT 10X Reaction buffer (10mM Tris-HCl pH 9.0 at 25°C, 50mM KCl, 0.1% Triton® X-100), 1µl 10mM dNTPs, 0.25µl RNasin (ribonuclease inhibitor), 0.3125µl Avian Myeloblastosis virus (AMV) reverse transcriptase and 0.5µl random primers. Samples were incubated at room temperature for 10 minutes before undergoing reverse transcription as follows (1) 42°C for 1 hour, (2) 95°C for 5 minutes and (3) 4°C for 5 minutes. Samples were then diluted with the addition of 10µl nuclease free water before being stored at -20°C.

2.6 Quantitive real-time PCR (qRT-PCR)

Relative expression of specific mRNAs were determined using qRT-PCR in relation to the abundant internal control 18S. qRT-PCR was performed either using custom-made primers (Alta Biosciences, Birmingham, UK) and probes (Eurogentec, Liège, Belgium) or with TaqMan® Gene Expression Assays (Life Technologies). The probes consisted of oligonucleotides containing a 5' fluorophore, FAM (6-carboxy-fluorescein) for all target genes and VIC for 18S controls, and a 3' quencher, TAMRA (6-carboxy-tetramethyl-rhodamine). The fluorophore is excited by the light source in the PCR machine, however without gene amplification the quencher is in close proximity to the fluorophore and can suppress any fluorescence due to fluorescence resonance energy transfer (FRET). FRET involves the transfer of energy from the excited high energy fluorophore to the low energy quencher. As the Taq polymerase extends the primer, the probe is broken down by exonuclease activity releasing the fluorophore thus disrupting the close proximity of the quencher and fluorophore. As a result of this distancing, the quencher can no longer suppress the fluorescence allowing fluorescence emission and detection of this excitation

by an ABI 7500 halogen light and charge-coupled device (CCD) camera. Hence the fluorescence detected is directly proportional to the level of cDNA template available for primer amplification.

Duplicates of 1µl cDNA were loaded into 96 well plates and 24µl 'PCR mastermix' added to each well. For custom-made primers and probe, the 'PCR mastermix' contained 4.5µl Forward Primer (5pmol/µl), 4.5µl Reverse Primer (5pmol/µl), 0.75µl Probe (5pmol/µl) (Alta Biosciences), 12.5µl 2x qPCR MasterMix Plus QGS (Eurogentec), 1.25µl Eukaryotic 18S (Applied Biosystems, Life Technologies) and 0.5µl nuclease-free water. All custom-made primers and probes were validated for multiplexing with 18S. When using TaqMan® Gene Expression Assays, the 'PCR mastermix' contained 1µl TaqMan® Gene Expression Assay (Life Technologies) for a specific gene, 12.5µl 2x qPCR MasterMix Plus QGS (Eurogentec) and 10.5µl nuclease-free water. TaqMan® Gene Expression Assays had not been independently validated for multiplex with 18S so it was necessary to singleplex when using these assays. 18S was set up with separate 1µl cDNA, 1µl Eukaryotic 18S (Applied Biosystems), 12.5µl 2x qPCR MasterMix Plus QGS (Eurogentec) and 10.5µl nuclease-free water.

qRT-PCR was performed on the ABI Prism 7500 real-time PCR system (Applied Biosystems). The steps were as follows: 50°C for 2 minutes; 95°C for 10 minutes; 40 cycles of 95°C for 15 seconds and 60°C for 1 minute. For each gene and 18s control, a threshold line was set in the exponential phase and the cycle threshold (C_T) calculated from the cycle number at which each logarithmic PCR plot crossed the threshold line. These values were then used to calculate ΔC_T values (ΔC_T = C_T target gene –C_T 18S) and fold change ($2^{-(\Delta CT \text{ of experimental samples} - \Delta CT \text{ control samples})}$).

2.7 Radioiodide Uptake

Radioiodide uptake assays were performed to assess functional NIS levels in cells. Cells were seeded in 24 well plates and assays were performed typically 48 hours after transfection. Control cells were incubated for one hour with 100µM sodium perchlorate (Sigma-Aldrich) prior to the addition of radioiodide. Sodium perchlorate inhibits NIS function allowing any changes in uptake to be attributed to NIS functionality by removing any inherent background uptake. Cells were incubated with 10^{-6}M NaI containing 0.05µCi ^{125}I (Hartmann Analytic) for an hour at 37°C. Cell medium was removed and any unincorporated radioiodide removed by rapidly washing the cells with Hank's balanced salt solution (HBSS). The cells were lysed with 100µl 2% SDS and radioactivity counted for one minute using a gamma counter (1260 Multigamma II, Wallac). A BCA assay (as described in 2.3.1) was then undertaken to calculate protein concentration of the lysates which were used to standardise the observed counts.

2.8 Table of antibodies used

Antibody	Clone	Company	Western Concentration	IF Concentration
Anti- PBF	Rabbit polyclonal	Eurogentec (Custom-made)	1:500	1:100
Anti-pY174 PBF	Rabbit polyclonal	Covalab (Custom-made)	1:1000	1:50
Anti-β-actin	Mouse monoclonal (AC-15)	Sigma Aldrich (A5441)	1:20000	N/A
Anti-NIS	Rabbit polyclonal	Abcam (ab104920 – discontinued)	1:1000	1:500
Anti-NIS	Rabbit polyclonal	ProteinTech (24324-1-AP)	1:1000	1:500
Anti-Myc tag	Mouse monoclonal (9B11)	Cell Signalling (2276S)	1:1000	1:750
Anti-HA tag	Mouse monoclonal (16B12)	Covance (MMS-101P)	1:1000	1:200
Anti-HA tag	Rabbit polyclonal (Y-11)	Santa Cruz (sc-805)	1:500	1:100
Anti-CD8	Mouse monoclonal (UCHT4)	Ancell (153-200)	N/A	1:250
Anti-Src	Rabbit monoclonal (32G6)	Cell Signalling (2123)	1:1000	N/A
Anti Src (phospho Y418)	Rabbit polyclonal	Abcam (ab4816)	1:1000	N/A
Anti-FAK	Rabbit monoclonal (EP695Y)	Abcam (ab40794)	1:1000	N/A
Anti-FAK (phospho Y576 + Y577)	Rabbit monoclonal (EP1832Y)	Abcam (ab76244)	1:1000	N/A
Anti-α-tubulin	Mouse monoclonal (B-7)	Santa Cruz (sc-5286)	1:1000	N/A

Table 2-3. Antibodies used in this study.

2.9 Statistics

Data were analysed using SigmaPlot (SPSS Science Software UK Ltd). The Shapiro-Wilk test was performed on each data set to ensure the data followed a Gaussian distribution before it was further analysed using a Student's t-test or one-way ANOVA. For data that did not possess a normal distribution a Mann-Whitney U test was used for analysis. Significance was taken as $p < 0.05$. For qRT-PCR, statistics were performed on ΔCt to avoid potential bias through transformation of data using $2^{-\Delta\Delta Ct}$.

CHAPTER 3 - PBF ALTERS NIS LOCALISATION AND REPRESSES RADIOIODIDE UPTAKE IN BREAST CANCER CELLS

3.1 Introduction

As discussed in 1.4 there is substantial evidence for an association between PBF and NIS in thyroid cancer (Boelaert et al., 2007; Smith et al., 2009; Smith et al., 2013). The PBF protein has been observed to bind directly to the NIS protein in thyroid cancer cells (Smith et al., 2009). Upon binding of the two proteins, PBF alters the subcellular localisation of NIS, translocating it away from the plasma membrane into intracellular vesicles. This mislocalisation of NIS impairs its functionality and reduces the ability of the cells to take up radioiodide (Smith et al., 2009).

In thyroid cells, PBF exerts an effect not only on the NIS protein but also on the NIS gene (Boelaert et al., 2007). Overexpression of PBF decreased NIS mRNA expression by 95% in primary thyrocytes, and PBF was observed to repress NIS transcription through interactions with both the proximal NIS promoter and the NUE in FRTL-5 cells. However in primary thyrocytes PBF had no effect on the proximal promoter and was only capable of repressing NIS expression via the NUE (Boelaert et al., 2007), which has previously been described to be a thyroid-specific enhancer of NIS (Schmitt et al., 2002; Taki et al., 2002).

The aim of the work described in this chapter was to establish whether the two proteins have the same relationship in the context of breast cancer. NIS and PBF have both been observed to be minimally expressed in normal breast tissue but are upregulated in the majority of breast tumours (Tazebay et al., 2000; Watkins et al., 2010). However, it is not known if PBF can interact with or regulate the expression of NIS in the breast cancer disease state. The effect of PBF on NIS expression and function was determined in MCF-7 and MDA-MB-231 breast cancer cells.

3.2 Materials and Methods

3.2.1 Breast Cancer Samples

Four matched normal and breast cancer samples were kindly donated by the Breast Cancer Campaign. Samples were first homogenised on ice in RIPA buffer containing sodium orthovanadate and phosphatase and protease inhibitor cocktails using a conventional rotor-stator homogeniser. Samples were then further homogenised using a dounce homogeniser followed by use of a micro pestle. Homogenates were centrifuged at 13000rpm for 20 minutes at 4°C, the upper fat layer was removed and the supernatant transferred to a new tube. Lysates were then quantified and PBF and NIS protein expression analysed by Western blotting as described in sections 2.3.1 and 2.3.2 respectively.

3.2.2 Cell Culture

MCF-7 and MDA-MB-231 cells were maintained as described in 2.1.2 with stably transfected MCF-7 cells being cultured in medium containing G418 (1 mg/ml) and lentivirally-transduced MDA-MB-231 cells being cultured in medium containing blasticidin (15 μg/ml). All cell lines were seeded at 30,000 cells per well in a 24 well plate for radioiodide uptake and at 150,000 and 200,000 cells per well in a 6 well plate for immunofluorecent microscopy and protein extraction respectively.

3.2.3 ATRA and Dexamethasone Treatment

MCF-7 and MDA-MB-231 cells were treated with varying concentrations of all *trans*-retinoic acid (ATRA) and dexamethasone. ATRA (Sigma) was dissolved in dimethyl sulfoxide (DMSO) to create a stock solution of 10mM and stored at -80°C. Dexamethasone (Sigma) was dissolved in ethanol as per manufacturer's instructions to create a stock solution at 1mM and stored at -20°C. Further dilutions of both ATRA and dexamethasone were performed in cell medium to minimise the toxicity of DMSO and ethanol to the cells. In all combination treatments, an equal volume of ethanol and DMSO in cell media was used as a control.

3.2.4 Development of Stable and Lentiviral Cell lines

3.2.4.1 NIS Lentiviral Cells

Lentivirally-transduced MDA-MB-231 cells were generated as described in 2.2.5. The MDA-MB-231 cells utilised in this chapter were control clone 1 and NIS clones 1 and 2, selected due to their consistent cell growth, cell survival, NIS and PBF expression and high levels of radioiodide uptake.

3.2.4.2 PBF Knockdown Lentiviral Cells

To stably knockdown PBF within cell lines, lentiviral particles containing shRNA targeted to PBF mRNA (SMARTvector Human Lentiviral PTTG1IP - VSH6063/SH-011820) were used (Dharmacon, GE Healthcare, Buckinghamshire, UK) along with SMARTvector Non-targeting hCMV-TurboGFP Control Particles (S-005000-01; Dharmacon). The viral particles contained a puromycin resistance gene and a CMV promoter. The viral vectors express PBF shRNA modelled on precursor microRNA (pre-miRNA) that are transcribed under the control of

RNA Polymerase III (Pol III) promoters. shRNAs are produced as single-stranded molecules consisting of 50-70 nucleotides. They form a stem-loop structure with a 19-29 base-pair region of double-stranded RNA (the stem) bridged by a region of single-stranded RNA (the loop) and a short 3' overhang. Once transcribed, the shRNAs translocate from the nucleus to the cytoplasm where they are cleaved at the loop by the nuclease Dicer. Following cleavage they enter the RNA-induced silencing complex (RISC) to direct cleavage and subsequent degradation of complementary mRNA.

Prior to lentiviral transduction, a puromycin kill curve was performed to determine the concentration of puromycin required to kill 100% of cells without the resistance gene. MDA-MB-231 and MCF-7 cells both required 4 µg/ml puromycin for 100% death after 7-10 days. For transduction, cells were seeded into 96 well plates (1000 cells per well) and incubated for 24 hours before medium was replaced with 45µl serum free medium (SFM). Viral mixtures (30 µl) containing polybrene (1 µl) and either control or PBF shRNA particles (5 µl) in SFM were prepared and 5µl was added into each well. Cells were then incubated for 6 hours before 50µl complete medium was added. Medium was replaced after 24 hours and then again 48 hours later with the addition of puromycin. For lentiviral PBF knockdown, MCF-7 cells were utilised along with MDA-MB-231 cells that had previously been lentivirally-transduced with control-RFP (clone A) and NIS (clone 1 and 2) particles. Cells were assessed for PBF knockdown using qRT-PCR (described in section 3.2.9) and were maintained in medium supplemented with puromycin for all future cultures.

3.2.4.3 Stable Transfection

MCF-7 and MDA-MB-231 cells were stably transfected with empty vector and PBF in pCI-neo vectors as described in section 2.2.4 (plasmids kindly gifted by Dr Vicki Smith) (Smith et al., 2009). Stable transfection was confirmed using qRT-PCR.

3.2.5 Transient Transfection

Transfection efficiency experiments were performed to determine optimal cell numbers and transfection reagents. TransIT®-LT1 Transfection Reagent produced the highest levels of transfection efficiency using a Green fluorescent protein (GFP) plasmid in MCF-7 (75% efficiency) andMDA-MB-231 (80% efficiency) cells with the least amount of cytotoxicity compared to Fugene 6 (Promega) and Lipofectamine (Thermo Fisher Scientific) (data not shown). The cell numbers described in Table 2-2 provided the optimal number of cells with for transfection without cell crowding after 48 hours for both MCF-7 and MDA-MB-231 cells.

Transfection was performed as described in section 2.2.3 using an empty vector, PBF, PBF-HA, and NIS-MYC in pcDNA3.1 (+) vectors (Smith et al., 2009).

3.2.6 Radioiodide uptake

Radioiodide uptake was performed as described in 2.7. Transient transfection or treatment with ATRA and dexamethasone was performed 48 hours prior to the addition of ^{125}I to cells.

3.2.7 Western Blotting

Protein extraction and Western blotting were performed as described in sections 2.3.1 and 2.3.2 respectively. In order to preserve protein phosphorylation and allow the detection of pY174 PBF prior to harvesting, cells were treated for 20 minutes with the irreversible tyrosine phosphatase inhibitor pervanadate (100 µM from a 30mM stock of 951.1 µL PBS, 6 µL hydrogen peroxide, 42.9 µL sodium orthovanadate (Na_3VO_4) that had been incubated in the dark for 15 minutes). Cells were harvested as normal in RIPA buffer with the addition of 1 mM Na_3VO_4along with normal protease and phosphatase inhibitors. Antibodies used were anti-pY174 PBF antibody (Covalab) (Smith et al., 2013), anti-PBF (Smith et al., 2009), anti-phospho-Src (Y418) (Abcam), anti-Src (Cell Signalling) and β-actin (Sigma-Aldrich) (refer to section 2.8). Appropriate secondary antibodies were used.

3.2.8 Fluorescence immunocytochemistry

Fluorescence immunocytochemistry was performed as described in 2.4. Cells were treated with pervanadate (as in Section 1.2.7) prior to fixation to allow the detection of pY174 PBF. Antibodies used included anti-pY174 PBF antibody (1:50) (Covalab) (Smith et al., 2013), anti-HA tag (mouse) (1:200) (Covance), anti-HA tag (rabbit) (1:100) (Santa Cruz) and anti-Myc tag (1:750) (Cell Signalling).

3.2.9 RNA extraction and qRT-PCR

RNA extraction, reverse transcription and qRT-PCR were performed as described in 2.5 and 2.6. Expression of PBF was assessed using the PBF TaqMan® Gene Expression Assay

(Hs01036322_m1)(Life Technologies). Expression of NIS was assessed using custom-made primers and probe (Table 3-1).

	Sequence
Forward Primer	**5'** CCCCAGCTCAGGAATGGA **3'**
Reverse Primer	**5'** CGTAATAAGATAGGAGATGGCATAGAA **3'**
FAM-labelled Probe	**5'** CCAGCCGGCCCGCCTTAGC **3'**

Table 3-1. Sequence of custom-made primers and probe for NIS qRT-PCR.

3.2.10 Statistics

Data were analysed using Sigma Plot (SPSS Science Software UK Ltd). The student's t-test was utilised to compare data between two groups whereas the one-way ANOVA was used to compare more than two groups of parametric data with significance taken at $p < 0.05$ for both.

3.3 Results

3.3.1 PBF and NIS are expressed in breast cancer

PBF has previously been observed to be upregulated in breast tumours compared to normal breast tissue (Watkins et al., 2010). NIS has been demonstrated to be upregulated in 70-80% of breast tumours (Kilbane et al., 2000; Tazebay et al., 2000). The breast cancer campaign kindly donated four matched normal and tumour samples for preliminary investigation into NIS and PBF expression in breast cancer tumours. The four matched normal and tumour breast samples displayed increased PBF expression compared with their normal counterparts. On average the tumours displayed a 9-fold increase in PBF levels compared with the normal tissue (Figure 3-1). PBF can be detected by Western blotting at multiple different sizes due to post-translational modifications and oligomerisation (unpublished observations); monomeric PBF protein is detected at around 28kDa with a fully glycosylated form being detected around 37kDa (Smith et al., 2009). NIS is primarily detected by Western blotting at approximately 75kDa as a fully glycosylated form; other prominent bands include the unglycosylated 55kDa form and the 100kDa dimer of the unglycosylated form (Tazebay et al., 2000). Only 3 of the 4 tumours had increased expression of glycosylated NIS, with tumours displaying on average a 4-fold increase in NIS levels (Figure 3-1). Though the sample size was low, there did appear to be a correlation between NIS and PBF expression within tumour samples.

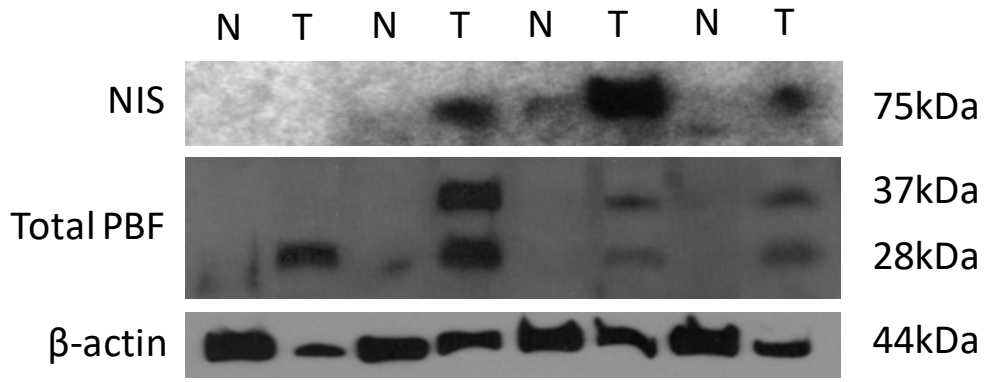

Figure 3-1. PBF and NIS expression in breast tumour samples. Western blot of protein from matched normal/tumour patient samples. Total PBF and NIS were detected with β-actin used a loading control. n=1

3.3.2 Endogenous NIS expression and function in MCF-7 and MDA-MB-231 cells

Both MCF-7 and MDA-MB-231 cells have endogenous levels of PBF and NIS expression. To allow further investigation of the two proteins in breast cancer cells, it is important to assess these endogenous expression levels. Both cell-lines display approximately equal levels of PBF mRNA expression (MCF-7 ΔCT=12.8 and MDA-MB-231 ΔCT=12.3) (Figure 3-2A). MDA-MB-231 cells have higher endogenous levels of NIS mRNA (ΔCT=17.6) than MCF-7 cells (ΔCT=20.5) (Figure 3-2A).

To establish whether the higher levels of NIS mRNA in MDA-MB-231 cells resulted in increased functional NIS levels compared to MCF-7 cells, endogenous radioiodide uptake in the two cell-lines was assessed. The cell-lines were left untreated or treated with sodium perchlorate ($NaClO_4$) for one hour prior to the addition of ^{125}I. Sodium perchlorate is a NIS specific inhibitor that was utilised to assess background radioiodide uptake, allowing for differences in NIS specific uptake to be quantified between conditions. TPC-1 cells, a cell-line derived from papillary thyroid carcinoma, was utilised for comparison. Both MCF-7 and

MDA-MB-231 cells were capable of 0.18 and 0.19 pmol ^{125}I/µg protein NIS-specific uptake (Figure 3-2B). Both breast cancer cell-lines displayed similar levels of NIS-specific uptake to the thyroid cancer cell-line, with TPC-1 cells displaying 0.18 pmol ^{125}I/µg protein of NIS-specific. uptake (Figure 3-2B). This data suggests that although MDA-MB-231 cells have increased NIS mRNA levels compared to MCF-7 cells, this increased expression does not translate to increased function.

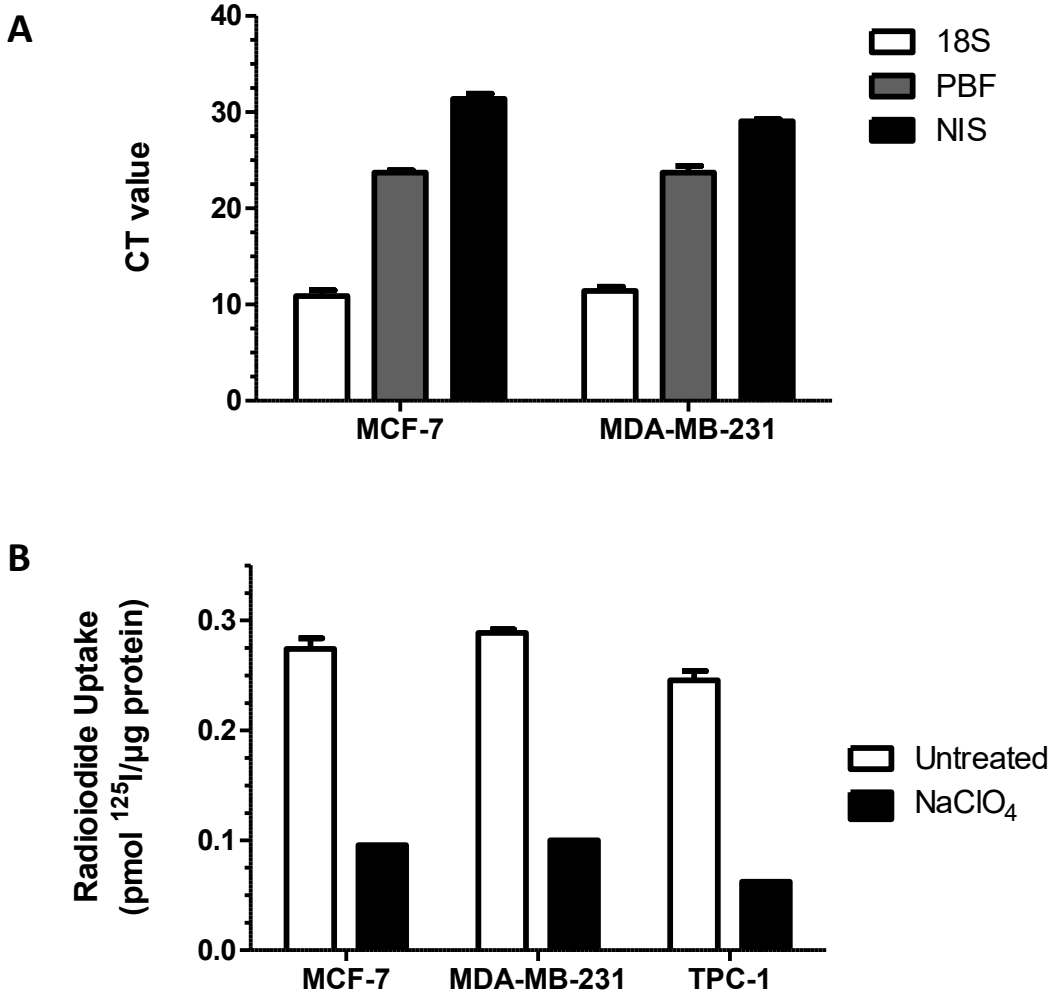

Figure 3-2- Endogenous expression and radioiodide uptake of MCF-7and MDA-MB-231. (A) The expression of 18s, PBF and NIS in untreated MCF-7 cells and MDA-MB-231 cells. Data displayed as ΔCT values with smaller bars indicating higher expression. n=3 (B) MCF-7, MDA-MB-231 and TPC-1 cells were left untreated or treated with sodium perchlorate ($NaClO_4$) 1 hour prior to the addition of ^{125} I to establish baseline NIS-specific radioiodide uptake . n=2 with 4 replicates in each n.

3.3.3 Creation of Stable Cell lines

3.3.3.1 Characterisation of PBF Stables

To enable the study of PBF in breast cancer cells, MCF-7 and MDA-MB-231 cells with stably-transfected with an empty vector and PBF were generated. Transfection of MCF-7 cells with PBF significantly boosted PBF expression with a 3.8-fold increase compared to cells transfected with the empty pCI-neo vector (Figure 3-3). MDA-MB-231 showed a significant 9.3-fold increase in PBF expression (Figure 3-3).

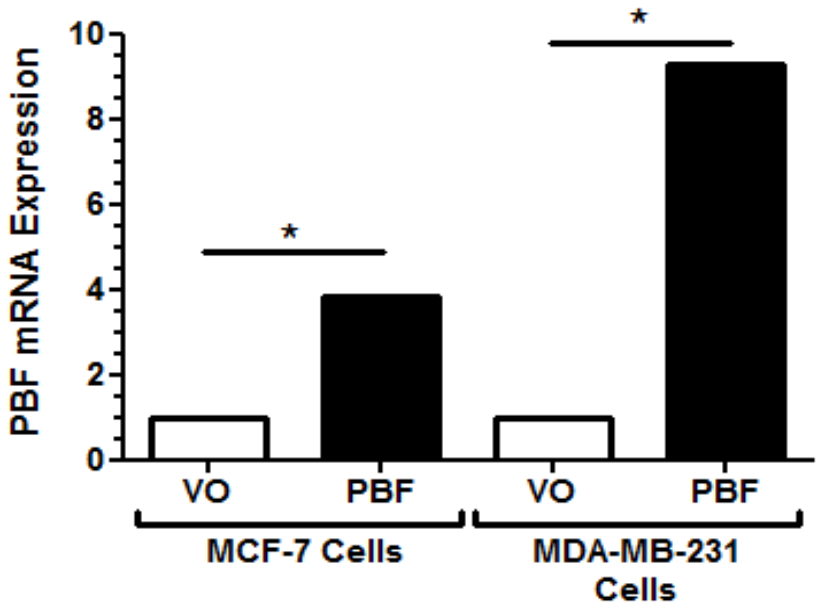

		Average ΔCT	ΔCT SEM	Fold Change	*p* value
MCF-7	**VO**	15.702	0.145	3.840	0.048
	PBF	13.769	0.002		
MDA-MB-231	**VO**	11.762	0.144	9.266	0.026
	PBF	8.595	0.504		

Figure 3-3. Stable expression of PBF in MCF-7 and MDA-MB-231 cells. MCF-7s and MDA-MB-231 cells were stably-transfected with empty pCI-neo vector (VO) and PBF. RNA was extracted from cells and qRT-PCR used to assess PBF mRNA expression using 18s as the internal housekeeping gene. Graph displays fold change compared with empty vector transfected cells. Statistics were performed on ΔCT values. n=3 with 4 replicates in each n. = p<0.05.*

3.3.3.2 Creation of NIS Lentiviral Stables

To maximise the radioiodide uptake of breast cancer cells, MDA-MB-231 cells were transduced with control or NIS lentiviral particles. Three clones of control and five clones of NIS lentiviral cells were selected and assessed for their PBF expression, NIS expression and radioiodide uptake. The five NIS clones displayed dramatically increased levels of radioiodide uptake as expected (Figure 3-5) whereas the control transduced cells had minimal radioiodide uptake that were similar to background radioiodide levels (Figure 3-5). Increased NIS expression in the NIS lentiviral cells compared with the controls was confirmed (Figure 3-5A). Both the NIS and control lentiviral transduced cells had similar levels of PBF expression (Figure 3-5B).

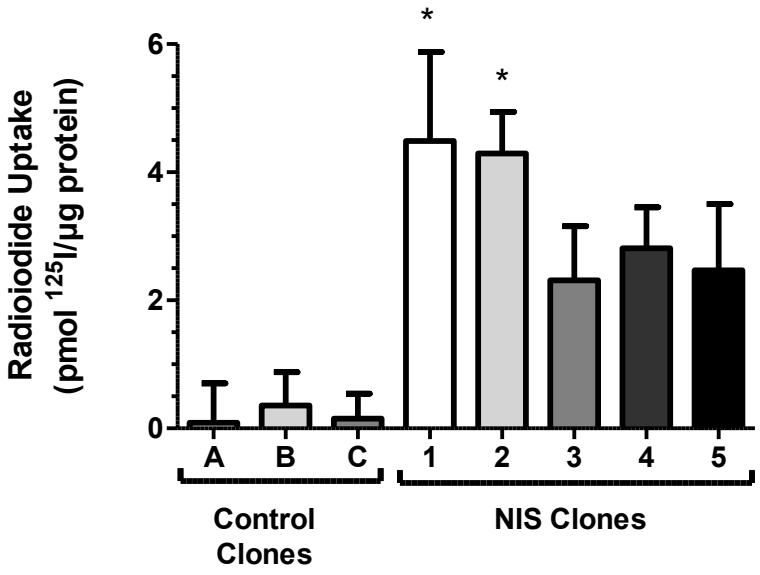

*Figure 3-4. Functionality of NIS lentiviral clones. Radioiodide uptake in the control and NIS lentiviral transduced MDA-MB-231 cell clones normalised to sodium perchlorate ($NaClO_4$) controls to display NIS-specific activity. n=2 with 3 replicates in each n. * = p<0.05 compared to all three control clones (A,B, & C).*

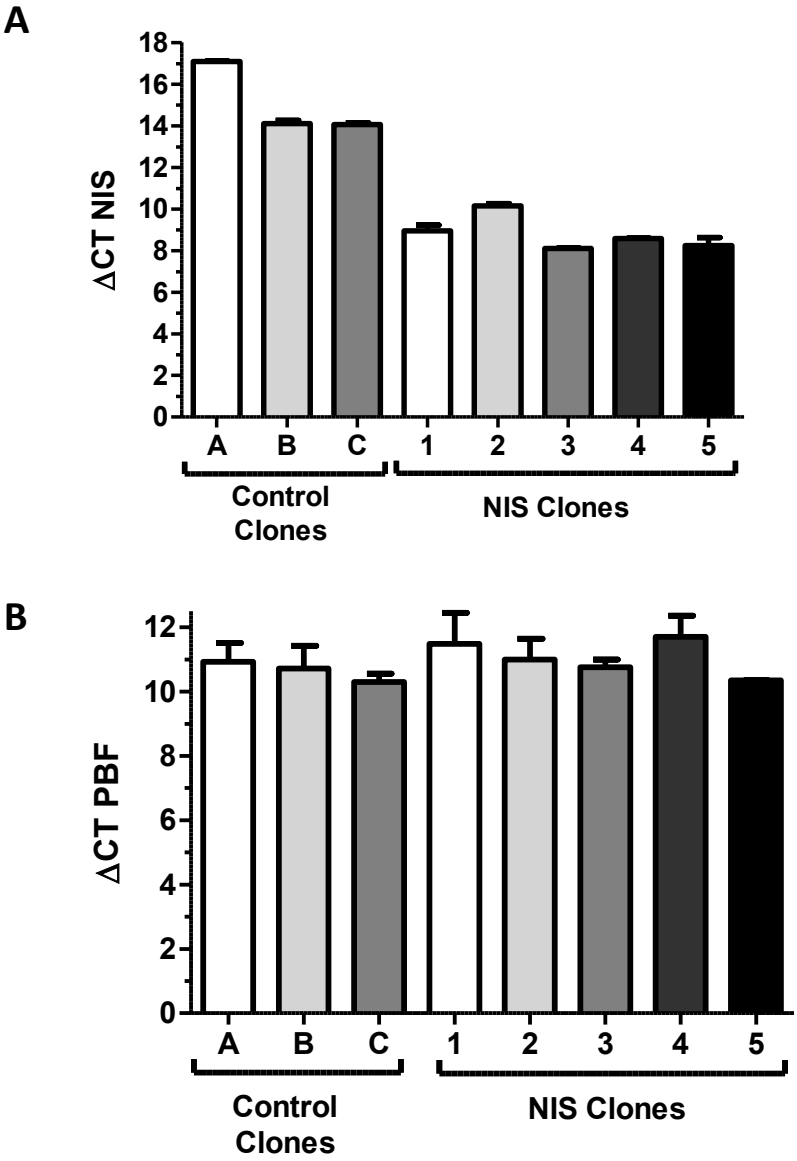

Figure 3-5. Expression NIS lentiviral clones. The expression of NIS (A) and PBF (B) mRNA in the individual clones of control and NIS lentiviral transduced MDA-MB-231 cells grown from a single cell colony. Displayed as ΔCT values with smaller bars indicating the higher expression. n=2 with 3 replicates in each n.

3.3.3.3 Creation of PBF Knockdown Lentiviral Stables

To enable the investigation of breast cancer cells lacking PBF expression, PBF was knocked down in breast cancer cells using PBF shRNA lentiviral particles. PBF was successfully

knocked down in MCF-7 cells with a 60% reduction in PBF expression compared with scrambled control MCF-7 cells (Figure 3-6).

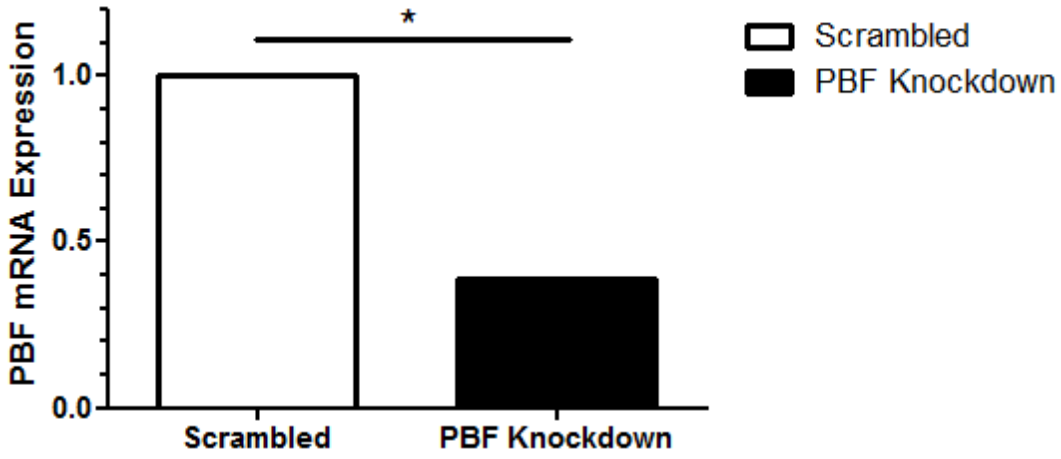

	Average ΔCT	ΔCT SEM	Fold Change	*p* value
Scrambled	14.242	0.100	0.407042	0.0461
PBF Knockdown	15.538	0.868		

*Figure 3-6. Lentiviral knockdown of PBF in MCF-7 cells. MCF-7 cells were lentivirally transduced with scrambled or PBF shRNA. PBF was efficiently knocked down as determined by qRT-PCR. Statistics were performed on ΔCT values. n=3 with 4 replicates in each n. *=p<0.05*

PBF was also knocked down in MDA-MB-231 cells that had been transduced previously with control particles or NIS lentiviral particles, resulting in efficient knockdown of over 95% (Figure 3-7).

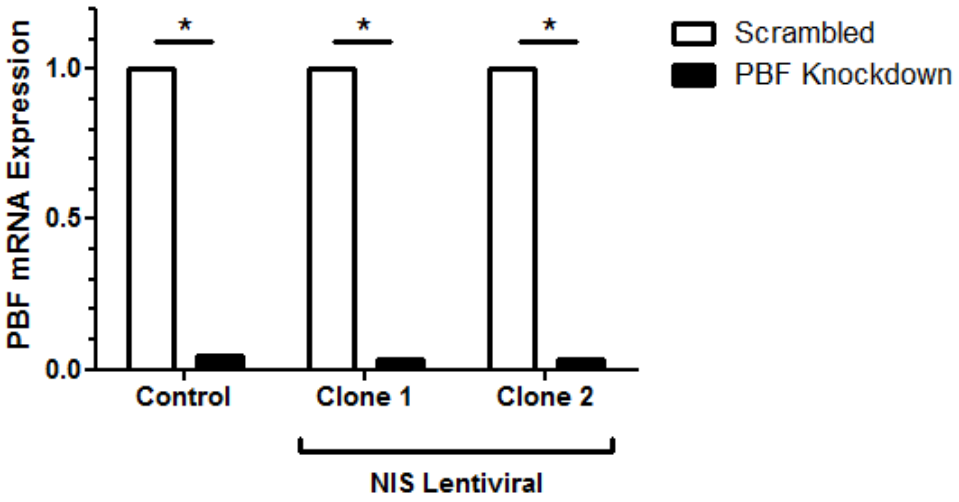

		Average ΔCT	ΔCT SEM	Fold Change	*p* value
Control	**Scrambled**	11.030	0.016	0.038	0.033
	PBF Knockdown	15.732	0.881		
Clone 1	**Scrambled**	11.648	1.285	0.023	0.0426
	PBF Knockdown	17.061	0.138		
Clone 2	**Scrambled**	10.536	0.251	0.024	0.0270
	PBF Knockdown	15.898	0.864		

*Figure 3-7. Lentiviral PBF knockdown in MDA-MB-231 NIS Lentiviral Cells. MDA-MB-231 cells that had previously been lentivirally-transduced with either control or NIS particles were further transduced with Scrambled shRNA or PBF shRNA. PBF was efficiently knocked down in all cell lines. n=2 with 4 replicates in each n. *=p<0.05*

3.3.4 Treatment with ATRA and Dex increases NIS expression but does not affect PBF expression

Treatment of MCF-7 cells with ATRA and dexamethasone has been previously observed to increase NIS mRNA and protein levels (Kogai et al., 2005). To confirm the MCF-7 cells used in this project were comparable to those used in previous studies, they were treated with varying doses of ATRA and dexamethasone for 48 hours prior to harvesting. Levels of NIS

mRNA were quantified using qRT-PCR. Treatment with 100nM ATRA and 1µM dexamethasone provided the largest increase in NIS (192-fold, *p*=0.004) compared with vehicle-only treated cells (Figure 3-8). This is comparable to published data where the same concentration induced a 150-fold increase (Kogai et al., 2005).

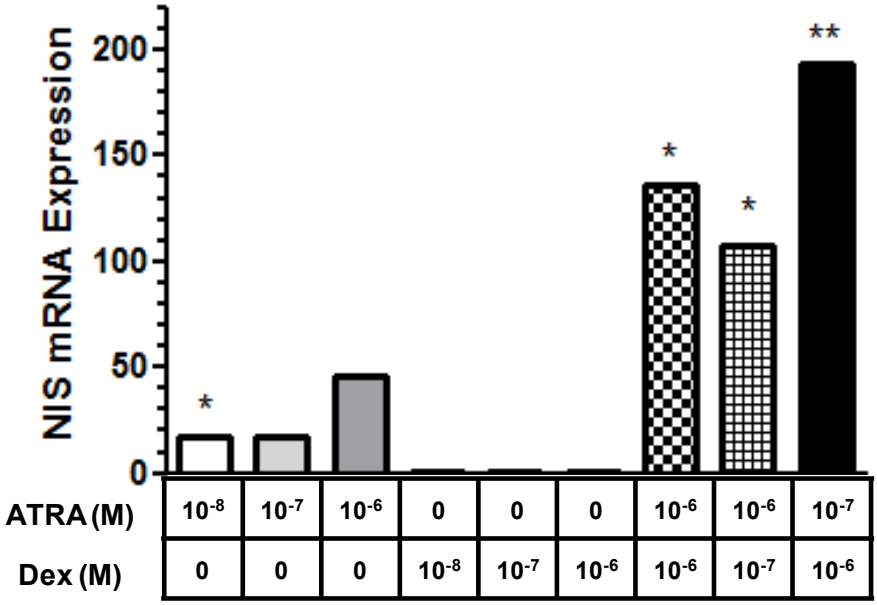

Figure 3-8. Treatment with ATRA/Dex increases NIS mRNA expression in MCF-7 cells. MCF-7 cells treated with varying doses of ATRA and dexamethasone for 48 hours were analysed by qRT-PCR for NIS mRNA expression using 18s as the internal housekeeping gene. Graph displays fold change compared with vehicle-only treated cells. Statistics were performed on ΔCT values. n=3 with 4 replicates in each n. = p<0.05. **=p<0.01.*

Though the effect of ATRA and dexamethasone on NIS levels in MCF-7 cells has been widely reported and exploited, the effect of these drugs on PBF levels has not been studied. Treatment of MCF-7 cells with varying concentrations of ATRA and dexamethasone had no significant effect on PBF mRNA levels (Figure 3-9).

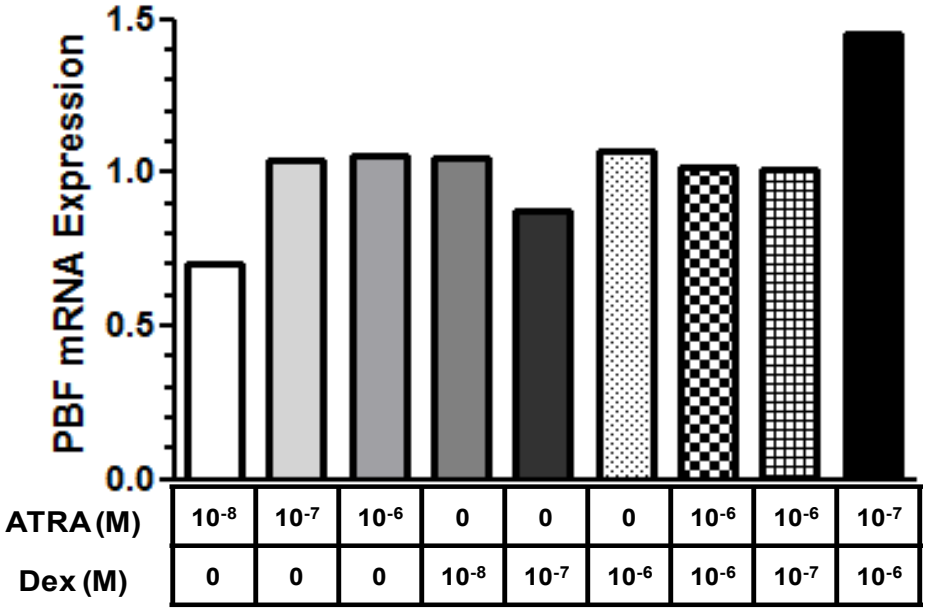

Figure 3-9. Treatment with ATRA/Dex does not significantly alter PBF mRNA expression. MCF-7 cells treated with varying doses of ATRA and dexamethasone for 48 hours were analysed by qRT-PCR for PBF mRNA expression using 18s as the internal housekeeping gene. Graph displays fold change compared with vehicle-only treated cells. Statistics were performed on ΔCT values. n=3 with 4 replicates in each n.

3.3.5 PBF expression increases NIS expression levels in breast cells

To assess whether exogenous expression of PBF had any effect on levels of NIS expression, qRT-PCR was performed on RNA extracted from MCF-7 cells stably-expressing PBF. Here, exogenous expression of PBF increased NIS expression by over 12-fold compared with vector-only expressing cells (p=0.001) (Figure 3-10).

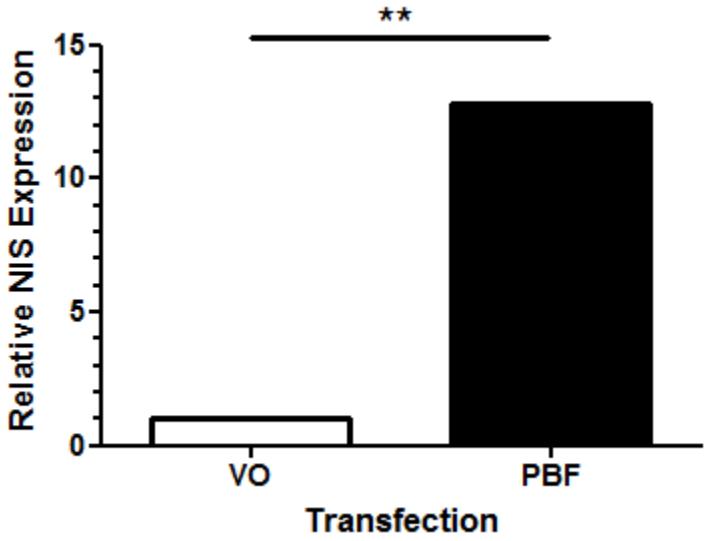

	Average ΔCT	ΔCT SEM	Fold Change	*p* value
VO	20.339	0.143	12.810	0.001
PBF	16.660	0.177		

*Figure 3-10. Exogenous PBF increases NIS mRNA expression. MCF-7 cells stably transfected with an empty vector (VO) and PBF were analysed by qRT-PCR for NIS mRNA expression using 18s as the internal housekeeping gene. Statistics were performed on ΔCT values. n=2 with 4 replicates in each n. **=p<0.01.*

Transient transfection of PBF suggested a trend of increasing NIS expression levels in MCF-7 cells (2-fold increase)(Figure 3-11). Transient transfection of PBF also further induced NIS

expression in ATRA/Dex treated cells with a 1.8-fold increase compared with empty vector transfected ATRA/Dex treated cells (*p*=0.025)(Figure 3-11).

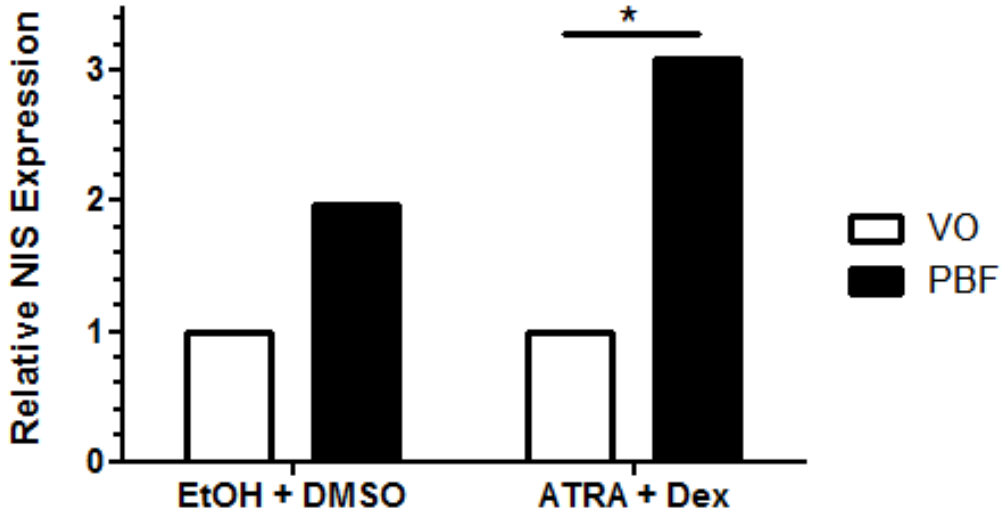

		Average ΔCT	ΔCT SEM	Fold Change
EtOH + DMSO	VO	18.374	0.591	1.973
	PBF	17.394	0.557	
ATRA + Dex	VO	14.019	0.070	3.309
	PBF	12.486	0.603	

*Figure 3-11. Transient transfection of PBF increases NIS mRNA expression. MCF-7 cells that had been transiently transfected with an empty vector (VO) or PBF and treated with ethanol and DMSO (vehicle only) or 100nM ATRA and 1µM dexamethasone were analysed by qRT-PCR for NIS mRNA expression. Statistics performed on ΔCT values. n=2 with 4 replicates in each n.. *=p<0.01.*

3.3.6 PBF Knockdown decreases NIS expression

Following induction of NIS mRNA with PBF overexpression, it was important to assess if knockdown of PBF could have the converse effect. PBF was efficiently lentivirally knocked down in MCF-7 (Figure 3-6) and MDA-MB-231 cells (Figure 3-7). Knockdown of PBF in all cell lines reduced NIS expression (Figure 3-12). In MDA-MB-231 cells lentivirally transduced

with NIS, PBF knockdown reduced NIS mRNA levels by 88% (p=0.002). PBF knockdown in MCF-7 cells decreased NIS by 44% (p=0.04).

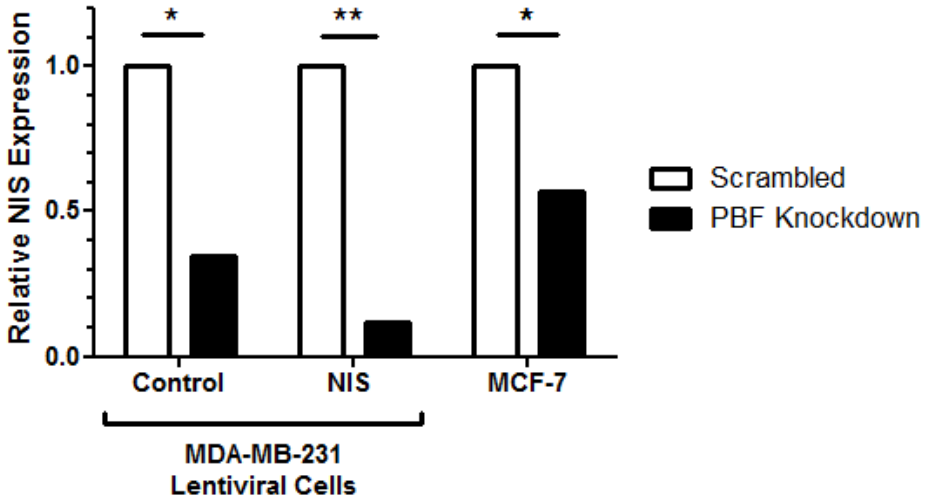

		Average ΔCT	ΔCT SEM	Fold Change	*p* value
Control	**Scrambled**	17.364	0.100	0.347	0.024
	PBF Knockdown	19.389	0.217		
NIS	**Scrambled**	8.575	0.139	0.118	0.002
	PBF Knockdown	11.653	0.081		
MCF-7	**Scrambled**	18.539	0.100	0.562	0.0426
	PBF Knockdown	19.371	0.868		

*Figure 3-12. PBF knockdown decreases NIS mRNA. MCF-7 cells and MDA-MB-231 cells lentivirally-transduced with NIS were lentivirally-transduced with scrambled or PBF shRNA. Expression levels of NIS mRNA were quantified using qRT-PCR. Statistics performed on ΔCT values. n=2 with 4 replicates in each n.. *=p<0.05. **=p<0.01.*

3.3.7 PBF reduces radioiodide uptake

To establish the effect that PBF has on NIS function, radioiodide uptake studies were performed. MCF-7 cells treated with ATRA and dexamethasone displayed increased radioiodide uptake compared with vehicle-only treated cells (8.76-fold increase, p=0.036)

in a similar manner to that observed in Kogai et al (2005)(Figure 3-13). Stable transfection of PBF within these treated cells reduced radioiodide uptake by a 28% (p=0.023) (Figure 3-13). Figure 3-13 demonstrates the levels of radioiodide uptake witnessed when cells are treated with the NIS specific inhibitor, sodium perchlorate. All future radioiodide uptake graphs have been normalised to the sodium perchlorate controls and only show specific NIS activity.

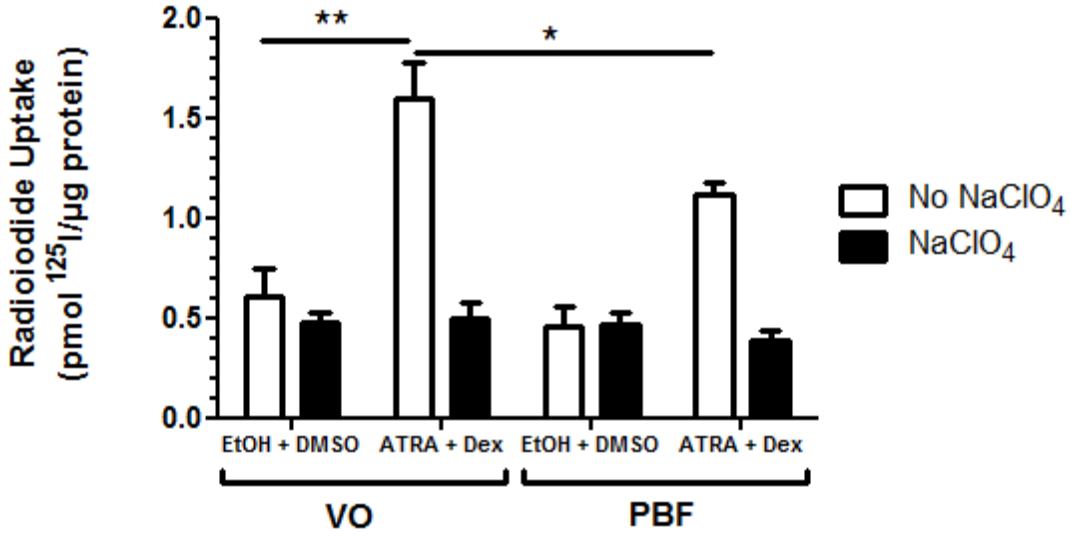

*Figure 3-13. PBF decreases the radioiodide uptake of ATRA/Dex treated MCF-7 cells. MCF-7 cells stably transfected with either a control empty vector (VO) or PBF were treated with ethanol and DMSO (vehicle) or 100nM ATRA and 1µM dexamethasone for 48 hours prior to the addition of ^{125}I. Sodium perchlorate ($NaClO_4$) controls plotted to show NIS-specific activity. n=3 with 4 replicates in each n. * = p<0.05. ** = p<0.01.*

Initial optimisation experiments were performed by varying the cell number and transfection time prior to radioiodide addition (24 hour, 48 hour and 72 hour) to allow for maximum radioiodide uptake. MDA-MB-231 cells that had been transiently transfected with NIS-MYC had a three-fold increase in radioiodide compared to control empty vector

transfected cells (Figure 3-14). Co-transfection of NIS-MYC with PBF decreased radioiodide uptake by 30% (*p*=0.0042) (Figure 3-14).

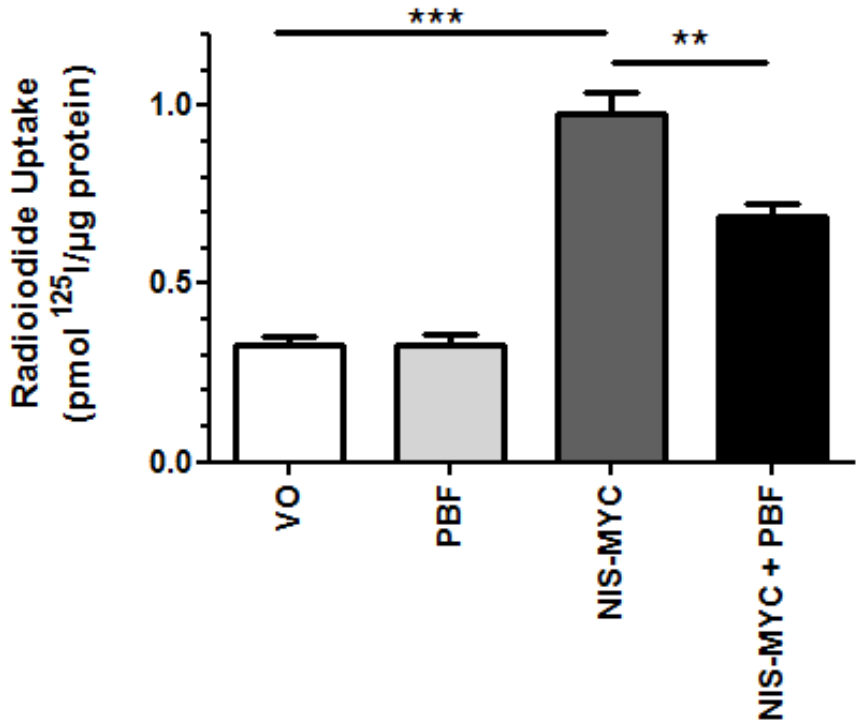

*Figure 3-14. Overexpression of PBF decreases radioiodide uptake in MDA-MB-231 cells expressing NIS. MDA-MB-231 cells were transiently transfected with an empty vector (VO), PBF and NIS-MYC for 48 hours prior to the addition of ^{125}I. Normalised to sodium perchlorate ($NaClO_4$) controls to display only NIS-specific activity. n=3 with 4 replicates in each n. ** = p<0.01. *** = p<0.001.*

3.3.8 Knockdown of PBF does not have a significant effect on radioiodide uptake

Having demonstrated that PBF overexpression reduces radioiodide uptake, it was then important to establish whether silencing PBF expression could increase radioiodide uptake. PBF was effectively silenced in MCF-7 (Figure 3-6) and MDA-MB-231 (Figure 3-7) cells using

lentiviral particles. In MCF-7 cells treated with ATRA and dexamethasone, a trend towards increased radioiodide uptake was seen with PBF knockdown (43% increase) but the data were not statistically significant (Figure 3-15A). MDA-MB-231 cells that had been transduced with NIS displayed a more modest effect with radioiodide uptake marginally increasing with PBF knockdown (19.8% and 7% for clone 1 and 2 respectively) (Figure 3-15B).

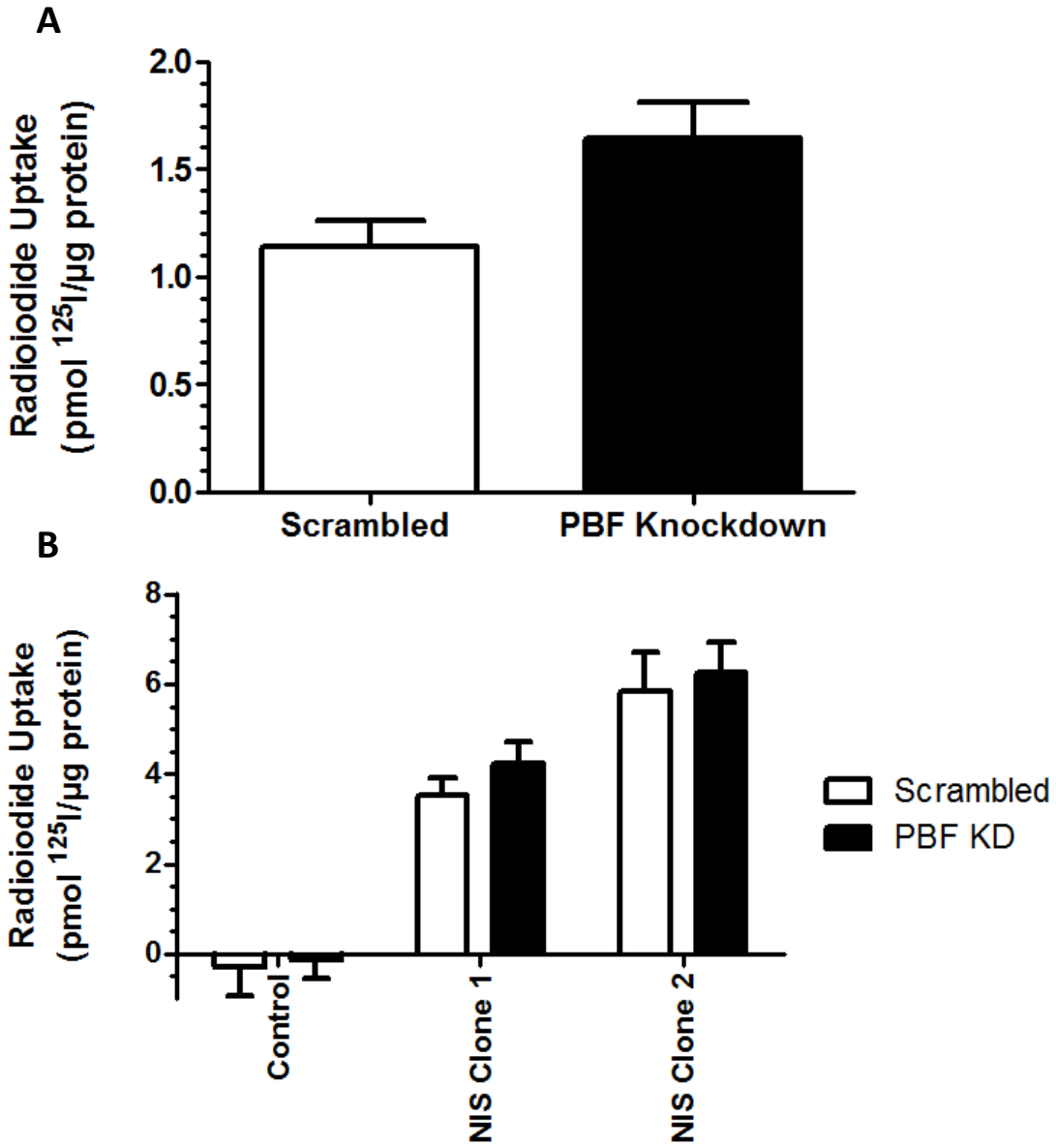

Figure 3-15. PBF knockdown effect on radioiodide uptake. (A) MCF-7 cells lentivirally-transduced with control and PBF shRNA were assessed for radioiodide uptake. n=3. (B) MDA-MB-231 cells that had been lentivirally-transduced with RFP-control (clone A) and NIS (clones 1 and 2) particles were further transduced with control and PBF shRNA particles and assessed for their ability to take up radioiodide. Normalised to sodium perchlorate ($NaClO_4$) controls to display only NIS-specific activity. n=3 with 4 replicates in each n.

3.3.9 PBF alters the subcellular localisation of NIS in breast cancer cells

Transient transfection of NIS-MYC into MCF-7 cells resulted in expression of NIS throughout the cell with some evidence of plasma membrane and cytoplasmic vesicle staining (Figure 3-16A). However when PBF-HA was co-transfected into MCF-7 cells alongside NIS-MYC there was increased cytoplasmic vesicle staining of NIS-MYC (Figure 3-16B+C) and high vesicular colocalisation between the two proteins (represented by yellow staining). Figure 3-16C in particular displays a high number of vesicles (depicted by localised yellow spots) containing NIS and PBF, compared to Figure 3-16A which has very little NIS in these locations.

3.3.10 NIS and pY174 PBF colocalise

As PBF and NIS have been observed to colocalise in breast cancer cells (3.3.9), it was important to establish whether NIS and pY174 PBF (phosphorylated PBF) were capable of colocalising in breast cancer cells. Immunofluorescence studies revealed clear colocalisation between pY174 PBF and NIS-MYC in MCF-7 cells at both the plasma membrane and in intracellular vesicles (Figure 3-17).

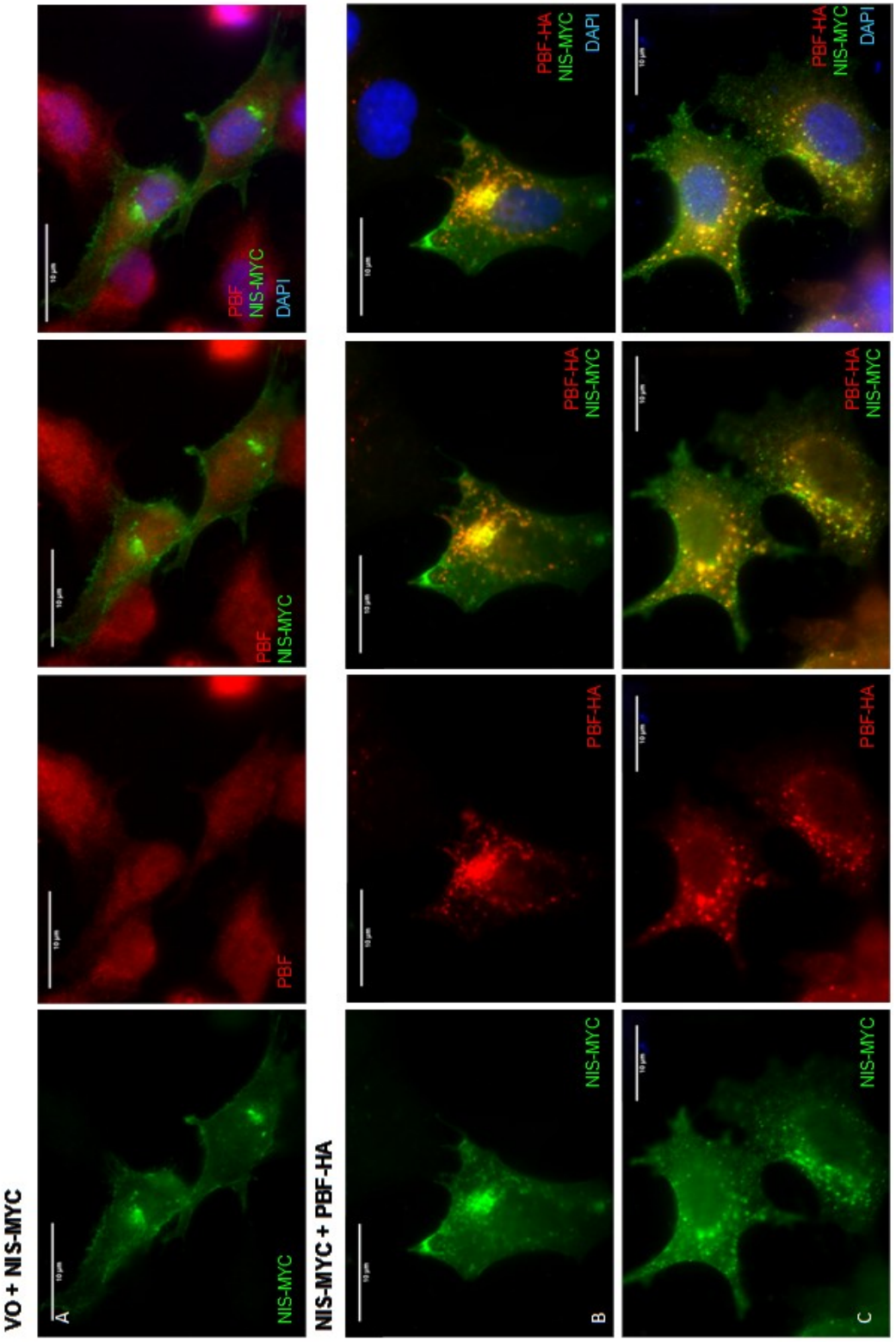

Figure 3-16. PBF alters the subcellular localisation of NIS. MCF-7 cells were co-transfected with empty pcDNA(3.1+) vector (VO) and NIS-MYC or PBF-HA + NIS-MYC. In A, NIS-MYC is visualised using a mouse anti-MYC antibody in green and a rabbit anti-PBF antibody in red. In B + C, PBF-HA is visualised using a rabbit anti-HA antibody in red and NIS-MYC visualised using a mouse anti-MYC tag antibody in green. In all images nuclei are visualised in blue using Hoechst stain. 100x magnification. n=3.

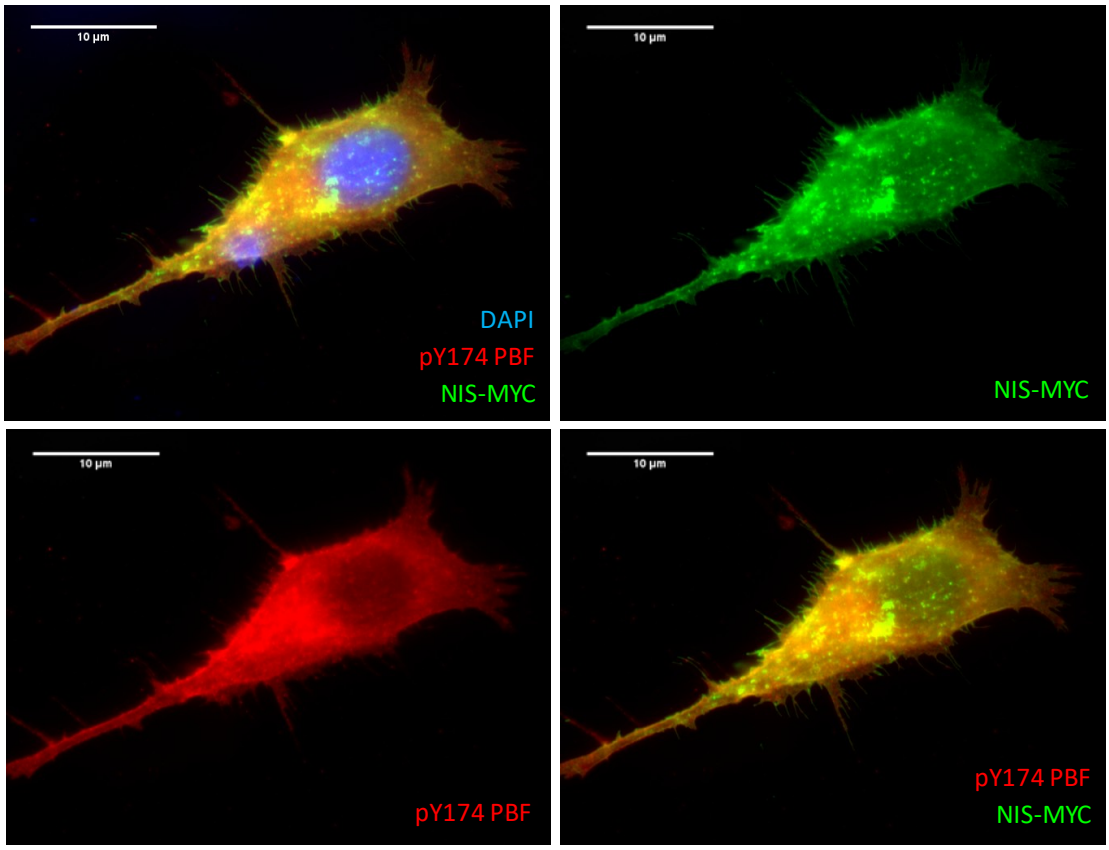

Figure 3-17. pY174 PBF and NIS colocalise within MCF-7 cells. Immunofluorescent detection of pY174 PBF (red) and NIS-MYC (green) in MCF-7 cells transfected with PBF and NIS-MYC. Yellow staining is indicative of colocalisation between pY174 PBF and NIS. Nuclei are visualised in blue with Hoechst staining. Magnification x100. n=3.

3.4 Discussion

The main aim of this chapter was to establish whether PBF and NIS were associated in breast cancer, and from the results detailed above it is clear the two proteins have a relationship in breast cancer cells.

3.4.1 PBF and NIS are both expressed in breast cancer

Though PBF and NIS expression have both independently been observed in breast cancer (Tazebay et al., 2000; Watkins et al., 2010), their expression has not previously been correlated in breast cancer. Data in this chapter showed that in 3/4 of matched normal and tumour samples both PBF and NIS are upregulated at the protein level in breast cancer tumours. Although this suggests a potential correlation between the two proteins it is important to note that this is a particularly small sample size and a large number of samples would be needed to verify this association. Unfortunately no further samples were made available to us during this PhD.

Both MCF-7 and MDA-MB-231 cells expressed endogenous levels of PBF and NIS mRNA. Although both cell-lines displayed similar levels of PBF mRNA, there was a marked difference in their NIS mRNA levels. Despite MDA-MB-231 cells having increased NIS mRNA levels compared to MCF-7 cells, there was little difference between the endogenous radioiodide uptake between the two cell-lines. This may suggest that increased levels of NIS mRNA may not necessarily lead to increased protein translation within MDA-MB-231 cells. Alternatively, the protein product may be non-functional or be aberrantly localised away from the plasma membrane. Western blotting would be

required to assess if increased NIS mRNA results in increased NIS protein in MDA-MB-231 cells compared to MCF-7 cells.

3.4.2 PBF enhances NIS mRNA expression

In thyroid cancer cell lines, PBF overexpression downregulates NIS mRNA expression through repression of both the proximal NIS promoter and the NUE, though the repression of NIS by PBF at the proximal promoter is controversial and was not witnessed in primary thyrocytes (Boelaert et al., 2007). Here we did not observe any repression of NIS mRNA or protein expression by PBF; instead overexpression of PBF appeared to enhance NIS expression. PBF was capable of increasing NIS mRNA levels in both the presence of endogenous NIS, ATRA/Dex-induced NIS and exogenous NIS. Conversely, the knockdown of PBF in breast cancer cells decreased NIS expression, further suggesting a positive correlation between PBF and NIS expression.

These data directly contradict the relationship observed between PBF and NIS in thyroid cancer. However as the repression of NIS by PBF has been reported to occur primarily by interaction with the NUE, an enhancer that has been identified to be thyroid-specific, the lack of repression is unsurprising. The novel finding is that NIS is upregulated by PBF. One potential hypothesis for this induction could be due to Akt, a known downstream target of the PI3K pathway which has been heavily associated with NIS regulation in breast cancer cells (Kogai et al., 2008). In transgenic mice with thyroid-specific overexpression of PBF, significantly increased levels of the phosphorylated forms of p-Akt have been reported compared to WT mice, with no change to total Akt levels (Read et al., 2011). If PBF overexpression influences Akt phosphorylation and activity, it

may constitute a mechanism for the upregulation of NIS witnessed in the presence of PBF overexpression.

Western blotting would be required to establish that the effects observed with NIS mRNA translate to protein expression. However due to limitations with the PBF antibody this could unfortunately not be performed as part of this work. There were few commercial PBF antibodies available each with limited functionalities so for throughout this project a custom made PBF antibody was utilised which was not fully optimised during this initial phase of the thesis.

3.4.3 PBF represses NIS function

As previously observed in thyroid cancer, PBF overexpression reduced radioiodide uptake in breast cells. Here we have shown that PBF affects NIS functionality in a similar manner in breast cells. The reduction in radioiodide uptake in breast cancer cells is consistently above 25% in the presence of PBF whether NIS is exogenously expressed or endogenously enhanced. However, the knock-down of PBF was incapable of increasing radioiodide uptake in several experimental scenarios. It is possible that this conflicting data may be due to the fact that NIS expression is greatly reduced in cells that have PBF silenced and with the overall reduction in NIS levels it may be difficult to observe the effect PBF knockdown has on the protein function alone.

3.4.4 PBF alters the subcellular localisation of NIS in breast cancer

As in thyroid cancer, PBF was observed to colocalise with NIS and alter its subcellular localisation. Overexpression of both proteins in breast cancer cells increased NIS staining in intracellular vesicles where a high level of colocalisation with PBF was apparent. Not only did NIS colocalise with total PBF, there was also a high level of colocalisation with pY174 PBF within both the plasma membrane and intracellular vesicles in breast cancer cells. These data agree with the previous findings in thyroid cancer (Smith et al., 2011; Smith et al., 2009; Smith et al., 2013). NIS has previously been described to be located intracellularly within breast cancer cells (Beyer et al., 2009; Tazebay et al., 2000) and as hypothesised this may be due to its interaction with upregulated PBF in breast cancer.

Overall, it is clear from these data that PBF and NIS have a functional relationship in breast cancer. PBF can alter the subcellular localisation of NIS and repress NIS function within breast cancer cells. This is similar to the relationship observed in thyroid cancer cells between PBF and NIS. This is potentially therapeutically important as it supports the hypothesis that PBF represses radioiodide uptake in breast cancer cells and that inhibition of PBF and NIS interaction may increase radioiodide uptake. Therefore it was of great interest to establish whether phosphorylation of Y174 in PBF is critical for the interaction between NIS and PBF in breast cancer cells as observed in thyroid cancer.

CHAPTER 4 - PHOSPHORYLATION MUTANTS OF PBF DO NOT BIND TO NIS OR DECREASE RADIOIODIDE UPTAKE

4.1 Introduction

PBF has been described as a membrane glycoprotein with expression primarily at the plasma membrane and in cellular vesicles (Smith et al., 2009). The presence of a tyrosine-based sorting signal within the C-terminal region of PBF has been observed to be critical for the correct trafficking of PBF in cells (Smith et al., 2013). Tyrosine-based sorting signals have a prominent role in endocytosis (Collawn et al., 1990) and sorting to lysosomes (Guarnieri et al., 1993) with the motif sequence being YXXϕ (where Y is tyrosine, X is any amino acid and ϕ is an amino acid with a bulky hydrophobic side chain) (Canfield et al., 1991). The YXXϕ signals are recognised by homologous μ1, μ2, μ3 and μ4 subunits of the corresponding heterotetrameric adaptor protein (AP) complexes AP-1, AP-2, AP-3 and AP-4 that function as cargo adaptors (Mardones et al., 2013). PBF conforms to the YXXϕ motif between amino acids 174-177 where the sequence is YARF and mutation of either Y174 or F177 to alanine leads to accumulation of PBF at the plasma membrane (Smith et al., 2013).

Residue Y174 of PBF appears to be critical for multiple roles within the protein, being both the lead tyrosine of the sorting signal as well as being strongly predicted to be phosphorylated. Phosphorylation at this residue has been confirmed in many cell-lines including both COS-7 (monkey kidney epithelial) and K1 (human thyroid cancer) cell-lines (Smith et al., 2013). PBF phosphorylated at Y174 was demonstrated to colocalise with NIS in a variety of cell lines including T47D breast cancer cells. An interaction between Y174A PBF and NIS was assessed and mutation of the tyrosine to alanine almost completely abrogated PBF binding to NIS (Smith et al., 2013).

The evidence thus far suggested that Y174 is critical for PBF localisation and for interaction with NIS. However it was not obvious whether differences in interaction with NIS are due to differences in PBF phosphorylation or localisation. To assess whether phosphorylation alone is critical for the interaction, a mutant that retains normal PBF localisation but is unable to be phosphorylated was required. In this chapter the consensus sequence for kinase recognition of PBF was identified and mutated. It was proposed that mutating this consensus sequence would abrogate phosphorylation of PBF but retain PBF's native cellular trafficking as the sorting signal would remain intact. Here, a mutant retaining normal PBF localisation yet lacking phosphorylation was identified, described and assessed in comparison to WT and Y174A PBF.

4.2 Material and Methods

4.2.1 Prediction Tools

To aid with the generation of a phospho-Y174 (pY174)-null mutant form of PBF, phosphorylation prediction software was utilised. The primary software employed was the online tool NetPhos 2.0 (Blom et al., 1999). The PBF peptide sequence was obtained from NCBI (accession number - AAH31097), altered to have mutations in the amino acid sequence surrounding Y174 and inputted to NetPhos 2.0 in FASTA format. To confirm predictions additional phosphorylation tools were utilised:- PhosphoMotif Finder (Amanchy et al., 2007), GPS3.0 (Xue et al., 2008) and KinasePhos2.0 (Wong et al., 2007).

4.2.2 Cell Culture

MCF-7 and MDA-MB-231 cells were maintained as described in 2.1.2 with stably-transfected MCF-7 cells cultured in medium containing G418 (1 mg/ml) and lentivirally-transduced MDA-MB-231 cells cultured in medium containing blasticidin (15 µg/ml). All cell lines were seeded at $3x10^4$cells per well in a 24 well plate for radioiodide uptake and at $1.5x10^5$ and $2x10^5$ cells per well in a 6 well plate for fluorescence immunocytochemistry and protein extraction respectively.

4.2.3 ATRA and Dexamethasone Treatment

MCF-7 cells were treated with 100 nM ATRA and 1 µM dexamethasone as described in section 3.2.3. An equal volume of ethanol and DMSO in cell media was used as a control.

4.2.4 Mutagenesis

The pcDNA3.1 (+)_PBF and pcDNA3.1 (+)_PBF-HA plasmids were mutated using the QuikChange II XL Site-Directed Mutagenesis kit (Agilent, California, USA). Forward and reverse primers for mutagenesis were designed and produced (Sigma) in accordance with the kit protocol to ensure maximum efficiency. 10 ng plasmid DNA was combined with 125ng mutagenic forward and reverse primers (Table 4-1), 5 µl 10x reaction buffer, 1 µl dNTP mix, 3 µl Quiksolution, 2.5 U *PfuUltra* HF DNA polymerase and made up to a total volume of 50 µl with nuclease free water. Following an initial denaturation step at 95°C for 1 minute, 18 cycles of PCR were performed including denaturation (95°C for 50 seconds), primer annealing (60°C for 50 seconds) and primer extension (68°C for 6 minute). After an additional 7 minutes at 68°C, the reaction was cooled to 37°C. 10U *Dpn*, a restriction enzyme which specifically cleaves methylated and hemi-methylated DNA, was added to each reaction and incubated for 1 hour at 37°C to digest parental supercoiled dsDNA. XL10-Gold® Ultracompetent bacterial cells were transformed by the addition of 2 µl of the reaction mixture, incubated on ice for 30 minutes, followed by heat shock at 42°C for 30 seconds and returned to ice for a further 2 minutes. The cells were then plated on Lysogeny broth-carbenicillin (100 µg/ml) plates and incubated overnight at 37°C.

	Sequence
EEN170-172AAA Forward	**5'** GA AAA AAA TAT GGC CTG TTT AAA G**C**A G**C**A **GC**C CCG TAT GCT AGA TTT G **3'**
EEN170-172AAA Reverse	**5'** C AAA TCT AGC ATA CGG G**GC** T**G**C T**G**C TTT AAA CAG GCC ATA TTT TTT TC **3'**

Table 4-1. Mutagenesis primers for EEN170-172AAA PBF. The red letters signify changes to the PBF sequence that result in amino acid substitutions.

4.2.5 Plasmid Purification and Sequencing

Carbenicillin-resistant bacterial colonies were used to inoculate 5ml LB containing carbenicillin (100 µg/ml) and incubated at 37°C for 16 hours with shaking at 200 rpm. Purification was performed using the Wizard® Plus SV Miniprep DNA Purification System (Promega) according to manufacturer's instructions. 1.5 ml of the bacterial suspension was centrifuged at 10,000 x g for 5 minutes and the supernatant discarded. Cells were re-suspended in 250 µl Cell Resuspension Solution and lysed using 250 µl Cell Lysis Solution and incubation at room temperature until the suspension had cleared. The lysate was incubated for 10 minutes with 10 µl alkaline protease to inactivate any endonucleases released during cell lysis. To terminate lysis, 350 µl Neutralisation Solution was added and the suspension inverted 4 times before centrifuging for 10 minutes at 14,000 x g. The cleared lysate was transferred to a spin column and further centrifuged at 14,000 x g for 1 minute, discarding the eluate. Plasmid DNA was washed twice by centrifugation with Column Wash Solution (750 µl wash 1, 250 µl wash 2). Finally, the DNA was eluted with 100 µl nuclease free water. DNA quantification was carried out using a NanoDrop© ND-1000 Spectrophotometer (NanoDrop) and accompanying ND-1000 v3.3 software on the DNA-50 setting. DNA was then sequenced as described in 2.2.2.3.

To further amplify the mutated plasmid, purified plasmid DNA was used to transform DH5-α bacterial cells as described in 2.2.2.1 and the DNA then amplified using the Sigma GenElute™ HP Plasmid Maxiprep kit as described in 2.2.2.2.

4.2.6 Development of Stable and Lentiviral Cell lines

4.2.6.1 Stable Transfection

MCF-7 and MDA-MB-231 cells were stably transfected with an empty pCI-neo vector, PBF (kindly gifted by Dr Vicki Smith), Y174A (kindly gifted by Waraporn Imruetaicharoenchoke) and EEN170-172AAA in the pCI-neo vector as described in 2.2.4. Stable transfection was confirmed using qRT-PCR.

4.2.7 Transient Transfection

Transfection was performed as described in 2.2.3. WT PBF-HA, EEN/AAA PBF-HA, Y174 PBF-HA, NIS-MYC (kindly gifted by Dr Vicki Smith) and EEN170-172AAA in the pcDNA3.1 (+) vector were transfected into MCF-7 cells in 6 well plates for use in fluorescence immunocytochemistry and Western blotting. For radioiodide uptake, cells were seeded in 24 well plates and transfected with untagged forms of WT, EEN170-172AAA and Y174A PBF alongside NIS-MYC.

4.2.8 Radioiodide uptake

Radioiodide uptake was performed as described in 2.7. Transfection and drug treatments were performed 48 and 24 hours respectively before the addition of ^{125}I to cells.

4.2.9 Western Blotting

Protein extraction and Western blotting were performed as described in 2.3.1 and 2.3.2 respectively. Cells were treated with 100µM sodium pervanadate for 20 minutes prior to harvesting to allow the detection of pY174 PBF. Antibodies used were anti-pY174 PBF antibody (Smith et al., 2013), anti-PBF (Smith et al., 2009), anti-phospho-Src (Y418) (Abcam), anti-Src (Cell Signalling) and β-actin (Sigma-Aldrich) (refer to section 2.8). Appropriate secondary antibodies were used.

4.2.10 Fluorescence immunocytochemistry

Fluorescence immunocytochemistry was performed as described in 2.4. Cells were treated with 100µM sodium pervanadate for 20 minutes prior to fixing to allow the detection of pY174 PBF. Antibodies used included anti-pY174 PBF antibody (1:50) (Covalab) (Smith et al., 2013), anti-HA tag (mouse) (1:200) (Covance), anti-HA tag (rabbit) (1:100) (Santa Cruz) and anti-Myc tag (1:750) (Cell Signalling).

4.2.11 BrdU proliferation

Proliferation was assessed using a cell proliferation ELISA BrdU (5-bromo-2'-deoxyuridine) (colorimetric) assay (Roche). BrdU is a synthetic pyrimidine analogue, which is incorporated in place of thymidine into DNA during replication. This analogue can be detected by a peroxidase-conjugated BrdU antibody, which cleaves tetramethylbenzidine (TMB) substrate producing a blue colouring, therefore providing a method to quantify proliferation.

The BrdU assays were performed according to the manufacturer's instructions. Cells were seeded at 2,500 per well in a 96 well plate for 24 hours prior to the assay being performed. Cells were incubated with 10 µM BrdU labelling solution at 37°C for 4 hours. After removal of the labelling solution, cells were incubated at room temperature for 30 minutes with 200 µl FixDenat Solution. Once removed, 50 µl anti-BrdU-POD (Monoclonal antibody from mouse-mouse hybrid cells (clone BMG 6H8, Fab fragments) conjugated with peroxidase (POD)) (10 µM) were added to each well and left for 90 minutes. Antibody solution was then removed and the wells washed 3 times with 200 µl BrdU wash solution before 100 µl BrdU-POD substrate (tetrametyl-benzidine) solution was added to each well. After brief shaking, the absorbance was then read at 405nm using the Wallac Victor plate reader.

4.2.12 Co-immunoprecipitation Assay (Co-IP)

Cells were cultured in T75 flasks and transfected as described in 2.2.3 for 48 hours. Prior to harvesting cells were treated for 20 minutes with 100 µM sodium pervanadate. Cells were then washed in PBS and harvested in 1 ml RIPA containing 60 µl/ml protease

inhibitor cocktail (Sigma) and phosphatase inhibitor cocktails 2 and 3 (1% v/v) (Sigma). Lysates were subjected to end-over-end rotation for 10 minutes at 4°C before being sonicated for 30 seconds (medium setting, Bioruptor Standard, Diagenode, Liège, Belgium) and undergoing an additional 10 minutes end-over-end rotation. Cell debris was then pelleted and lysate transferred to a fresh micro-centrifuge tube. 100 µl of lysate were removed and stored at -20°C for use as the whole cell lysate. The remaining lysate was incubated with primary anti-Myc antibody (7.5 µl) overnight at 4°C with end-over-end rotation. Protein G sepharose beads (GE Lifesciences, Little Chalfont, Buckinghamshire, UK) were washed in RIPA buffer before a 1:1 (v:v) bead slurry was prepared in RIPA. The bead slurry (50 µl) was then added to each sample and incubated for 3 hours at 4°C with end-over-end rotation. The samples were briefly centrifuged, the supernatant discarded and the pelleted beads washed in 500 µl RIPA three times. Bound proteins were eluted from the beads in 50 µl 2x Laemmli buffer (Bio-Rad) containing 1:20 β-mercaptoethanol (Sigma) by heating for 30 minutes at 37°C. The samples were pelleted and the supernatants transferred to fresh tubes and stored at -20°C ready for Western blotting as described in 2.3.2. The whole cell lysates retained earlier were denatured in 5x Laemmli buffer (250 mM Tris-HCl pH6.8, 10% SDS, 0.02% bromophenol blue, 50% glycerol and 12.5% β-mercaptoethanol) prior to Western blotting.

4.2.13 RNA extraction and qRT-PCR

RNA extraction, reverse transcription and qRT-PCR were performed as described in 2.5 and 2.6. Expression of PBF was assessed using the PBF TaqMan® Gene Expression Assay (Hs01036322_m1) (Life Technologies). Expression of NIS was assessed using custom-made primers and probe (Table 3-1).

4.2.14 Statistics

Data were analysed using Sigma Plot (SPSS Science Software UK Ltd). The student's t-test was utilised to compare data between two groups whereas the one-way ANOVA was used to compare more than two groups of parametric data with significance taken at $p < 0.05$ for both.

4.3 Results

4.3.1 Prediction of non-phosphorylated forms of PBF

NetPhos 2.0 (Blom et al., 1999) was initially utilised to predict the effect of mutating amino acids upstream of Y174 on the phosphorylation of this tyrosine residue. Figure 4-1 shows that WT PBF is predicted to be phosphorylated at Y174 and mutation of this tyrosine to alanine removes all phosphorylation potential. Single amino acid substitutions were subsequently made to residues upstream of Y174, however individual mutations were not capable of reducing phosphorylation potential below the threshold (data not shown). Multiple substitutions were then run through the prediction tool (data not shown) and EEN170-172AAA (EEN/AAA) was found to reduce the phosphorylation potential to below the predicted threshold at Y174 (Figure 4-1). Mutating these residues to similarly charged amino acids could not reduce phosphorylation potential (data not shown). The sequence of the prospective EEN/AAA mutant was further tested for phosphorylation potential using different phosphorylation prediction tools that confirmed this mutant was not likely to be phosphorylated.

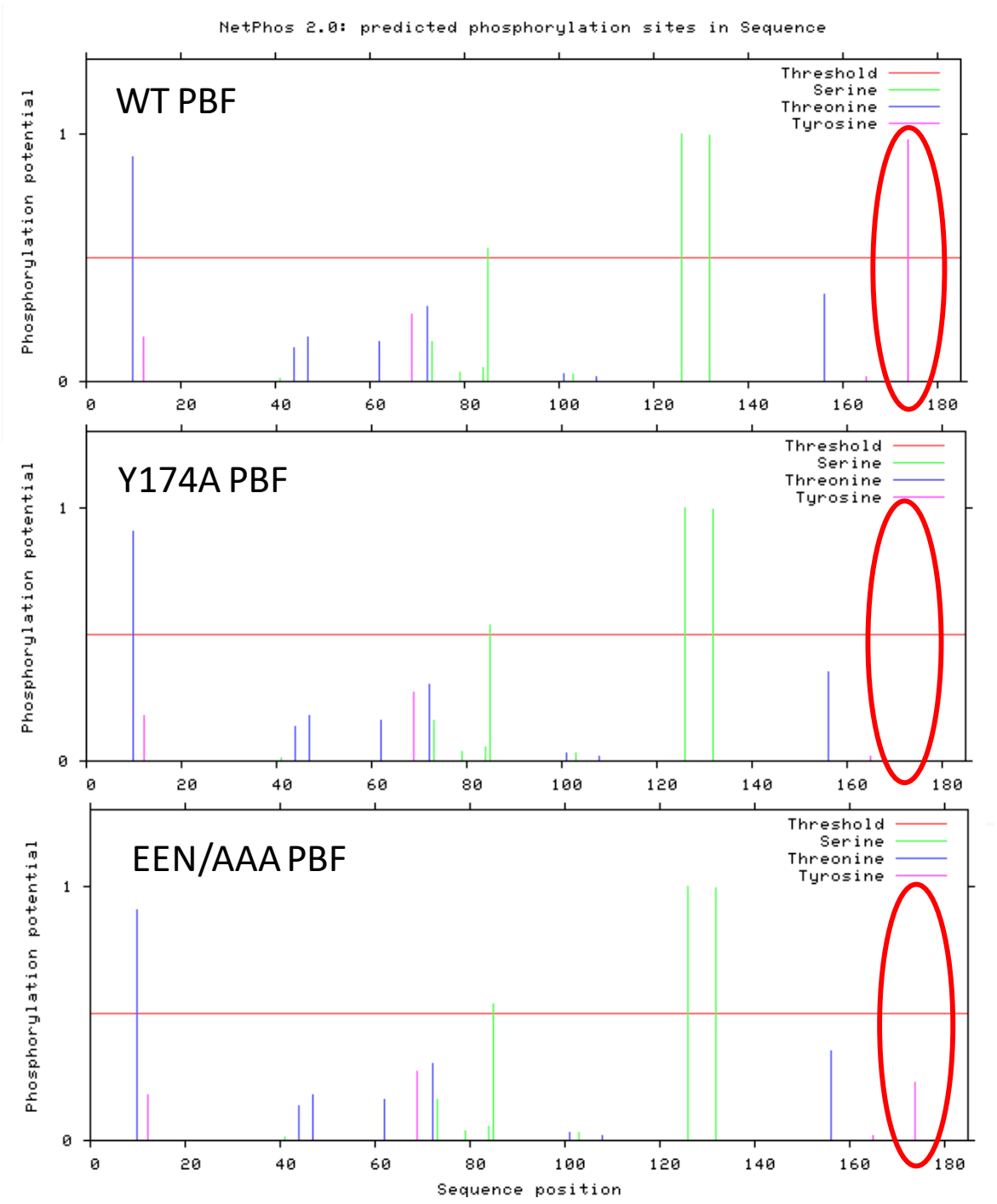

Figure 4-1. Phosphorylation potential of WT PBF and mutant forms. NetPhos 2.0 (Blom et al., 1999) was utilised as a phosphorylation prediction tool. The charts show the phosphorylation potential of proteins at serine (green), threonine (blue) and tyrosine (pink) residues. Peaks crossing the red threshold line are considered to be phosphorylated (Blom et al., 1999). Red circles highlight the residue of interest –Y174.

4.3.2 Creation of EEN/AAA

Wild-type PBF was successfully mutated to EEN170-172AAA (EEN/AAA) using site-directed mutagenesis. The new plasmid was sequenced and NCBI tools nucleotide BLAST (http://blast.ncbi.nlm.nih.gov/Blast.cgi?PROGRAM=blastn&PAGE_TYPE=BlastSearch&LINK_LOC=blasthome) and BLAST x (http://blast.ncbi.nlm.nih.gov/Blast.cgi?PROGRAM=blastx&PAGE_TYPE=BlastSearch&LINK_LOC=blasthome) were used to compare the sequences. BLAST confirmed the correct mutation of the PBF plasmid, with both the nucleotide sequence (Figure 4-2) and translated amino acid sequence revealing the correct mutation.

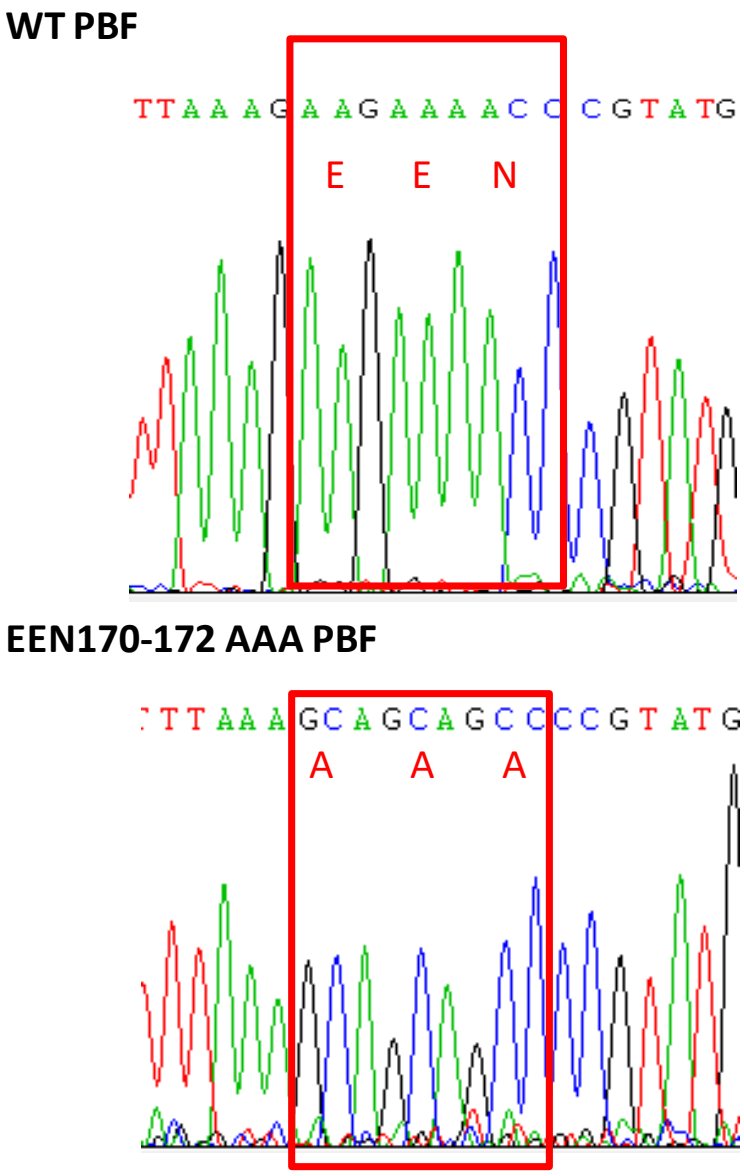

*Figure 4-2. Successful mutation of PBF at residues 170-172. Sequencing of the pcDNA 3.1 plasmid containing human PBF confirmed successful mutagenesis of GAA GAA AAC (EEN/AAA) to G**C**A G**C**A **GC**C (AAA).*

4.3.3 Predicted Structure of WT and EEN/AAA PBF

The sequence of PBF and the two mutants, Y174A and EEN/AAA, were entered into the Protein Homology/analogY Recognition Engine V 2.0 (Phyre2) online tool (Kelley et al., 2015) which predicts protein structure based on homology and analogy to proteins that have had their structure determined. WT PBF is primarily made up of α-helix and

unstructured regions (Figure 4-3). The C-terminal end of WT PBF, which contains the residue of interest Y174, is predicted to be largely unstructured. When this tyrosine residue at position 174 is mutated to alanine, the C-terminal end encompassing this residue changes structure and is predicted to be an α-helix. However, the C-terminal structure of EEN/AAA PBF is very similar to WT with the region being largely unstructured (Figure 4-3).

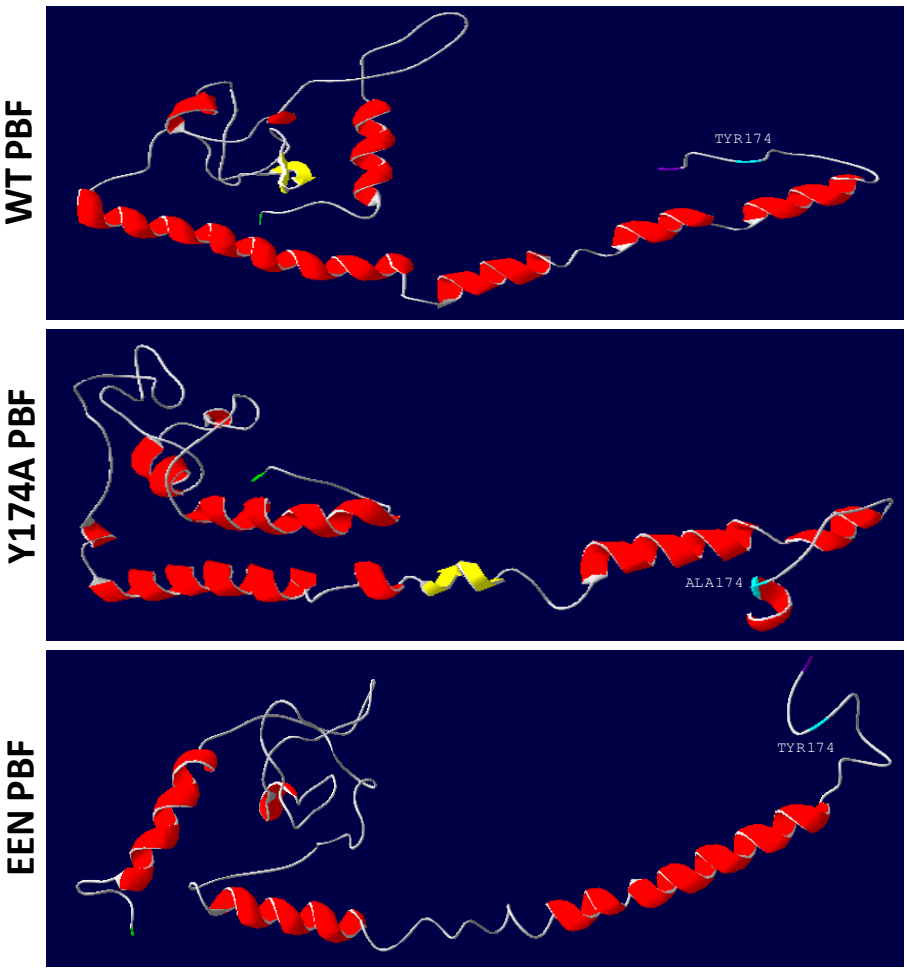

Figure 4-3. Structure of WT, Y174A and EEN/AAA PBF. The sequences of the 3 forms of PBF were entered into the Protein Homology/analogY Recognition Engine V 2.0 (Phyre2) online tool (Kelley et al., 2015) creating a model which could be manipulated within Swiss Pdb viewer. Red ribbon represents α-helices with yellow ribbon representing β-sheets. N-terminal residues are lime green and located to the left of the image whereas C-terminal residues are displayed in violet to the right of the image. The baby blue labelled residue represents the residue of interest Y174.

4.3.4 EEN/AAA PBF is not phosphorylated at Y174

To determine the phosphorylation status of the EEN/AAA PBF mutant, WT, EEN/AAA and Y174A PBF were transiently transfected into MCF-7 cells. Western blotting using the pY174-specific antibody demonstrated strong pY174 PBF expression with WT PBF transfection but pY174 PBF was not detected in either the EEN/AAA or Y174A PBF transfected cells (Figure 4-4). Both total PBF and β-actin showed equal expression in all three cell lysates (Figure 4-4), suggesting that the prediction tools were correct and EEN/AAA PBF is incapable of being phosphorylated at Y174.

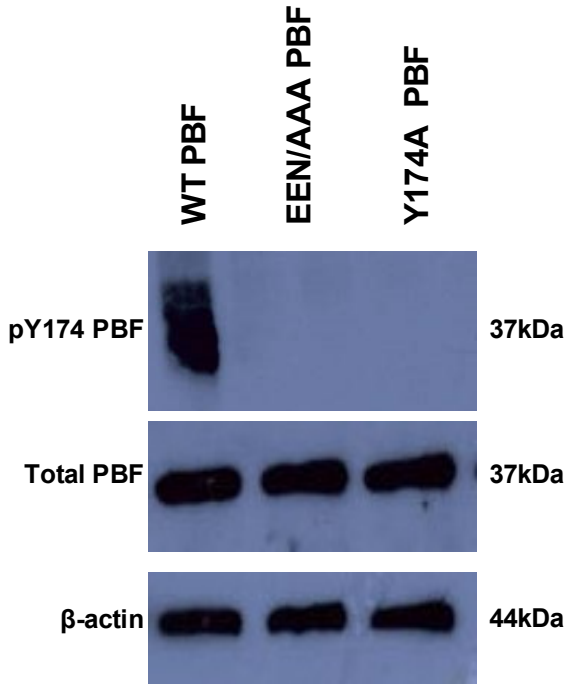

Figure 4-4. EEN/AAA PBF is not phosphorylated at Y174. MCF-7 cells were transfected with WT, EEN/AAA and Y174A PBF for 48 hours prior to harvesting. pY174 PBF and total PBF were detected with β-actin used as a loading control. n=3.

4.3.5 Generation of Stable Cell lines

To enable the study of PBF in breast cancer cells, MCF-7 and MDA-MB-231 cells were stably transfected with WT, EEN/AAA and Y174A PBF. Stable transfection in MDA-MB-231 cells significantly increased PBF mRNA expression with a 9.3, 3.3 and 29.4-fold increase retrospectively compared to empty vector transfected cells (Figure 4-5). This increased expression of PBF was confirmed by Western blotting, where although limited pY174 PBF was detected in cells transfected with EEN/AAA and Y174 PBF, there was a distinct increase in total PBF levels compared to empty vector transfected cells. Endogenous pY174 PBF was also detected in both cell-lines as observed in the pCI-neo empty vector stably transfected cells. MCF-7 cells also had significantly increased PBF expression after transfection with WT, EEN/AAA and Y174A PBF with an increase of 3.8, 5.5 and 4.6 -fold respectively (Figure 4-6).

A

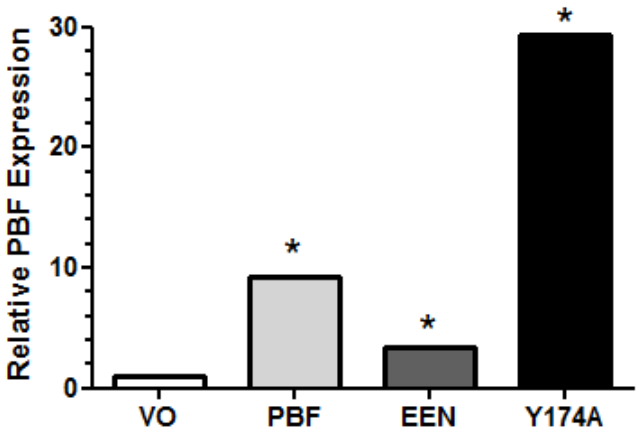

	Average ΔCT	ΔCT SEM	Fold Change	*p* value
VO	11.762	0.144	-	-
PBF	8.595	0.504	9.266	0.026
EEN	10.089	0.302	3.343	0.038
Y174A	7.035	0.527	29.415	0.013

B

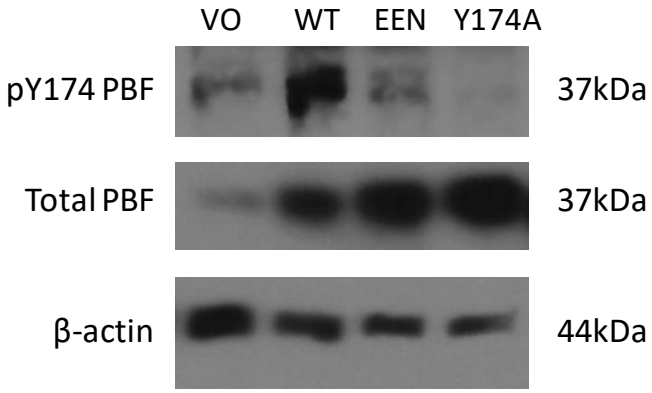

*Figure 4-5. Expression of pY174 PBF, total PBF and NIS in stably transfected MDA-MB-231 cells. (A) Relative expression of PBF as determined by qRT-PCR in MDA-MB-231 cells stably transfected with pCI-neo empty vector (VO), WT, EEN/AAA and Y174A PBF normalised to the empty vector control. Statistics were performed on ΔCT values. n=3 with 4 replicates in each n. *=p<0.05 compared to the empty vector control. (B) Western blotting of MDA-MB-231 cells stably transfected with pCI-neo empty vector (VO), WT, EEN/AAA and Y174A PBF. pY174 and total PBF were detected with β-actin used a loading control. n=2.*

A

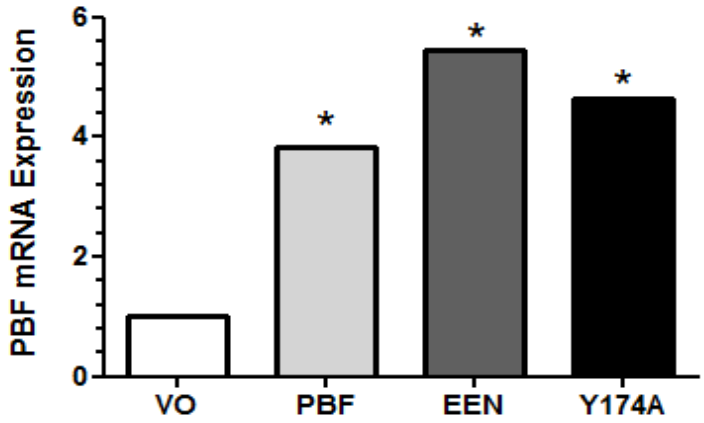

	Average ΔCT	ΔCT SEM	Fold Change	*p* value
VO	15.702	0.145	-	-
PBF	13.769	0.002	3.840	0.048
EEN	13.260	0.274	5.456	0.033
Y174A	13.579	0.272	4.640	0.049

B

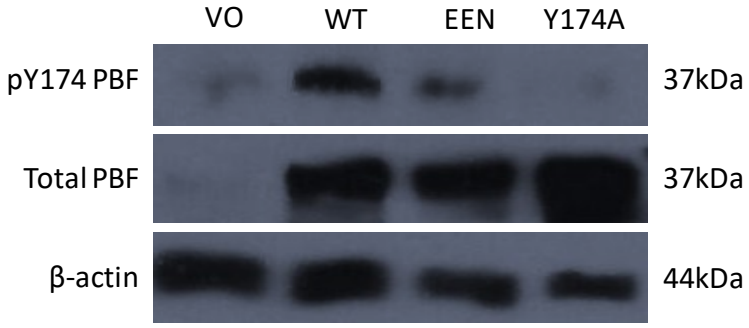

Figure 4-6. Expression of pY174 PBF, total PBF and NIS in stably transfected MCF-7 cells. (A) Relative expression of PBF as determined by qRT-PCR in MCF-7 cells stably transfected with pCI-neo empty vector (VO), WT, EEN/AAA and Y174A PBF normalised to the empty vector control transfected cells. Statistics were performed on ΔCT values. n=3 with 4 replicates in each n.=p<0.05 compared to the empty vector control. (B) Western blotting of MCF-7 cells stably transfected with pCI-neo empty vector (VO), WT, EEN/AAA and Y174A PBF. pY174 and total PBF were detected with β-actin used a loading control. n=2.*

4.3.6 Proliferation is not affected by the phosphorylation status of PBF

PBF has previously been observed to be mildly pro-proliferative in transgenic mouse thyroids (Read et al., 2011). To establish whether the phosphorylation status of PBF had

any effect on proliferation, BrdU assays were employed in cells stably transfected with WT PBF and the phosphorylation mutants. In MCF-7 and MDA-MB-231 cells proliferation following PBF overexpression was not significantly different from the empty vector control but there was a slight trend towards being mildly proliferative (Figure 4-7). There was no significant difference in proliferation between WT PBF and the two phosphorylation mutants in either cell-line (Figure 4-7).

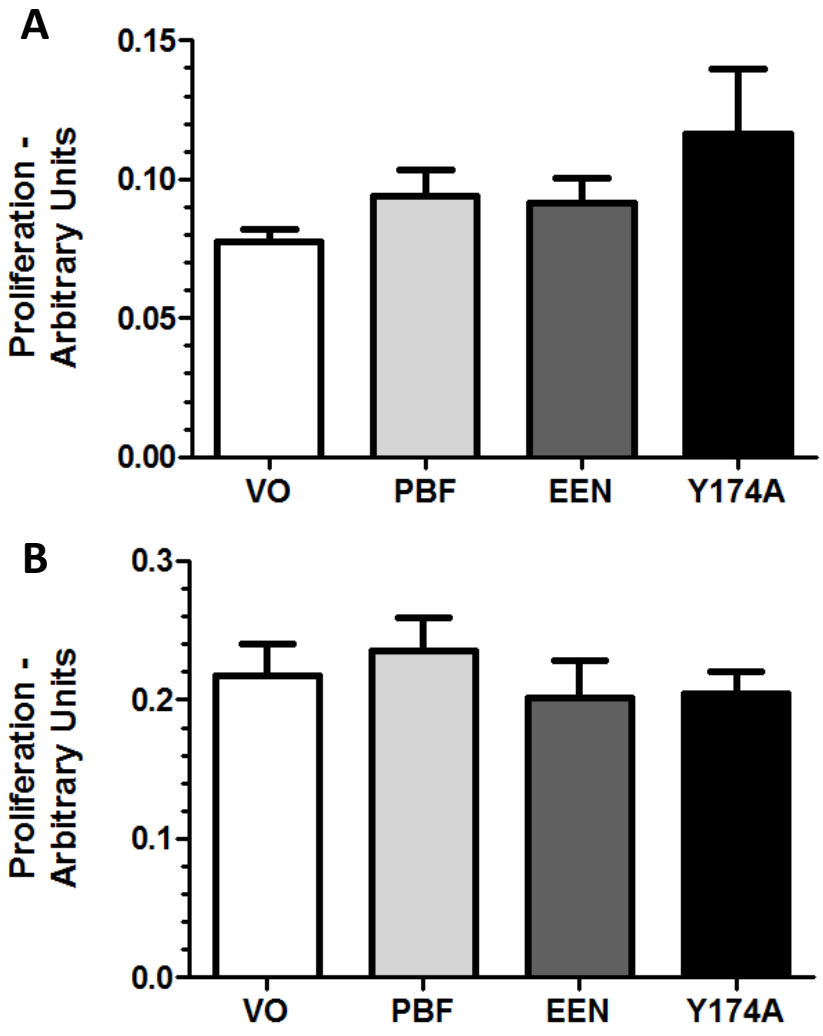

Figure 4-7. Phosphorylation status of PBF does not affect proliferation. BrdU assays were performed on MCF-7 (A) and MDA-MB-231 (B) cells stably-transfected with empty vector (VO), WT, EEN/AAA and Y174A PBF. n=3 with 4 replicates in each n.

4.3.7 EEN/AAA PBF is not retained in the plasma membrane

Fluorescence immunocytochemistry was utilised to assess the localisation of EEN/AAA PBF within MCF-7 cells. WT PBF was localised ubiquitously throughout the cells, with some plasma membrane expression but the majority located within the cytoplasm (Figure 4-8). As demonstrated previously (Smith et al., 2013), Y174A PBF was retained in the plasma membrane and was apparent within cell ruffles and lamellipodia (Figure 4-8). In contrast, EEN/AAA PBF localised in a similar manner to WT PBF, primarily being located within the cytoplasm but with some staining in the plasma membrane and into lamellipodia (Figure 4-8).

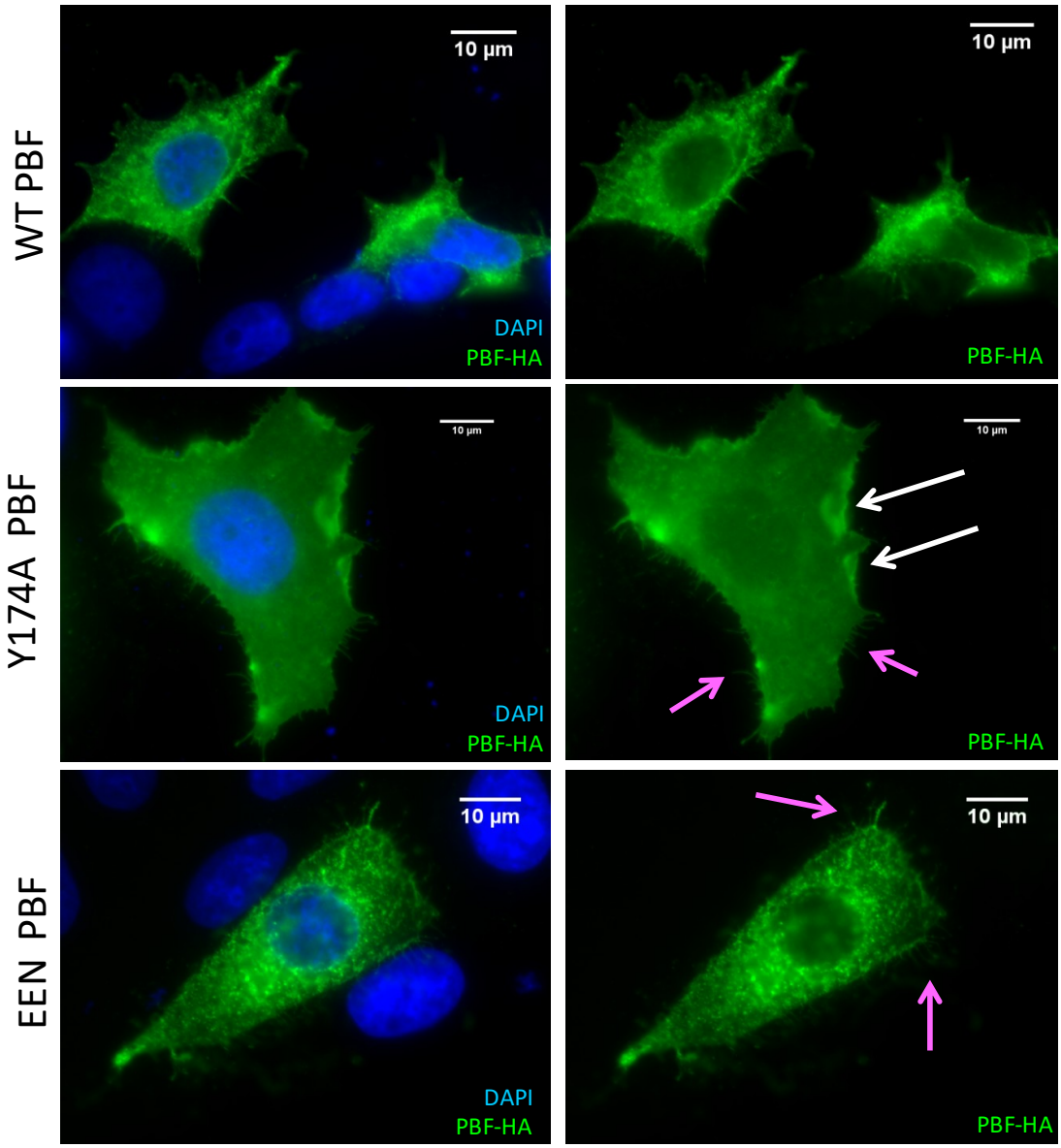

Figure 4-8. Fluorescence immunocytochemistry demonstrating the localisation of WT and mutant PBF. MCF-7 cells were transfected with WT, EEN/AAA or Y174A PBF-HA for 48 hours prior to fixing. HA-tagged PBF is identified in green using a mouse anti-HA antibody with the nuclei visualised in blue using Hoechst stain. White arrows indicate ruffles with pink arrows depicting lamellipodia. 100x magnification. n=3.

4.3.8 EEN/AAA PBF does not alter NIS subcellular localisation

Although EEN/AAA PBF has a similar subcellular localisation to WT PBF, it was important to assess its affect on the localisation of NIS within breast cancer cells. To investigate this, MCF-7 cells were co-transfected with WT PBF-HA, EEN/AAA PBF-HA or Y174A PBF-HA

alongside NIS-MYC and assessed using fluorescence immunocytochemistry. Cells transfected with WT PBF displayed intracellular colocalisation between NIS and PBF with limited NIS staining at the plasma membrane (Figure 4-9). In contrast, Y174A PBF was retained in the plasma membrane and there was a reduction in intracellular NIS levels. EEN/AAA PBF primarily localised within intracellular vesicles in a similar manner to PBF. However, there was an increase in the level of NIS staining at the plasma membrane, alongside a sharp reduction in the amount of co-localisation between NIS and PBF (Figure 4-9).

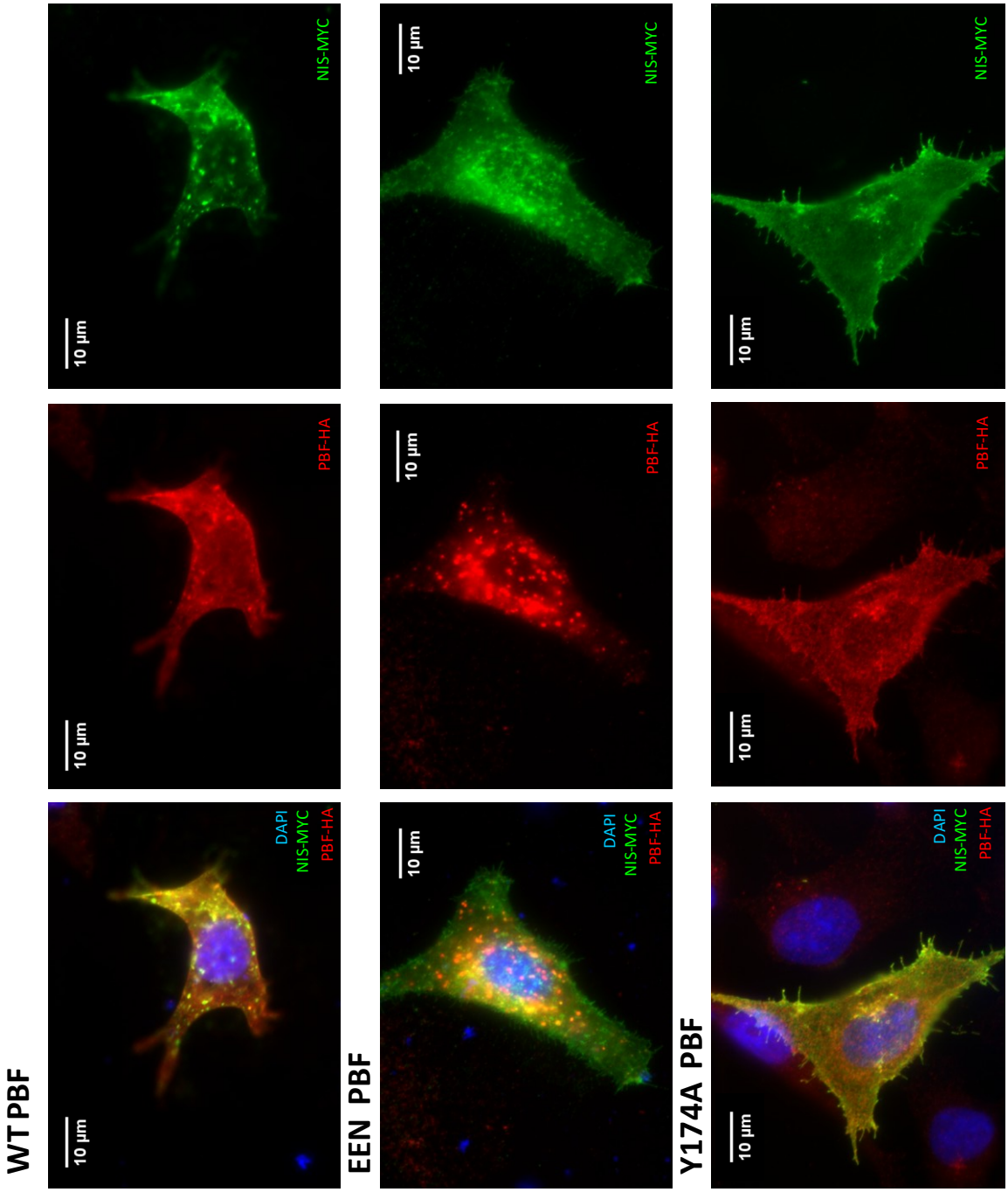

Figure 4-9. EEN/AAA PBF does not sequester NIS in intracellular vesicles. MCF-7 cells were transfected with WT, EEN/AAA or Y174A PBF-HA for 48 hours prior to fixing. MYC-tagged NIS is identified in green using a mouse anti-MYC antibody and HA-tagged PBF is identified in red using a mouse anti-HA antibody with the nuclei visualised in blue using Hoechst stain. 100x magnification. n=3.

4.3.9 EEN/AAA PBF does not decrease radioiodide uptake

Radioiodide uptake of EEN/AAA and Y174A PBF was assessed to determine if mutants lacking phosphorylation of PBF at Y174 could affect NIS function. WT PBF was previously demonstrated to be capable of decreasing radioiodide uptake in MCF-7 and MDA-MB-231 cells exogenously expressing NIS (Figure 4-10 A&B) and MCF-7 cells treated with ATRA and dexamethasone (Figure 4-10 C). In contrast to WT PBF, both EEN/AAA PBF and Y174 PBF were not capable of reducing radioiodide uptake in either cell-line tested with exogenously expressed or ATRA/Dex-induced NIS. Both EEN/AAA and Y174A PBF had significantly increased radioiodide uptake compared with WT PBF and there was no significant difference from empty vector control transfected cells.

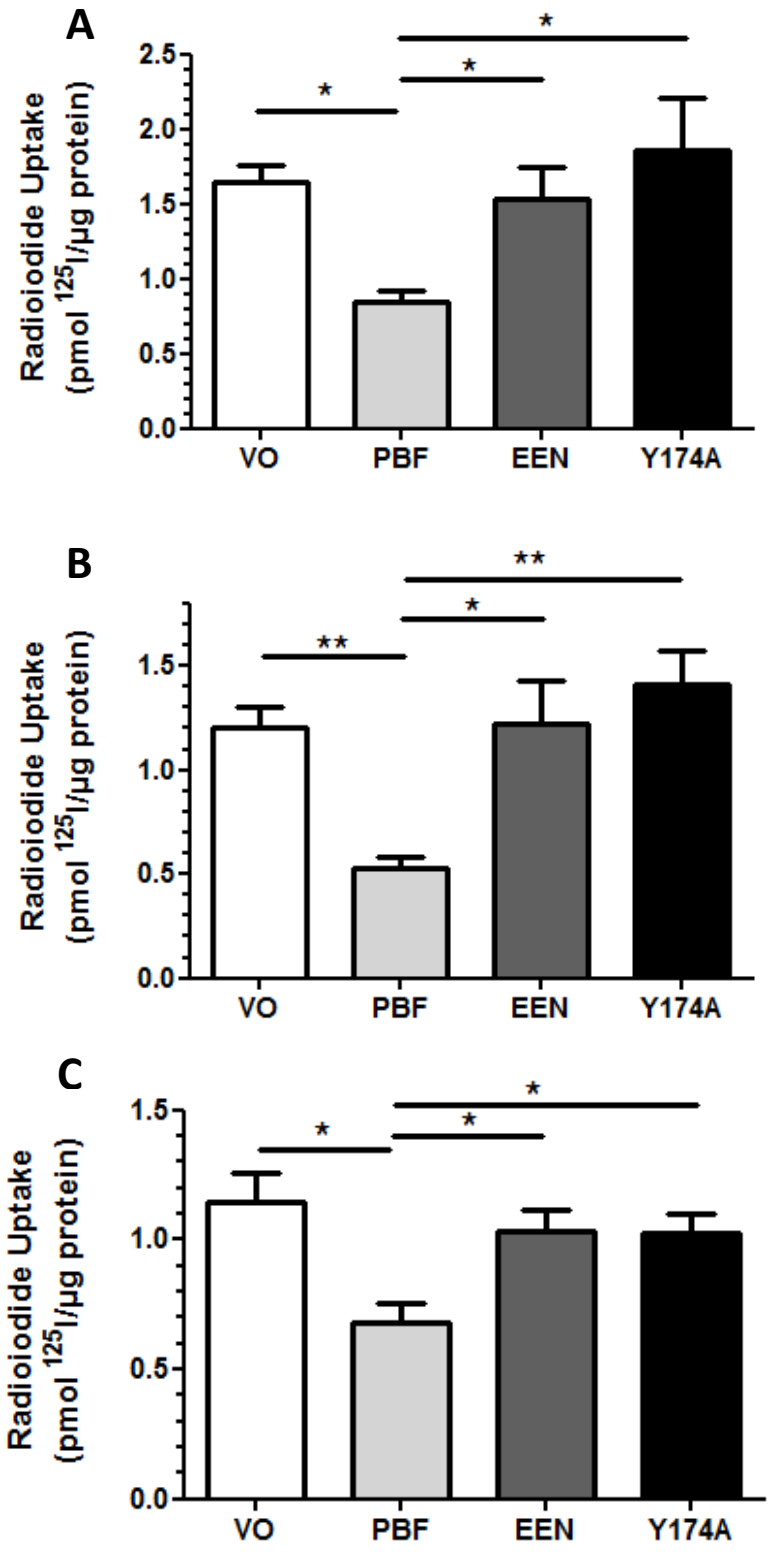

*Figure 4-10. EEN/AAA and Y174A PBF cannot reduce radioiodide uptake in the same manner as WT PBF. (A) MCF-7 and (B) MDA-MB-231 cells were transiently co-transfected with NIS-MYC and empty vector (VO), WT PBF, EEN/AAA PBF or Y174A PBF 48 hours prior to the addition of ^{125}I. (C) MCF-7 cells stably transfected with empty vector (VO), WT, EEN/AAA or Y174A PBF were treated with ATRA and dexamethasone 48 hours prior to the addition of ^{125}I. n=3 with 4 replicates in each n for all experiments. *= p<0.05.**= p<0.01.*

4.3.10 EEN/AAA PBF does not bind to NIS

Co-immunoprecipitation (Co-IP) assays in COS-7 cells previously revealed binding between PBF and NIS. However when Y174A was transfected into these cells Y174A PBF was not capable of binding to NIS (Smith et al., 2013). A possible interaction between PBF and NIS was assessed here in breast cancer cells. In MCF-7 cells, it was clear that PBF-HA and NIS-MYC maintain a physical relationship with strong binding being observed between the two proteins (Figure 4-11). Again, Y174A PBF-HA demonstrated a significant reduction in the ability to bind NIS-MYC with the alanine substitution at the Y174 residue almost completely abrogating the binding between PBF and NIS. Mutation of PBF-HA to EEN/AAA PBF-HA also drastically reduced binding of NIS and PBF in MCF-7 cells, with binding being almost completely lost (Figure 4-11).

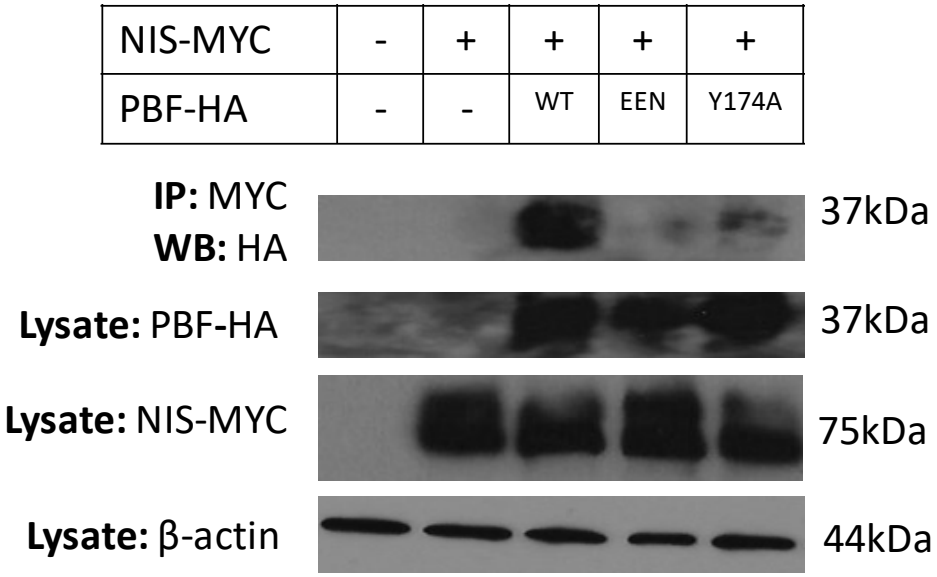

Figure 4-11. Unphosphorylated forms of PBF do not bind NIS. MCF-7 cells were co-transfected with NIS-MYC alongside empty vector (VO), WT, EEN/AAA or Y174A PBF-HA for 48 hours prior to harvesting. In the Co-IP, proteins were pulled down using the MYC antibody and probed with the HA antibody. Whole cell lysate was probed with HA, MYC and β-actin as a loading control. n=1.

4.4 Discussion

4.4.1 EEN/AAA PBF is not phosphorylated

The utilisation of phosphorylation prediction websites provided a vital tool in the identification of the pY174-null PBF. Although the tools were essential in the identification of potential mutants lacking phosphorylation, it was critical to confirm the phenotype *in vitro*. Similarly to Y174A PBF, EEN/AAA PBF was observed to be unphosphorylated *in vitro* by Western blotting allowing further investigation into the role of PBF phosphorylation.

One of the limitations observed with the PBF antibody is the epitope in which it binds to is located within the C-terminus of PBF, in the regions surrounding Y174. The presence of a phosphate group at Y174 of PBF can disrupt the binding efficacy of the PBF antibody. When phosphorylation is inhibited or not possible due to PBF mutation, increased levels of total PBF can be detected by Western blotting; as observed in Figure 4-5 and Figure 4-6. This effect rendered quantification of Western blotting by densitometry inappropriate as total PBF levels could not be utilised as a control for phospho-PBF levels.

The creation of an alternative mutant of PBF with an additional YARF motif was intended to be created and characterised alongside EEN/AAA PBF, but unfortunately due to mutagenesis limitations this was not possible. The mutation involved the addition of 4 amino acids to the Y174A PBF protein, with an intended amino acid sequence of KEENPAARFYARFENN. It was expected that the Y174A mutation would prevent PBF phosphorylation but the additional YARF would provide the tyrosine-based sorting signal.

This mutant alone would not have been ideal as there were questions as to whether the introduced tyrosine residue would become phosphorylated as well as whether the structure of PBF would be affected by the addition of 4 amino acids. Alongside the EEN/AAA mutant, it would have provided insight into a form of PBF that would hopefully not be phosphorylated but would localise correctly. However, the introduction of 12 nucleic acids was not possible after multiple attempts to optimise the mutagenesis technique using several different mutagenesis kits and varying the PCR cycle lengths and temperatures.

4.4.2 Characterisation of EEN/AAA PBF

Modelling of EEN/AAA PBF revealed a similar structure between WT PBF and EEN/AAA PBF, particularly at the C-terminal end of PBF where the mutation is found. Although there were minor differences in this C-terminal section, both proteins had a small α-helix followed by a largely unstructured section in this region. With the structures of PBF and EEN/AAA PBF being similar, phenotypic differences between WT and EEN/AAA PBF are more likely to be attributable solely to the lack of phosphorylation at Y174.

To make further comparisons between the mutated and WT forms of the protein, several characteristics of PBF were assessed to identify the effect of phosphorylation. WT PBF has previously been described to be mildly pro-proliferative in thyroid cancer cells. In breast cancer cells, there was no difference in the proliferation between WT PBF and empty vector transfected cells. Both Y174A and EEN/AAA PBF did not alter proliferation significantly compared to both WT PBF and empty vector transfected cells suggesting that the phosphorylation of PBF does not affect the proliferation of breast cancer cells.

4.4.2.1 Localisation

Establishing the localisation of EEN/AAA PBF is fundamental to understanding the interaction between NIS and PBF in breast cancer. EEN/AAA PBF contains an intact tyrosine-based sorting signal (YARF) so was predicted to be capable of endocytosis similar to WT PBF. Immunofluorescence studies revealed that EEN/AAA PBF is localised throughout the cell, with a presence at both the plasma membrane and in intracellular vesicles. The localisation of EEN/AAA PBF was synonymous with that seen with WT PBF and in sharp contrast to the enhanced plasma membrane staining witnessed with Y174A PBF.

It has been previously hypothesised that phosphorylation of PBF regulates its localisation, with phosphorylation of Y174 impairing the interaction with clathrin-associated adaptor complexes thereby inhibiting endocytosis (Smith et al., 2013). There is currently conflicting data as to whether phosphorylation enhances interaction with adaptor protein (AP) complexes that recognise YXXϕ signals. Phosphorylation of the T cell co-stimulatory receptor CTLA-4 on the lead tyrosine of the receptor sorting signal (YVKM) blocks the protein's interaction with the μ2 subunit of the AP complex and inhibits receptor internalisation (Shiratori et al., 1997). This form of regulation can be easily explained by the impossibility of the binding pocket to sterically accommodate a large negatively charged phosphate group. However, in contrast to this negative regulation, phosphorylation of aquaporin 4 (AQP4) enhances the interaction between the protein and subunit μ3 of the AP complex increasing lysosomal targeting of the protein, although the structural basis for this regulation remain to be elucidated (Madrid et al., 2001). To determine whether phosphorylation does regulate the localisation of PBF, a constitutively phosphorylated form of PBF would need to be compared to both WT PBF and EEN/AAA

PBF. From these data, it is apparent that phosphorylation is not critical for the internalisation of PBF in breast cancer cells but does not establish how endocytosis of the protein is regulated.

4.4.2.2 Interaction with NIS

Within this chapter there is substantial evidence to suggest that unphosphorylated EEN/AAA PBF cannot interact with NIS *in vitro*. Immunofluorescence studies have previously revealed high levels of colocalisation between WT PBF and NIS in breast cancer cells, with staining of NIS primarily being in intracellular vesicles with some staining at the plasma membrane. Use of the unphosphorylated EEN/AAA mutant form of PBF reduced colocalisation between exogenous NIS and PBF and altered the localisation of NIS. These data agree with previous studies where Y174A PBF expression has been unable to internalise NIS, although there were questions as to whether this was due to plasma membrane retention of the Y174A form of PBF (Smith et al., 2013). The decreased colocalisation between EEN/AAA PBF and NIS observed using immunofluorescence is supported by the co-immunopreciptitation studies where little to no binding was detected between the two proteins. Both EEN/AAA and Y174A forms of PBF did not bind to NIS within breast cancer cells, with both forms having a lack of phosphorylation in common. In addition to this reduced binding, the presence of EEN/AAA PBF and Y174A PBF did not repress radioiodide uptake in the same manner as the expression of exogenous WT PBF in breast cancer cells.

These data suggest that phosphorylation of PBF at Y174 is critical for the interaction between NIS and PBF. The importance of the phosphorylation in protein binding has previously been witnessed with studies identifying that phosphosites have a

tendency to be located on the binding interfaces of protein complexes. Phosphorylation has been hypothesised to modulate the strength of interactions and bring about changes in binding energy that may trigger the transitions between conformational states, removing previous potential steric constraints (Nishi et al., 2011).

Overall these data suggest that the phosphorylation of PBF at Y174 is essential for the interaction between PBF and NIS. Forms of PBF that cannot be phosphorylated are incapable of binding to NIS, altering its subcellular localisation and reducing radioiodide uptake, suggesting that therapeutically reducing pY174 PBF levels in breast cancer cells may increase radioiodide uptake. With phosphorylation of Y174 being observed to be critical, rather than the integrity of the endocytosis motif and PBF subcellular localisation, it is important to identify methods to abrogate Y174 phosphorylation to overcome PBF repression of NIS function. If PBF phosphorylation can be inhibited, the exact mechanics of the interaction between NIS and PBF can begin to be fully elucidated and exploited to boost NIS function and radioiodide uptake within breast cancer cells.

CHAPTER 5 - SRC FAMILY KINASE INHIBITORS INCREASE RADIOIODIDE UPTAKE

5.1 Introduction

Previous work in thyroid cancer has identified that the use of a Src family kinase (SFK) inhibitor, PP1, can decrease phosphorylation of PBF (Smith et al., 2013). Use of PP1 in thyroid cancer cells also overcame the reduction in radioiodide uptake witnessed with PBF overexpression (Smith et al., 2013). With radioiodide uptake being proposed as a potential treatment for breast cancer, it is important to identify whether SFK inhibition can enhance radioiodide uptake in breast cancer cells and determine which inhibitors are the most specific and have the greatest effect.

5.1.1 Src and Src Family Kinases

Src, also referred to as c-Src, is a non-receptor tyrosine kinase that is the prototype member of the Src family of tyrosine kinases (SFKs), a family consisting of eight other members: Lck, Fyn, Lyn, Hck, Yes, Fgr, Blk and Yrk. All members of the family are closely related, having significant amino acid homology along with structural similarities such as SH2 (Src Homology 2), SH3 and kinase catalytic domains. SFKs modulate many signalling cascades involved in processes including cell proliferation, survival, differentiation, adhesion, migration and invasion (Thomas and Brugge, 1997). SFKs are aberrantly expressed or functionally dysregulated in many human cancers including breast, colorectal, pancreatic, prostatic and ovarian carcinomas (Summy and Gallick, 2003). In breast cancer, Src was found to be present in 95% of triple negative (TN) samples and 84% of other breast cancer types. TN tumours exhibited increased membranous expression of Src with activated Src being localised within peripheral membrane-associated focal adhesions (Tryfonopoulos et al., 2011). Src expression has also been

linked to aggressive disease and poor prognosis (Elsberger et al., 2009), and has been identified as a common signalling axis in trastuzumab resistance in breast cancer (Zhang et al., 2011). Due to SFK frequent dysregulation in multiple cancers, SFK inhibitors are being assessed in multiple cancers to inhibit cell proliferation, migration, tumour growth and invasion.

5.1.2 SFK inhibitors

5.1.2.1 PP1

PP1 (1-(1,1-Dimethylethyl)-1-(4-methylphenyl)-1*H*-pyrazolo[3,4-*d*]pyrimidin-4-amine) is a potent small molecular inhibitor (Figure 5-1) of SFKs that was first identified in 1996 (Hanke et al., 1996), with an IC_{50} of around 5nM, 6nM and 170nM for Lck, Fyn and Src respectively. PP1 was also identified as an inhibitor of other proteins such as ZAP-70 and JAK2 but at a much lower potency (IC_{50} >100μM and >50μM respectively). PP1 inhibits SFKs by interacting with the amino acid corresponding to Thr341 in c-Src, via interaction of a C3 phenyl ring, acting as an ATP competitive inhibitor (Liu et al., 1999). PP1 has since been extensively studied and identified as a moderate inhibitor of a plethora of proteins including p38, CSK (Bain et al., 2003), PDGF receptors, RET-derived oncogenes (Carlomagno et al., 2002), c-Kit and Bcr-Abl (Tatton et al., 2003). Due to its lack of specificity, PP1 is not used therapeutically but is a useful tool in identifying whether SFKs are involved in cellular processes *in vitro*. More potent and specific SFK inhibitors such as Dasatinib and Saracatinib are now being investigated.

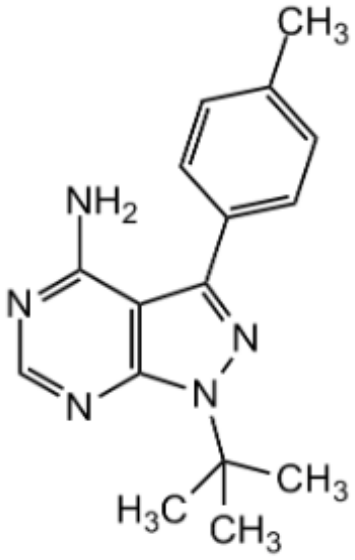

Figure 5-1. The chemical structure of PP1. Taken from the Adipogen website (http://www.adipogen.com/productmanagement/resource/download/type/sheet/id/3347/).

5.1.2.2 Dasatinib

Dasatinib is a small molecular inhibitor (Figure 5-2) that targets Bcr-Abl, SFKs and c-Kit (IC_{50} <1nM, 0.8nM and 79nM respectively) and has been FDA approved for the treatment of Philadelphia chromosome-positive chronic myeloid leukaemia (CML) and acute lymphoblastic leukaemia (ALL) (FDA, 2010a). MDA-MB-231 cells have been observed to be sensitive to dasatinib with treatment decreasing cell proliferation, migration and invasion (Tryfonopoulos et al., 2011). Dasatinib has also been used in a number of phase II clinical trials in patients with advanced breast cancer, with partial responses and disease stabilisation being reported in some patients (Mayer et al., 2011). It has also been shown to significantly decrease growth, survival and colony formation in thyroid cancer cell-lines (Chan et al., 2012).

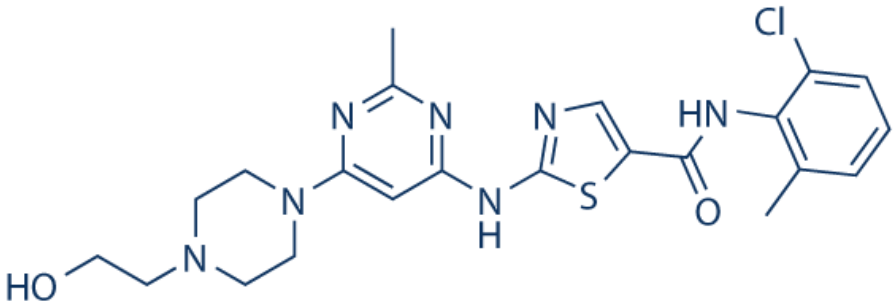

Figure 5-2. The chemical structure of dasatinib. Taken from the SelleckChem website (http://www.selleckchem.com/products/Dasatinib.html).

5.1.2.3 Saracatinib

Saracatinib (AZD0530) is another small molecular inhibitor (Figure 5-3) that targets Src and other SFKs (IC_{50} 2.7nM and 4-10nM respectively); it is also capable of inhibiting Bcr-Abl and EGFR but at much lower potencies (IC_{50} 30nM and 66nM respectively). Saracatinib has been observed to inhibit growth and invasion of four thyroid cancer cell-lines in both two- and three-dimensional culture (Schweppe et al., 2009). Studies in MCF-7 cells have also shown saracatinib to have a synergistic effect with tamoxifen, decreasing growth and cell anchorage (Herynk et al., 2006). However phase II clinical trials of Saracatinib in patients with hormone receptor-negative metastatic breast cancer, no patients displayed evidence of stable disease or partial response when the drug was used in isolation over a 6 month period (Gucalp et al., 2011).

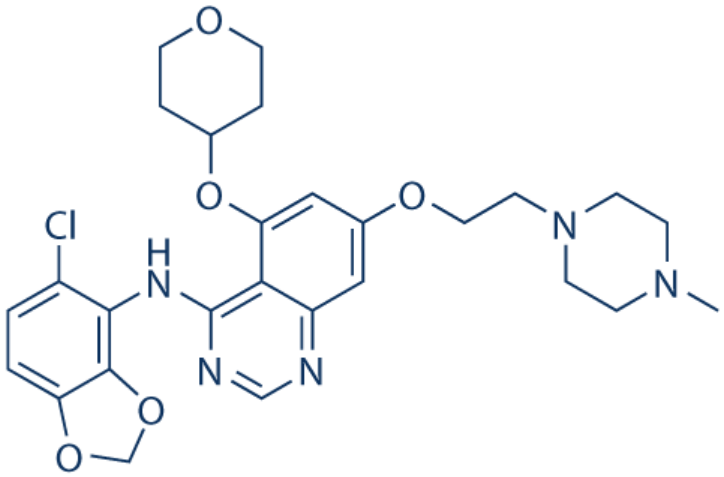

Figure 5-3. The chemical structure of saracatinib. Taken from the SelleckChem website (http://www.selleckchem.com/products/AZD0530.html).

5.1.3 Focal Adhesion Kinase (FAK)

Focal adhesion kinase (FAK) is a non-receptor protein tyrosine kinase that is a critical substrate of Src and the cellular functions of the two kinases are closely linked (Schweppe et al., 2009). FAK plays an important role in signal transduction pathways that are initiated at sites of integrin-mediated cell adhesions and by growth factor receptors. Like Src, FAK is a key regulator of survival, proliferation, migration and invasion and has been seen to have increased activity in many cancers including breast cancer (van Nimwegen and van de Water, 2007).

5.1.3.1 PF573228

PF573228 is a potent FAK inhibitor (IC_{50} 4nM) (Figure 5-4) that is ~50 to 250-fold more selective for FAK than its other target kinases Pyk2, CDK1/7 and GSK-3β. PF573228 binds to FAK in its ATP-binding domain and prevents FAK autophosphorylation on Y397. Although PF573228 has not been reported to have any effect on the growth of MCF-7

cells, it has been found to decrease adhesion and migration of MCF-7 cells resistant to tamoxifen and fulvestrant (Hiscox et al., 2011).

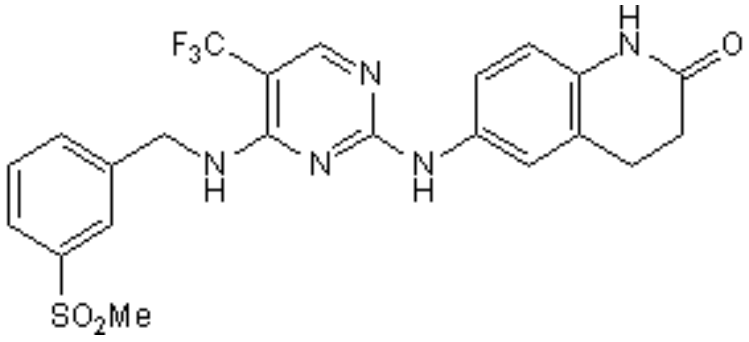

Figure 5-4. The chemical structure of PF573228. Taken from the Tocris website (https://www.tocris.com/dispprod.php?ItemId=213493#.Vy9lheTe76k).

The aim of the work carried out in this chapter was to establish whether the inhibition of SFK could decrease levels of phosphorylated PBF and enhance radioiodide uptake in breast cancer in a similar manner to that witnessed in thyroid cancer (Smith et al., 2013). The inhibition of FAK was also investigated to determine whether SFK inhibition directly affects PBF or whether it may be through downstream kinases such as FAK. Specific SFK inhibitors that have been approved for clinical use were investigated with the intention of identifying a compound that has the potential to maximise radioiodine therapy in breast cancer patients. The effect of SFK inhibition on PBF phosphorylation and NIS function was determined in MCF-7 and MDA-MB-231 breast cancer cells.

5.2 Materials and Methods

5.2.1 Cell Culture

MCF-7 and MDA-MB-231 cells were maintained as described in 2.1.2 with stably transfected MCF-7 cells being cultured in medium containing G418 (1 mg/ml) and lentivirally-transduced MDA-MB-231 cells being cultured in medium containing blasticidin (15 µg/ml). All cell lines were seeded at 30,000 cells per well in a 24 well plate for radioiodide uptake and at 150,000 and 200,000 cells per well in a 6 well plate for fluorescence immunocytochemistry and protein extraction respectively.

5.2.2 Drug Treatments

MCF-7 cells were treated with ATRA and dexamethasone as described in section 3.2.3 at 100nM and 1µM respectively. Cells were cultured with ATRA and dexamethasone for 48 hours prior to harvesting or treatment with ^{125}I. Src Family Kinase inhibitors PP1 (Tocris, Bristol, UK), Dasatinib (Selleck Chemicals, Houston, Texas, USA) and Saracatinib (Selleck Chemicals) and the FAK inhibitor, PF573228 (Tocris) were dissolved in DMSO to a stock concentration of 10mM.

5.2.3 Transfection

Transfection was performed as described in 2.2.3. WT PBF-HA and NIS-MYC (kindly gifted by Dr Vicki Smith) in pcDNA3.1 (+) vectors were transfected into MCF-7 and MDA-MB-231 cells in 6 well plates for use in fluorescence immunocytochemistry and Western blotting.

For radioiodide uptake cells were seeded in 24 well plates and transfected with untagged PBF and NIS-MYC.

5.2.4 Radioiodide uptake

Radioiodide uptake was performed as described in 2.7. Transfection and drug treatments were performed 48 and 24 hours respectively before the addition of ^{125}I to cells.

5.2.5 Western Blotting

Protein extraction and Western blotting were performed as described in 2.3.1 and 2.3.2 respectively. Cells were treated with sodium pervanadate prior to harvesting to allow the detection of pY174 PBF. Antibodies used were anti-pY174 PBF antibody (Covalab) (Smith et al., 2013), anti-PBF (Eurogentec) (Smith et al., 2009), anti-phospho-Src (Y418) (Abcam), anti-Src (Cell Signalling) and β-actin (Sigma-Aldrich)(refer to section 2.8). Appropriate secondary antibodies were used.

5.2.6 Fluorescence immunocytochemistry

Fluorescence immunocytochemistry was performed as described in 2.4. Antibodies used include anti-HA tag (rabbit) (1:100) (Santa Cruz) and anti-Myc tag (1:750) (Cell Signalling).

5.2.7 BrdU Proliferation Assays

The BrdU assays were performed as described in section 4.2.11. Cells were seeded at 2,500 per well in a 96 well plate for 24 hours prior to the assay being performed.

5.2.8 RNA extraction and qRT-PCR

RNA extraction, reverse transcription and qRT-PCR were performed as described in 2.5 and 2.6. Expression of PBF was assessed using the PBF TaqMan® Gene Expression Assay (Hs01036322_m1)(Life Technologies). Expression of NIS was assessed using custom-made primers and probe (Table 3-1).

5.2.9 Statistics

Data were analysed using Sigma Plot (SPSS Science Software UK Ltd). The student's t-test was utilised to compare data between two groups whereas the one-way ANOVA was used to compare more than two groups of parametric data with significance taken at $p<0.05$ for both.

5.3 Results

5.3.1 PP1 decreases levels of phosphorylated PBF in breast cancer cell lines

PP1 has previously been demonstrated to inhibit the phosphorylation of PBF in thyroid cancer cells at a concentration of 2µM (Smith et al., 2013). To determine whether PP1 was capable of inhibiting PBF phosphorylation in breast cells a dose response was performed for 24 hours in both MCF-7 and MDA-MB-231 cells. PP1 decreased pY174 PBF levels in a dose-dependent manner in both cell lines. In MCF-7 cells phosphorylation of PBF was completely abolished using 2µM of PP1 (Figure 5-5A), as previously demonstrated in thyroid cancer. Concentrations lower than 2µM were not capable of fully inhibiting the phosphorylation of PBF (Figure 5-5A). In MDA-MB-231 cells the phosphorylation of PBF was completely inhibited after treatment with 100nM of PP1 (Figure 5-5B).

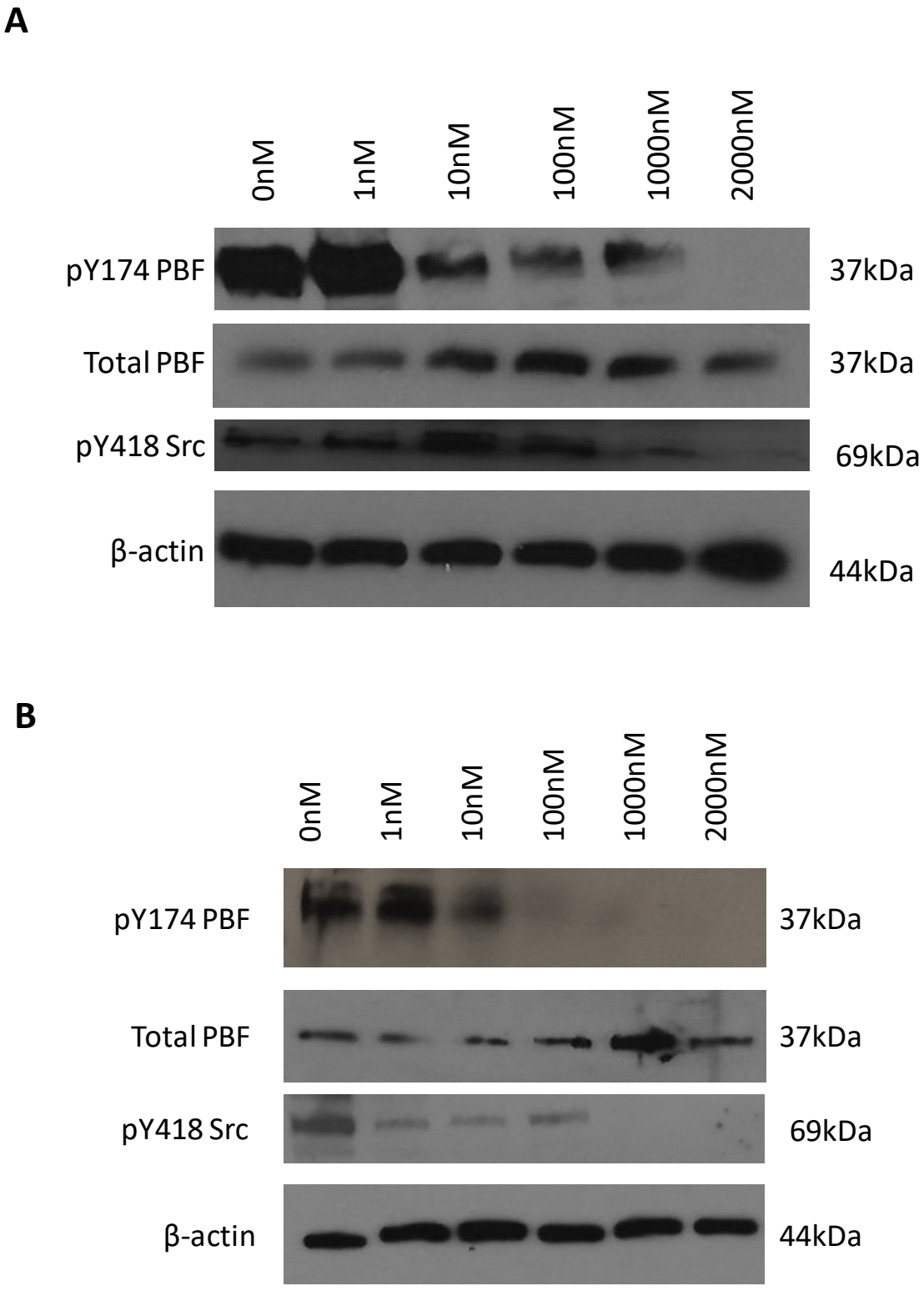

Figure 5-5. PP1 inhibits the phosphorylation of PBF. (A) MCF-7 cells and (B) MDA-MB-231 cells were treated with varying doses of PP1 (0nM-2000nM) for 24 hours before protein harvesting. Western blots were probed for pY174 PBF and total PBF with β-actin used a loading control. n=3.

5.3.2 PP1 rescues radioiodide uptake in breast cancer cell lines

PP1 has previously been demonstrated to restore radioiodide uptake in PBF expressing thyroid cancer cell-lines. PBF has already been demonstrated to reduce radioiodide uptake in breast cancer cell-lines including MCF-7 and MDA-MB-231 cells, so it was of interest to establish whether inhibition of SFK could restore radioiodide uptake in these cell-lines. Exogenous expression of PBF decreased radioiodide uptake by 25% (p=0.0008) in NIS-MYC co-transfected MCF-7 cells incubated with vehicle only (DMSO) for 24 hours (Figure 5-6A). However when PBF expressing cells were treated with 2μM PP1 for 24 hours, radioiodide uptake was restored with a significant increase of 23.5% compared to vehicle only treated cells (p= 0.011) (Figure 5-6A). The uptake observed in the presence of PBF and PP1 was comparable to the uptake of MCF-7 cells lacking exogenous PBF (6.7% difference, p=0.69) (Figure 5-6A).

PP1 also had a similar effect on MDA-MB-231 cells. Exogenous expression of PBF reduced radioiodide uptake by 32% (p=0.008) in vehicle only treated cells (Figure 5-6B). Treatment with PP1 lead to a significant increase in radioiodide uptake in these cells (41%, p=0.0005) (Figure 5-6B). PP1 treatment also displayed a trend of increasing radioiodide uptake in NIS-MYC expressing cells compared to vehicle only treatment however the effect was not significant (p=0.056). MCF-7 cells treated with ATRA and dexamethasone were also assessed to evaluate whether this effect was exclusive to cells exogenously expressing NIS. Expression of PBF decreased radioiodide uptake by 22% (p=0.03) compared to empty vector in vehicle only treated cells (Figure 5-6C). Treatment with PP1 significantly increased radioiodide uptake in PBF transfected cells by 56% (p=0.007) (Figure 5-6C).

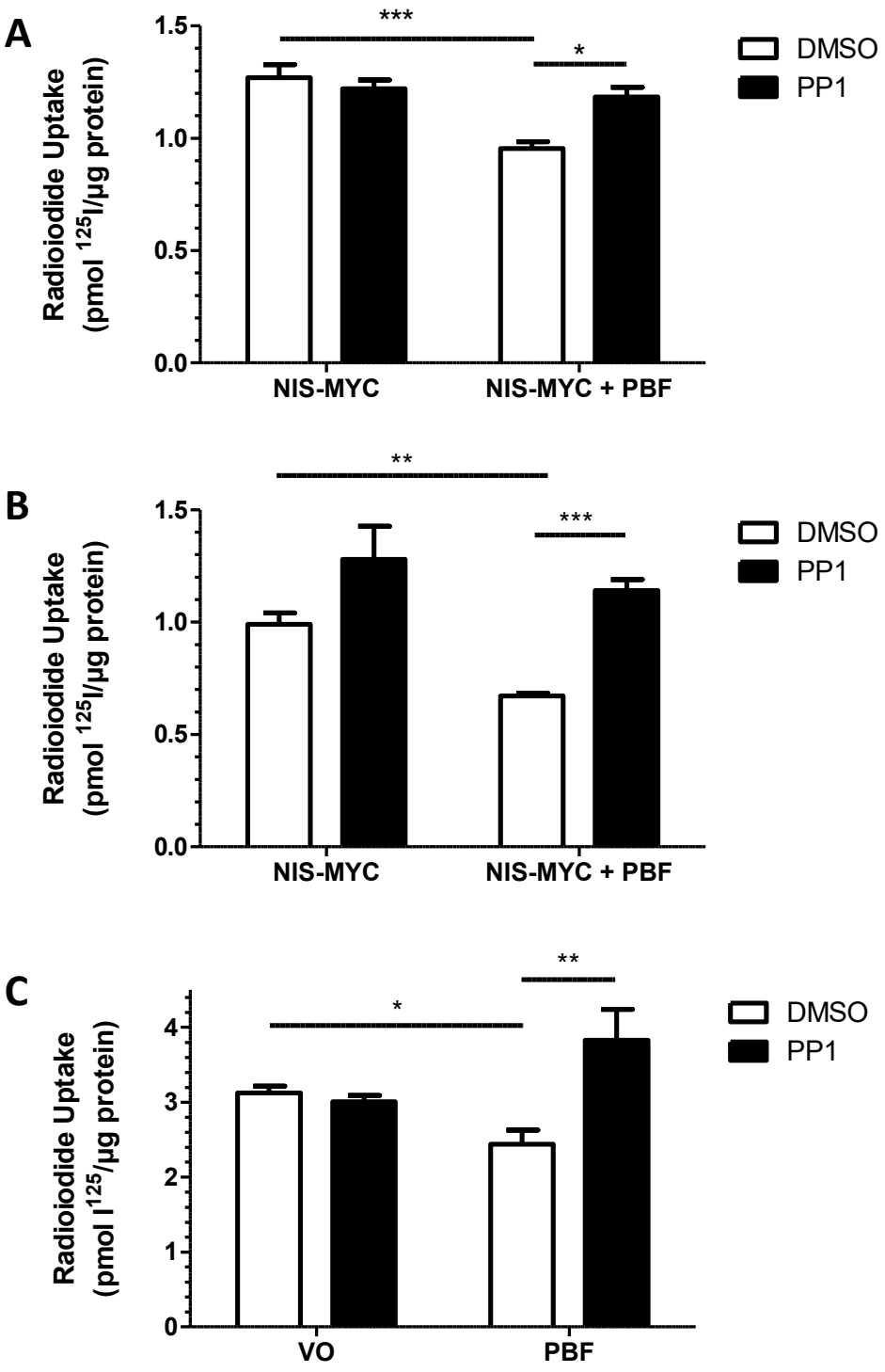

*Figure 5-6. PP1 restores radioiodide uptake in breast cancer cells. (A) MCF-7 and (B) MDA-MB-231 cells were transfected for 48 hours with empty vector (VO) + NIS-MYC or NIS-MYC + PBF and treated with 2µM PP1 for 24 hours prior to the addition of ^{125}I. (C) MCF-7 cells were stably transfected with empty vector (VO) or PBF and treated with ATRA and dexamethasone 48 hours prior to the addition of ^{125}I. n=3 with 4 replicates in each n for all experiments. *=p<0.05.**=p<0.01. ***=p<0.001.*

5.3.3 Dasatinib and Saracatanib decrease pY174 PBF levels in a dose-dependent manner

With PP1 being capable of inhibiting the phosphorylation of PBF and restoring radioiodide uptake in breast cancer cells, it was of interest to establish whether more specific and therapeutically relevant SFK inhibitors can act in the same way. To test this, MCF-7 and MDA-MB-231 cells were treated with dasatinib and saracatinib at concentrations ranging from 1nM - 2µM for 24 hours. A time response experiment was also performed varying the treatment time from 2 - 48 hours (data not shown) over the differential dose levels, with 24 hours identified as the most optimal for the inhibition for pY418 Src.

Dasatinib reduced the levels of pY418 Src at concentrations as low as 10nM in both cell-lines and fully abolished phosphorylation at 10nM in MCF-7 cells (Figure 5-7A). Dasatinib was the more effective inhibitor of PBF phosphorylation with pY174 PBF levels being almost completely abolished at 1nM in both MCF-7 and MDA-MB-231 cells (Figure 5-7).

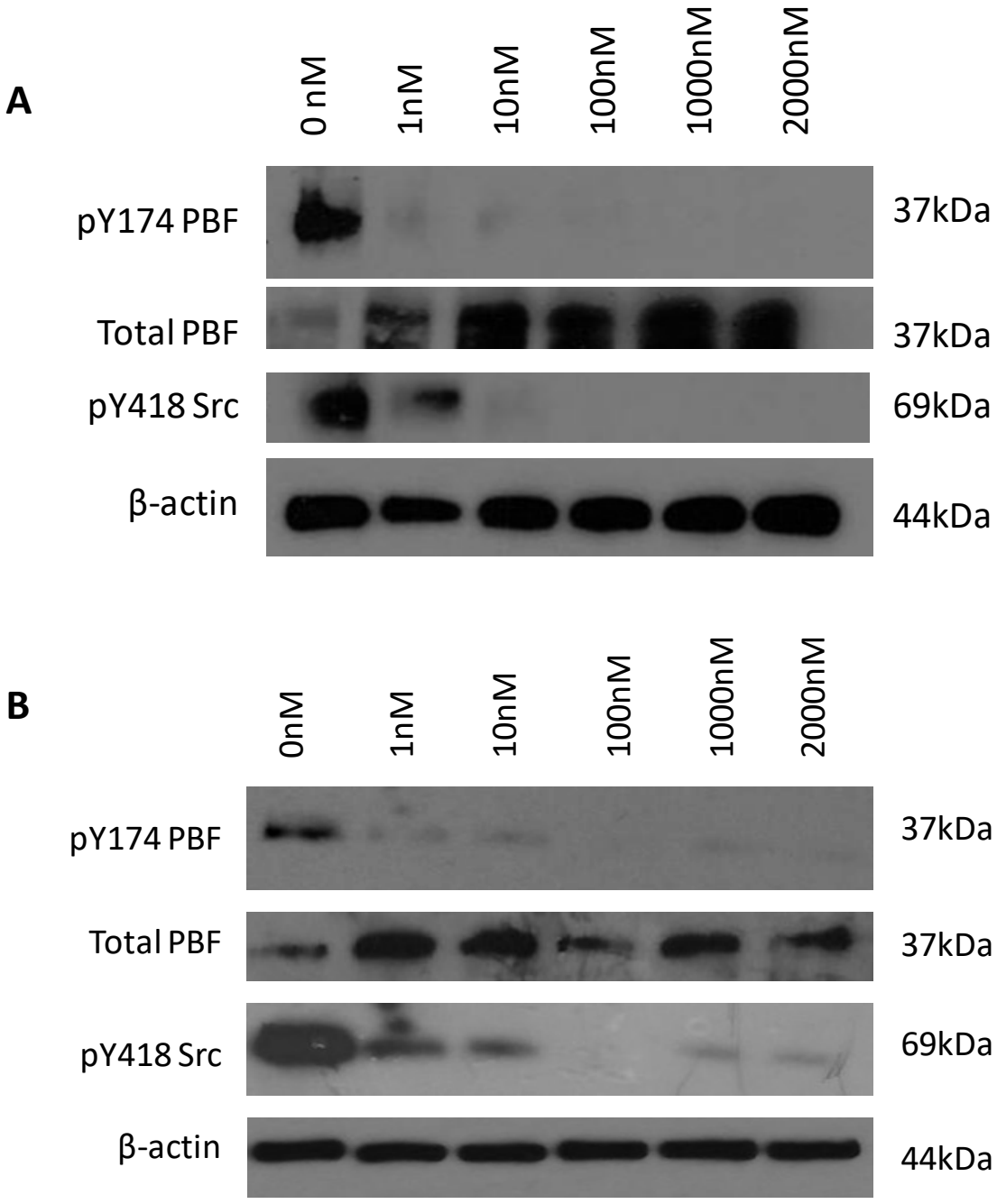

Figure 5-7. Dasatinib inhibits the phosphorylation of PBF. (A) MCF-7 cells and (B) MDA-MB-231 cells were treated with varying doses of dasatinib (0nM-2000nM) for 24 hours before protein harvesting. Western blots were probed for pY174 PBF, pY418 Src and total PBF with β-actin used a loading control. n=3.

Saracatinib completely inhibited pY418 Src at concentrations as low as 10nM in MDA-MB-231 cells (Figure 5-8B). Saracatinib was not as potent at inhibiting PBF phosphorylation as dasatinib, with phosphorylation of Y174 not being completely eradicated below concentrations of 100nM (Figure 5-8).

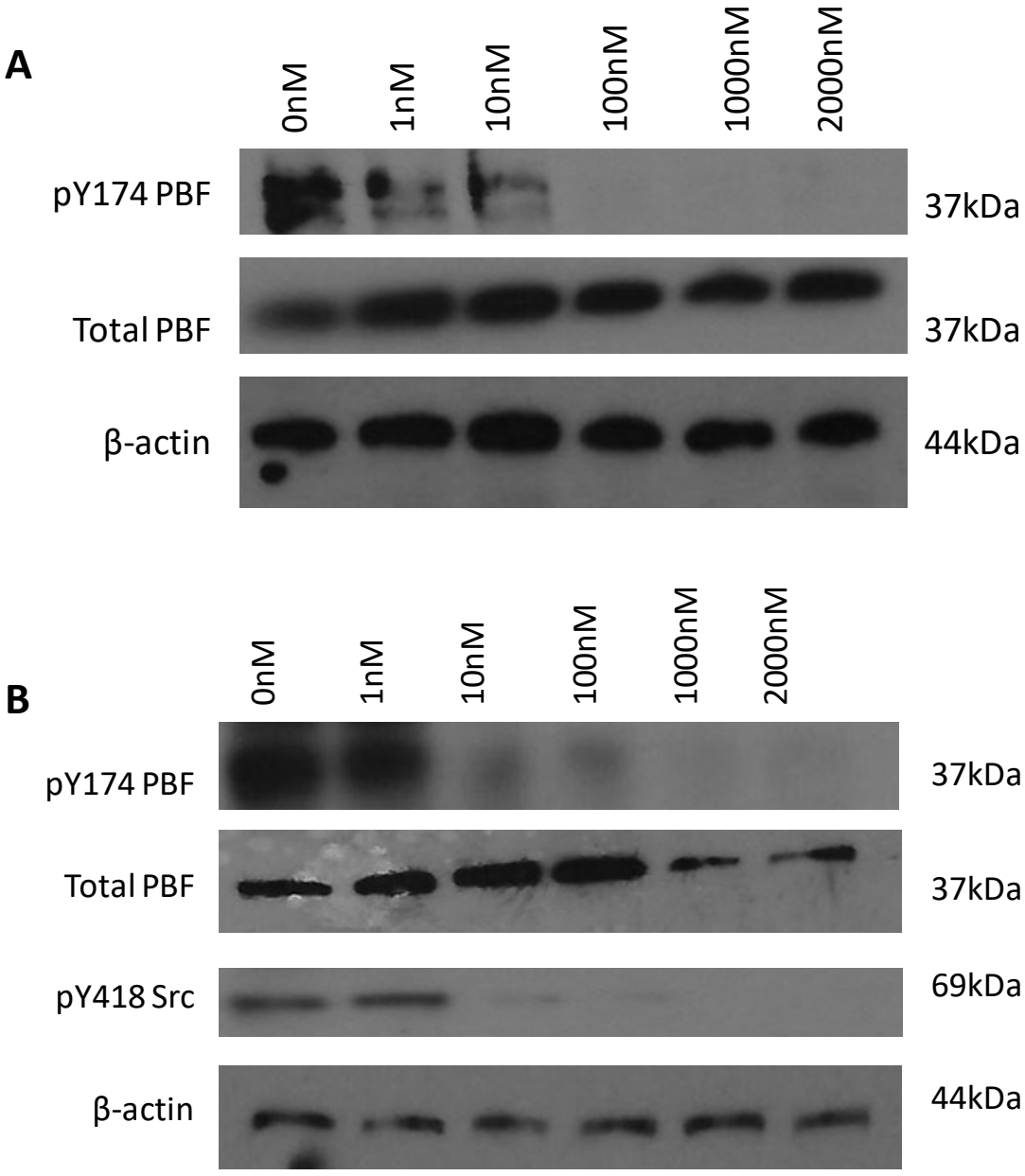

Figure 5-8. Saracatinib inhibits the phosphorylation of PBF. (A) MCF-7 cells and (B) MDA-MB-231 cells were treated with varying doses of saracatinib (0nM-2000nM) for 24 hours before protein harvesting. Western blots were probed for pY174 PBF, pY418 Src and total PBF with β-actin used a loading control. n=3.

5.3.4 Inhibiting FAK has no effect on pY174 PBF levels

To assess whether the inhibition of SFK has a direct effect on the phosphorylation of PBF or whether the effect is due to lack of activation of downstream targets such as FAK, inhibition of FAK was assessed. To investigate this MCF-7 and MDA-MB-231 cells were treated with a PF573228 at concentrations ranging from 1nM - 2µM for 24 hours.

Treatment with PF573228 did not reduce phosphorylated PBF levels until a concentration of 1µM was reached in MCF-7 cells. Even at concentrations as high as 2µM, phosphorylation of PBF could not be fully inhibited (Figure 5-9A). Although treatment with 1µM and 2µM did not fully abolish PBF phosphorylation in MCF-7 cells, treatment with these high concentrations caused a high level of cell death (data not shown). Treatment with PF573228 in MDA-MB-231 cells did not reduce pY174 PBF levels over the range of concentrations used (Figure 5-9B). For further experiments a concentration of 100nM PF573228 was utilised as this was the highest concentration that did not compromise cell number in both cell-lines (data not shown).

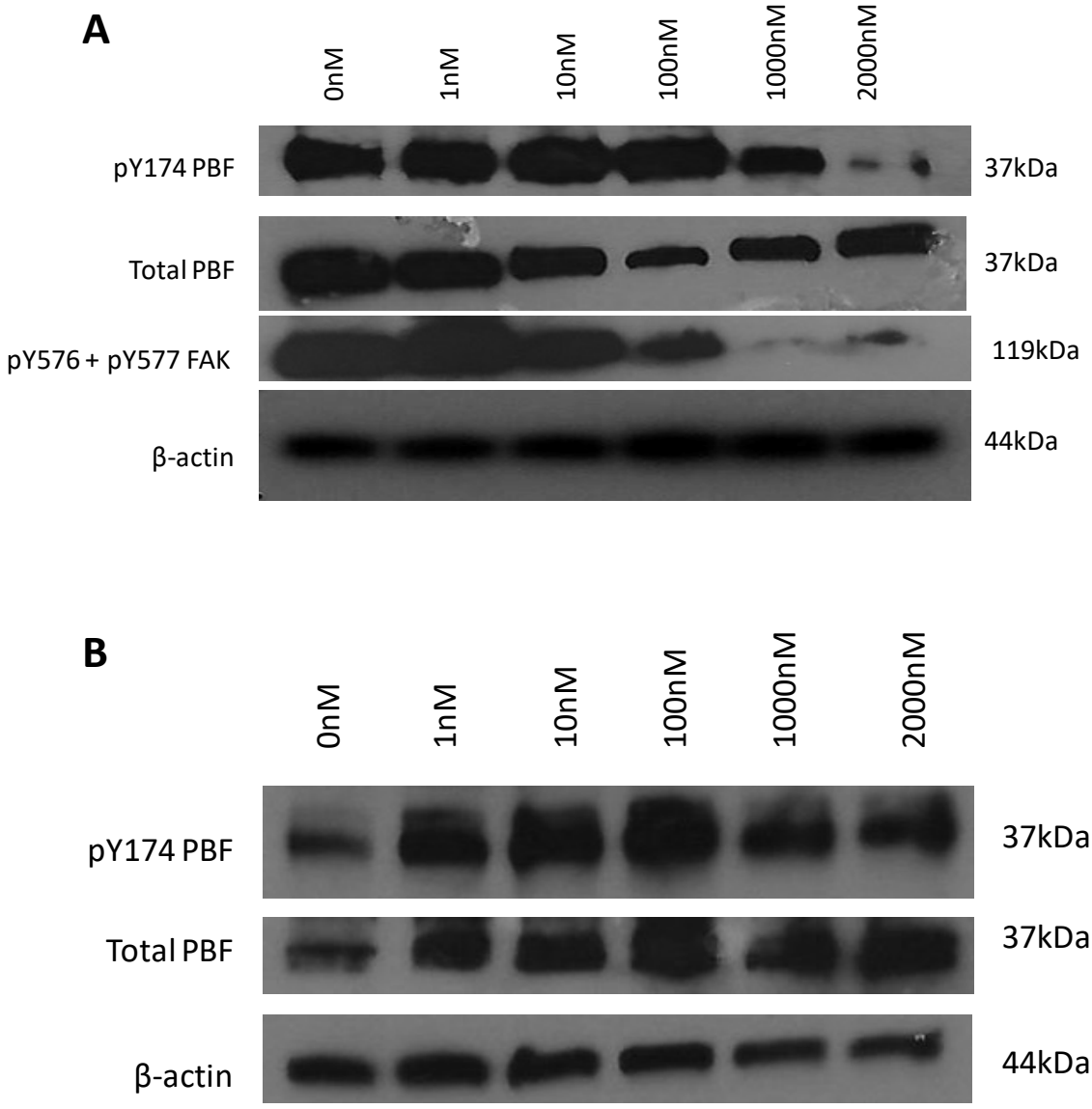

Figure 5-9. Inhibition of FAK does not significantly alter the phosphorylation status of PBF. (A) MCF-7 cells and (B) MDA-MB-231 cells were treated with varying doses of PF573228 (0nM-2000nM) for 24 hours before protein harvesting. Western blots were probed for pY174 PBF, total PBF and pY576/pY577 FAK with β-actin used a loading control. n=3.

5.3.5 Effect of drugs on PBF and NIS mRNA expression

To assess whether inhibition of SFK affected PBF or NIS expression, qRT-PCR was performed and relative expression of NIS and PBF determined in both MCF-7 and MDA-MB-231 cells. Treatment of MCF-7 and MDA-MB-231 cells with SFK or FAK inhibitors did not significantly alter PBF expression (Figure 5-10). Treatment with the SFK and FAK inhibitors did not alter NIS expression in a significant manner in either cell-line (Figure 5-11).

A

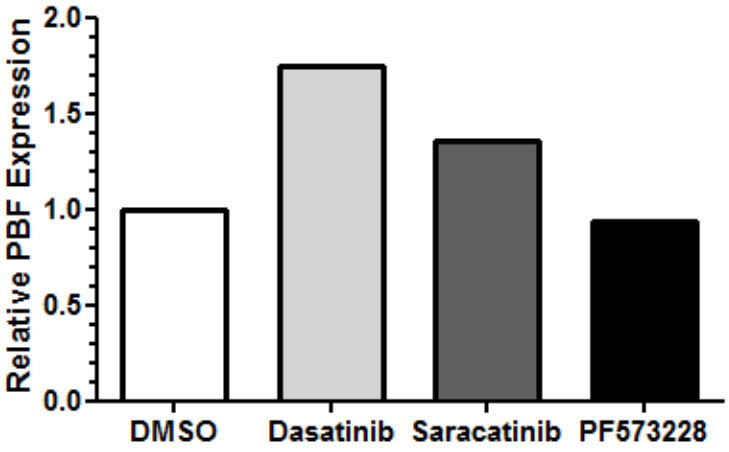

	Average ΔCT	ΔCT SEM	Fold Change	*p* value
DMSO	13.08	0.422	-	-
Dasatinib	12.39	0.663	1.748	0.439
Saracatinib	12.73	0.494	1.356	0.627
PF573228	13.22	0.589	0.936	0.856

B

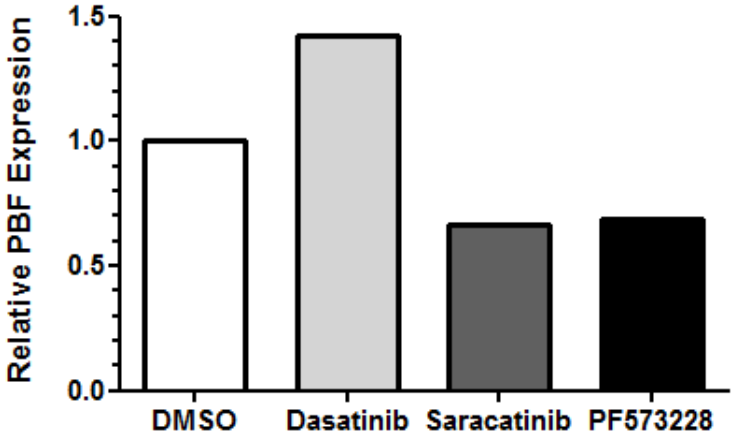

	Average ΔCT	ΔCT SEM	Fold Change	*p* value
DMSO	11.37	0.146	-	-
Dasatinib	11.07	0.448	1.424	0.385
Saracatinib	12.18	0.459	0.664	0.299
PF573228	12.07	0.364	0.690	0.649

Figure 5-10. Inhibiting Src and FAK has no significant effect on PBF expression levels. (A) MCF-7 and (B) MDA-MB-231 cells were treated with DMSO, 1nM dasatinib, 10nM Saracatinib or 100nM PF573228 for 24hours prior to harvesting RNA. Expression levels of PBF mRNA were quantified using qRT-PCR. Expression levels normalised to DMSO. All statistical analyses performed on ΔCT values. n=3 with 4 replicates in each n.

A

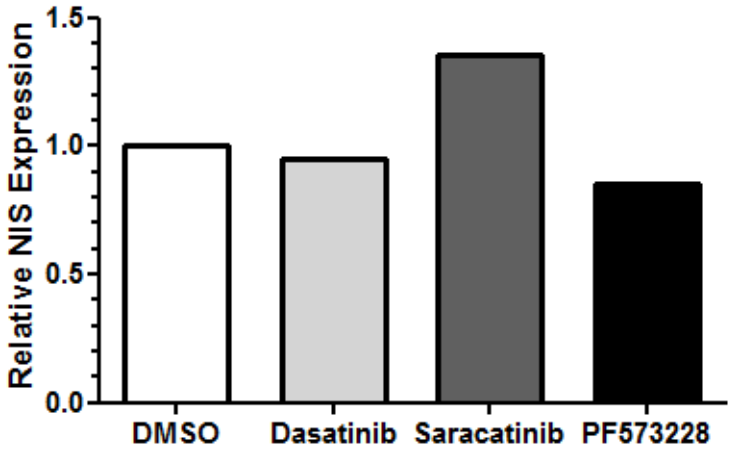

	Average ΔCT	ΔCT SEM	Fold Change	*p* value
DMSO	18.65	0.197	-	-
Dasatinib	18.78	0.278	0.916	0.735
Saracatinib	18.29	0.379	1.278	0.468
PF573228	18.89	0.237	0.85	0.481

B

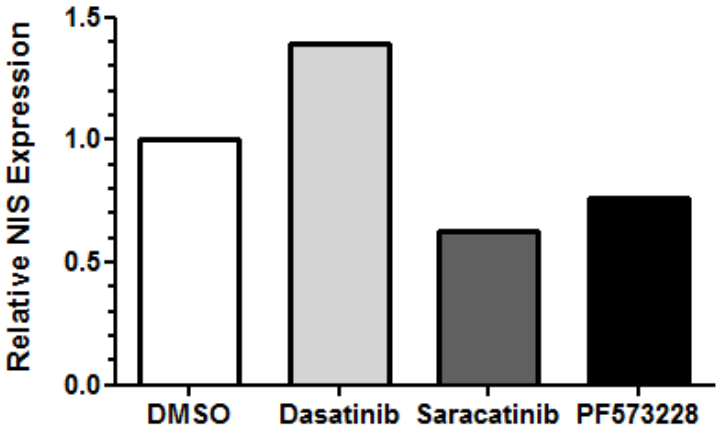

	Average ΔCT	ΔCT SEM	Fold Change	*p* value
DMSO	17.18	0.819	-	-
Dasatinib	16.17	0.828	1.389	0.716
Saracatinib	17.48	0.789	0.815	0.806
PF573228	17.91	0.533	0.604	0.533

Figure 5-11. Inhibiting Src and FAK has no significant effect on NIS expression levels. (A) MCF-7 and (B) MDA-MB-231 cells were treated with DMSO, 1nM dasatinib, 10nM Saracatinib or 100nM PF573228 for 24 hours prior to harvesting RNA. Expression levels of NIS mRNA were quantified using qRT-PCR. Expression levels normalised to DMSO. All statistical analyses performed on ΔCT values. n=3 with 4 replicates in each n.

5.3.6 Cell proliferation is not affected by Src or FAK inhibition

The effects of dasatinib, saracatinib and PF573228 on cell proliferation were assessed using BrdU assays. The use of dasatinib or saracatinib did not significantly alter the proliferation from control DMSO treatment in either cell-line across any of the transfections (Figure 5-12). Similarly PF573228 inhibition of FAK did not significantly alter cellular proliferation in any of the transfections and cell lines tested (Figure 5-12). For the BrdU experiments and all further experiments, 1nM dasatinib was utilised as this was the concentration of dasatinib that effectively inhibited PBF phosphorylation in both MCF-7 and MDA-MB-231 cells. For Saracatinib a concentration of 10nM was utilised as this was the lowest concentration that displayed a marked reduction in PBF phosphorylation in both cell-lines. A concentration of 100nM PF573228 was MCF-7 and MDA-MB-231 cells (data not shown).

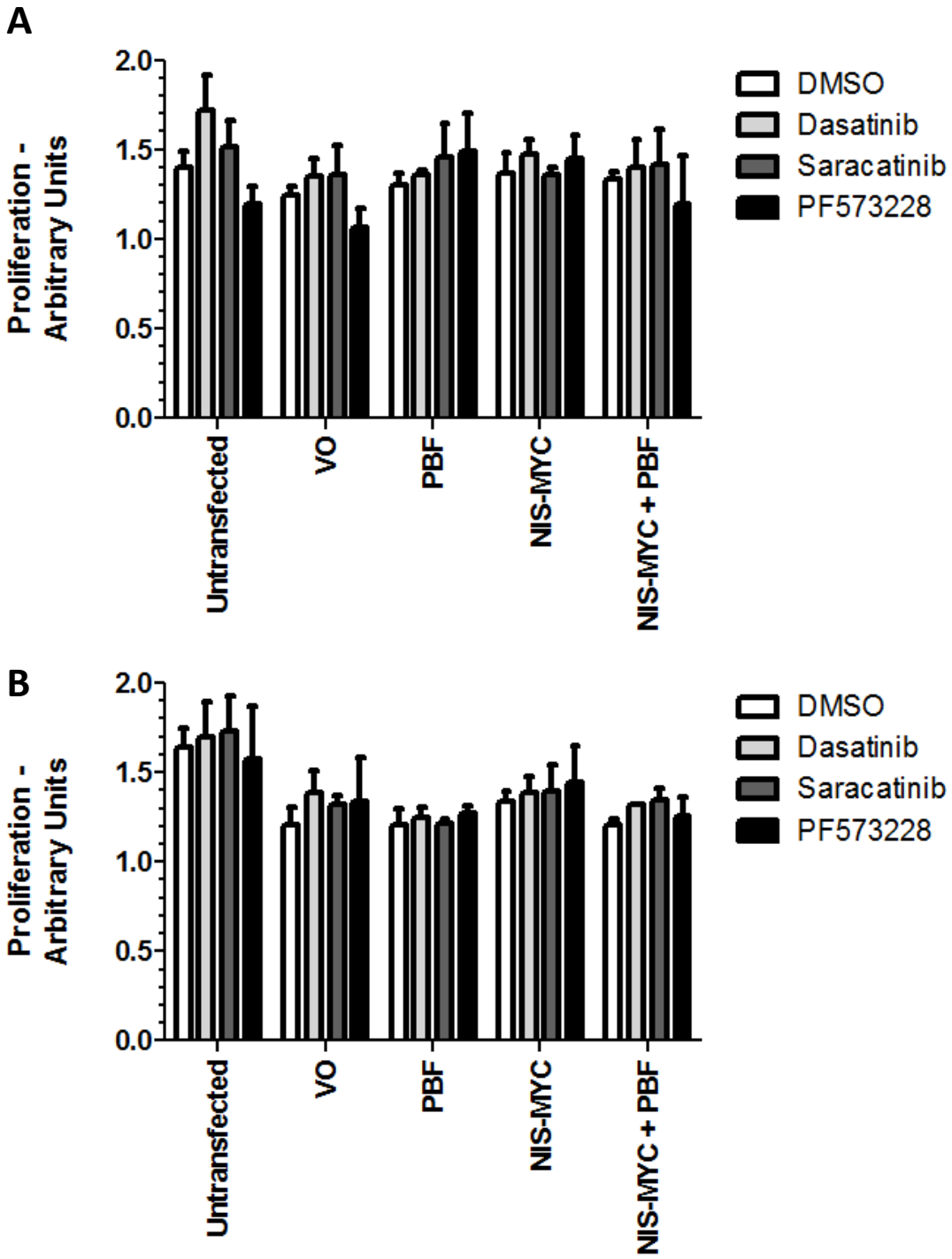

Figure 5-12. Inhibition of Src and FAK does not significantly affect cell proliferation. MCF-7 (A) and MDA-MB-231 (B) cells were transiently transfected with empty vector (VO), PBF and NIS-MYC for 48 hours and treated with DMSO, 1nM dasatinib, 10nM saracatinib or 100nM PF573228 for 24 hours prior to addition of BrdU labelling solution. n=3 with 3 replicates in each n.

5.3.7 Dasatinib and Saracatanib restore radioiodide uptake

Both dasatinib and saracatinib can inhibit the phosphorylation of PBF at concentrations as low as 1nM and 10nM respectively in breast cancer cells. Neither drug was capable of significantly increasing NIS expression in both MCF-7 and MDA-MB-231 cells so it was of great interest to establish whether the drugs could increase radioiodide uptake through the post-translational regulation of NIS. In MCF-7 cells, treatment with 1nM dasatinib and 10nM saracatinib restored radioiodide uptake in cells exogenously expressing PBF (Figure 5-13A). In DMSO treated cells, PBF expression reduced radioiodide uptake by 33% (p=0.002). Treatment with 1nM dasatinib increased uptake in PBF transfected cells by 65% (p= 0.038) (Figure 5-13A). This restoration of radioiodide uptake was also observed with treatment with 10nM saracatinib where there was an increase of 28% (p=0.021) compared to DMSO treatment) (Figure 5-13A). Treatment with neither dasatinib nor saracatinib could increase radioiodide uptake in MCF-7 cells not transfected with PBF (Figure 5-13A).

In MDA-MB-231 cells, exogenously expressed PBF significantly decreased radioiodide uptake by 33% (p=0.0016) (Figure 5-13B). Treatment with 1nM dasatinib rescued radioiodide uptake with an increase of 84% (p=0.0016) compared to DMSO treated PBF transfected cells and a difference of 23% (p=0.0355) compared to DMSO treated MDA-MB-231 cells lacking PBF transfection (Figure 5-13B). Again, saracatinib produced very similar results with an increase of 64% (p=0.049) compared to DMSO treated cells (Figure 5-13B). As observed in the MCF-7 cells, neither treatment could significantly influence radioiodide uptake in cells lacking exogenous PBF expression.

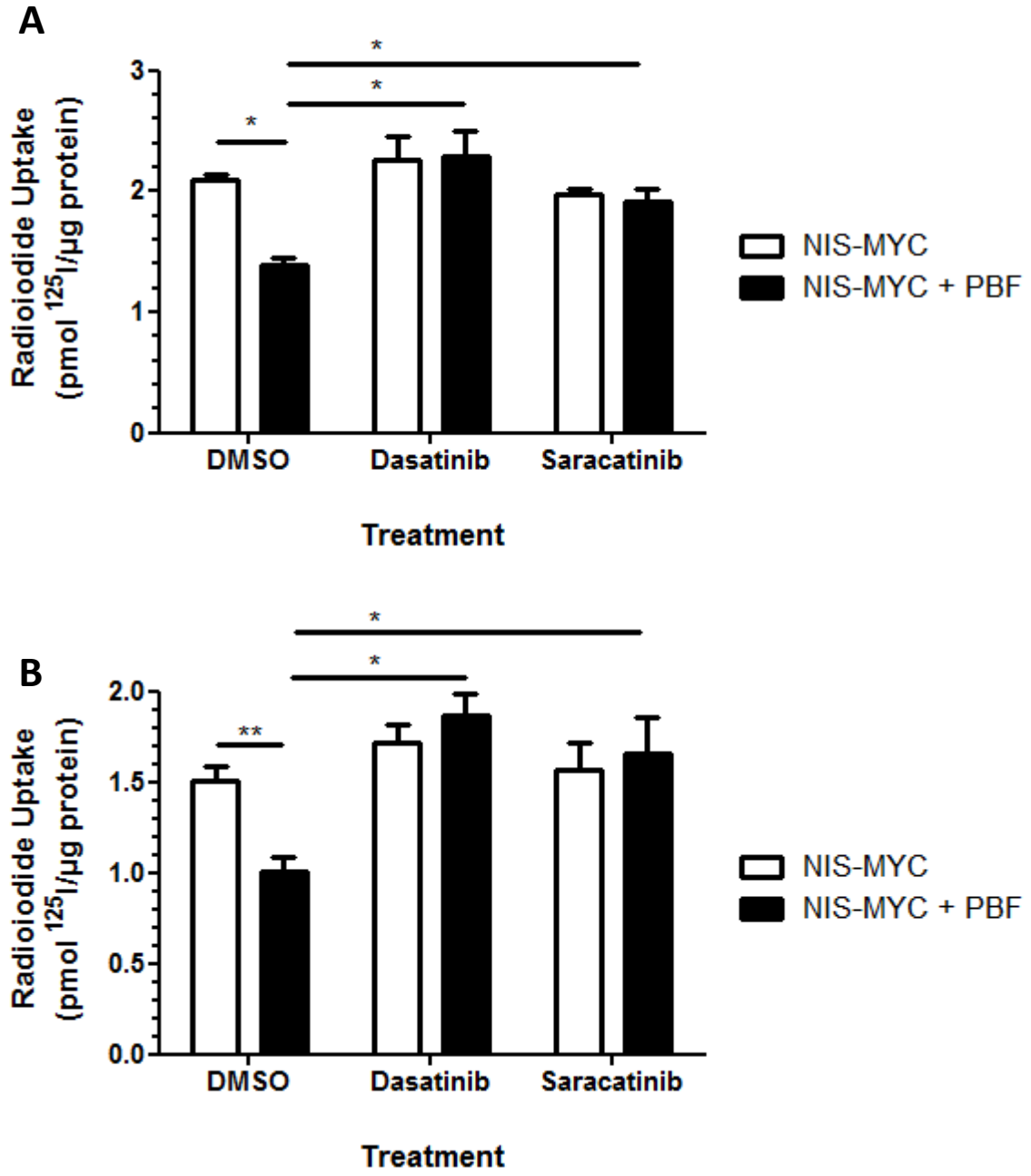

*Figure 5-13. Dasatinib and Saracatinib restore radioiodide uptake in breast cancer cells. (A) MCF-7 and (B) MDA-MB-231 cells were transfected for 48 hours with empty vector (VO) + NIS-MYC or NIS-MYC + PBF and treated with 1nM dasatinib or 10nM Saracatinib for 24 hours prior to the addition of ^{125}I. n=3 with 4 replicates in each n. *= p<0.05.**= p<0.01.*

5.3.8 Inhibiting FAK has differing effects on radioiodide uptake

Although inhibition of FAK did not appear to decrease PBF phosphorylation in breast cancer cells, it was of interest to see if it had any effect on radioiodide uptake. In MCF-7 cells, PBF reduced radioiodide uptake by 34% (p=0.0015) in DMSO treated cells (Figure 5-14A). Treatment with 100nM PF573228 restored radioiodide uptake in PBF expressing MCF-7 cells, increasing radioiodide uptake by 70% (p=0.001) compared to DMSO treated cells with a 13% difference from DMSO treated MCF-7 cells lacking PBF transfection (Figure 5-14A). The effect of FAK inhibition on radioiodide uptake in MCF-7 cells was in stark contrast to that witnessed with MDA-MB-231 cells as treatment with 100nM PF573228 did not restore radioiodide uptake in MDA-MB-231 cells (Figure 5-14B). PBF transfection reduced radioiodide by 33% (p=0.00218) in DMSO treated cells and there was no significant difference compared to PF573228 treated cells (10% difference, p=0.281) (Figure 5-14B).

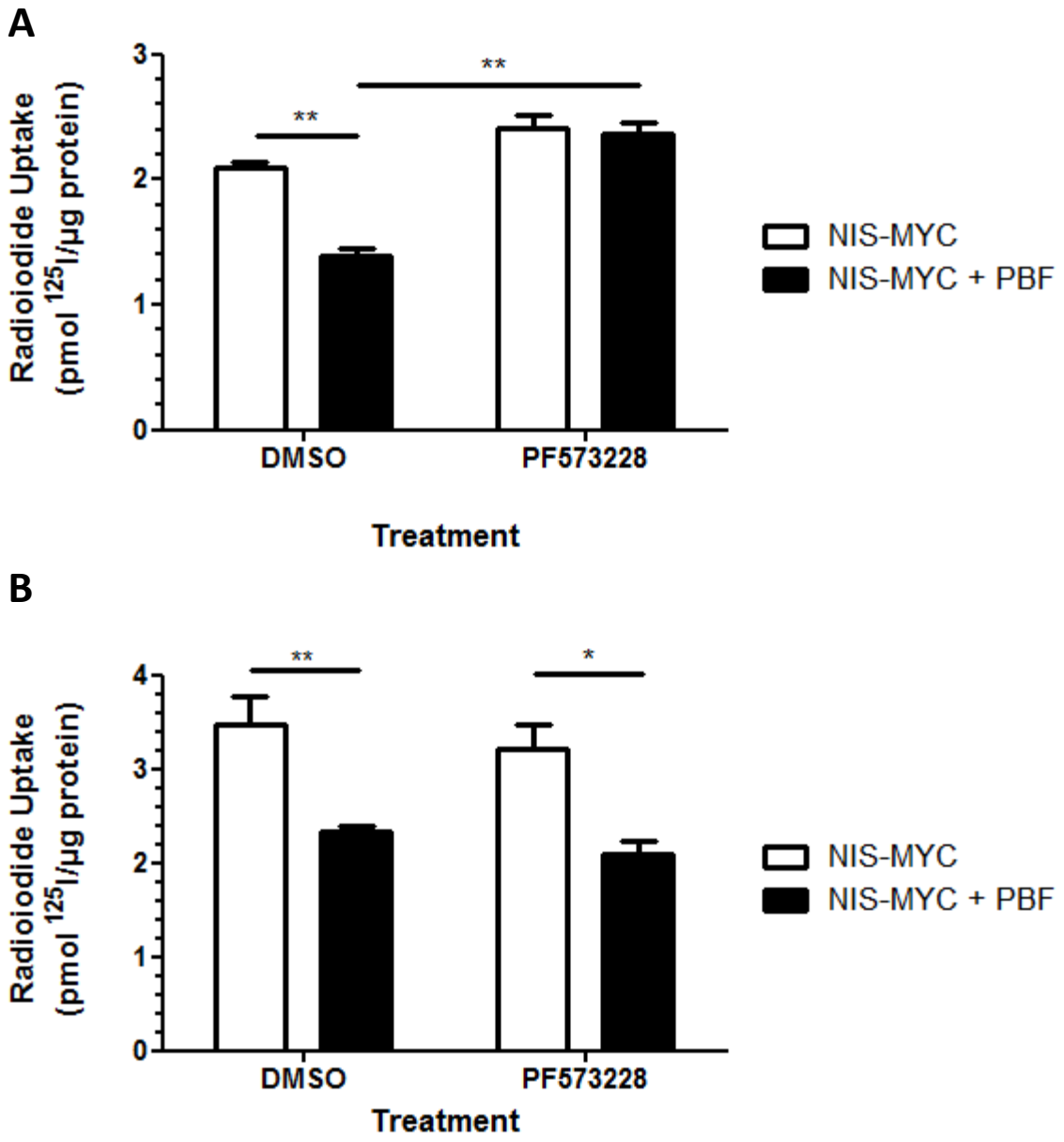

*Figure 5-14. Inhibition of FAK restores radioiodide uptake in MCF-7 breast cancer cells. (A) MCF-7 and (B) MDA-MB-231 cells were transfected for 48 hours with empty vector (VO) + NIS-MYC or NIS-MYC + PBF and treated with 100nM PF573228 for 24 hours prior to the addition of ^{125}I. n=3 with 4 replicates in each n. *= p<0.05.**= p<0.01.*

5.3.9 Saracatinib increase radioiodide uptake in cells with endogenous expression of PBF

To assess whether tyrosine kinase inhibitors (TKIs) could increase radioiodide uptake in MCF-7 cells possessing only endogenous PBF expression, MCF-7 cells were treated with ATRA and dexamethasone and TKI/FAK inhibitors. Treatment with ATRA and dexamethasone significantly increased radioiodide uptake (p<0.05) across all treatments compared to vehicle only (VeO) MCF-7 cells (treated with ethanol and DMSO). In ATRA and dexamethasone treated cells, treatment with PP1 and PF573228 did not increase radioiodide uptake compared to DMSO treated cells. Treatment with dasatinib had a trend towards increased radioiodide uptake with a 1.57-fold increase in uptake but was not statistically significant. Treatment with saracatinib significantly increased radioiodide uptake compared to DMSO treated cells with a 2-fold increase in uptake.

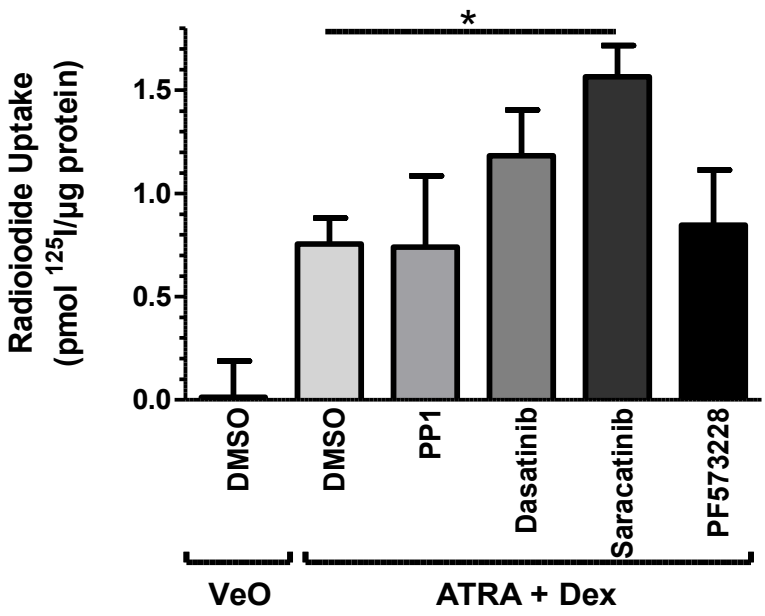

*Figure 5-15. TKIs can increase radioiodide uptake in cells with endogenous PBF expression. MCF-7 cells were transfected for 48 hours with VeO (ethanol and DMSO) or ATRA and dexamethasone for 48 hours and treated with DMSO, 2µM PP1, 1nM dasatinib, 10nM saracatinib or 100nM PF573228 for 24 hours prior to the addition of ^{125}I. n=3 with 4 replicates in each n. *= p<0.05 compared to DMSO, ATRA and dexamethasone treated cells.*

5.4 Discussion

5.4.1 Inhibition of SFK inhibits PBF phosphorylation and restores radioiodide uptake in breast cancer cells

The SFK kinase inhibitor PP1 has previously been demonstrated to inhibit the phosphorylation of PBF in thyroid cancer cell-lines (Smith et al., 2013). Both Src and Lyn are documented to be overexpressed in thyroid cancer, with limited expression of other members of the SFK family (Chan et al., 2012). Although Lyn is commonly overexpressed in thyroid cancers, evidence suggests that Src is the dominant SFK in thyroid carcinoma (Chan et al., 2012). With differential expression of SFK in breast cancer, it was important to assess the ability of PP1 and other SFK inhibitors to induce radioiodide uptake in breast cancer cells to establish whether targeting SFK prior to ^{131}I delivery could be a potential therapy in this disease.

5.4.1.1 PP1

In thyroid cancer cells PP1 was capable of inhibiting the phosphorylation of PBF at a concentration of 2μM (Smith et al., 2013). The data generated using PP1 in breast cancer cells was comparable to that in thyroid cancer cells with PBF phosphorylation being inhibited at concentrations of 2μM in MCF-7 cells and 100nM in MDA-MB-231 cells. Use of PP1 in breast cancer cells not only inhibited phosphorylation in both cell-lines at 2μM but also decreased NIS staining in intracellular vesicles and rescued radioiodide uptake (Smith et al., 2013). Again, this is comparable to the data generated in primary thyroid cells where treatment with 2μM PP1 rescued the reduction in radioiodide uptake observed with exogenous PBF expression.

Although PP1 is a potent SFK inhibitor, it has limited specificity and can target multiple kinases, so it was important to assess more specific inhibitors to determine SFK role in PBF phosphorylation.

5.4.1.2 Dasatinib and Saracatinib

Currently, there is no published evidence to suggest that the SFK inhibitors dasatinib or saracatinib can directly or indirectly influence NIS activity in any cell line or disease. In this chapter it was demonstrated that both dasatinib and saracatinib can inhibit PBF phosphorylation and ultimately rescue radioiodide uptake in cells overexpressing PBF. Dasatinib was observed to inhibit PBF phosphorylation at concentrations as low as 1nM in both MCF-7 and MDA-MB-231 cells, whilst a slightly increased concentration of 10nM was required for saracatinib to have the same effect. Not only did both inhibitors reduce PBF phosphorylation, they were also capable of reversing PBF's repression of radioiodide uptake. At the concentrations utilised in these experiments, neither compounds altered the proliferation of either MCF-7 or MDA-MB-231 cells across a range of different transfections, or significantly altered the expression of PBF or NIS in either cell-line. Saracatinib was also capable of significantly increasing radioiodide uptake in MCF-7 cells with only endogenous PBF expression and ATRA and dexamethasone boosted NIS expression. This effect could be to due to saracatinib increasing the levels of NIS expression within MCF-7 cells as seen by qRT-PCR.

Utilisation of these drugs to increase radioiodide uptake is potentially therapeutically important. Dasatinib already has FDA clearance for leukaemia treatments and saracatinib is currently being appraised in several clinical trials. Dasatinib was deemed to be tolerable for patients allowing a dose of 180 mg once daily over an

extended period (FDA, 2010b). In the proposed treatment regime for radioiodine therapy for breast cancer patients, dasatinib would be used as a pre-treatment for the therapy, only used in the days prior to radioiodine therapy to boost NIS activity and increase radioiodide uptake into breast cancer cells. The advantage of this short period of treatment with dasatinib is that patients are unlikely to experience the side-effects associated with prolonged treatment.

5.4.2 FAK does not modulate PBF phosphorylation

Previous mass spectrometry work identified FAK as a potential binding partner for PBF (unpublished data from the McCabe Group, Birmingham, UK), although the relationship between FAK and PBF has not been further investigated. From the data presented in this chapter it is evident that FAK does not modulate the phosphorylation status of PBF in breast cancer cells. Assessment of concentrations of PF573228 up to 2µM did not abolish pY174 PBF levels as determined by Western blotting and FAK inhibition was also incapable of restoring radioiodide uptake in MDA-MB-231 cells.

SFK and FAK are well-documented to have a complex relationship and one potential explanation for the discrepancies observed between the two cells lines may be due to the differential expression and different activation pathways of both SFKs and FAK in MCF-7 and MDA-MB-231 cells. The initiation of FAK activation involves FAK autophosphorylation at Y397, which creates a high-affinity SH2-dependent binding site for Src (Schaller et al., 1994). Src then further phosphorylates FAK at five tyrosine residues (Y407, Y576, Y577, Y861 and Y925) (Calalb et al., 1995; Calalb et al., 1996). In turn this leads to the activation of Src through the formation of a bipartite kinase

complex (Schaller et al., 1994). It could be hypothesised from the data in this chapter that inhibition of FAK may lead to indirect inhibition of Src in MCF-7 cells, whereas in MDA-MB-231 cells activation of Src may be independent of FAK. This is potentially supported by the fact that FAK expression has also been positively associated with Her2 expression in breast cancer (Schmitz et al., 2005). MCF-7 cells are known to have a positive Her2 status and so potentially have increased FAK levels compared with Her2 negative MDA-MB-231 cells. Another potential hypothesis is that although FAK inhibition can indirectly inhibit Src in both cell lines, Src may not be the dominant SFK in MDA-MB-231 cells, with PBF phosphorylation being modulated by a different SFK. However this is largely speculation and substantial further work would be needed to establish the complex mechanisms involved in the interplay between Src and FAK and their roles in PBF phosphorylation and modulation of radioiodide uptake.

Overall these data suggest that PBF is phosphorylated by members of the SFK family. Inhibition of the SFK family can reduce PBF phosphorylation which in turn reduces NIS mislocalisation and restores radioiodide uptake. Dasatinib and saracatinib appear to be of potential therapeutic value in breast cancer with both appearing to restore PBF's reduction in radioiodide uptake. Both Src (Smith et al., 2013) and Lyn (unpublished data) have the ability to bind to PBF *in vitro*, thus in order to further understand the mechanism of PBF phosphorylation in the hope of exploiting it, it is fundamental to establish which SFK is responsible for PBF phosphorylation.

CHAPTER 6 - SRC REGULATES/POTENTIALLY PHOSPHORYLATES PBF

6.1 Introduction

The data presented so far in this thesis has provided strong evidence that the phosphorylation of PBF is critical for its interaction with NIS. PBF phosphorylation can be inhibited by SFK inhibitors. In thyroid cancer Src kinase is the dominant SFK with the only other family member expressed being Lyn (Chan et al., 2012). As SFKs are differentially expressed in breast cancer, it is important to understand which SFK is responsible for the phosphorylation of PBF within the disease.

6.1.1 Expression of SFK in breast cancer

In breast cancer, all 8 SFK family members have been shown to be expressed with Src and Lyn having the highest expression and being associated with poor prognosis and clinical outcome (Elsberger et al., 2010). Src was found to be primarily cytoplasmic with some nuclear and membranous expression in breast cancer whereas Lyn was localised mainly in the cytoplasm and nucleus with limited plasma membrane staining (Elsberger et al., 2010). Lck is the only SFK member that has been associated with ER status, with ER negative tumours having the highest expression levels. However, Src expression was significantly associated with decreased disease-specific survival in ER-positive breast cancer patients compared to those with ER-negative tumours (Elsberger et al., 2010). Src has also been linked to high tumour grade and reduced recurrence-free survival in DCIS (Wilson et al., 2006).

6.1.2 Src

Src was the first characterised member of the SFK family, and is as such the most studied. The human Src protein is 536 amino acids in length and has a similar structure to all SFK, being comprised of a myristoylation site, a unique region, an SH3 and SH2 domain followed by a protein-tyrosine kinase SH1 domain (Waksman et al., 1993; Xu et al., 1999; Yu et al., 1992) (Figure 6-1). During biosynthesis, the N-terminal methionine is removed resulting in an N-terminal glycine that becomes myristoylated (Peseckis et al., 1993) (discussed further in Chapter 7) (Figure 6-1). Chicken and avian Rous sarcoma viral Src (v-Src) have also been extensively investigated, sharing 99.6% and 95.8% homology with human c-Src respectively (Roskoski, 2015). Src contains two tyrosine residues whose phosphorylation is critical to regulation of the protein: Y418 and Y529. Tyrosine-Y529 (Y527 in chicken Src) is an autoinhibitory phosphorylation site whereas Y418 is within the kinase (SH1) domain and phosphorylation of this residue results in a kinase with full catalytic activity (Nada et al., 1991; Smart et al., 1981). *In vivo*, Src kinases are phosphorylated on either Tyr 418 (in their active state) or Tyr 529 (in the inactive state) (Figure 6-1).

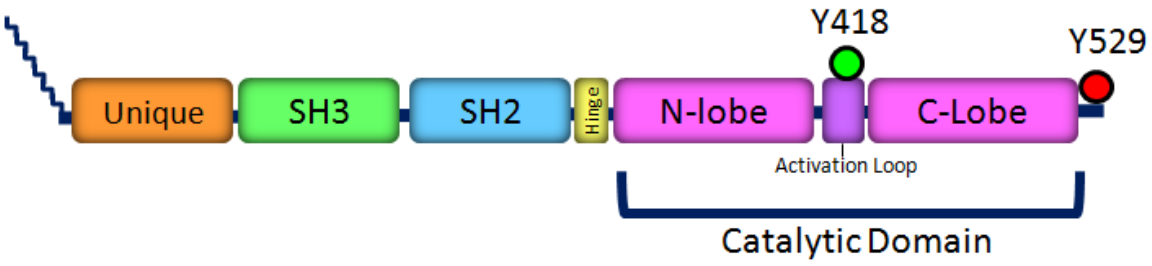

Figure 6-1. A schematic diagram detailing the structure of Src. Src is comprised of unique region, Src homology 3 and 2 domains (SH3/2), a hinge region and a catalytic kinase domain. N-terminal myristoylation is illustrated along with important pY motifs that are phosphorylated in the inactive (pY529, red) and active (pY418, green) kinase.

Src is a non-receptor tyrosine kinase that can be activated by cytoplasmic proteins including FAK and Crk-associated substrate (CAS). Interaction with proteins such as FAK disrupts the intermolecular interactions within Src, altering the conformation and leading to Src activation (Figure 6-2). Src is expressed ubiquitously throughout many human tissues and has been associated with many cellular processes including proliferation, differentiation, survival, adhesion and migration. Many cancers have been observed to have increased Src expression or activity due to overexpression or deregulation of upstream growth factor receptors such as EGFR or HER2 (Luttrell et al., 1994).

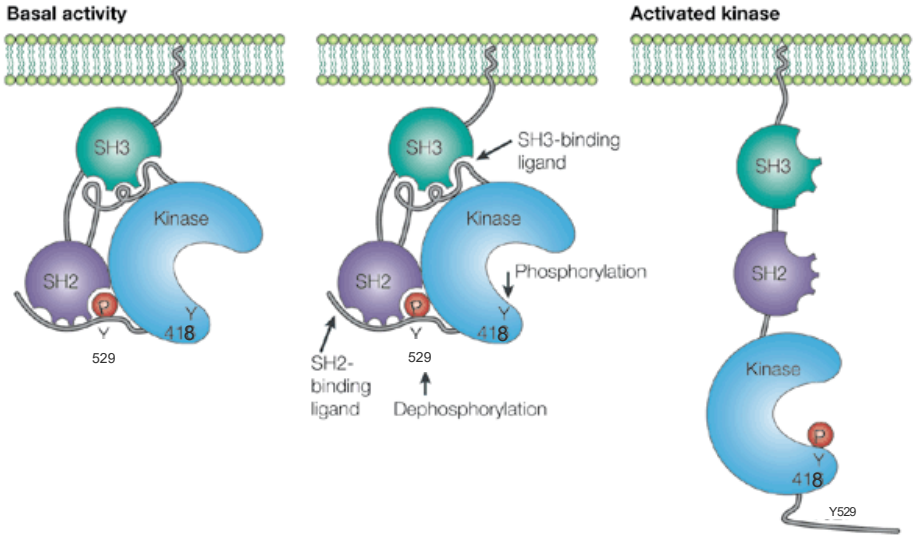

Figure 6-2. The activation of Src. In the inactive conformation (the left panel), the phosphorylated Y529 interacts with the SH2 domain, positioning the SH3 domain to interact with the linker between the hinge region between the SH2 and SH1 domain. The middle panel illustrates the mechanisms by which Src can be activated with the right panel depicting activated Src. Adapted from Martin, 2001.

Src kinase activity is approximately 4-20 fold higher in breast tumours compared to normal breast tissue (Egan et al., 1999; Rosen et al., 1986), although overexpression of Src alone is insufficient to transform fibroblasts in culture (Shalloway et al., 1984). Src was

found to be upregulated in 95% of triple negative (TN) samples and 84% of other breast cancer types, with TN tumours having increased membranous expression of Src, where active Src was localised within peripheral membrane-associated focal adhesions (Tryfonopoulos et al., 2011). Src has a fundamental role in signalling and cross-talk between growth-promoting pathways known to be active in breast cancer such as the ER and EGFR family signalling pathways. Expression of Src is required for EGF-induced mitogenesis (Wilson et al., 1989) and for the induction of mammary tumours using the polyomavirus middle T oncogene (Guy et al., 1994). *In vitro*, hypoxia has been found to activate Src resulting in upregulation of vascular endothelial growth factor (VEGF), a signalling molecule fundamental for malignant angiogenesis (Mukhopadhyay et al., 1995). Src has also been deemed a pivotal protein in cell migration with Src suppression resulting in significantly reduced cell migration, attachment and spread in MCF-7 cells (Gonzalez et al., 2006). Expression of phosphorylated Src and STAT3 have also been correlated with invasive carcinoma, with levels being significantly higher in invasive tumours compared to non-neoplastic tissue (Diaz et al., 2006). Src has also been identified as part of a common signalling axis in trastuzumab (Herceptin) resistance in breast cancer (Zhang et al., 2011).

As aforementioned in chapter 5, several Src and SFK inhibitors are being investigated in the treatment of breast cancer. Phase I and II clinical trials are on-going to assess dasatinib within the disease, along with a trial to specifically assess the potential of dasatinib as a treatment for in breast cancer bone metastasis (Finn, 2008; Mitri et al., 2016). However, a gatekeeper mutation has been identified in Src that leads to a dasatinib-resistant, constituently active form of the kinase (Azam et al., 2008).

6.1.3 Src Gatekeeper residue (T341)

Many small molecule inhibitors of kinases target the ATP binding pocket of the protein and dasatinib is no exception, functioning by competing for binding to this site with ATP. Threonine-341 (T341) in Src (T338 in chicken Src) is often referred to as the gatekeeper residue within the kinase due to the size of the residue's side chain governing the volume and shape of the ATP-binding pocket and thereby determining the size of the ATP-competitive ligands that can bind.

The Src protein kinase domain is comprised of a small amino-terminal lobe and large carboxy-terminal lobe that form a cleft that serves as a docking site for ATP. The larger lobe can exist in two forms; an extended open conformation when Src is activated and a closed conformation when inactive. Within the activation segment of the kinase domain there are three key amino acids DFG (Asp-Phe-Gly). When the kinase is dormant, the aspartate side chain of the conserved DFG-sequence faces away from the active site (termed the DFG-Asp out conformation). When Src is activated the aspartate side faces into the ATP-binding pocket (DFG-Asp in conformation) and coordinates a Mg^{2+} ion (Hubbard, 1997; Hubbard et al., 1994). There are two major classes of reversible ATP-competitive protein kinase inhibitors: type I and type II. Dasatinib is a type I inhibitor binding to the DFG-Asp in kinase conformation (Getlik et al., 2009)(Figure 6-3). Dasatinib interacts with A296 and L396 and forms hydrophobic contacts with Y343, T341, M339 and V284 (Figure 6-3). T341 has been deemed the gatekeeper molecule, with mutation of the residue to isoleucine or a bulkier amino acid stabilising a 'hydrophobic spine' which further stabilises Src in an active conformation (Figure 6-4). Mutation to T341I Src not only results in a constituently active form of Src but also causes significant steric

hindrance from the presence of a bulkier side chain that is unable to form hydrophobic bonds with small-molecule inhibitors creating a dasatinib resistant form of the kinase (Azam et al., 2008).

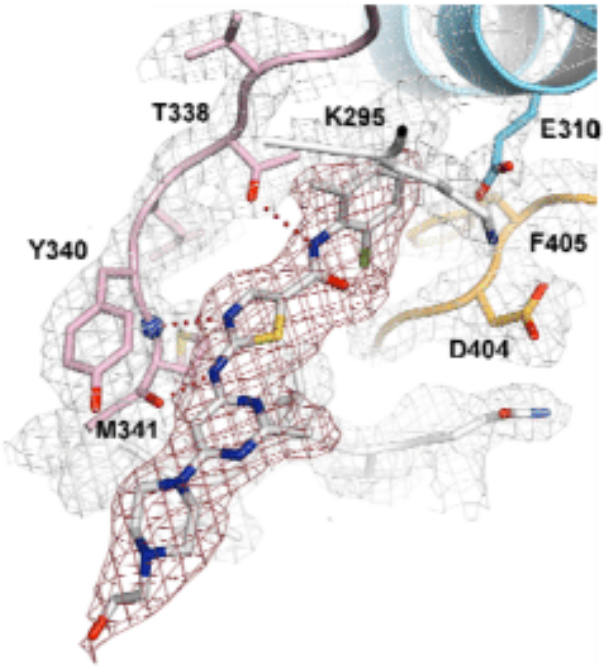

Figure 6-3. Crystal structure of the c-Src-dasatinib complex. Electron density map of dasatinib bound to the ATP-pocket of the active DFG-Asp in Src. Src is shown in grey with dasatinib in red with chicken Src nomenclature for amino acid numbering. Taken from Getlik et al., 2009.

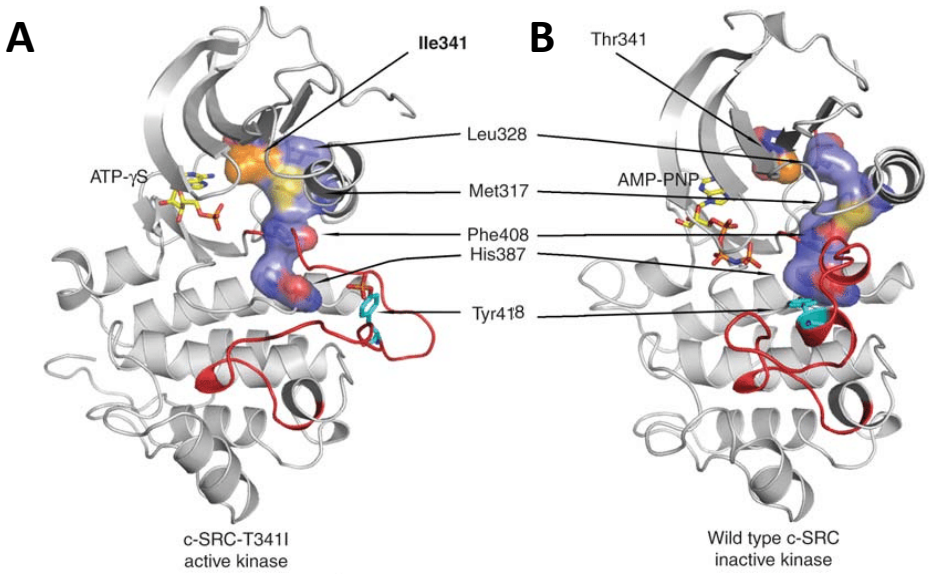

Figure 6-4. The hydrophobic spine in active and inactive Src kinases. (A) Crystal structure T341I Src bound to ATP. The residues Leu328, Met317, Phe408 and His387, which constitute the hydrophobic spine, are shown in blue. The gatekeeper isoleucine residue is shown in orange. The activation loop is shown in red. (B) The inactive conformation of WT Src, coloured as in (A). Adapted from Azam et al., 2008.

In vitro studies have shown that mutation of T341 in lung cancer cells rescued cell viability from dasatinib over a range of concentrations (Li et al., 2010). This effect has also been observed in thyroid cancer cells where expression of the gatekeeper mutant blocked the growth inhibitory effects of dasatinib, shifting the IC_{50} value from ~40 nmol/L to 1,200 nmol/L (Chan et al., 2012). Up to now, two mutations to T341 have been identified in the COSMIC database, a lung cancer sample with a T341R mutation (COSMIC Database, 2016c) and an endometrial carcinoma with a T341A mutation (COSMIC Database, 2016b).

The aim of the work described in this chapter was to establish whether Src has a fundamental role in the phosphorylation of PBF *in vitro.* Thus far inhibition of SFK has been observed to decrease PBF phosphorylation and restore radioiodide uptake in PBF expressing cells. Both Src (Smith et al., 2013) and Lyn (unpublished data) can bind to PBF in thyroid cancer cells with the expression of other SFKs being limited in this disease (Chan et al., 2012). In breast cancer, all family members of the SFK are expressed (Elsberger et al., 2010) increasing the number of possible kinases that could be responsible for PBF phosphorylation. To maximise radioiodide uptake it is fundamental to establish which kinase is responsible for PBF phosphorylation in breast cancer with the hope of identifying a specific and potent inhibitor.

6.2 Materials and Methods

6.2.1 Cell Culture

MCF-7 and MDA-MB-231 cells were maintained as described in 2.1.2 with stably-transfected MCF-7 cells cultured in medium containing G418 (1 mg/ml) and lentivirally-transduced MDA-MB-231 cells cultured in medium containing blasticidin (15 μg/ml). All cell lines were seeded at 30,000 cells per well in a 24 well plate for radioiodide uptake and at 150,000 and 200,000 cells per well in a 6 well plate for fluorescence immunocytochemistry and protein extraction respectively.

6.2.2 Drug Treatments

MCF-7 cells were treated with 100nM ATRA and 1μM dexamethasone as described in section 3.2.3. In all combination treatments, an equal volume of ethanol and DMSO in cell media was used as a control. Cells were treated with dasatinib as described in 5.2.2 at a concentration of 10nM.

6.2.3 Mutagenesis

Mutagenesis was performed as described in 4.2.4. A pcDNA3.1 (+) vector containing WT Src (kindly gifted by Neil Sharma, University of Birmingham) was utilised to create a T341I mutant form of Src. The sequence for the forward and reverse mutagenesis primers for T341I Src (Sigma-Aldrich) (Table 6-1) were designed and manufactured as recommended

by the QuikChange II XL Site-directed mutagenesis kit. Mutated plasmid DNA was then purified, sequenced and amplified in the same manner as described 4.2.5.

	Sequence
T341I Src Forward	**5'** GAG CCC ATT TAC ATC GTC ATC GAG TAC ATG AGC AAG GGG **3'**
T341I Src Reverse	**5'** CCC CTT GCT CAT GTA CTC GAT GAC GAT GTA AAT GGG CTC **3'**

Table 6-1. Mutagenesis primers for T341I Src. The red letter signifies changes to the Src sequence intended for the creation of a mutant Src.

6.2.4 Transfection

Transfection was performed as described in 2.2.3. WT PBF-HA, Y174 PBF-HA (kindly gifted by Dr Vicki Smith), EEN/AAA PBF-HA, WT Src, Src T341I and EEN170-172AAA PBF-HA in pcDNA3.1 (+) vectors were transfected into MCF-7 cells in 6 well plates for use in fluorescence immunocytochemistry and Western blotting. For radioiodide uptake cells were seeded in 24 well plates and transfected with untagged forms of WT, EEN170-172AAA and Y174A PBF.

6.2.5 Fluorescence immunocytochemistry

Fluorescence immunocytochemistry was performed as described in 2.4. Cells were treated with 100µM sodium pervanadate for 20 minutes prior to fixing to allow the

detection of pY418 Src. Antibodies used included anti-HA tag (mouse) (1:200) (Covance), anti-pY418 Src (rabbit) (1:50) (Abcam) and anti-Src (mouse) (1:100) (Abcam).

6.2.6 Co-immunoprecipitation Assay (Co-IP)

Co-IP was performed as described in 4.2.12. Cells were cultured in T75 flasks and transfected with Src and empty pcDNA3.1(+) vector, PBF-HA, EEN/AAA PBF-HA or Y174A PBF-HA. Protein was IP-ed with mouse anti-HA tag antibody (Covance) (7.5µl) overnight at 4°C with end-over-end rotation.

6.2.7 Western Blotting

Protein extraction and Western blotting were performed as described in sections 2.3.1 and 2.3.2 respectively. Cells were treated with 100µM sodium pervanadate for 20 minutes prior to harvesting to allow the detection of pY174 PBF. Antibodies used were anti-pY174 PBF antibody (Covalab) (Smith et al., 2013), anti-PBF (Eurogentec) (Smith et al., 2009), anti-phospho-Src (Y418) (Abcam), anti-Src (Cell Signalling) and β-actin (Sigma-Aldrich)(refer to section 2.8). Appropriate secondary antibodies were used.

6.2.8 Radioiodide uptake

Radioiodide uptake was performed as described in 2.7. Transfection and drug treatments were performed 48 and 24 hours respectively before the addition of ^{125}I to cells.

6.2.9 Statistics

Data were analysed using Sigma Plot (SPSS Science Software UK Ltd). The one-way ANOVA was used to compare groups of parametric data with significance taken at $p<0.05$.

6.3 Results

6.3.1 PBF colocalises with Src and pY418 Src

Transient transfection of Src into MCF-7 cells resulted in Src expression within the cytoplasm and at the plasma membrane (Figure 6-5A) with activated pY418 Src locating primarily at the plasma membrane (Figure 6-5B). Co-transfection with PBF revealed colocalisation between Src and PBF primarily in cytoplasmic vesicles (depicted by localised yellow spots) with limited plasma membrane yellow (Figure 6-5A). pY418 Src that also appeared to colocalise with PBF in intracellular vesicles (Figure 6-5B). Co-transfection of PBF and Src appeared to alter the subcellular localisation of Src increasing levels of cytoplasmic Src (Figure 6-5A).

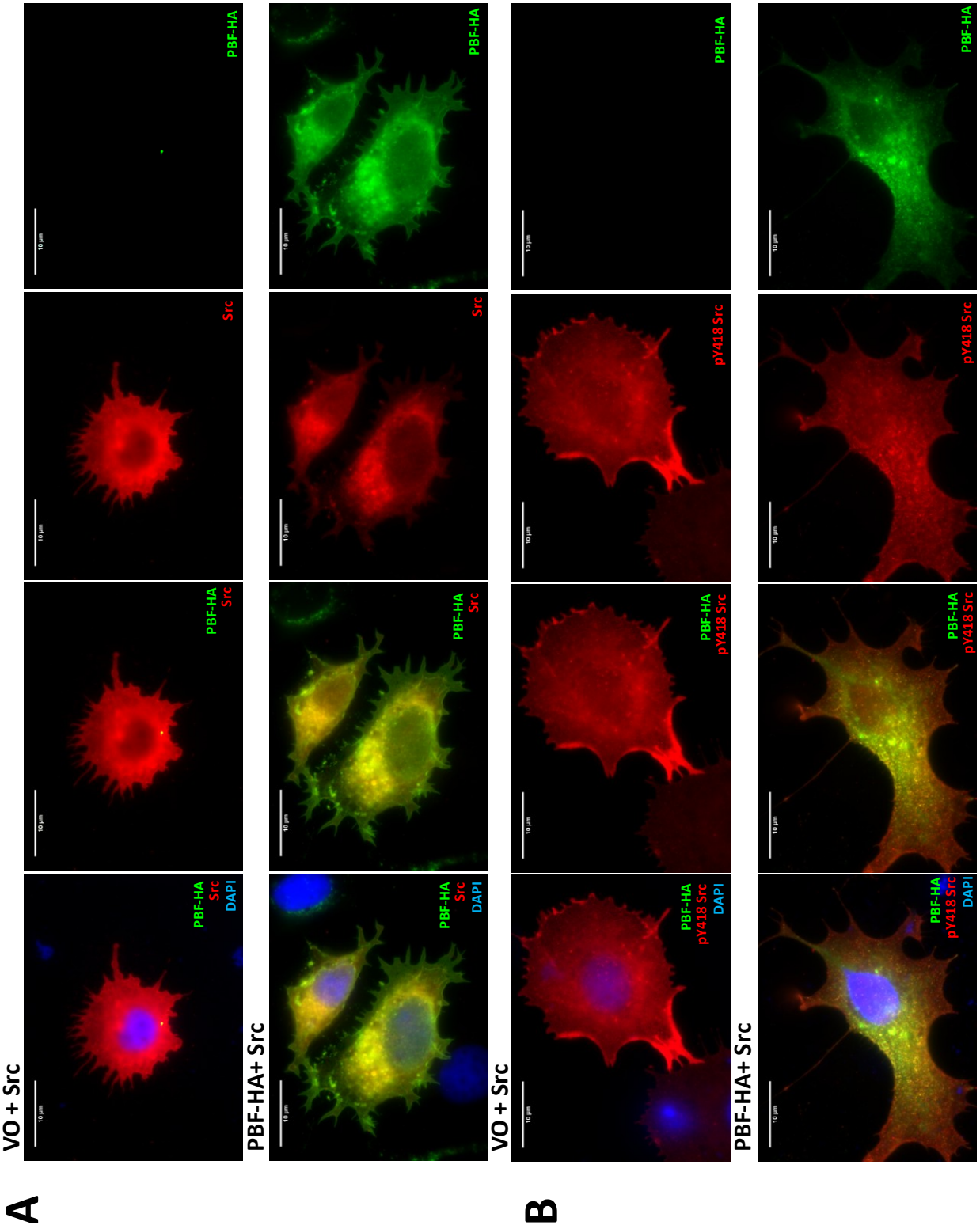

Figure 6-5. PBF colocalises with Src and pY418 Src. MCF-7 cells were co-transfected with empty pcDNA3.1(+) vector (VO) + Src or PBF-HA + Src. In A, Src is visualised using a rabbit anti-Src antibody in red and PBF-HA with a mouse anti-HA antibody in green. In B, pY418 Src is visualised using a rabbit anti-pY418 Src antibody in red and PBF-HA visualised using a mouse anti-HA tag antibody in green. In all images nuclei are visualised in blue using Hoechst stain with yellow staining indicating colocalisation. 100x magnification. n=2.

6.3.2 Src and PBF bind in breast cancer cells

To assess whether Src and PBF bind *in vitro,* co-immunoprecipitation studies were performed by pulling down HA-tagged PBF and assessing the levels of bound Src. In MCF-7 cells, binding was observed between WT PBF-HA and Src (Figure 6-6). Although the antibody staining was not particularly strong, there was evidence to suggest that WT, EEN/AAA and Y174A PBF were all capable of binding Src with little difference in the binding affinity (Figure 6-6).

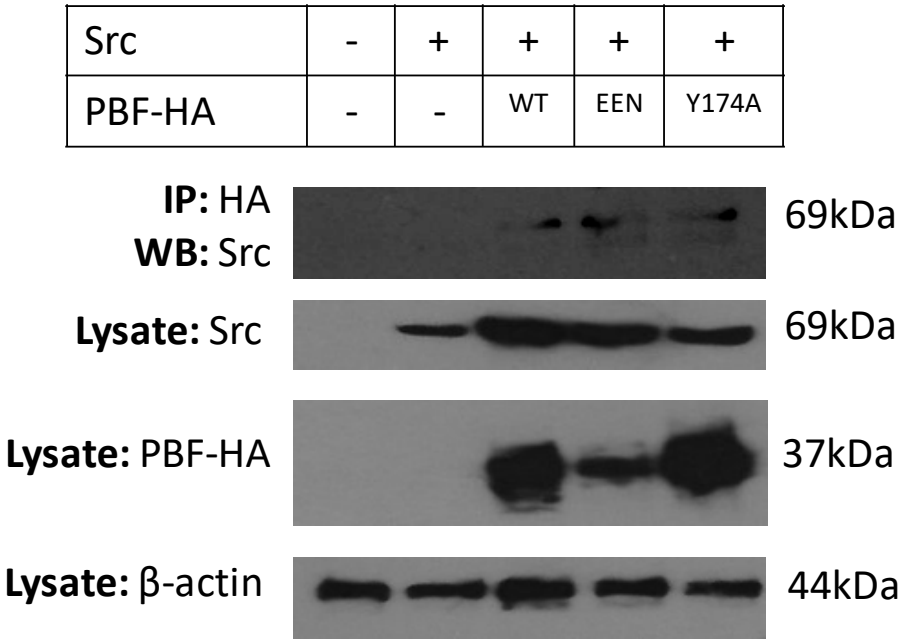

Figure 6-6. All forms of PBF bind to Src. MCF-7 cells were co-transfected with Src alongside empty pcDNA3.1(+) vector (VO), WT, EEN/AAA or Y174A PBF-HA for 48 hours prior to harvesting. In the Co-IP, proteins were pulled down using the HA antibody and probed with the Src antibody. Whole cell lysate was probed with HA, Src and β-actin as a loading control. n=2.

6.3.3 Exogenous Src increases levels of pY174 PBF

To assess the effect of Src on the phosphorylation status of PBF, Src was transfected into MCF-7 and MDA-MB-231 cells and protein was extracted. Western blotting confirmed Src transfection to be successful in both cell lines through increased levels of both total Src and pY418 active Src (Figure 6-7). Exogenous Src expression also led to increased levels of pY174 PBF while levels of total PBF remained unchanged (Figure 6-7).

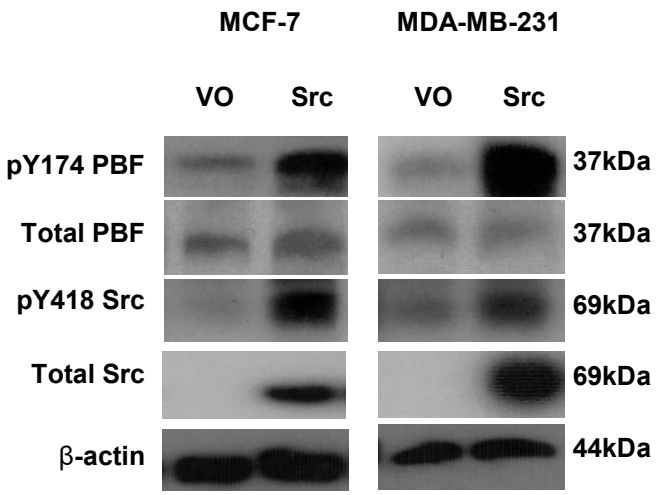

Figure 6-7. Exogenous Src expression increases levels of pY174 PBF. MCF-7 and MDA-MB-231 cells were transfected with empty pcDNA3.1(+) vector (VO) or Src for 48 hours prior to protein harvesting. pY174 PBF, total PBF, pY418 Src and total Src were detected with β-actin used a loading control. n=3.

6.3.4 Exogenous Src decreases radioiodide uptake

To assess whether exogenous Src affects the radioiodide uptake of breast cancer cells, ATRA and dexamethasone-treated MCF-7 cells stably transfected with empty pCI-neo vector, WT, EEN/AAA and Y174A PBF were then transiently transfected with Src or empty pcDNA3.1(+) vector. Exogenous Src was capable of significantly reducing radioiodide uptake across each of the stable cell lines compared to empty pcDNA3.1(+) vector transfected cells except for EEN/AAA PBF (Figure 6-8). Stable transfection of PBF reduced radioiodide uptake by 43% (p= 0.02) compared to control pCI-neo vector transfected cells and this was even further reduced in the presence of Src (33% decreased compared to PBF + empty pcDNA3.1(+) vector, p=0.045) (Figure 6-8). PBF stable transfection also reduced radioiodide uptake significantly compared to stable transfection with EEN/AAA and Y174A PBF (42% and 37% reduction, p=0.01 and p=0.02 respectively). Stable transfection of EEN/AAA PBF was unable to significantly reduce radioiodide uptake compared to empty pCI-neo vector stable transfection (3% reduction, p=0.8), with transfection of Src again not significantly reducing radioiodide uptake (21% reduction, p=0.15) (Figure 6-8). Y174A PBF stable transfection did not reduce significantly radioiodide uptake compared to stable transfection with empty pCI-neo vector (11% reduction, p=0.4) however transient transfection with Src did significantly decrease radioiodide uptake in Y174A PBF stable cells compared to Y174A PBF co-transfected with empty vector (29% reduction, p=0.0098) (Figure 6-8).

Transfection of PBF and Src was also capable of reducing radioiodide uptake compared to empty vector and Src (42% reduction, p=0.006). EEN/AAA PBF + Src and

Y174A PBF + Src were not significantly different to empty vector + Src (15% increase and 2% reduction, p=0.34 and p=0.84 respectively).

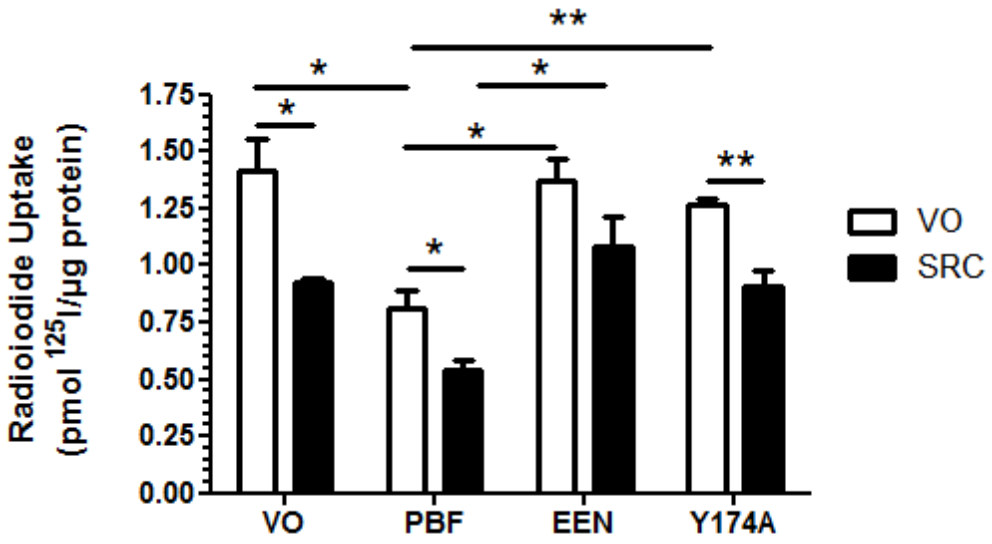

*Figure 6-8. Src reduces radioiodide uptake in MCF-7 cells. ATRA and dexamethasone treated MCF-7 cells stably transfected with empty pCI-neo vector (VO), PBF, EEN/AAA or Y174A PBF were transiently transfected with empty vector (VO) or Src and radioiodide uptake assessed. Cells were transiently transfected for 48 hours prior to the addition of radioiodide. n=3 with 4 replicates in each n. * = p<0.05. ** = p<0.01.*

6.3.5 Successful production of the mutant T341I Src

Wild-type Src was successfully mutated to T341I via mutagenesis. The new plasmid was sequenced and BLAST used to compare the sequences. BLAST confirmed the correct mutation of the Src plasmid, with both the nucleotide sequence (Figure 6-9) and translated amino acid sequence displaying the correct mutation.

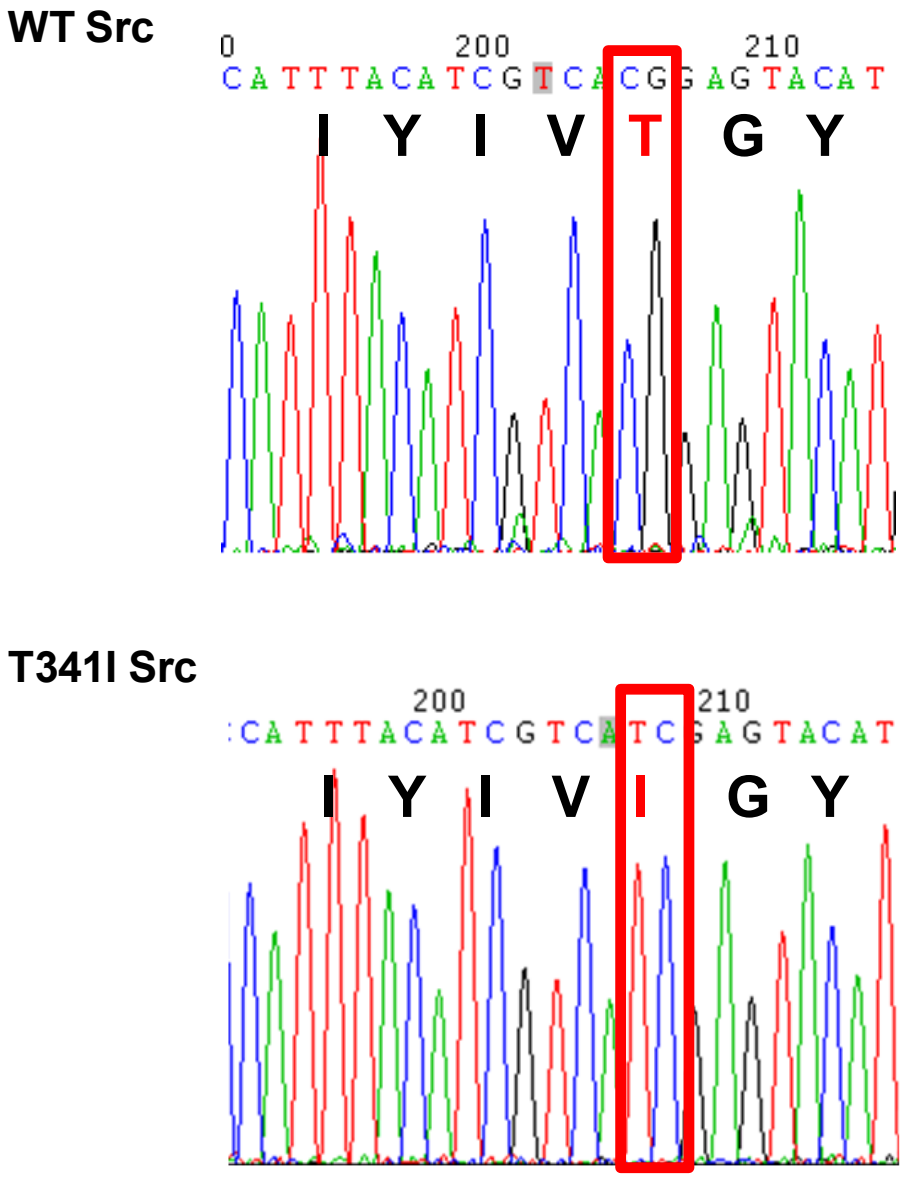

Figure 6-9. Successful mutation of Src at residue 341. Sequencing of the pcDNA 3.1 plasmid containing human Src confirmed successful mutagenesis with the presence of ATC instead of ACG.

6.3.6 T341I Src increases pY174 PBF levels in the presence of dasatinib

Exogenous WT Src is capable of increasing levels of phosphorylated Y174 PBF as observed in Figure 6-7. However this increase in pY174 PBF was abrogated in the presence of 10nM dasatinib (Figure 6-10). Treatment with dasatinib decreased levels of active pY418 Src in both empty vector and WT Src-expressing cells whereas cells containing mutant T341I Src

did not display a decrease in pY418 Src, confirming this mutant Src is constitutively active (Figure 6-10). Expression of mutant T341I Src was still capable of increasing levels of pY174 PBF compared to empty vector control in DMSO treated cells (Figure 6-10). However, unlike WT Src, T341I Src was resistant to dasatinib and could still increase pY174 PBF levels in the presence of this inhibitor. Dasatinib had no effect on the levels of total PBF or Src (Figure 6-10).

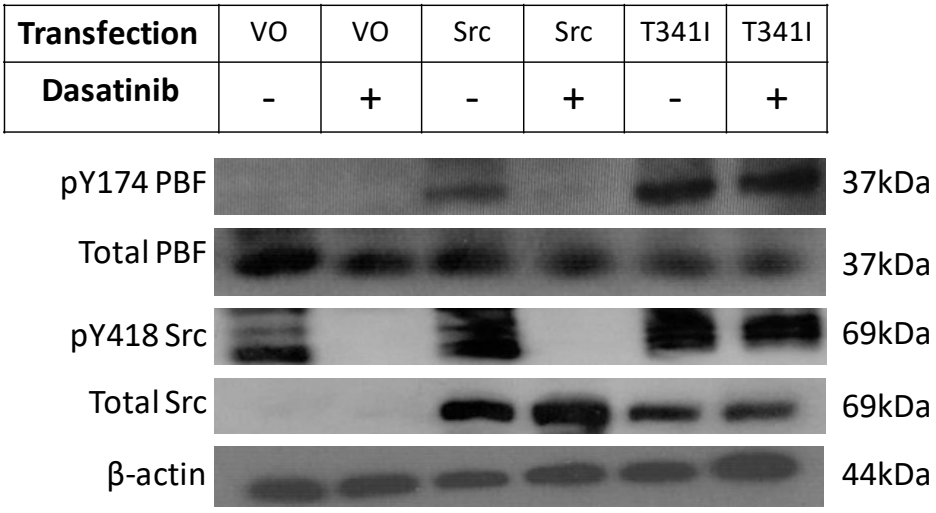

Figure 6-10. T341I Src increases pY174 PBF levels irrespective of dasatinib treatment. MCF-7 cells were transfected with empty vector (VO), WT Src or T341I Src for 48 hours and treated with 10nM dasatinib 24 hours prior to protein harvesting. pY174 PBF, total PBF, pY418 Src and total Src were detected with β-actin used a loading control. n=3.

6.3.7 T341I Src reduces radioiodide uptake in the presence of dasatinib

To assess whether exogenous Src affects the radioiodide uptake of breast cancer cells, ATRA and dexamethasone-treated MCF-7 cells stably transfected with empty pCI-neo vector, WT, EEN/AAA and Y174A PBF were then transiently transfected with empty pcDNA3.1(+) vector, or Src and treated with either DMSO or 10nM dasatinib. In DMSO treated, control empty vector transiently transfected cells stable transfection of PBF

reduced radioiodide uptake (37% decrease, *p*=0.02) whereas stable transfection with EEN/AAA and Y174A PBF could not significantly reduce radioiodide uptake (1% and 3% reduction, *p*=0.83 and *p*=0.80 respectively) (Figure 6-11). This reduction in radioiodide uptake with WT PBF was restored after treatment with 10nM dasatinib (49% increase, *p*=0.04) replicating earlier data in this thesis (Figure 6-11).

In DMSO treated cells, transient transfection with Src reduced radioiodide uptake in cells stably transfected with empty vector, WT and Y174A PBF (31%, 36% and 35% reduction, *p*=0.03 *p*=0.02 and *p*=0.01 respectively compared to the respective stable transfection with transient empty vector transfection)(Figure 6-11). Transfection with PBF + Src significantly reduced radioiodide uptake compared to empty vector + Src with a 42% reduction (*p*=0.048) replicating data from 6.3.4. EEN/AAA PBF + Src and Y174A PBF + Src did not reduce radioiodide significantly compared to empty vector + Src (13% increase and 9% decrease, *p*=0.46 and *p*=0.64 respectively). In PBF + Src expressing cells dasatinib was capable of rescuing Src's reduction in radioiodide uptake with a 126% increase (*p*=0.01) restoring radioiodide uptake to near empty vector levels (7% difference, *p*=0.40)(Figure 6-11). Dasatinib also rescued radioiodide uptake in empty vector + Src (43% increase, *p*=0.045) expressing cells (Figure 6-11).

To establish whether dasatinib was acting on Src or another kinase, the T341I dasatinib-resistant form of Src was utilised. Across stable transfection with empty pCI-neo vector, WT, EEN/AAA and Y174A PBF, T341I Src reduced radioiodide uptake in the same manner as wild-type Src. T341I Src significantly reduced radioiodide uptake in PBF stably transfected cells by 30% (*p*=0.039). However unlike with WT Src transfection, dasatinib was not capable of rescuing radioiodide uptake with T341I Src in any of the stable

transfections (Figure 6-11), suggesting Src is the kinase responsible for PBF phosphorylation and repression of NIS function.

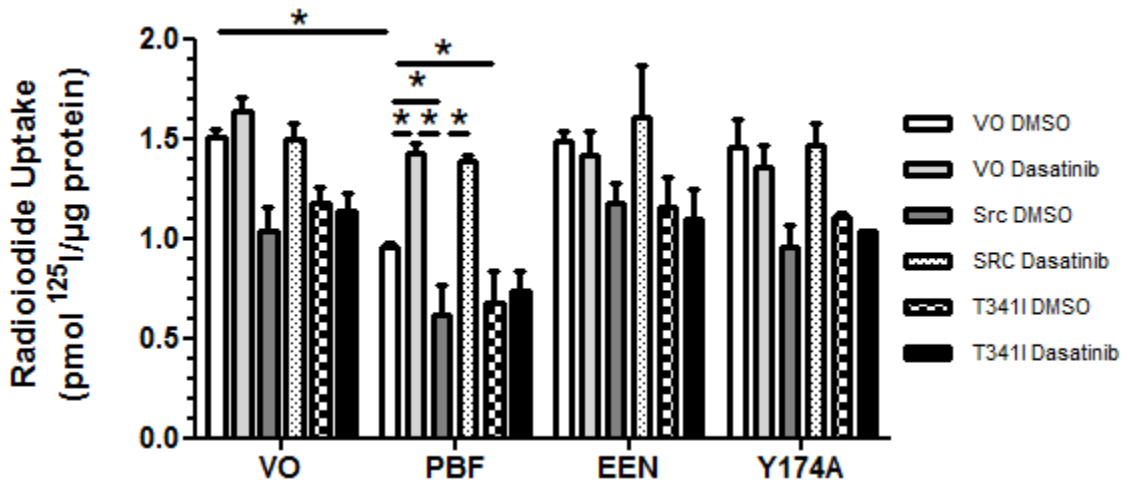

*Figure 6-11. Dasatinib cannot restore radioiodide uptake with T341I Src. ATRA and dexamethasone treated MCF-7 cells stably transfected with empty pCI-neo vector (VO), PBF, EEN/AAA or Y174A PBF were transiently transfected with empty pcDNA3.1(+) vector (VO), Src or T341I Src and treated with DMSO or 10nM dasatinib before radioiodide uptake was assessed. Cells were transiently transfected for 48 hours and treated for 24 hours prior to the addition of radioiodide. n=2 with 4 replicates in each n. * = p<0.05.*

6.4 Discussion

6.4.1 Src binds to PBF and increases PBF phosphorylation

The evidence presented in this thesis chapter suggests that Src and PBF interact within breast cancer cells and that Src can phosphorylate PBF. Investigations revealed that Src kinase can colocalise with and bind to PBF *in vitro* and that overexpression of Src results in increased levels of pY174 PBF. These data reflect studies carried out in thyroid cancer cells where Src was identified as a binding partner for PBF by mass spectrometry and Co-IP with Src overexpression increasing PBF phosphorylation (Smith et al., 2013). Further to the work in thyroid cancer cells, it was observed here that overexpression of Src could decrease radioiodide uptake in breast cancer cells. Not only did Src decrease radioiodide uptake in MCF-7 cells stably transfected with empty pCI-neo vector, radioiodide uptake was further reduced in cells overexpressing both Src and PBF. However co-transfection of Src alongside EEN/AAA PBF could not significantly reduce radioiodide uptake further. The EEN/AAA form of PBF was generated to have a mutation upstream from Y174 to reduce Src's recognition of Y174 as a potential phosphorylation site. Although EEN/AAA PBF could not be phosphorylated by Src, as evidenced via Co-IP, it appeared that it was still able to interact with Src. There are three potential hypotheses as to why: (i) it may be that Src cannot phosphorylate EEN/AAA PBF due to the mutant having a slightly altered conformation, (ii) Src may bind to and phosphorylate PBF at an different site such as Y165, or (iii) alternatively that Src is unable to recognise Y174 as a potential phosphorylation site as the consensus sequence for the SH1 kinase domain is no longer intact. Although Src was capable of further reducing radioiodide uptake *in vitro,* use of the potent SFK inhibitor dasatinib restored radioiodide uptake. These results support the

data presented in chapter 5, where use of SFK kinase inhibitors prevented PBF phosphorylation and rescued radioiodide uptake.

6.4.2 Src regulates and can phosphorylate PBF

Although there is much evidence to suggest that Src can phosphorylate PBF, it is important to fully assess Src's role as it may not be the only kinase involved in the phosphorylation of PBF in breast cancer. Mass spectrometry in thyroid cancer cells also revealed that Lyn was a binding partner of PBF suggesting that it can also phosphorylate PBF (unpublished data). Here, a mutant form of Src was created that was constitutively active and could not be inhibited by dasatinib, as confirmed by Western blotting. The use of this mutant in radioiodide uptake experiments showed that it was capable of reducing radioiodide uptake with a similar potency to that of WT Src, although dasatinib could not restore radioiodide uptake in cells expressing T341I Src. Western blotting and radioiodide uptake studies suggest that dasatinib is inhibiting WT Src directly and this has a direct effect on PBF phosphorylation and radioiodide uptake. If another SFK was phosphorylating PBF and is inhibited by dasatinib, it could be hypothesised that dasatinib could restore radioiodide uptake even in the presence of T34I Src.

While these results do not prove that Lyn or another SFK have no role, the data produced with the T341 Src mutant provides evidence that Src has an important role in PBF phosphorylation. This is further supported by the similarity in the data produced in breast cancer cells and thyroid cancer (Smith et al., 2013), a disease where Src has been reported to be the dominant SFK (Chan et al., 2012).

Overall these data suggest that PBF interacts with and can be phosphorylated by Src. Overexpression of Src led to increased PBF phosphorylation and reduced radioiodide uptake in breast cancer cells, with the potent SFK inhibitor dasatinib restoring radioiodide uptake in cells with Src overexpression. This rescue is therapeutically important as many breast cancers have upregulated Src activity compared to normal tissue (Egan et al., 1999; Rosen et al., 1986). Thus, for radioiodide to be an effective treatment in breast cancer dasatinib would be required to overcome the reduction in radioiodide uptake even in tumours with the highest levels of Src expression. Use of the T341I Src mutant revealed that the effect of dasatinib was Src-specific as the inhibitor was not able to restore radioiodide uptake in the presence of this resistant mutant. Although these data do not rule out PBF involvement with other SFK, they present evidence suggesting that PBF can be regulated and phosphorylated by Src in breast cancer cells.

CHAPTER 7 - INHIBITION OF *N*-MYRISTOYLATION INCREASES RADIOIODIDE UPTAKE

7.1 Introduction

7.1.1 *N*-Myristoylation

Protein *N*-myristoylation is a form of irreversible post-translational modification to a subset of eukaryotic and viral proteins (Sefton and Buss, 1987). The term refers to the covalent attachment of a 14-carbon saturated fatty acid, myristate, to the *N*-terminal glycine of proteins. Although the process is referred to as a post-translational modification, it usually occurs co-translationally (Wilcox et al., 1987), when fewer than 100 residues of the target protein have been polymerised by the ribosome (Deichaite et al., 1988). The modification usually occurs imminently following removal of the initiator methionine residue by methionylaminopeptidases (Wilcox et al., 1987) (Figure 7-1). More rarely, myristoylation can occur after the exposure of internal glycine following protein cleavage as found in the apoptosis pathway where pro-apoptotic proteins such as BID are myristoylated after cleavage by caspases (Zha et al., 2000) (Figure 7-1). Not all proteins with a *N*-terminal glycine are myristoylated; the consensus sequence for protein substrates is Gly-X-X-X-Ser/Thr (Johnson et al., 1994).

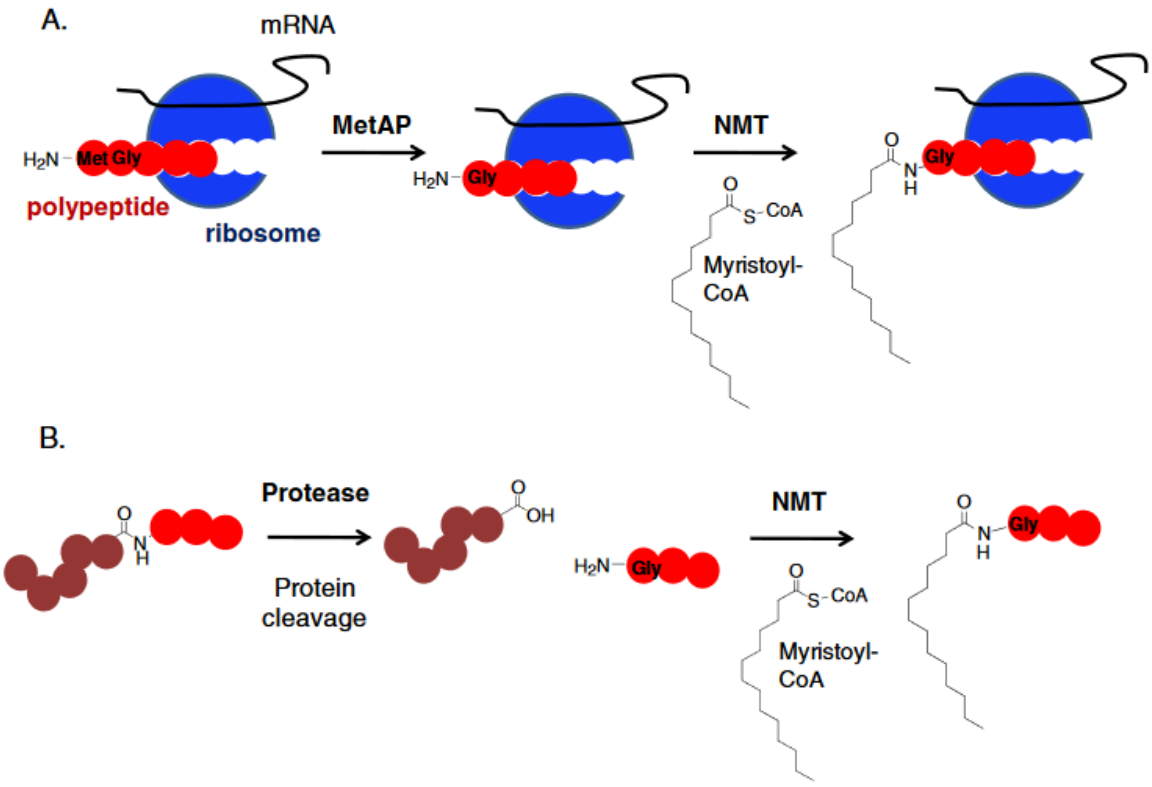

Figure 7-1. Mechanisms of N-myristoylation. A schematic diagram illustrating the two mechanisms of N-myristoylation. (A) Co-translationally, N-terminal methionines are cleaved from proteins by methionylaminopeptidases (MetAP). Following cleavage, NMT catalyses the addition of a myristrate to the exposed newly N-terminal glycine. (B) Proteins are cleaved by proteases revealing a new N-terminal glycine that can be myristoylated by NMT. Taken from Wright et al., 2010.

N-terminal myristoylation of proteins is catalysed by myristoyl-CoA:protein*N*-myristoyltransferase (NMT), a member of the Gcn5-related *N*-acetyltransferases (GNAT) superfamily of proteins (Weston et al., 1998). Nineteen different NMT have thus far been identified from fifteen species with human, mouse and cow each possessing two NMT termed NMT type I and type II (Giang and Cravatt, 1998). Both types show a high level of homology across species with the two forms being 76% homologous to each other. The greatest divergence is situated within the *N*-terminal region of the protein (Giang and Cravatt, 1998). The *N*-terminal divergence is hypothesised to allow the two isoforms of

NMT to localise differentially in the cell to influence co-translational ribosome-based or post-translational cytosol-based protein myristoylation (Glover et al., 1997) (Farazi et al., 2001).

It is estimated that 0.5-3% of all proteins are myristoylated (Martinez et al., 2008; Maurer-Stroh et al., 2002). Myristoylation of target proteins has multiple effects including influencing protein-protein interaction, protein stability and enhancing interaction of protein with cellular organelles or membranes (Wright et al., 2010). X-ray crystallography studies have revealed that myristoylation is required to stabilise the three-dimensional protein conformation of several *N*-myristoylated proteins, including protein kinase A (PKA) where the myristate is positioned in the hydrophobic pocket of the kinase and is necessary for both structural and thermal stability of the protein (Zheng et al., 1993). Many proteins require *N*-terminal myristoylation to associate with the plasma membrane or other intracellular membranes.

7.1.2 *N*-myristoylation of Src

One of the best studied families of myristoylated proteins are the SFK, particularly Src. All members of the SFK family are known to be myristoylated (Resh, 1994). Myristoylation of SFK is necessary for the kinases to anchor to the membrane but is not sufficient for anchorage with a second signal being required. For Src, this second signal for anchorage is a cluster of polybasic amino acids that can interact with the acidic phospholipids on the inner leaflet of the membrane bilayer (Cross et al., 1984; Murray et al., 1998). Myristoylation-null mutant forms of Src have been observed to lose the ability to bind to membranes, and cannot mediate cellular transformation (Cross et al., 1984; Kamps et al.,

1985). This is a defining feature of Src with the other SFK family members relying on the attachment of a 16-carbon saturated fatty acid palmitate to Cys3 and Cys5/6 alongside myristoylation to anchor to the membrane (Resh, 1999). Src is yet to be crystallised, but it is hypothesised that the myristate is situated within a myristate binding pocket in a similar manner to that observed in c-Abl (Cowan-Jacob et al., 2005).

Membrane binding is critical for many of the cellular functions of Src. Non-myristoylated Src has been observed to be cytoplasmic, with membrane localisation of Src being essential for mitotic Src activation (Bagrodia et al., 1993). Myristoylation has also been hypothesised to play a role in the regulation of nuclear translocation of Src (David-Pfeuty et al., 1993). The expression of non-myristoylated Src *in vitro* was found to be higher than expression of the myristoylated form, with non-myristoylated Src being degraded at a slower rate than the myristoylated form (Patwardhan and Resh, 2010). However myristoylated Src has been observed to have a higher rate of kinase activity than non-myristoylated Src (Patwardhan and Resh, 2010). With myristoylation-null mutants being less active than WT Src and being unable to mediate cellular transformation, NMT inhibitors have been investigated as anti-cancer reagents.

7.1.3 Clinical uses of NMT inhibitors

NMT has been investigated as a therapeutic target in multiple disease states but also for use as a fungicide or antiprotozoan. Although NMT enzymes are relatively well conserved amongst species, it has been possible to differentiate between viral, parasitic and mammalian NMT allowing for the creation of drugs to target species-specific NMT (Wright et al., 2010). The identification of species-specific inhibitors has focused on the

peptide binding pocket as this is the least conserved region of NMT enzymes (Wright et al., 2010). The NMT enzyme is essential for the human pathogen *C. albicans* to grow and be virulent, and inhibitors have been identified that are approximately 250-fold more selective for *C. albicans* NMT than human NMT (Devadas et al., 1995). NMT has also been identified to be a critical enzyme for *L. major, T. brucei* and *P. falciparum* which have been associated with diseases including leishmaniasis, African sleeping sickness and malaria, for which selective inhibitors are being investigated to aid in the treatment of these diseases (Bowyer et al., 2007; Gunaratne et al., 2000; Panethymitaki et al., 2006; Price et al., 2003). NMT inhibitors have also been suggested for use in the treatment of HIV-1 infection, however there have been concerns about toxicity in targeting human NMT to combat disease and the effects on uninfected cells (Furuishi et al., 1997; Seaton and Smith, 2008; Takamune et al., 2008).

NMT enzymes were first proposed as chemotherapuetic targets in 1995 due to their interaction with proteins involved in the regulation of cell proliferation and growth (Felsted et al., 1995). Overexpression of NMT has been associated with several neoplasms including colorectal, gallbladder, brain and oral squamous cell carcinomas (Lu et al., 2005; Magnuson et al., 1995; Rajala et al., 2000; Raju et al., 1997; Shrivastav et al., 2007). NMT expression has also been correlated with proliferative capacity in mammary epithelial cells (Clegg et al., 1999). Inhibition and knockdown of NMT *in vitro* has been observed to reduce cell proliferation by approximately 27%, to reduce Src phosphorylation on Y418 and to inhibit signalling through the c-Raf/MEK/ERK/Elk pathway (Ducker et al., 2005). However, inhibition of myristoylation in carcinogenesis may also have negative effects on tumour suppressor genes. One tumour suppressor gene known to be myristoylated is

Fus1, a protein implicated in lung cancers that can promote apoptosis (Ji and Roth, 2008). Non-myristoylated forms of Fus1 lose tumour suppressor activity and cannot induce cellular apoptosis (Uno et al., 2004). Although potential use of NMT inhibitors for treatment of cancer appears to have merit, the findings are very preliminary and there are multiple factors to consider. Currently there are no NMT inhibitors in clinical trials but as interest grows in the enzymes and effective inhibitors are identified then it is expected that these inhibitors may prove a potent strategy in the fight against cancer.

The aim of this chapter is to assess the ability of three NMT inhibitors, kindly donated by the Drug Discovery Group at the University of Dundee, to reduce Src myristoylation, inhibit the phosphorylation of PBF and increase radioiodide uptake in breast cancer cells. The Drug Discovery Group was working to inhibit parasitic NMT with the aim to combat parasites commonly affecting third world countries. Two of the three compounds they donated to this project were found to inhibit human NMT as well as parasitic NMT rendering them unsuitable for treatment of parasitic disease. The group decided to redeploy the compounds and establish whether the compounds had anti-cancer properties or could be used in the treatment of cancer. In this collaboration, the three compounds were individually assessed to establish their effect on radioiodide uptake. With NMT inhibition being known to affect Src activity it is hypothesised that inhibition of NMT will increase radioiodide uptake in a similar manner to that observed with SFK inhibitors. Of the three drugs the most potent was taken forward to establish the effect that NMT inhibition has on PBF phosphorylation and radioiodide uptake both on its own and in combination with dasatinib with the aim of maximising radioiodide uptake.

7.2 Materials and Methods

7.2.1 Cell Culture

MCF-7 and MDA-MB-231 cells were maintained as described in 2.1.2 with stably-transfected MCF-7 cells being cultured in media containing G418 (1 mg/ml) and lentivirally transduced MDA-MB-231 cells being cultured in media containing blasticidin (15 μg/ml). All cell lines were seeded at 30,000 cells per well in a 24 well plate for radioiodide uptake and at 150,000 and 200,000 cells per well in a 6 well plate for fluorescence immunocytochemistry and protein extraction respectively.

7.2.2 Drug Treatments

MCF-7 cells were treated with ATRA and dexamethasone as described in section 3.2.3 at 100nM and 1μM respectively. Cells were cultured with ATRA and dexamethasone for 48 hours prior to harvesting or treatment with ^{125}I. Cells were treated with dasatinib as described in 5.2.2 at a concentration of 1nM.

NMT Inhibitor compounds 1 (MW= 463), 2 (MW=523) and 3 (MW=610) (kindly donated from the Drug Discovery Group, University of Dundee) were dissolved in DMSO to give a stock concentration of 10mM. Cells were treated with dilutions of NMT inhibitor 1, 2 and 3 ranging from 1nM - 1μM in RPMI media. DMSO was used as a vehicle-only control in all experiments.

7.2.3 Radioiodide uptake, retention and efflux

Radioiodide uptake was performed as described in section 2.7. NMT inhibitor dose curves were generated following treatment with NMT for 2 hours prior to the addition of ^{125}I upon recommendation from the University of Dundee.

Radioiodide retention and efflux were performed simultaneously. MCF-7 cells were treated with ATRA and dexamethasone for 48 hours and with DMSO/dasatinib/NMT inhibitor 3 for 24 hours prior to the addition of ^{125}I. Cells were incubated at 37°C for 1 hour with 1µM NaI containing 0.05µCi ^{125}I (Hartmann Analytic) before cell media was removed and replaced with fresh RPMI media. The cells were then incubated at 37°C for a further 1, 2 or 4 hours. After the appropriate amount of time, media was removed and assessed using a gamma counter (1260 Multigamma II, Wallac) for 60 seconds to determine iodide efflux. The cells then were lysed with 100µl 2% SDS and the radioactivity of the lysate assessed for one minute using the gamma counter. A BCA assay was undertaken to calculate the protein concentration of the lysates, which was then used to standardise the counts observed.

7.2.4 Western Blotting

Protein extraction and Western blotting were performed as described in sections 2.3.1 and 2.3.2 respectively. Cells were treated with 100µM sodium pervanadate for 20 minutes prior to harvesting to allow the detection of pY174 PBF. Antibodies used were anti-pY174 PBF antibody (Covalab) (Smith et al., 2013), anti-PBF (Eurogentec) (Smith et al., 2009), anti-phospho-Src (Y418) (Abcam), anti-Src (Cell Signalling) and β-actin (Sigma-Aldrich) (refer to section 2.8). Appropriate secondary antibodies were used.

7.2.5 Statistics

Data were analysed using Sigma Plot (SPSS Science Software UK Ltd). One-way ANOVA was used to compare groups of parametric data with significance taken at $p < 0.05$.

7.3 Results

7.3.1 Both NIS and PBF are not predicted to be targeted by NMT

Online prediction software (http://mendel.imp.ac.at/myristate/SUPLpredictor.htm) (Eisenhaber et al., 2003) did not detect any potential sites in either PBF or NIS that could be targeted by NMT. The NMT enzymes are well documented to target *N*-terminal glycines after cleavage of methionines, but neither PBF nor NIS have a glycine in the second position of their amino acid sequences. NMT is also capable of acting on *N*-terminal glycines after proteolytic processing of pro-proteins, and although PBF is predicted to be cleaved following the signal peptide, any potential cleavage to the protein does not create an *N*-terminal glycine.

Src has previously been described to be myristoylated, having an *N*-terminal glycine following methionine cleavage. For this reason Src was used as a positive control, with the prediction software correctly identifying Src as a target for myristoylation.

7.3.2 Inhibition of NMT increases radioiodide uptake

Radioiodide uptake experiments were performed using the three NMT inhibitor compounds donated from The Drug Discovery Group at the University of Dundee. Prior to experiments, it was disclosed that one of the compounds was inactive whereas the other two readily inhibited NMT at varying efficacies. To ensure an unbiased experiment the identity of the compounds were blinded and labelled NMTi 1, NMTi 2 and NMTi 3. In NIS lentivirally transduced MDA-MB-231 cells, NMTi 3 appeared to be the most active compound increasing radioiodide uptake by the cells by 51% at 50nM when compared to

the DMSO control (Figure 7-2). NMTi 3 maximally increased radioiodide uptake at a concentration of 200nM where a 68% increase in uptake was observed (p = 0.004) (Figure 7-2). NMTi 1 appeared to be the inactive compound with radioiodide uptake being unaffected by the presence of the inhibitor at any dose (Figure 7-2). NMTi 2 marginally increased radioiodide uptake in a dose-dependent manner up to 100nM; however this uptake was not significant (Figure 7-2). Subsequently, the Drug Discovery group in Dundee confirmed that inhibitor 3 was the most active NMTi in their biological tests, followed by 2, and that 1 was an inactive compound.

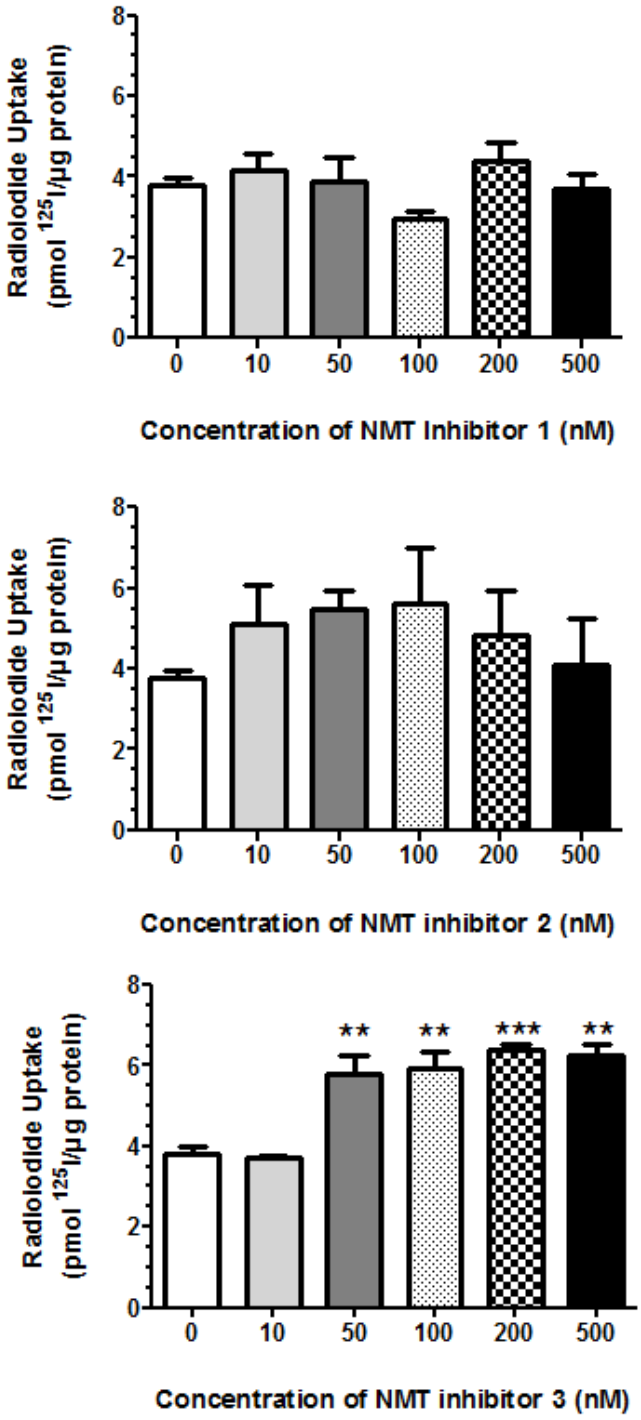

*Figure 7-2. Treatment with NMT inhibitor 3 increases radioiodide uptake. NIS lentivirally transduced MDA-MB-231 cells were treated with varying doses of NMT inhibitor compounds 1, 2 and 3 for 2 hours prior to the addition of ^{125}I. n=3 with 4 replicates in each n. ** = p < 0.01. *** = p <0.001 compared to cells treated with vehicle control (0nM).*

7.3.3 NMT Inhibitor 3 reduces pY418 Src plasma membrane localisation

To determine the effect of NMT inhibitor 3 on the localisation of pY418 Src MCF-7 cells were transfected with NIS-MYC and treated with 100nM NMT inhibitor 3. In control DMSO treated cells, pY418 Src was located ubiquitously throughout the cells with strong staining at the plasma membrane (Figure 7-3). The use of NMT inhibitor 3 decreased plasma membrane staining for pY418 Src suggesting the NMT inhibitor 3 inhibits the myristoylation of Src effectively (Figure 7-3).

In DMSO treated cells, NIS-MYC appeared to be expressed in defined intracellular vesicles, with little plasma membrane staining (Figure 7-3). However in NMT inhibitor 3 treated cells there was a marked increase in plasma membrane NIS and increased visualisation of lamellipodia-like structures in the NIS stained cells. NIS was also present in a similar number of defined intracellular vesicles in DMSO treated cells, suggesting a potential increase in total NIS levels (Figure 7-3).

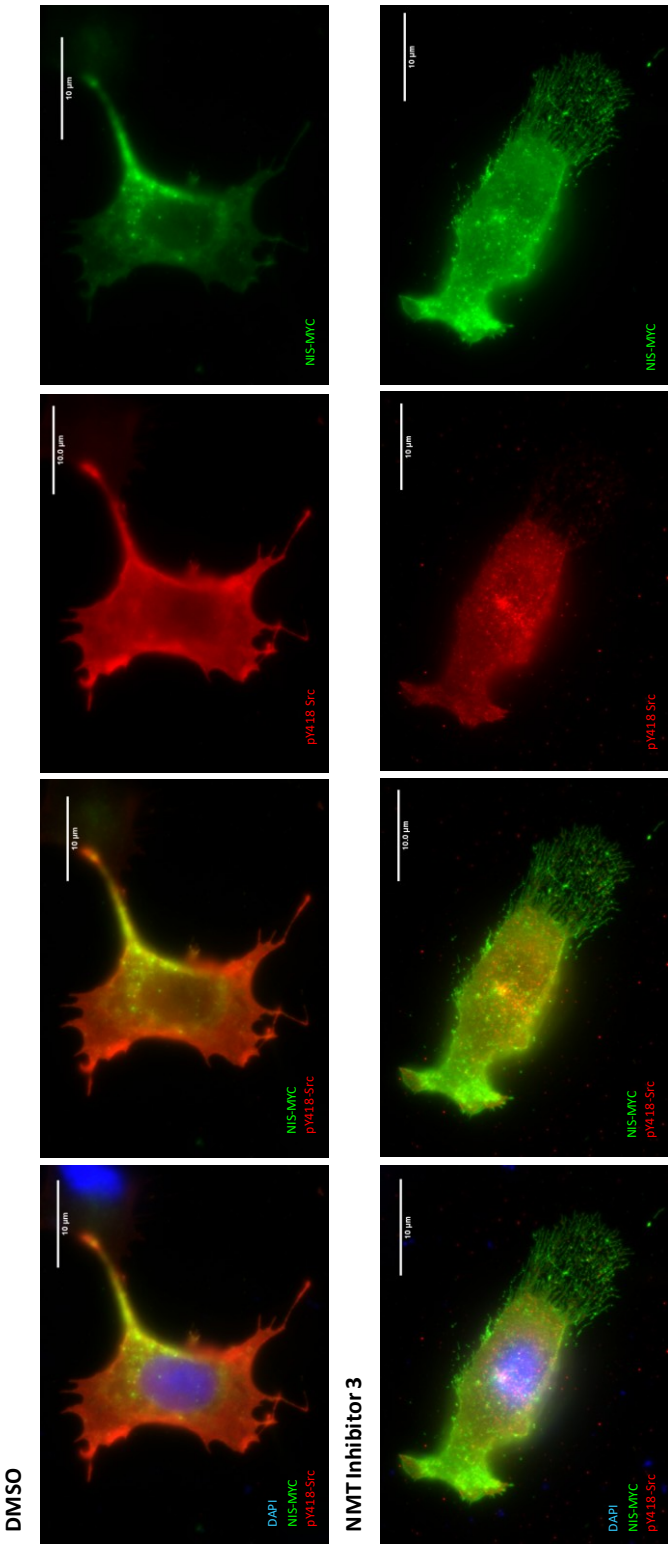

Figure 7-3. NMT inhibitor 3 decreases pY418 Src plasma membrane localisation and increases NIS plasma membrane localisation. MCF-7 cells were transfected with empty pcDNA3.1 (+) vector and NIS-MYC for 48 hours and treated with DMSO or 100nM NMT inhibitor 3 for 24 hours prior to fixing. MYC-tagged NIS is identified in green using a mouse anti-MYC antibody,pY418 Src is visualised using a rabbit anti-pY418 Src antibody in red and PBF-HA visualised using a mouse anti-HA tag antibody in green. In all images nuclei are visualised in blue using Hoechst stain. 100x magnification. n=2.

7.3.4 Phosphorylation of PBF is not affected by NMT inhibitor 3

To determine the effect of NMT inhibitor 3 on the phosphorylation of PBF and Src, NIS lentivirally transduced MDA-MB-231 cells were treated with NMT inhibitor 3 at varying doses before protein was extracted and Western blotted. NMTi 3 did not alter the levels of phosphorylated PBF at any concentration compared to the DMSO control (Figure 7-4). Levels of total PBF were also unchanged. Expression levels of pY418 Src and total Src were also unaltered within the 2 hour treatment (Figure 7-4).

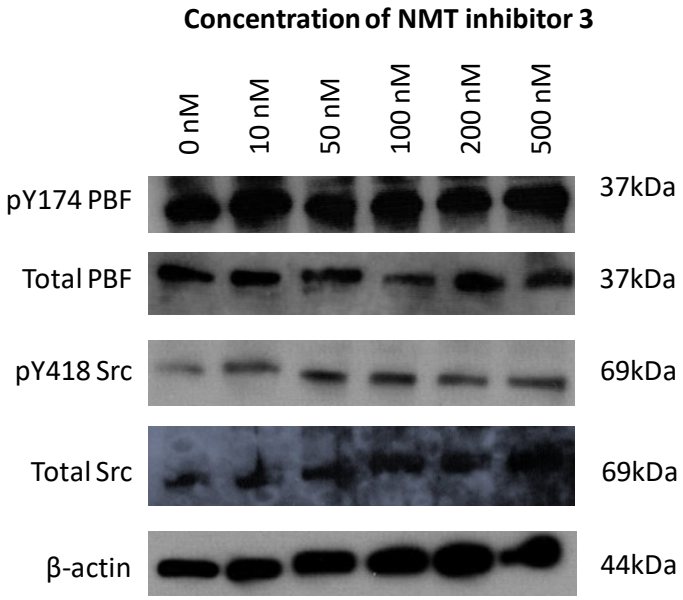

Figure 7-4. Treatment with increasing NMT inhibitor 3 doses. NIS lentivirally transduced MDA-MB-231 cells were treated with varying concentrations of NMT inhibitor 3 for 2 hours prior to harvesting. pY174 PBF, total PBF, pY418 Src and total Src were detected, with β-actin used as a loading control. n=2 .

7.3.5 NMT inhibitor 3 cannot restore radioiodide in the presence of exogenous PBF

To assess whether NMT inhibitor 3 was capable of rescuing radioiodide uptake in cells overexpressing PBF, ATRA and dexamethasone-treated MCF-7 and NIS lentivirally transduced MDA-MB-231 cells were employed. In both DMSO-treated cell lines, PBF transfection significantly reduced radioiodide uptake compared to empty vector transfected cells (29% reduction, p= 0.0015 and 29% reduction, p=0.0297 in MCF-7 and MDA-MB-231 cells respectively) (Figure 7-5). This reduction was rescued after treatment with 1nM dasatinib for 24 hours (100% increase compared to DMSO + PBF, p=0.0283 and 78% increase, p=0.0344 in MCF-7 and MDA-MB-231 cells respectively) (Figure 7-5). NMT inhibitor 3 could not significantly rescue PBF's reduction in radioiodide uptake at either time-point in either cell line (Figure 7-5). Treatment with NMT inhibitor 3 for 2 hours significantly increased radioiodide uptake in MDA-MB-231 cells transfected with empty vector (32% increase, p=0.0474) (Figure 7-5B). MCF-7 and MDA-MB-231 cells transfected with empty vector displayed increased uptake with NMTi 3 at 24 hours but the increase was not statistically significant (Figure 7-5).

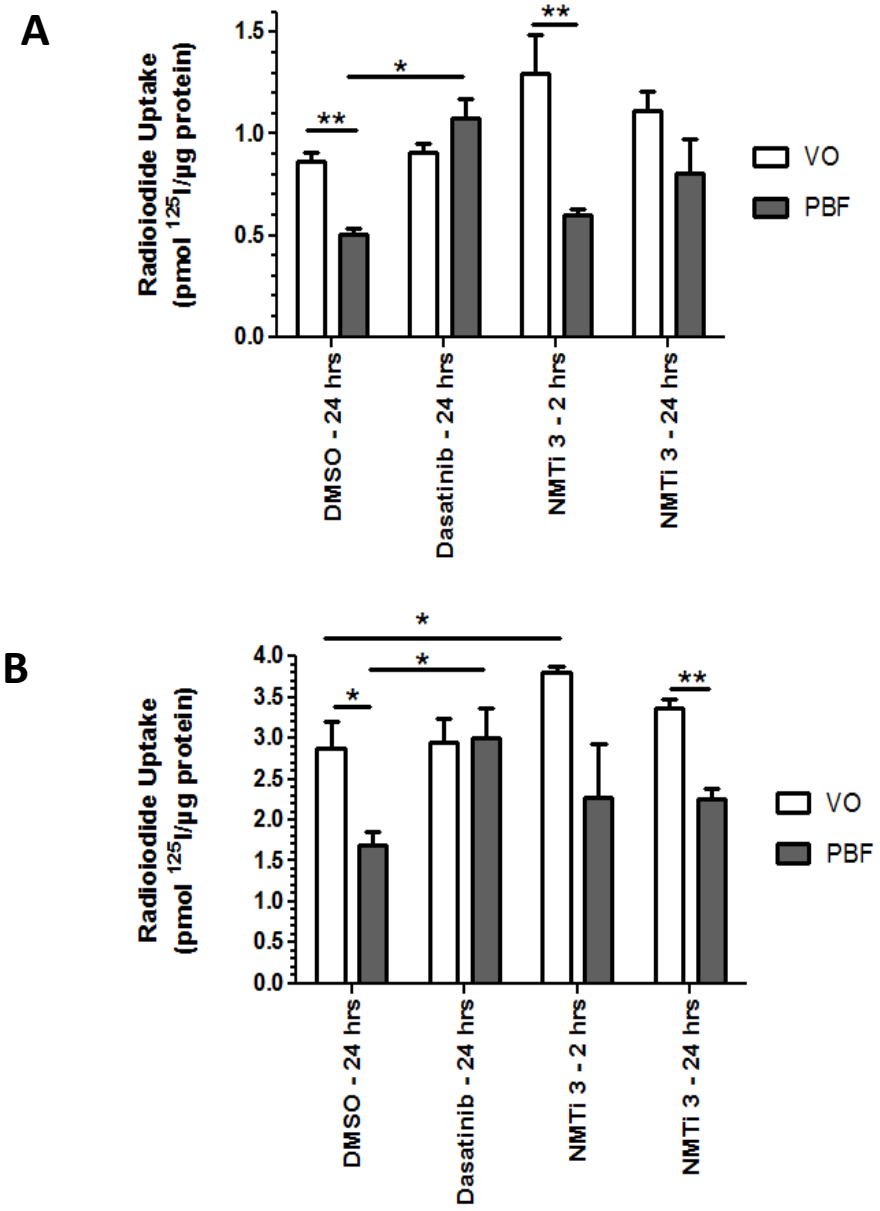

*Figure 7-5. NMT inhibitor 3 cannot restore radioiodide uptake in the same manner as dasatinib. (A) ATRA and dexamethasone-treated MCF-7 cells stably transfected with empty vector (VO) or PBF and (B) NIS lentivirally transduced MDA-MB-231 cells transiently transfected with empty vector (VO) or PBF were treated with DMSO, 1nM dasatinib or 100nM NMT inhibitor 3 for either 24 or 2 hours before the addition of ^{125}I. Radioiodide counts were normalised to protein concentration. n=3 with 4 replicates in each n. *= p<0.05. ** = p<0.01.*

7.3.6 NMT inhibition combined with dasatinib affects MCF-7 and MDA-MB-231 cells differently

When ATRA and dexamethasone-treated MCF-7s were treated with a combination of dasatinib and NMT inhibitor 3, an increased uptake was observed in comparison to single drug treatments (Figure 7-6A). A pre-treatment with NMT inhibitor 3 for 2 hours prior to the addition of dasatinib gave the highest levels of radioiodide uptake, with a 96% increase in radioiodide uptake compared to control DMSO treated cells (p=0.003) (Figure 7-6A). Simultaneous treatment with both drugs also provided a 71% increase in MCF-7 radioiodide uptake (p=0.015), and 24 hour dasatinib treatment with NMTi 3 in the final 2 hours gave an increase of 63% compared to control treated cells (p=0.0008) (Figure 7-6A).

Treatment of NIS lentivirally transduced MDA-MB-231 cells with dasatinib and NMT inhibitor 3 in combination did not significantly alter radioiodide uptake from control-treated cells (Figure 7-6B). NMT inhibitor 3 treatment alone for 2 hours was the only treatment that significantly altered radioiodide uptake from the control DMSO-treated cells (p=0.0474) (Figure 7-6B).

It was evident in both cell lines that the phosphorylation status of PBF was not reduced by the presence of NMT inhibitor 3 (Figure 7-7). These preliminary data suggested that in both cell lines dasatinib alone was the best modulator of PBF phosphorylation, with combination treatments appearing to have higher levels of pY174 PBF than dasatinib alone (Figure 7-7). MDA-MB-231 cells treated with 100nM NMT inhibitor 3 for both 2 and 24 hours appeared to have increased levels of pY174 PBF compared to DMSO (Figure 7-7B); however this effect was not observed in the MCF-7 cells (Figure 7-7A).

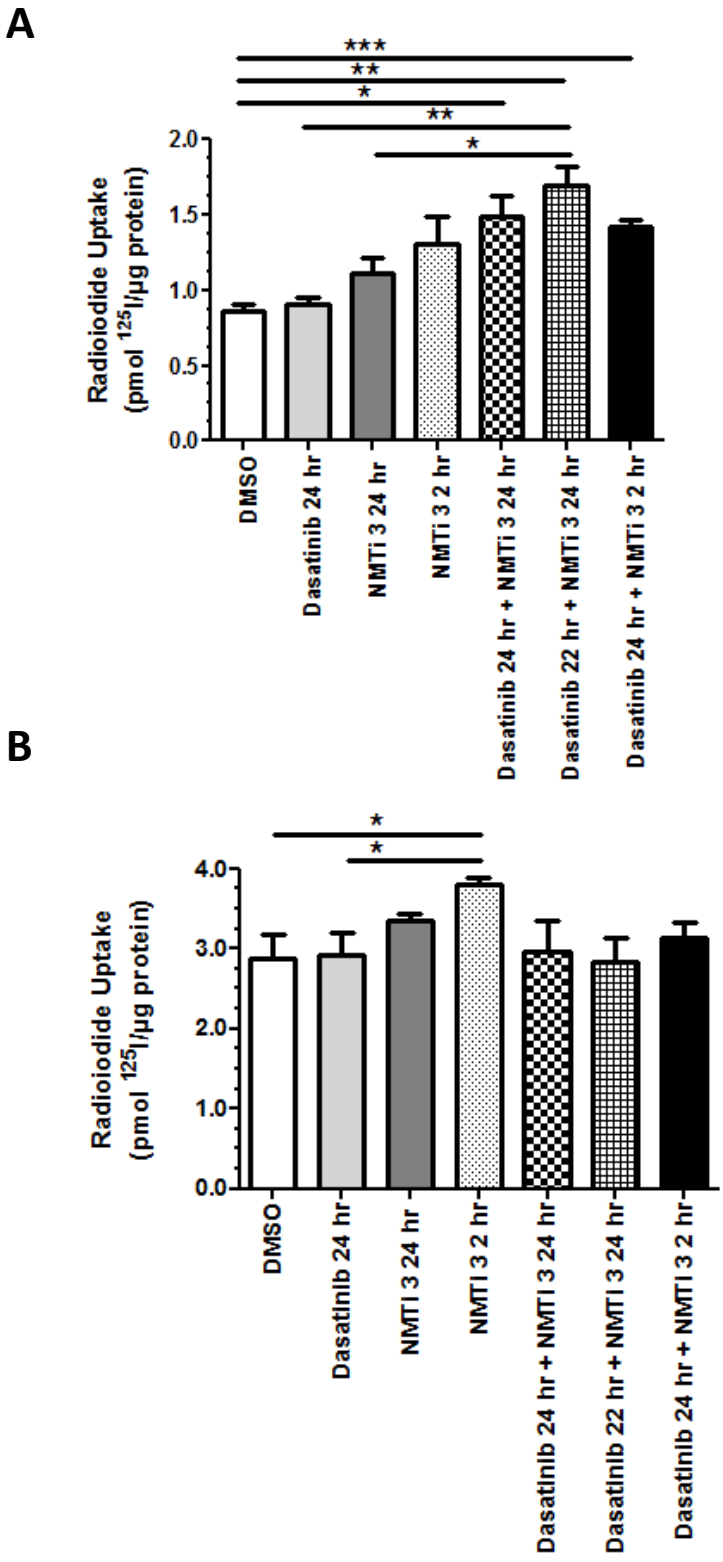

*Figure 7-6. Combination treatments affect MCF-7 and MDA-MB-231 cells differently. (A) ATRA and dexamethasone-treated MCF-7 and (B) NIS-lentivirally transduced MDA-MB-231 cells transiently transfected were treated with DMSO, 1nM dasatinib and 100nM NMT inhibitor 3.Timepoints indicate treatment time prior to the addition of ^{125}I. n=3 with 4 replicates in each n. *= p<0.05. ** = p<0.01. *** = p<0.01.*

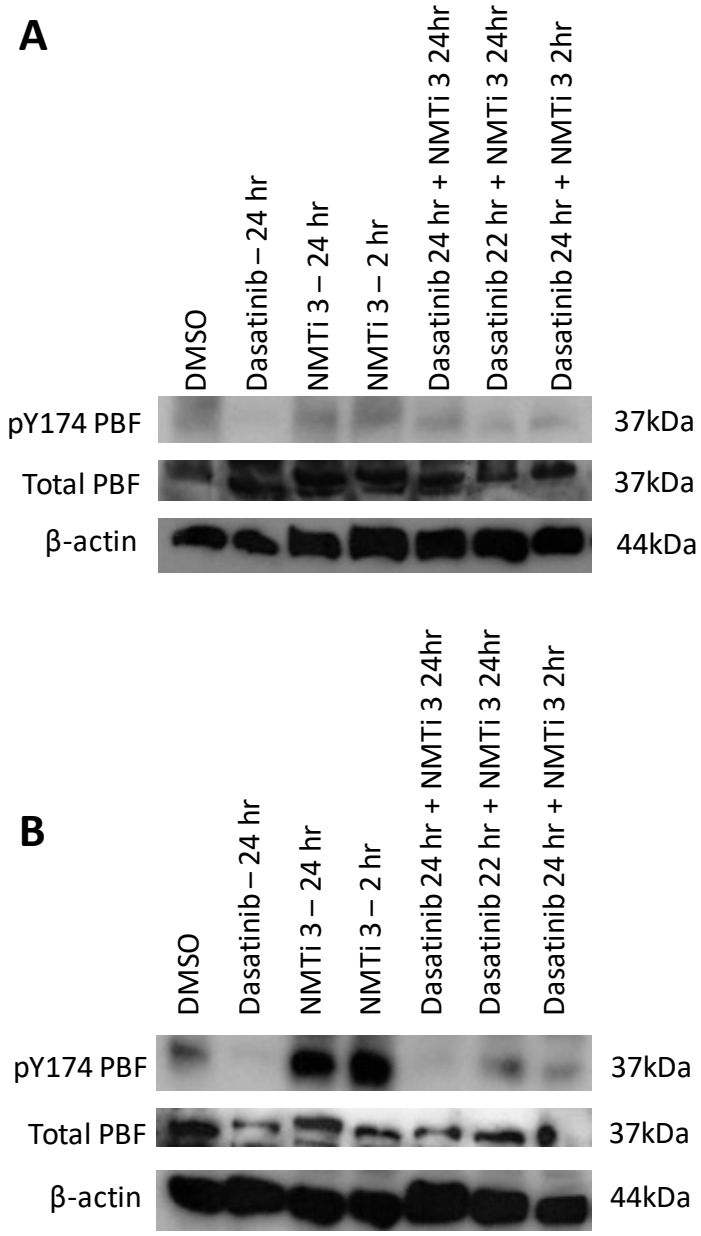

Figure 7-7. Dasatinib alone reduces pY174 PBF levels the most effectively. (A) MCF-7 cells and (B) NIS lentivirally transduced MDA-MB-231 cells treated with DMSO, dasatinib or NMT inhibitor 3 or a combination of the two drugs. pY174 and total PBF were detected with β-actin used a loading control. n=1.

7.3.7 NMT inhibition does not have an additive effect on the rescue of PBF-repressed radioiodide uptake by dasatanib

As observed throughout this thesis, PBF was capable of significantly reducing radioiodide uptake in MCF-7 and MDA-MB-231 cells (31% and 42% decrease, p=0.048 and *p*=0.026 respectively) (Figure 7-8). Treatment with NMT inhibitor 3 did not have an additive effective when paired with dasatinib on rescuing exogenous PBF's reduction of radioiodide uptake. Three different time combinations were investigated but none of the tested combinations produced results significantly above dasatinib treatment alone in both cell lines (Figure 7-8). Conversely, treatment with dasatinib for 24 hours and NMT inhibitor 3 for the final two hours in MDA-MB-231 cells appeared to reverse the rescue effect dasatinib treatment alone has on radioiodide uptake (Figure 7-8B).

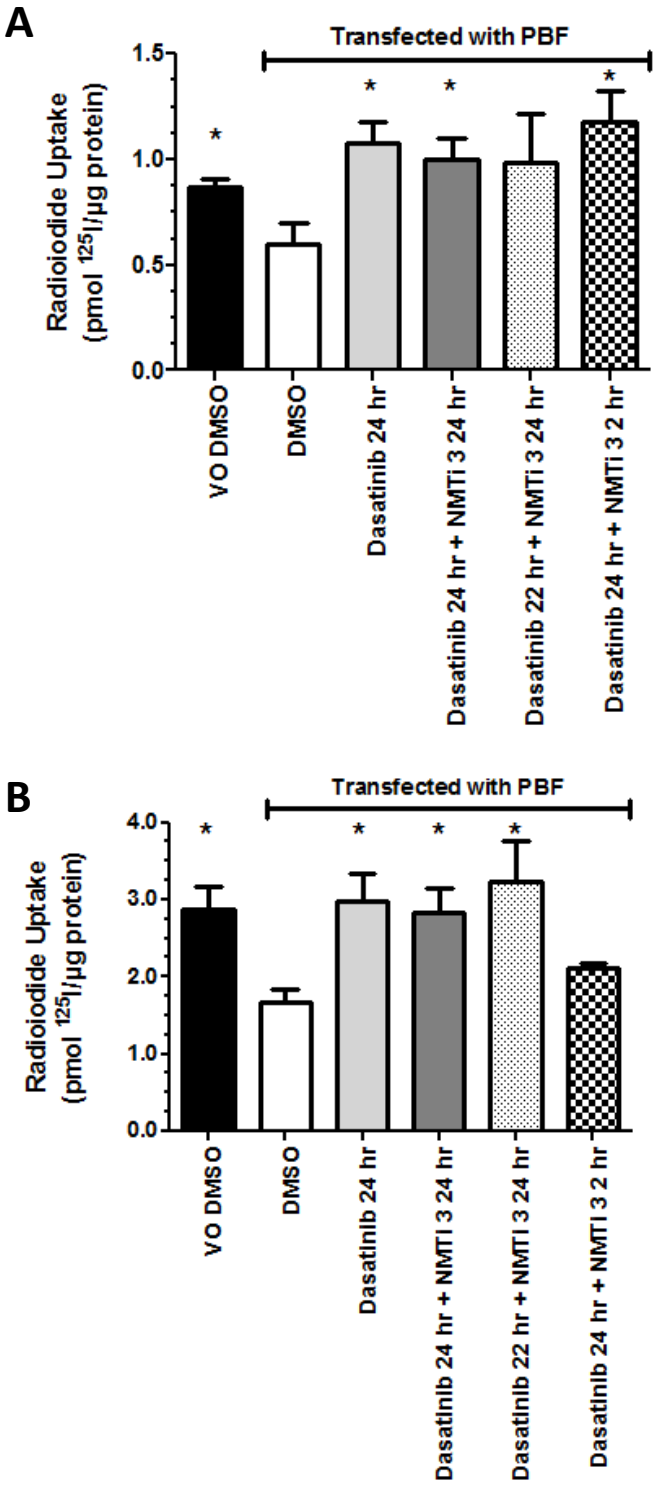

*Figure 7-8. Dasatinib and NMT inhibitor 3 do not have an additive effective when rescuing radioiodide uptake in the presence of PBF. (A) ATRA and dexamethasone-treated MCF-7 cells stably transfected with PBF and (B) NIS-lentivirally transduced MDA-MB-231 cells transiently transfected with PBF were treated with DMSO, 1nM dasatinib and 100nM NMT inhibitor 3. n=3 with 4 replicates in each n. *= p<0.05 compared to PBF + DMSO.*

7.3.8 NMT Inhibitor 3 does not reduce co-localisation between PBF and NIS

In MCF-7 cells there has been significant evidence to suggest PBF and NIS co-localise in intracellular vesicles. Here, it was demonstrated that dasatinib can disrupt the relationship between NIS and PBF. In MCF-7 cells treated with DMSO, there were clear signs of colocalisation (depicted in yellow and indicated by white arrows in Figure 7-9) with minimal plasma membrane staining for NIS. Treatment with dasatinib for 24 hours decreased intracellular colocalisation between NIS and PBF and increased the plasma membrane staining of NIS, increasing the visualisation of apparent lamellipodia in NIS stained cells (Figure 7-9). MCF-7 cells treated with NMT inhibitor 3 for 24 hours appeared to have similar levels of PBF and NIS colocalisation as those cells treated with vehicle only DMSO. However in the NMT inhibitor treated cells there was also increased visualisation of lamellipodia-like structures in NIS stained cells, potentially suggesting an increase in total NIS levels (Figure 7-9).

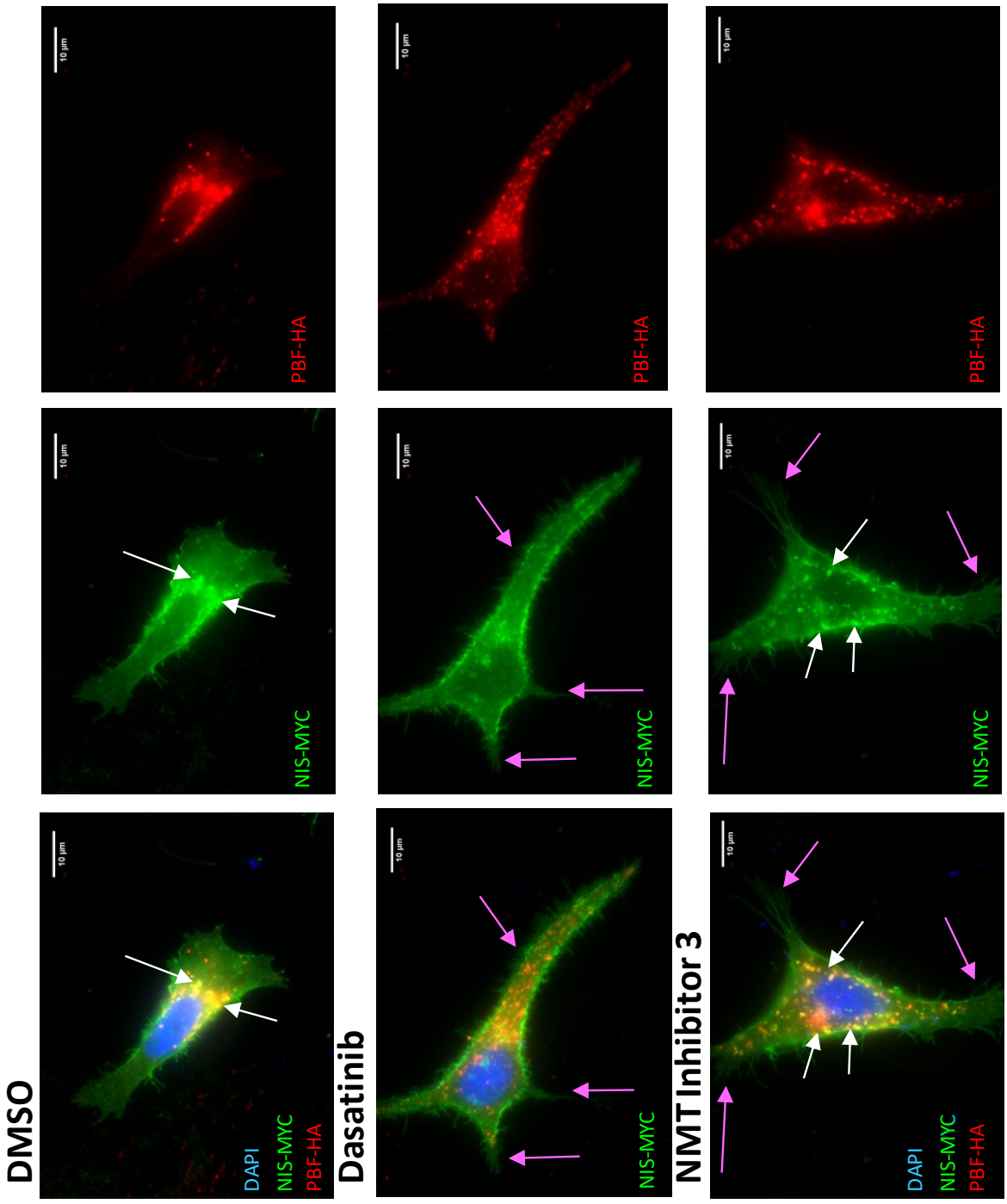

Figure 7-9. NMT inhibition cannot reduce colocalisation between NIS and PBF. MCF-7 cells were transfected with WT PBF-HA and NIS-MYC for 48 hours and treated with DMSO, 1nM dasatinib or 100nM NMT inhibitor 3 for 24 hours prior to fixing. MYC-tagged NIS is identified in green using a mouse anti-MYC antibody and HA-tagged PBF is identified in red using a mouse anti-HA antibody with the nuclei visualised in blue using Hoechst stain. White arrows indicate high levels of colocalisation as depicted by yellow staining. 100x magnification. Pink arrows indicate lamellipodia-like structures. 100x magnification. n=2.

7.3.9 NMTi 3 and dasatinib affect radioiodide retention and efflux

To assess whether dasatinib and NMT inhibitor 3 were capable of extending the time that breast cancer cells were able to retain radioiodide, retention and efflux experiments were performed. The preliminary data suggested that 24 hour treatment with NMT inhibitor 3 was capable of extending iodide retention in empty vector transfected MCF-7 cells as they appeared to retain 88% more radioiodide after 1 hour and 36% more after 2 hours than DMSO control-treated cells (Figure 7-10). Dasatinib-treated empty vector transfected MCF-7 cells were also capable of retaining 88% more radioiodide than DMSO-treated cells after 2 hours (Figure 7-10). A combination of the two drugs also enhanced radioiodide retention but not above the levels of single drug treatments (Figure 7-10).

Cells overexpressing PBF displayed decreased radioiodide uptake at 0 hours compared to empty vector transfected cells, which was partially restored in the presence of dasatinib (Figure 7-10). Dasatinib-treated PBF stable cells retained 33% more radioiodide after 1 hr and 15% after 2 hours compared to their DMSO treated counterparts (Figure 7-10). NMT inhibitor 3 had very little effect on the retention of radioiodide even in combination with dasatinib (Figure 7-10).

Apart from dasatinib-treated cells, all of the PBF transfected cells appeared to efflux less radioiodide than their empty vector transfected counterparts across all timepoints (Figure 7-11) but this may be due to not taking up as much radioiodide initially. DMSO-treated MCF-7 cells with PBF overexpression effluxed the least amount of radioiodide after 4 hours (Figure 7-11).

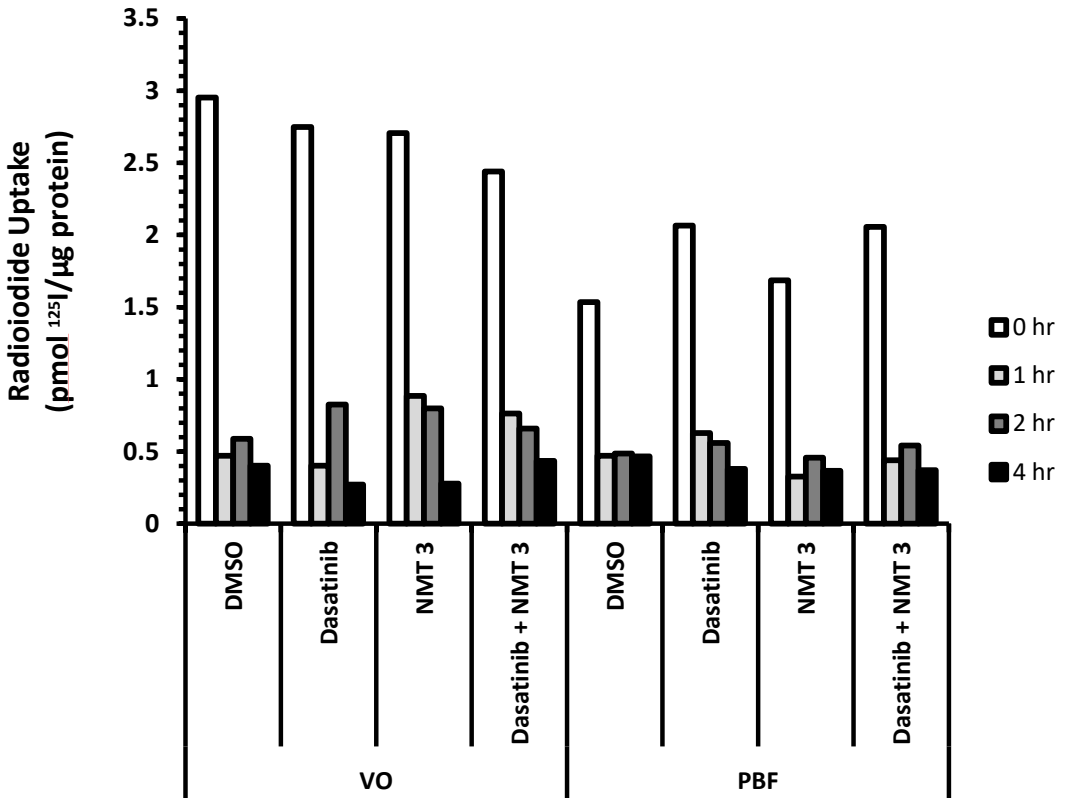

Figure 7-10. Radioiodide retention. ATRA and dexamethasone-treated MCF-7 cells stably transfected with empty pCI-neo vector (VO) or PBF were treated with DMSO, 1nM dasatinib, 100nM NMT inhibitor 3 or a combination of the two drugs for 24 hours before the addition of ^{125}I. After 1 hour media was replaced and cells were harvested after 0, 1, 2 or 4 hours. n=1 with six replicates.

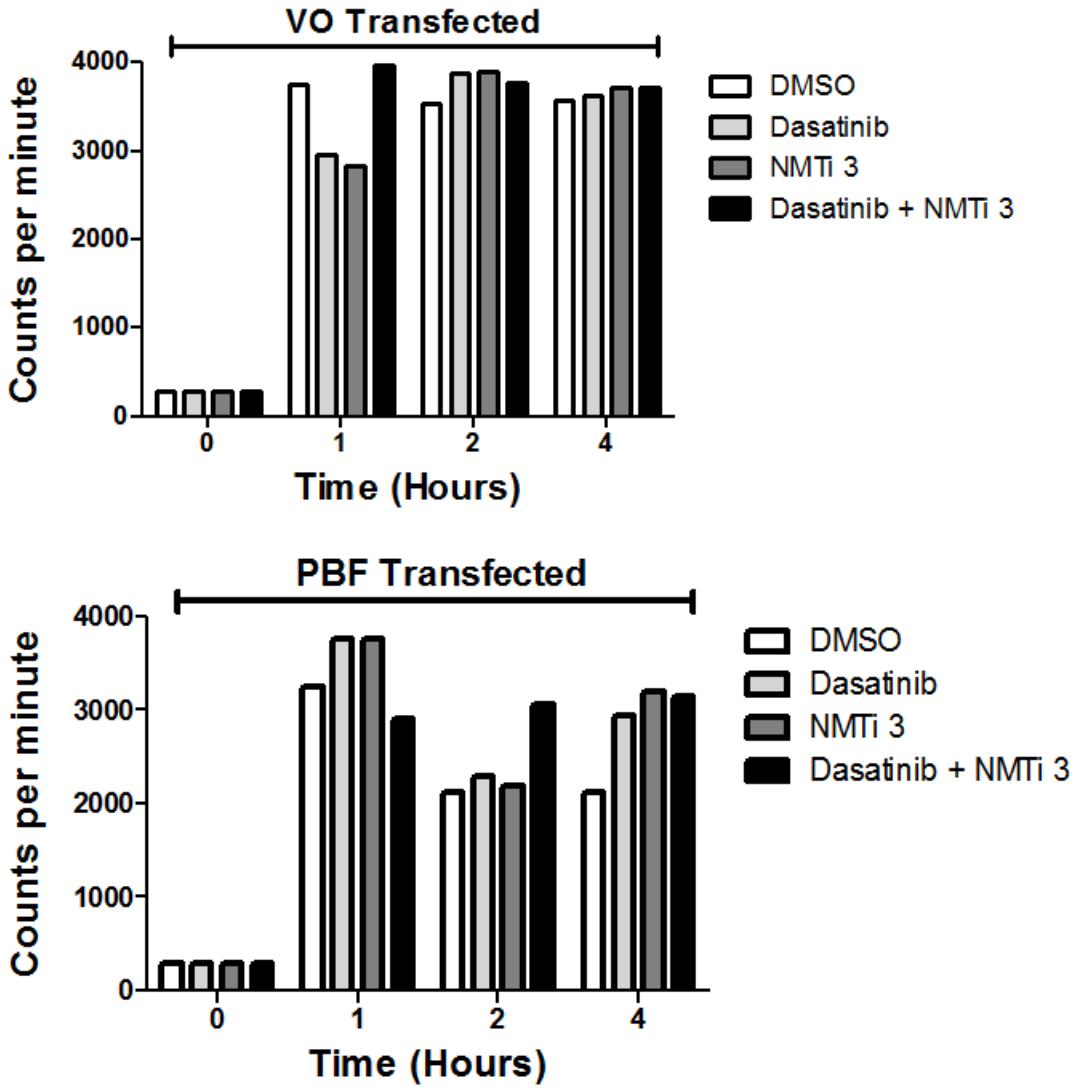

Figure 7-11. Radioiodide efflux. ATRA and dexamethasone-treated MCF-7 cells stably transfected with empty pCI-neo vector (VO) or PBF were treated with DMSO, 1nM dasatinib, 100nM NMT inhibitor 3 or a combination of the two drugs for 24 hours before the addition of ^{125}I. After 1 hour medium was replaced and then the medium was harvested and counted after 0, 1, 2 or 4 hours. n=1.

7.4 Discussion

7.4.1 Inhibition of NMT increases radioiodide uptake

The University of Dundee Drug Discovery Group identified two potent inhibitors of NMT and a structurally related negative control compound. The initial assessment of these compounds using radioiodide uptake studies over a range of doses correctly identified the two active compounds as observed by increased radioiodide. NMT inhibitor 3 was observed to be the most effective compound, significantly increasing radioiodide uptake. This compound had previously been identified as the most potent NMT inhibitor by the Drug Discovery Group. Thus far, the data in this thesis have suggested that Src is responsible for the phosphorylation of PBF and a reduction in radioiodide uptake in breast cancer cells. With the *N*-myristoylation of Src by NMT being critical for Src association with the plasma and intracellular membrane where Src is known to be activated, it is logical that inhibition of NMT would increase radioiodide uptake in breast cancer cells. This increase in radioiodide uptake is a key finding as the treatment time utilised in these dose curves is two hours prior to the addition of ^{125}I. This short treatment time would negate any of the side effects of NMT inhibition such as deactivation of Fus1 as exposure time would be minimal.

7.4.2 Inhibition of NMT does not affect PBF phosphorylation

To assess whether the increase in radioiodide uptake witnessed with the use of NMT inhibitor 3 was PBF dependent, the effect of the inhibitor on PBF phosphorylation was assessed. Inhibition of NMT was identified not to affect PBF phosphorylation with levels

of pY174 PBF remaining unaltered over a range of doses. However the levels of activated pY418 Src also remained consistent over the range of doses. The protein utilised for Western blotting was harvested two hours after treatment with NMT. Since *N*-myristoylation of Src occurs co-translationally, this two hour treatment may have not allowed for sufficient time to alter the cellular phosphorylation of Src and therefore PBF. These data suggest that the increase in radioiodide uptake observed with NMT inhibitor 3 treatment may be through a PBF independent mechanism.

To test this hypothesis that NMT inhibition is acting independently of PBF to increase radioiodide uptake, it was assessed whether NMT inhibition could rescue the reduction in radioiodide uptake with PBF in a similar manner to dasatinib. The use of NMT inhibitor 3 for 2 hours did not rescue radioiodide uptake in either MCF-7 or MDA-MB-231 cells. Although there was a small trend towards increased radioiodide uptake after 24 hours treatment with NMT inhibitor 3, the compound again could not rescue radioiodide uptake. These data suggest again that the increase in radioiodide uptake identified when using NMT inhibitor 3 is PBF independent. This was further supported by immunofluorescence studies where treatment with NMT inhibitor 3 for 24 hours did not decrease the colocalisation between PBF and NIS in breast cancer cells.

7.4.3 Src and NMT inhibition may have synergistic effects

Both NMT inhibition and Src inhibition have been observed to increase radioiodide uptake when used separately, and it was therefore of interest to assess the effect the two drugs had in combination. In untransfected MCF-7 cells, treatment with 100nM NMT inhibitor 3 for 24 hours and dasatinib for 22 hours provided the highest level of

radioiodide uptake across all the treatment combinations tested. However this synergistic effect was not observed in MDA-MB-231 cells suggesting the effect may be cell type specific. The combination of the two drugs was also ineffective at combating the effect of PBF transfection on radioiodide uptake with dual treatment being no more effective than dasatinib alone in both MCF-7 and MDA-MB-231 cells.

In radioiodide retention experiments, the combination of treatment with dasatinib and NMT inhibitor 3 did not initially show increased radioiodide activity after one or 2 hours but empty vector transfected MCF-7 cells treated with both dasatinib and NMT inhibitor 3 retained the most ^{125}I after 4 hours. However, with initial treatment after 1 hour cells treated with a combination treatment effluxed the most radioiodide. In cells transfected with PBF, the addition of NMT inhibitor 3 in combination did not affect the retention of radioiodide when compared with dasatinib treatment alone.

Although initial radioiodide uptake studies in MCF-7 cells suggested that treatment with dasatinib and NMT inhibitor 3 may be synergistic increasing radioiodide uptake beyond solo treatment, it appears this effect may be cell type specific as it was not observed in MDA-MB-231 cells. The results presented in this chapter are preliminary and further experiments are required before a definitive conclusion can be made on the combined effects of the drugs.

7.4.4 Hypotheses and further work

Although the mechanism by which NMT inhibition increases radioiodide uptake is unknown, there are several hypotheses that can be formed from this study. Firstly, the

increased radioiodide uptake observed with NMTi 3 treatment could be as a result of NMT inhibition increasing NIS expression or stability. NIS expression after treatment with NMTi 3 could easily be assessed by qRT-PCR and Western blotting, and protein stability could be assessed by using the protein synthesis inhibitor anisomycin and monitoring the expression of NIS protein by Western blotting over a period of several hours. If NMT inhibition is observed to promote NIS stability or increase NIS expression, the additional radioiodide uptake observed can be accounted for. However, should this not be the case then further work is required to elucidate the mechanism by which NMT inhibitor 3 is increasing radioiodide uptake.

Another hypothesis may be that although neither NIS nor PBF are predicted to be *N*-myristoylated, there may be another putitative binding partner of NIS capable of influencing its activity. NIS activity has been observed to increase when its binding partner hsp90 is inhibited (Marsee et al., 2004) and with hsp90 containing a *N*-myristoylation site (Chen et al., 2005) it is possible that NMT inhibition is indirectly increasing NIS function via hsp90 inhibition. With 0.5-3% of all proteins predicted to be *N*-myristoylated, there are a plethora of reasons that NMT inhibition could be increasing radioiodide uptake.

It was also observed that MCF-7 and MDA-MB-231 cells behaved differently in the presence of PBF and NMT inhibition. An explanation for this may lie within intrinsic differences in expression of NMT isoforms between the two cell lines. The two cell-lines may express differing levels of both NMT 1 and NMT 2, with NMTi 3 having different affinities for the two isoforms of the enzyme effecting the level to which NMT is inhibition on a whole.

Overall these data suggest that the inhibition of NMT with a potent inhibitor can increase radioiodide uptake in breast cancer cells. This increased radioiodide uptake appears to be independent of PBF suggesting another mechanism to increase plasma membrane NIS expression in breast cancer cells. Further work is required to elucidate whether inhibition of NMT is increasing total NIS levels or is solely increasing plasma membrane expression, with an aim to exploit the mechanism for therapeutic purposes. Once this mechanism is identified it would be advantageous to further assess whether inhibition of NMT could be used synergistically with Src inhibition to further increase radioiodide uptake in breast cancer cells.

CHAPTER 8 – FINAL CONCLUSIONS AND FUTURE STUDIES

The work described in this thesis investigated the relationship between PBF and NIS in breast cancer cells with the primary focus of increasing the ability of breast cancer cells to uptake radioactive iodide. This was based on previous work detailing the important role of PBF in thyroid cancer and the protein's ability to decrease radioiodide uptake in these cells. In thyroid cancer, PBF is capable of binding to and altering the subcellular localisation of NIS, rendering the transporter inactive due to its aberrant localisation (Smith et al., 2009). The phosphorylation of PBF at Y174 is critical for this interaction between NIS and PBF with abrogation of phosphorylation restoring radioiodide uptake in thyroid cancer cells (Smith et al., 2013). PBF and NIS have been individually described to be upregulated in the majority of breast cancers (Tazebay et al., 2000; Watkins et al., 2010), however prior to this thesis the relationship between the two proteins had never been investigated in breast cancer.

8.1 PBF and NIS interact in breast cancer

Previous studies have demonstrated that in thyroid cancer PBF binds directly to NIS and can alter its subcellular localisation, translocating it away from the plasma membrane into intracellular vesicles resulting in decreased radioiodide uptake. In this thesis, it has been demonstrated over a small number of samples that both NIS and PBF are overexpressed within breast cancer tumours compared to matched normal tissue. However, in future studies, more matched tissue samples would be necessary to correlate the expression between the two proteins. In a similar manner to thyroid cancer, PBF was observed to bind to NIS in breast cancer cells. Overexpression of PBF increased intracellular staining of NIS *in vitro* and decreased radioiodide uptake as hypothesised.

Although the posttranslational effects of PBF and NIS are similar in thyroid and breast cancer, the relationship between the two appears to differ between the diseases in terms of gene regulation. In thyroid cancer, NIS expression has been reported to be repressed by PBF expression. This is through PBF's interaction with the NUE (Boelaert et al., 2007), a thyroid-specific enhancer of NIS (Schmitt et al., 2002; Taki et al., 2002). As hypothesised, PBF overexpression did not repress NIS expression in the absence of an active NUE. However, and more unexpectedly, PBF overexpression was actually capable of upregulating NIS mRNA. Although NIS expression is increased in the presence of PBF, there is no increase in activity due to the aberrant subcellular localisation of NIS within breast cancer cells. Further work is required to identify the mechanism by which PBF can increase NIS expression within breast cancer cells. One hypothesised mechanism is through PBF's induction of Akt, a protein that has been associated with NIS regulation in breast cancer (Kogai et al., 2008). This hypothesis could be tested by treating PBF transfected cells with an Akt inhibitor prior to harvesting RNA. If Akt is involved with upregulating NIS expression, then the Akt inhibitor should counteract this effect and the increase in NIS mRNA would not be observed.

From the data presented in this thesis it is clear that PBF and NIS have a functional relationship in breast cancer similar to that observed in thyroid cancer. Overexpression of PBF in breast cancer cells consistently reduced radioiodide uptake by at least 25%. This loss of activity in NIS functionality can be attributed to increased intracellular NIS observed in the presence of PBF overexpression. In 80% of breast tumours that express NIS, the majority of them are observed to have primarily intracellular NIS, rendering radioiodide uptake ineffective in these patients. It would be of great interest to obtain

more breast cancer tumour samples, correlate the levels of PBF and NIS within the samples and identify whether there is an association between PBF levels and the intracellular localisation of NIS. However it is already clear from the data presented that PBF and NIS have a functional relationship in breast cancer, and minimising their interaction can increase the radioiodide uptake of breast cancer cells.

8.2 PBF phosphorylation is critical for protein interaction with NIS

In this thesis, a new mutant form of PBF lacking Y174 phosphorylation was identified and characterised. Though this form is unlikely to be witnessed within breast cancer tumours, it served as an ideal tool to study the effect PBF phosphorylation has on PBF's interaction with NIS. The EEN/AAA PBF mutant was observed to lack phosphorylation at Y174 *in vitro* similar to the previously characterised Y174A PBF mutant. However the major difference between the two mutant forms was EEN/AAA PBF's ability to localise within cells in the same manner as WT PBF. The Y174A PBF mutant is known to have an interrupted endocytosis motif and be retained in the plasma membrane. The ability for EEN/AAA PBF to localise like WT PBF allowed the study of the effects of phosphorylation alone. Neither phospho-mutant forms of PBF appeared to be capable of interacting with NIS, with EEN/AAA PBF exhibiting reduced colocalisation with NIS compared with WT PBF. This lack of interaction was confirmed with Co-IP data in which NIS and EEN/AAA PBF or Y174A PBF did not bind whereas strong binding was witnessed with WT PBF. In cells expressing EEN/AAA PBF, there appeared to be reduced intracellular NIS compared to cells

containing WT PBF and neither EEN/AAA PBF nor Y174A PBF were able to reduce radioiodide uptake *in vitro* as WT PBF had. Taken together the data suggest that PBF phosphorylation at Y174 is critical for PBF's interaction with NIS.

To further assess the role that PBF phosphorylation plays in the relationship between PBF and NIS, SFK inhibitors were assessed. PP1, a potent SFK inhibitor had previously been identified to inhibit the phosphorylation of PBF in thyroid cells. Here, it was identified that the more specific and effective SFK inhibitors dasatinib and saracatinib can also inhibit the phosphorylation of PBF *in vitro*. Both inhibitors were capable of inhibiting PBF phosphorylation at concentrations much lower than previously demonstrated with PP1. All Src inhibitors tested were capable of restoring PBF's reduction in radioiodide uptake in breast cancer cells, again suggesting a link between unphosphorylated PBF being unable to interact with NIS and alter its subcellular localisation.

Together the data presented suggest that the phosphorylation of PBF at Y174 is critical for the interaction between NIS and PBF. Utilisation of FDA cleared dasatinib to inhibit PBF phosphorylation and increase radioiodide uptake is potentially therapeutically important. In the proposed treatment regime, dasatinib could be used as a pre-treatment, only used a few days prior to radioiodide therapy to boost plasma membrane localisation of NIS and increase radioiodide uptake into breast cancer cells, thereby avoiding any potential side effects caused by long term dasatinib exposure.

8.3 Src regulates/potentially phosphorylates PBF

Previous work has demonstrated that inhibition of SFK can inhibit PBF phosphorylation, with both Src (Smith et al., 2013) and Lyn (unpublished work) observed to bind to PBF. Here, it was demonstrated that Src can bind to PBF in breast cancer cell lines. Overexpression of Src increased PBF phosphorylation and decreased radioiodide in the presence of exogenous PBF further than PBF expression alone, suggesting that Src can regulate PBF phosphorylation. Dasatinib was capable of restoring radioiodide uptake in the presence of both Src and PBF. Phosphorylation mutants of PBF were observed to still be capable of binding to Src, but were unable to become phosphorylated or reduce radioiodide uptake in the presence of exogenous Src.

A constitutively active mutant form of Src was utilised to ascertain whether Src was the primary SFK responsible for phosphorylating PBF. The T341I Src mutant contains an activating mutation at Src's gatekeeper residue and is resistant to dasatinib inhibition. The data presented here suggest that Src can regulate PBF phosphorylation. Use of the T341I Src mutant increased PBF phosphorylation levels even in the presence of dasatinib, which was also unable to rescue T341I Src's reduction in radioiodide uptake. While these results do not prove that Lyn or another SFK do not have additional roles in PBF phosphorylation, they provide evidence that Src has a key role PBF phosphorylation and is thereby an indirect inhibitor of radioiodide uptake.

8.4 Inhibition of NMT does not affect PBF but can increase radioiodide uptake

The effect of NMT inhibition on the cellular ability to uptake radioiodide had previously never been investigated. Of the three compounds gifted to the study by The Drug Discovery Group at the University of Dundee, one compound referred to as NMT inhibitor 3 was capable of increasing radioiodide uptake in MCF-7 cells after 2hours at concentrations as low as 100nM. However, investigations into the inhibitor's effect on PBF showed that inhibition of NMT did not affect PBF's phosphorylation status at Y174. Further studies revealed that inhibition of NMT could not overcome PBF's repression of radioiodide uptake *in vitro* suggesting that the initial increase in radioiodide uptake observed with NMT inhibitor 3 is independent of PBF.

Although the effects of NMT inhibition on radioiodide uptake appear to be independent of PBF, it is of interest to establish whether NMT inhibitors can be administered alongside dasatinib to produce a positive synergistic effect on radioiodide uptake. In MCF-7 cells, treatment with both drugs increased radioiodide uptake above the levels witnessed with either drug in isolation. This effect was not observed in MDA-MB-231 cells, although both drugs in combination presented no adverse effects on radioiodide uptake. However even in MCF-7 cells there was no additive effect of dasatinib and NMT inhibition on restoring the radioiodide uptake observed in the presence of PBF. The combination of the two drugs did increase the radioiodide retention of MCF-7 cells after treatment with ^{125}I.

8.5 Critical Evaluation and Future Directions

Although this thesis constitutes a comprehensive study, there are notable limitations to several aspects of the study. Throughout the thesis, multiple differential *in vitro* models were utilised including endogenous cells, transient and stable transfection, lentiviral and chemically induced cells. The use of two or three models throughout the study may have provided a better overview and greater consistency. However, the use of multiple models can highlight the effectiveness of the work with the same effect being witnessed across the models. In this study, PBF expression whether transient or stable consistently decreased radioiodide uptake in cells expressing transfected, lentiviral and chemically induced NIS. As many of the experiments described in this thesis were protein expression and functional studies the use of multiple models demonstrates that the effects observed are not attributed solely to the method by which protein overexpression was achieved.

Transient transfection provided a quick method with which to assess the effect of single and combinatorial protein overexpression for short term experiments. It also provides a polyclonal mix of cells with differential levels of protein expression, simulating the heterogeneity of malignant tumours. Long term stable transfection and lentiviral expression of proteins provided a robust method for observing specific effects caused by overexpression of specific proteins.. As all cells were derived from a single cell clone, copy number and genomic transgene insertion points were consistent throughout experiments whereby lentiviral transduction was applied. Additionally, transient transfection can induce cellular stress with transfection reagents often being cytotoxic. With many transient transfection experiments typically spanning 48-72 hours, the cells may not have recovered sufficiently from the transfection process and thus behaved abberantly,

invalidating results. Stable transfection allows for ample time to recover from the procedure, thus avoiding this potential pitfall. The use of both models often alongside each other, has the advantage of assessing the overexpression of the protein in question, allowing for more confidence that any observable effects were due to protein overexpression rather than artefacts of the transfection process.

Western blotting was a powerful tool that provided a qualitative assessment of protein expression levels within a cell population. For quantitative analysis of protein expression, densitometry could have been employed. Densitometry was not utilised in this study due to the complexity of quantifying the loading controls. Many of the Western blots in this study were performed to assess the differences in the expression of phosphorylated proteins, such as PBF, and to accurately quantify the differences in phosphorylated protein both the loading control and and total target protein expression is required to normalise the data. With the limitations of the PBF antibody discussed in 3.4.2 and 4.4.1, accurate quantification of Western blotting was difficult to achieve and was therefore not included in the study.

To determine protein localisation within breast cancer cells, immunofluroscence microscopy was utilised, for which the use of the Zeiss Axioplan fluroescent microscope provided a reliable platform. However use of confocal microscopy could have allowed z-stacking and provided even greater accuracy of protein localisation within the cells. In future studies, counting an arbitrary number of cells and assessing the percentage of co-localisation would have also been a suitable method to quantify protein co-localisation over a population of cells. Proximity ligation assay (PLA) could also be utilised in future studies as a sensitive technique for identifying protein interactions *in situ*.

Additionally, the use of Src kinase inhibitors was heavily relied on during this study. There are many caveats to using inhibitors experimentally, such as their sensitivity and specificity. Dasatinib was utilised mainly as an inhibitor of Src, but is also known to inhibit all SFK along with Bcr-Abl and c-Kit. Although the use of T341I Src aided in the dissection of Src specific effects there are still flaws to the methodology. Use of Src siRNA and Src kinase assays should be utilised alongside inhibitors in future experiments to further aid in identifying the true effect of Src on PBF phosphorylation.

During the final weeks of this project, plasma membrane fractionation was undergoing optimisation. This technique would have been very useful for the study presented in this thesis as it would have provided a more quantifiable method to assess PBF's effect on the subcellular localisation of NIS within breast cancer cells. The technique allows the separation of the plasma membrane from all other membranes within the cell and thus would have provided a means of assessing the reduction of plasma membrane NIS in the presence of PBF.

In terms of NMT inhibition, future studies should involve elucidating the mechanism by which inhibition of NMT can increase radioiodide uptake. From the information presented in this study, it could be hypothesised that inhibition of NMT may influence the expression of NIS. Work could be done to assess NIS mRNA levels and protein levels after treatment with NMT inhibitors to test this hypothesis. With the short treatment times, it could be speculated that NMT inhibition may increase the stability of the NIS protein or the activity of the transporter.

Due to time and financial restraints, *in vivo* work was unable to be performed within the remit of this project. Had the study been without barriers, nude mice would

have been subjected to orthotopic MCF-7 tumours with either empty vector, WT PBF and EEN/AAA PBF stably expressing cells being injected into the mammary fat pad. Once the tumours were established, to boost endogenous NIS levels the mice would have been treated with ATRA and dexamethasone and then the three different transfection groups further divided into different experimental treatment groups. The first group would have been the control group, treated with saline containing vehicle only and DMSO. The second treatment group would have been treated with dasatinib and the third with a combination of dasatinib and NMT inhibitor 3. 24 hours after the treatment the mice would have been given ^{125}I and harvested the same day. Tumours would have been removed and radioiodide accumulation assessed. The study would have sought to validate all the work done *in vitro* and demonstrate that dasatinib can boost NIS activity within breast cancer cells overexpressing PBF making radioiodide therapy a potentially viable treatment for breast cancer.

8.6 Conclusions

This thesis has generated data that can improve the current understanding of the relationship between NIS and PBF within breast cancer cells. It has been demonstrated that PBF can bind to NIS and repress the ability of breast cancer cells to take up radioiodide. The interaction between PBF and NIS is regulated by PBF phosphorylation at Y174, with unphosphorylated forms of PBF being unable to interact with NIS. The phosphorylation of PBF in breast cancer cells can be inhibited using SFK inhibitors including the potent SFK inhibitor dasatinib, which not only abrogates pY174 PBF but also overcomes PBF's reduction in radioiodide uptake. Although further studies are required to establish the role NMT inhibition plays within radioiodide uptake and to validate the treatments *in vivo*, the data presented here have potentially important therapeutic implications. If the *in vitro* data prove to be translational, then there is potential for a novel treatment strategy for breast cancer patients that are unresponsive to current conventional treatments.

This work not only impacts breast cancer research but also has wider implications for thyroid and other cancer types. Methods to increase the efficacy of radioiodide therapy are of great value to the treatment of thyroid disease, particularly for patients with radioactive iodine-refractory differentiated thyroid cancer. Additionally, the work of Professor Christine Spitzweg (Muenchen) and other research groups could benefit greatly from these findings with their investigations into non-thyroidal NIS gene delivery, further widening the applicability of this research into cancers that do not express endogenous NIS. As PBF is overexpressed in many cancers, the conclusions of this thesis may help to overcome the major pitfall of NIS gene delivery in that PBF is identified as an orchestrator

of aberrant NIS localisation, thus reducing the effectiveness of NIS alone on radioiodide uptake. PBF is over-expressed within a plethora of cancers so delivery of NIS to tumours may not prove effective in terms of radioiodide uptake if NIS is aberrantly localised.

CHAPTER 9 - REFERENCES

Ali, S., and R.C. Coombes. 2002. Endocrine-responsive breast cancer and strategies for combating resistance. *Nat Rev Cancer*. 2:101-112.

Allegra, C.J., D.R. Aberle, P. Ganschow, S.M. Hahn, C.N. Lee, S. Millon-Underwood, M.C. Pike, S.D. Reed, A.F. Saftlas, S.A. Scarvalone, A.M. Schwartz, C. Slomski, G. Yothers, and R. Zon. 2009. NIH state-of-the-science conference statement: diagnosis and management of ductal carcinoma in situ (DCIS). *NIH Consens State Sci Statements*. 26:1-27.

Alotaibi, H., E. Yaman, D. Salvatore, V. Di Dato, P. Telkoparan, R. Di Lauro, and U.H. Tazebay. 2010. Intronic elements in the Na+/I- symporter gene (NIS) interact with retinoic acid receptors and mediate initiation of transcription. *Nucleic acids research*. 38:3172-3185.

Alotaibi, H., E.C. Yaman, E. Demirpence, and U.H. Tazebay. 2006. Unliganded estrogen receptor-alpha activates transcription of the mammary gland Na+/I- symporter gene. *Biochemical and biophysical research communications*. 345:1487-1496.

Alsayed, Y., S. Uddin, N. Mahmud, F. Lekmine, D.V. Kalvakolanu, S. Minucci, G. Bokoch, and L.C. Platanias. 2001. Activation of Rac1 and the p38 mitogen-activated protein kinase pathway in response to all-trans-retinoic acid. *J Biol Chem*. 276:4012-4019.

Amanchy, R., B. Periaswamy, S. Mathivanan, R. Reddy, S.G. Tattikota, and A. Pandey. 2007. A curated compendium of phosphorylation motifs. *Nat Biotechnol*. 25:285-286.

Angulo, A., C. Suto, R.A. Heyman, and P. Ghazal. 1996. Characterization of the sequences of the human cytomegalovirus enhancer that mediate differential regulation by natural and synthetic retinoids. *Molecular endocrinology*. 10:781-793.

Arriagada, A.A., E. Albornoz, M.C. Opazo, A. Becerra, G. Vidal, C. Fardella, L. Michea, N. Carrasco, F. Simon, A.A. Elorza, S.M. Bueno, A.M. Kalergis, and C.A. Riedel. 2015. Excess iodide induces an acute inhibition of the sodium/iodide symporter in thyroid male rat cells by increasing reactive oxygen species. *Endocrinology*. 156:1540-1551.

Arturi, F., E. Ferretti, I. Presta, T. Mattei, A. Scipioni, D. Scarpelli, R. Bruno, L. Lacroix, E. Tosi, A. Gulino, D. Russo, and S. Filetti. 2005. Regulation of iodide uptake and sodium/iodide symporter expression in the mcf-7 human breast cancer cell line. *The Journal of clinical endocrinology and metabolism*. 90:2321-2326.

Azam, M., M.A. Seeliger, N.S. Gray, J. Kuriyan, and G.Q. Daley. 2008. Activation of tyrosine kinases by mutation of the gatekeeper threonine. *Nat Struct Mol Biol*. 15:1109-1118.

Bagrodia, S., S.J. Taylor, and D. Shalloway. 1993. Myristylation is required for Tyr-527 dephosphorylation and activation of pp60c-src in mitosis. *Molecular and cellular biology*. 13:1464-1470.

Bain, J., H. McLauchlan, M. Elliott, and P. Cohen. 2003. The specificities of protein kinase inhibitors: an update. *Biochem J*. 371:199-204.

Baumann, E. 1896. Uber das Thyrojodin. *Munch Med Wschr*. 43:4.

Behl, C. 2002. Oestrogen as a neuroprotective hormone. *Nat Rev Neurosci*. 3:433-442.

Benson, J.R., I. Jatoi, M. Keisch, F.J. Esteva, A. Makris, and V.C. Jordan. 2009. Early breast cancer. *Lancet*. 373:1463-1479.

Benz, C.C., G.K. Scott, J.C. Sarup, R.M. Johnson, D. Tripathy, E. Coronado, H.M. Shepard, and C.K. Osborne. 1992. Estrogen-dependent, tamoxifen-resistant tumorigenic growth of MCF-7 cells transfected with HER2/neu. *Breast Cancer Res Treat*. 24:85-95.

Berclaz, G., S. Li, K.N. Price, A.S. Coates, M. Castiglione-Gertsch, C.M. Rudenstam, S.B. Holmberg, J. Lindtner, D. Erien, J. Collins, R. Snyder, B. Thurlimann, M.F. Fey, C. Mendiola, I.D. Werner, E. Simoncini, D. Crivellari, R.D. Gelber, A. Goldhirsch, and G. International Breast Cancer Study. 2004. Body mass index as a prognostic feature in operable breast cancer: the International Breast Cancer Study Group experience. *Ann Oncol*. 15:875-884.

Berditchevski, F., and E. Odintsova. 2007. Tetraspanins as regulators of protein trafficking. *Traffic*. 8:89-96.

Berx, G., A.M. Cleton-Jansen, F. Nollet, W.J. de Leeuw, M. van de Vijver, C. Cornelisse, and F. van Roy. 1995. E-cadherin is a tumour/invasion suppressor gene mutated in human lobular breast cancers. *EMBO J*. 14:6107-6115.

Beyer, S.J., R.E. Jimenez, C.L. Shapiro, J.Y. Cho, and S.M. Jhiang. 2009. Do cell surface trafficking impairments account for variable cell surface sodium iodide symporter levels in breast cancer? *Breast Cancer Res Treat*. 115:205-212.

Blom, N., S. Gammeltoft, and S. Brunak. 1999. Sequence and structure-based prediction of eukaryotic protein phosphorylation sites. *J Mol Biol*. 294:1351-1362.

Boelaert, K., C.J. McCabe, L.A. Tannahill, N.J. Gittoes, R.L. Holder, J.C. Watkinson, A.R. Bradwell, M.C. Sheppard, and J.A. Franklyn. 2003. Pituitary tumor transforming gene and fibroblast growth factor-

2 expression: potential prognostic indicators in differentiated thyroid cancer. *The Journal of clinical endocrinology and metabolism*. 88:2341-2347.

Boelaert, K., V.E. Smith, A.L. Stratford, T. Kogai, L.A. Tannahill, J.C. Watkinson, M.C. Eggo, J.A. Franklyn, and C.J. McCabe. 2007. PTTG and PBF repress the human sodium iodide symporter. *Oncogene*. 26:4344-4356.

Boland, A., M. Ricard, P. Opolon, J.M. Bidart, P. Yeh, S. Filetti, M. Schlumberger, and M. Perricaudet. 2000. Adenovirus-mediated transfer of the thyroid sodium/iodide symporter gene into tumors for a targeted radiotherapy. *Cancer research*. 60:3484-3492.

Bonifacino, J.S., and E.C. Dell'Angelica. 1999. Molecular bases for the recognition of tyrosine-based sorting signals. *J Cell Biol*. 145:923-926.

Bork, P., T. Doerks, T.A. Springer, and B. Snel. 1999. Domains in plexins: links to integrins and transcription factors. *Trends Biochem Sci*. 24:261-263.

Bowyer, P.W., R.S. Gunaratne, M. Grainger, C. Withers-Martinez, S.R. Wickramsinghe, E.W. Tate, R.J. Leatherbarrow, K.A. Brown, A.A. Holder, and D.F. Smith. 2007. Molecules incorporating a benzothiazole core scaffold inhibit the N-myristoyltransferase of Plasmodium falciparum. *Biochem J*. 408:173-180.

Buerger, H., F. Otterbach, R. Simon, K.L. Schafer, C. Poremba, R. Diallo, C. Brinkschmidt, B. Dockhorn-Dworniczak, and W. Boecker. 1999. Different genetic pathways in the evolution of invasive breast cancer are associated with distinct morphological subtypes. *J Pathol*. 189:521-526.

Burdon, T.G., J. Demmer, A.J. Clark, and C.J. Watson. 1994. The mammary factor MPBF is a prolactin-induced transcriptional regulator which binds to STAT factor recognition sites. *FEBS letters*. 350:177-182.

Bussolati, G., P. Cassoni, G. Ghisolfi, F. Negro, and A. Sapino. 1996. Immunolocalization and gene expression of oxytocin receptors in carcinomas and non-neoplastic tissues of the breast. *Am J Pathol*. 148:1895-1903.

Calalb, M.B., T.R. Polte, and S.K. Hanks. 1995. Tyrosine phosphorylation of focal adhesion kinase at sites in the catalytic domain regulates kinase activity: a role for Src family kinases. *Molecular and cellular biology*. 15:954-963.

Calalb, M.B., X. Zhang, T.R. Polte, and S.K. Hanks. 1996. Focal adhesion kinase tyrosine-861 is a major site of phosphorylation by Src. *Biochemical and biophysical research communications*. 228:662-668.

Cancer Research UK. 2015. Breast cancer incidence statistics. Vol. 2016.

Canfield, W.M., K.F. Johnson, R.D. Ye, W. Gregory, and S. Kornfeld. 1991. Localization of the signal for rapid internalization of the bovine cation-independent mannose 6-phosphate/insulin-like growth factor-II receptor to amino acids 24-29 of the cytoplasmic tail. *The Journal of biological chemistry*. 266:5682-5688.

Cao, X.Y., X.M. Jiang, Z.H. Dou, M.A. Rakeman, M.L. Zhang, K. O'Donnell, T. Ma, K. Amette, N. DeLong, and G.R. DeLong. 1994. Timing of vulnerability of the brain to iodine deficiency in endemic cretinism. *The New England journal of medicine*. 331:1739-1744.

Carey, L.A., C.M. Perou, C.A. Livasy, L.G. Dressler, D. Cowan, K. Conway, G. Karaca, M.A. Troester, C.K. Tse, S. Edmiston, S.L. Deming, J. Geradts, M.C. Cheang, T.O. Nielsen, P.G. Moorman, H.S. Earp, and R.C. Millikan. 2006. Race, breast cancer subtypes, and survival in the Carolina Breast Cancer Study. *JAMA*. 295:2492-2502.

Carlomagno, F., D. Vitagliano, T. Guida, M. Napolitano, G. Vecchio, A. Fusco, A. Gazit, A. Levitzki, and M. Santoro. 2002. The kinase inhibitor PP1 blocks tumorigenesis induced by RET oncogenes. *Cancer research*. 62:1077-1082.

Castro, M.R., E.R. Bergert, J.R. Goellner, I.D. Hay, and J.C. Morris. 2001. Immunohistochemical analysis of sodium iodide symporter expression in metastatic differentiated thyroid cancer: correlation with radioiodine uptake. *The Journal of clinical endocrinology and metabolism*. 86:5627-5632.

Cavalieri, E.L., and E.G. Rogan. 2016. Depurinating estrogen-DNA adducts, generators of cancer initiation: their minimization leads to cancer prevention. *Clin Transl Med*. 5:12.

Chan, C.M., X. Jing, L.A. Pike, Q. Zhou, D.J. Lim, S.B. Sams, G.S. Lund, V. Sharma, B.R. Haugen, and R.E. Schweppe. 2012. Targeted inhibition of Src kinase with dasatinib blocks thyroid cancer growth and metastasis. *Clinical cancer research : an official journal of the American Association for Cancer Research*. 18:3580-3591.

Chatterjee, S., R. Malhotra, F. Varghese, A.B. Bukhari, A. Patil, A. Budrukkar, V. Parmar, S. Gupta, and A. De. 2013. Quantitative immunohistochemical analysis reveals association between sodium iodide symporter and estrogen receptor expression in breast cancer. *PLoS One*. 8:e54055.

Chen, B., W.H. Piel, L. Gui, E. Bruford, and A. Monteiro. 2005. The HSP90 family of genes in the human genome: insights into their divergence and evolution. *Genomics*. 86:627-637.

Chen, G.G., Q. Zeng, and G.M. Tse. 2008. Estrogen and its receptors in cancer. *Med Res Rev*. 28:954-974.

Cheraghi, Z., J. Poorolajal, T. Hashem, N. Esmailnasab, and A. Doosti Irani. 2012. Effect of body mass index on breast cancer during premenopausal and postmenopausal periods: a meta-analysis. *PloS one*. 7:e51446.

Chien, W., and L. Pei. 2000. A novel binding factor facilitates nuclear translocation and transcriptional activation function of the pituitary tumor-transforming gene product. *The Journal of biological chemistry*. 275:19422-19427.

Cho, J.Y., R. Leveille, R. Kao, B. Rousset, A.F. Parlow, W.E. Burak, Jr., E.L. Mazzaferri, and S.M. Jhiang. 2000. Hormonal regulation of radioiodide uptake activity and Na+/I- symporter expression in mammary glands. *The Journal of clinical endocrinology and metabolism*. 85:2936-2943.

Choudhury, S., V. Almendro, V.F. Merino, Z. Wu, R. Maruyama, Y. Su, F.C. Martins, M.J. Fackler, M. Bessarabova, A. Kowalczyk, T. Conway, B. Beresford-Smith, G. Macintyre, Y.K. Cheng, Z. Lopez-Bujanda, A. Kaspi, R. Hu, J. Robens, T. Nikolskaya, V.D. Haakensen, S.J. Schnitt, P. Argani, G. Ethington, L. Panos, M. Grant, J. Clark, W. Herlihy, S.J. Lin, G. Chew, E.W. Thompson, A. Greene-Colozzi, A.L. Richardson, G.D. Rosson, M. Pike, J.E. Garber, Y. Nikolsky, J.L. Blum, A. Au, E.S. Hwang, R.M. Tamimi, F. Michor, I. Haviv, X.S. Liu, S. Sukumar, and K. Polyak. 2013. Molecular profiling of human mammary gland links breast cancer risk to a p27(+) cell population with progenitor characteristics. *Cell Stem Cell*. 13:117-130.

Clarke, M., R. Collins, S. Darby, C. Davies, P. Elphinstone, V. Evans, J. Godwin, R. Gray, C. Hicks, S. James, E. MacKinnon, P. McGale, T. McHugh, R. Peto, C. Taylor, Y. Wang, and G. Early Breast Cancer Trialists' Collaborative. 2005. Effects of radiotherapy and of differences in the extent of surgery for early breast cancer on local recurrence and 15-year survival: an overview of the randomised trials. *Lancet*. 366:2087-2106.

Cleary, M.P., and M.E. Grossmann. 2009. Minireview: Obesity and breast cancer: the estrogen connection. *Endocrinology*. 150:2537-2542.

Clegg, R.A., P.C. Gordge, and W.R. Miller. 1999. Expression of enzymes of covalent protein modification during regulated and dysregulated proliferation of mammary epithelial cells: PKA, PKC and NMT. *Adv Enzyme Regul*. 39:175-203.

Clemons, M., S. Danson, and A. Howell. 2002. Tamoxifen ("Nolvadex"): a review. *Cancer Treat Rev*. 28:165-180.

Cleveland, R.J., S.M. Eng, P.E. Abrahamson, J.A. Britton, S.L. Teitelbaum, A.I. Neugut, and M.D. Gammon. 2007. Weight gain prior to diagnosis and survival from breast cancer. *Cancer Epidemiol Biomarkers Prev*. 16:1803-1811.

Collaborative Group on Hormonal Factors in Breast, C. 2012. Menarche, menopause, and breast cancer risk: individual participant meta-analysis, including 118 964 women with breast cancer from 117 epidemiological studies. *Lancet Oncol*. 13:1141-1151.

Collawn, J.F., M. Stangel, L.A. Kuhn, V. Esekogwu, S.Q. Jing, I.S. Trowbridge, and J.A. Tainer. 1990. Transferrin receptor internalization sequence YXRF implicates a tight turn as the structural recognition motif for endocytosis. *Cell*. 63:1061-1072.

Conneely, O.M., and J.P. Lydon. 2000. Progesterone receptors in reproduction: functional impact of the A and B isoforms. *Steroids*. 65:571-577.

Connolly, R.M., N.K. Nguyen, and S. Sukumar. 2013. Molecular pathways: current role and future directions of the retinoic acid pathway in cancer prevention and treatment. *Clinical cancer research : an official journal of the American Association for Cancer Research*. 19:1651-1659.

Contesso, G., and J.Y. Petit. 1979. [Non-infiltrating intraductal carcinoma of the breast (author's transl)]. *Bull Cancer*. 66:1-8.

Cork, D.M., T.W. Lennard, and A.J. Tyson-Capper. 2008. Alternative splicing and the progesterone receptor in breast cancer. *Breast Cancer Res*. 10:207.

COSMIC Database, S. 2016a. Vol. 2015.

COSMIC Database, S. 2016b. SRC »p.T341A / c.1021A>G.

COSMIC Database, S. 2016c. SRC »p.T341R / c.1022C>G.

Cowan-Jacob, S.W., G. Fendrich, P.W. Manley, W. Jahnke, D. Fabbro, J. Liebetanz, and T. Meyer. 2005. The crystal structure of a c-Src complex in an active conformation suggests possible steps in c-Src activation. *Structure*. 13:861-871.

Cross, F.R., E.A. Garber, D. Pellman, and H. Hanafusa. 1984. A short sequence in the p60src N terminus is required for p60src myristylation and membrane association and for cell transformation. *Molecular and cellular biology*. 4:1834-1842.

Cuzick, J. 2005. Radiotherapy for breast cancer. *J Natl Cancer Inst*. 97:406-407.

Dai, G., O. Levy, and N. Carrasco. 1996. Cloning and characterization of the thyroid iodide transporter. *Nature*. 379:458-460.

David-Pfeuty, T., S. Bagrodia, and D. Shalloway. 1993. Differential localization patterns of myristoylated and nonmyristoylated c-Src proteins in interphase and mitotic c-Src overexpresser cells. *Journal of cell science*. 105 (Pt 3):613-628.

Deichaite, I., L.P. Casson, H.P. Ling, and M.D. Resh. 1988. In vitro synthesis of pp60v-src: myristylation in a cell-free system. *Molecular and cellular biology*. 8:4295-4301.

del Rincon, S.V., C. Rousseau, R. Samanta, and W.H. Miller, Jr. 2003. Retinoic acid-induced growth arrest of MCF-7 cells involves the selective regulation of the IRS-1/PI 3-kinase/AKT pathway. *Oncogene*. 22:3353-3360.

DeLong, G.R., P.W. Leslie, S.H. Wang, X.M. Jiang, M.L. Zhang, M. Rakeman, J.Y. Jiang, T. Ma, and X.Y. Cao. 1997. Effect on infant mortality of iodination of irrigation water in a severely iodine-deficient area of China. *Lancet*. 350:771-773.

Dentice, M., C. Luongo, A. Elefante, R. Romino, R. Ambrosio, M. Vitale, G. Rossi, G. Fenzi, and D. Salvatore. 2004. Transcription factor Nkx-2.5 induces sodium/iodide symporter gene expression and participates in retinoic acid- and lactation-induced transcription in mammary cells. *Molecular and cellular biology*. 24:7863-7877.

Devadas, B., M.E. Zupec, S.K. Freeman, D.L. Brown, S. Nagarajan, J.A. Sikorski, C.A. McWherter, D.P. Getman, and J.I. Gordon. 1995. Design and syntheses of potent and selective dipeptide inhibitors of Candida albicans myristoyl-CoA:protein N-myristoyltransferase. *J Med Chem*. 38:1837-1840.

Diaz, N., S. Minton, C. Cox, T. Bowman, T. Gritsko, R. Garcia, I. Eweis, M. Wloch, S. Livingston, E. Seijo, A. Cantor, J.H. Lee, C.A. Beam, D. Sullivan, R. Jove, and C.A. Muro-Cacho. 2006. Activation of stat3 in primary tumors from high-risk breast cancer patients is associated with elevated levels of activated SRC and survivin expression. *Clinical cancer research : an official journal of the American Association for Cancer Research*. 12:20-28.

Dorrington, J., and R.E. Gore-Langton. 1981. Prolactin inhibits oestrogen synthesis in the ovary. *Nature*. 290:600-602.

Ducker, C.E., J.J. Upson, K.J. French, and C.D. Smith. 2005. Two N-myristoyltransferase isozymes play unique roles in protein myristoylation, proliferation, and apoptosis. *Mol Cancer Res*. 3:463-476.

Dunning, A.M., C.S. Healey, P.D. Pharoah, M.D. Teare, B.A. Ponder, and D.F. Easton. 1999. A systematic review of genetic polymorphisms and breast cancer risk. *Cancer Epidemiol Biomarkers Prev*. 8:843-854.

Dupont, J., and D. Le Roith. 2001. Insulin-like growth factor 1 and oestradiol promote cell proliferation of MCF-7 breast cancer cells: new insights into their synergistic effects. *Molecular pathology : MP*. 54:149-154.

Duvic, M., K. Hymes, P. Heald, D. Breneman, A.G. Martin, P. Myskowski, C. Crowley, R.C. Yocum, and G. Bexarotene Worldwide Study. 2001. Bexarotene is effective and safe for treatment of refractory advanced-stage cutaneous T-cell lymphoma: multinational phase II-III trial results. *Journal of clinical oncology : official journal of the American Society of Clinical Oncology*. 19:2456-2471.

Dwyer, R.M., E.R. Bergert, K. O'Connor M, S.J. Gendler, and J.C. Morris. 2005. In vivo radioiodide imaging and treatment of breast cancer xenografts after MUC1-driven expression of the sodium iodide symporter. *Clinical cancer research : an official journal of the American Association for Cancer Research*. 11:1483-1489.

Dwyer, R.M., S. Khan, F.P. Barry, T. O'Brien, and M.J. Kerin. 2010. Advances in mesenchymal stem cell-mediated gene therapy for cancer. *Stem cell research & therapy*. 1:25.

Dwyer, R.M., J. Ryan, R.J. Havelin, J.C. Morris, B.W. Miller, Z. Liu, R. Flavin, C. O'Flatharta, M.J. Foley, H.H. Barrett, J.M. Murphy, F.P. Barry, T. O'Brien, and M.J. Kerin. 2011. Mesenchymal Stem Cell-mediated delivery of the sodium iodide symporter supports radionuclide imaging and treatment of breast cancer. *Stem cells*. 29:1149-1157.

Egan, C., A. Pang, D. Durda, H.C. Cheng, J.H. Wang, and D.J. Fujita. 1999. Activation of Src in human breast tumor cell lines: elevated levels of phosphotyrosine phosphatase activity that preferentially recognizes the Src carboxy terminal negative regulatory tyrosine 530. *Oncogene*. 18:1227-1237.

Eheman, C.R., K.M. Shaw, A.B. Ryerson, J.W. Miller, U.A. Ajani, and M.C. White. 2009. The changing incidence of in situ and invasive ductal and lobular breast carcinomas: United States, 1999-2004. *Cancer Epidemiol Biomarkers Prev*. 18:1763-1769.

Eisenhaber, F., B. Eisenhaber, W. Kubina, S. Maurer-Stroh, G. Neuberger, G. Schneider, and M. Wildpaner. 2003. Prediction of lipid posttranslational modifications and localization signals from protein sequences: big-Pi, NMT and PTS1. *Nucleic acids research*. 31:3631-3634.

Eliassen, A.H., G.A. Colditz, B. Rosner, W.C. Willett, and S.E. Hankinson. 2006. Adult weight change and risk of postmenopausal breast cancer. *JAMA*. 296:193-201.

Elsberger, B., R. Fullerton, S. Zino, F. Jordan, T.J. Mitchell, V.G. Brunton, E.A. Mallon, P.G. Shiels, and J. Edwards. 2010. Breast cancer patients' clinical outcome measures are associated with Src kinase family member expression. *British journal of cancer*. 103:899-909.

Elsberger, B., B.A. Tan, T.J. Mitchell, S.B. Brown, E.A. Mallon, S.M. Tovey, T.G. Cooke, V.G. Brunton, and J. Edwards. 2009. Is expression or activation of Src kinase associated with cancer-specific survival in ER-, PR- and HER2-negative breast cancer patients? *The American journal of pathology*. 175:1389-1397.

Eng, P.H., G.R. Cardona, S.L. Fang, M. Previti, S. Alex, N. Carrasco, W.W. Chin, and L.E. Braverman. 1999. Escape from the acute Wolff-Chaikoff effect is associated with a decrease in thyroid sodium/iodide symporter messenger ribonucleic acid and protein. *Endocrinology*. 140:3404-3410.

Eng, P.H., G.R. Cardona, M.C. Previti, W.W. Chin, and L.E. Braverman. 2001. Regulation of the sodium iodide symporter by iodide in FRTL-5 cells. *European journal of endocrinology / European Federation of Endocrine Societies*. 144:139-144.

Eskin, B.A., J.A. Parker, J.G. Bassett, and D.L. George. 1974. Human breast uptake of radioactive iodine. *Obstetrics and gynecology*. 44:398-402.

Farazi, T.A., G. Waksman, and J.I. Gordon. 2001. The biology and enzymology of protein N-myristoylation. *The Journal of biological chemistry*. 276:39501-39504.

FDA. 2010a. FDA - U.S. Food and Drug Administration - News and Events.

FDA. 2010b. SPRYCEL®(dasatinib) Tablet for Oral Use - HIGHLIGHTS OF PRESCRIBING INFORMATION B.-M.S. Company, editor, FDA.

Feigelson, H.S., R. McKean-Cowdin, G.A. Coetzee, D.O. Stram, L.N. Kolonel, and B.E. Henderson. 2001. Building a multigenic model of breast cancer susceptibility: CYP17 and HSD17B1 are two important candidates. *Cancer research*. 61:785-789.

Felsted, R.L., C.J. Glover, and K. Hartman. 1995. Protein N-myristoylation as a chemotherapeutic target for cancer. *J Natl Cancer Inst*. 87:1571-1573.

Ferrini, K., F. Ghelfi, R. Mannucci, and L. Titta. 2015. Lifestyle, nutrition and breast cancer: facts and presumptions for consideration. *Ecancermedicalscience*. 9:557.

Finn, R.S. 2008. Targeting Src in breast cancer. *Ann Oncol*. 19:1379-1386.

Foote, F.W., and F.W. Stewart. 1941. Lobular carcinoma in situ: A rare form of mammary cancer. *The American journal of pathology*. 17:491-496 493.

Forster, C., S. Makela, A. Warri, S. Kietz, D. Becker, K. Hultenby, M. Warner, and J.A. Gustafsson. 2002. Involvement of estrogen receptor beta in terminal differentiation of mammary gland epithelium. *Proceedings of the National Academy of Sciences of the United States of America*. 99:15578-15583.

Fulford, L.G., J.S. Reis-Filho, and S.R. Lakhani. 2004. Lobular in situ neoplasia. *Current Diagnostic Pathology*. 10:183-192.

Furuishi, K., H. Matsuoka, M. Takama, I. Takahashi, S. Misumi, and S. Shoji. 1997. Blockage of N-myristoylation of HIV-1 gag induces the production of impotent progeny virus. *Biochemical and biophysical research communications*. 237:504-511.

Gassmann, M., B. Grenacher, B. Rohde, and J. Vogel. 2009. Quantifying Western blots: pitfalls of densitometry. *Electrophoresis*. 30:1845-1855.

Gendler, S.J. 2001. MUC1, the renaissance molecule. *Journal of mammary gland biology and neoplasia*. 6:339-353.

Getlik, M., C. Grutter, J.R. Simard, S. Kluter, M. Rabiller, H.B. Rode, A. Robubi, and D. Rauh. 2009. Hybrid compound design to overcome the gatekeeper T338M mutation in cSrc. *J Med Chem*. 52:3915-3926.

Gholami, S., C.H. Chen, E. Lou, L.J. Belin, S. Fujisawa, V.A. Longo, N.G. Chen, M. Gonen, P.B. Zanzonico, A.A. Szalay, and Y. Fong. 2014. Vaccinia virus GLV-1h153 in combination with 131I shows increased efficiency in treating triple-negative breast cancer. *FASEB journal : official publication of the Federation of American Societies for Experimental Biology*. 28:676-682.

Giang, D.K., and B.F. Cravatt. 1998. A second mammalian N-myristoyltransferase. *The Journal of biological chemistry*. 273:6595-6598.

Giardina, C., G. Serio, G. Lepore, T. Lettini, A.M. Dalena, A. Pennella, G. D'Eredita, T. Valente, and R. Ricco. 2003. Pure ductal carcinoma in situ and in situ component of ductal invasive carcinoma of the breast. A preliminary morphometric study. *J Exp Clin Cancer Res*. 22:279-288.

Glover, C.J., K.D. Hartman, and R.L. Felsted. 1997. Human N-myristoyltransferase amino-terminal domain involved in targeting the enzyme to the ribosomal subcellular fraction. *The Journal of biological chemistry*. 272:28680-28689.

Gonzalez, L., M.T. Agullo-Ortuno, J.M. Garcia-Martinez, A. Calcabrini, C. Gamallo, J. Palacios, A. Aranda, and J. Martin-Perez. 2006. Role of c-Src in human MCF7 breast cancer cell tumorigenesis. *The Journal of biological chemistry*. 281:20851-20864.

Graus-Porta, D., R.R. Beerli, J.M. Daly, and N.E. Hynes. 1997. ErbB-2, the preferred heterodimerization partner of all ErbB receptors, is a mediator of lateral signaling. *EMBO J*. 16:1647-1655.

Guarnieri, F.G., L.M. Arterburn, M.B. Penno, Y. Cha, and J.T. August. 1993. The motif Tyr-X-X-hydrophobic residue mediates lysosomal membrane targeting of lysosome-associated membrane protein 1. *The Journal of biological chemistry*. 268:1941-1946.

Gucalp, A., J.A. Sparano, J. Caravelli, J. Santamauro, S. Patil, A. Abbruzzi, C. Pellegrino, J. Bromberg, C. Dang, M. Theodoulou, J. Massague, L. Norton, C. Hudis, and T.A. Traina. 2011. Phase II trial of saracatinib (AZD0530), an oral SRC-inhibitor for the treatment of patients with hormone receptor-negative metastatic breast cancer. *Clinical breast cancer*. 11:306-311.

Guinebretiere, J.M., E. Menet, A. Tardivon, P. Cherel, and D. Vanel. 2005. Normal and pathological breast, the histological basis. *Eur J Radiol*. 54:6-14.

Gunaratne, R.S., M. Sajid, I.T. Ling, R. Tripathi, J.A. Pachebat, and A.A. Holder. 2000. Characterization of N-myristoyltransferase from Plasmodium falciparum. *Biochem J*. 348 Pt 2:459-463.

Guy, C.T., S.K. Muthuswamy, R.D. Cardiff, P. Soriano, and W.J. Muller. 1994. Activation of the c-Src tyrosine kinase is required for the induction of mammary tumors in transgenic mice. *Genes & development*. 8:23-32.

Han, W.D., Y.L. Si, Y.L. Zhao, Q. Li, Z.Q. Wu, H.J. Hao, and H.J. Song. 2008. GC-rich promoter elements maximally confers estrogen-induced transactivation of LRP16 gene through ERalpha/Sp1 interaction in MCF-7 cells. *J Steroid Biochem Mol Biol*. 109:47-56.

Hanke, J.H., J.P. Gardner, R.L. Dow, P.S. Changelian, W.H. Brissette, E.J. Weringer, B.A. Pollok, and P.A. Connelly. 1996. Discovery of a novel, potent, and Src family-selective tyrosine kinase inhibitor. Study of Lck- and FynT-dependent T cell activation. *The Journal of biological chemistry*. 271:695-701.

Harvie, M., L. Hooper, and A.H. Howell. 2003. Central obesity and breast cancer risk: a systematic review. *Obes Rev*. 4:157-173.

Heaney, A.P., V. Nelson, M. Fernando, and G. Horwitz. 2001. Transforming events in thyroid tumorigenesis and their association with follicular lesions. *The Journal of clinical endocrinology and metabolism*. 86:5025-5032.

Heaney, A.P., R. Singson, C.J. McCabe, V. Nelson, M. Nakashima, and S. Melmed. 2000. Expression of pituitary-tumour transforming gene in colorectal tumours. *Lancet*. 355:716-719.

Hertz, S., and A. Roberts. 1942. Radioactive Iodine as an Indicator in Thyroid Physiology. V. The Use of Radioactive Iodine in the Differential Diagnosis of Two Types of Graves' Disease. *J Clin Invest*. 21:31-32.

Herynk, M.H., A.R. Beyer, Y. Cui, H. Weiss, E. Anderson, T.P. Green, and S.A. Fuqua. 2006. Cooperative action of tamoxifen and c-Src inhibition in preventing the growth of estrogen receptor-positive human breast cancer cells. *Mol Cancer Ther*. 5:3023-3031.

Hiscox, S., P. Barnfather, E. Hayes, P. Bramble, J. Christensen, R.I. Nicholson, and P. Barrett-Lee. 2011. Inhibition of focal adhesion kinase suppresses the adverse phenotype of endocrine-resistant breast cancer cells and improves endocrine response in endocrine-sensitive cells. *Breast Cancer Res Treat*. 125:659-669.

Holick, C.N., P.A. Newcomb, A. Trentham-Dietz, L. Titus-Ernstoff, A.J. Bersch, M.J. Stampfer, J.A. Baron, K.M. Egan, and W.C. Willett. 2008. Physical activity and survival after diagnosis of invasive breast cancer. *Cancer Epidemiol Biomarkers Prev*. 17:379-386.

Holmes, M.D., W.Y. Chen, D. Feskanich, C.H. Kroenke, and G.A. Colditz. 2005. Physical activity and survival after breast cancer diagnosis. *JAMA*. 293:2479-2486.

Honour, A.J., N.B. Myant, and E.N. Rowlands. 1952. Secretion of radioiodine in digestive juices and milk in man. *Clinical science*. 11:449-462.

Hortobagyi, G.N., J. de la Garza Salazar, K. Pritchard, D. Amadori, R. Haidinger, C.A. Hudis, H. Khaled, M.C. Liu, M. Martin, M. Namer, J.A. O'Shaughnessy, Z.Z. Shen, K.S. Albain, and A. Investigators. 2005. The global breast cancer burden: variations in epidemiology and survival. *Clinical breast cancer*. 6:391-401.

Howell, A., C.K. Osborne, C. Morris, and A.E. Wakeling. 2000. ICI 182,780 (Faslodex): development of a novel, "pure" antiestrogen. *Cancer*. 89:817-825.

Hsueh, C., J.D. Lin, Y.S. Chang, S. Hsueh, T.C. Chao, J.S. Yu, S.M. Jung, N.M. Tseng, J.H. Sun, S.Y. Kuo, and S.H. Ueng. 2013. Prognostic significance of pituitary tumour-transforming gene-binding factor (PBF) expression in papillary thyroid carcinoma. *Clin Endocrinol (Oxf)*. 78:303-309.

Hubbard, S.R. 1997. Crystal structure of the activated insulin receptor tyrosine kinase in complex with peptide substrate and ATP analog. *EMBO J*. 16:5572-5581.

Hubbard, S.R., L. Wei, L. Ellis, and W.A. Hendrickson. 1994. Crystal structure of the tyrosine kinase domain of the human insulin receptor. *Nature*. 372:746-754.

Ito, Y., T. Kobayashi, T. Kimura, N. Matsuura, E. Wakasugi, T. Takeda, T. Shimano, Y. Kubota, T. Nobunaga, Y. Makino, C. Azuma, F. Saji, and M. Monden. 1996. Investigation of the oxytocin receptor expression in human breast cancer tissue using newly established monoclonal antibodies. *Endocrinology*. 137:773-779.

Jakacka, M., M. Ito, J. Weiss, P.Y. Chien, B.D. Gehm, and J.L. Jameson. 2001. Estrogen receptor binding to DNA is not required for its activity through the nonclassical AP1 pathway. *The Journal of biological chemistry*. 276:13615-13621.

Jemal, A., R. Siegel, J. Xu, and E. Ward. 2010. Cancer statistics, 2010. *CA: a cancer journal for clinicians*. 60:277-300.

Ji, L., and J.A. Roth. 2008. Tumor suppressor FUS1 signaling pathway. *J Thorac Oncol*. 3:327-330.

Johnson, D.R., R.S. Bhatnagar, L.J. Knoll, and J.I. Gordon. 1994. Genetic and biochemical studies of protein N-myristoylation. *Annu Rev Biochem*. 63:869-914.

Jordan, V.C. 1993. Fourteenth Gaddum Memorial Lecture. A current view of tamoxifen for the treatment and prevention of breast cancer. *Br J Pharmacol*. 110:507-517.

Kamps, M.P., J.E. Buss, and B.M. Sefton. 1985. Mutation of NH2-terminal glycine of p60src prevents both myristoylation and morphological transformation. *Proceedings of the National Academy of Sciences of the United States of America*. 82:4625-4628.

Kang, J.X., Y. Li, and A. Leaf. 1997. Mannose-6-phosphate/insulin-like growth factor-II receptor is a receptor for retinoic acid. *Proceedings of the National Academy of Sciences of the United States of America*. 94:13671-13676.

Kastner, P., A. Krust, B. Turcotte, U. Stropp, L. Tora, H. Gronemeyer, and P. Chambon. 1990. Two distinct estrogen-regulated promoters generate transcripts encoding the two functionally different human progesterone receptor forms A and B. *EMBO J*. 9:1603-1614.

Kelley, L.A., S. Mezulis, C.M. Yates, M.N. Wass, and M.J. Sternberg. 2015. The Phyre2 web portal for protein modeling, prediction and analysis. *Nat Protoc*. 10:845-858.

Kelsey, J.L., M.D. Gammon, and E.M. John. 1993. Reproductive factors and breast cancer. *Epidemiol Rev*. 15:36-47.

Kenemans, P., and A. Bosman. 2003. Breast cancer and post-menopausal hormone therapy. *Best Pract Res Clin Endocrinol Metab*. 17:123-137.

Key, T., P. Appleby, I. Barnes, G. Reeves, H. Endogenous, and G. Breast Cancer Collaborative. 2002. Endogenous sex hormones and breast cancer in postmenopausal women: reanalysis of nine prospective studies. *J Natl Cancer Inst*. 94:606-616.

Key, T.J., N.E. Allen, E.A. Spencer, and R.C. Travis. 2003. Nutrition and breast cancer. *Breast*. 12:412-416.

Kilbane, M.T., R.A. Ajjan, A.P. Weetman, R. Dwyer, E.W. McDermott, N.J. O'Higgins, and P.P. Smyth. 2000. Tissue iodine content and serum-mediated 125I uptake-blocking activity in breast cancer. *The Journal of clinical endocrinology and metabolism*. 85:1245-1250.

Kirkbride, K.C., B.H. Sung, S. Sinha, and A.M. Weaver. 2011. Cortactin: a multifunctional regulator of cellular invasiveness. *Cell Adh Migr*. 5:187-198.

Knostman, K.A., J.Y. Cho, K.Y. Ryu, X. Lin, J.A. McCubrey, T. Hla, C.H. Liu, E. Di Carlo, R. Keri, M. Zhang, D.Y. Hwang, W.C. Kisseberth, C.C. Capen, and S.M. Jhiang. 2004. Signaling through 3',5'-cyclic adenosine monophosphate and phosphoinositide-3 kinase induces sodium/iodide symporter expression in breast cancer. *The Journal of clinical endocrinology and metabolism*. 89:5196-5203.

Knostman, K.A., J.A. McCubrey, C.D. Morrison, Z. Zhang, C.C. Capen, and S.M. Jhiang. 2007. PI3K activation is associated with intracellular sodium/iodide symporter protein expression in breast cancer. *BMC cancer*. 7:137.

Kogai, T., and G.A. Brent. 2012. The sodium iodide symporter (NIS): regulation and approaches to targeting for cancer therapeutics. *Pharmacology & therapeutics*. 135:355-370.

Kogai, T., T. Endo, T. Saito, A. Miyazaki, A. Kawaguchi, and T. Onaya. 1997. Regulation by thyroid-stimulating hormone of sodium/iodide symporter gene expression and protein levels in FRTL-5 cells. *Endocrinology*. 138:2227-2232.

Kogai, T., Y. Kanamoto, L.H. Che, K. Taki, F. Moatamed, J.J. Schultz, and G.A. Brent. 2004. Systemic retinoic acid treatment induces sodium/iodide symporter expression and radioiodide uptake in mouse breast cancer models. *Cancer research*. 64:415-422.

Kogai, T., Y. Kanamoto, A.I. Li, L.H. Che, E. Ohashi, K. Taki, R.A. Chandraratna, T. Saito, and G.A. Brent. 2005. Differential regulation of sodium/iodide symporter gene expression by nuclear receptor ligands in MCF-7 breast cancer cells. *Endocrinology*. 146:3059-3069.

Kogai, T., Y.Y. Liu, K. Mody, D.V. Shamsian, and G.A. Brent. 2012. Regulation of sodium iodide symporter gene expression by Rac1/p38beta mitogen-activated protein kinase signaling pathway in MCF-7 breast cancer cells. *J Biol Chem*. 287:3292-3300.

Kogai, T., E. Ohashi, M.S. Jacobs, S. Sajid-Crockett, M.L. Fisher, Y. Kanamoto, and G.A. Brent. 2008. Retinoic acid stimulation of the sodium/iodide symporter in MCF-7 breast cancer cells is mediated by the insulin growth factor-I/phosphatidylinositol 3-kinase and p38 mitogen-activated protein kinase signaling pathways. *The Journal of clinical endocrinology and metabolism*. 93:1884-1892.

Kogai, T., J.J. Schultz, L.S. Johnson, M. Huang, and G.A. Brent. 2000. Retinoic acid induces sodium/iodide symporter gene expression and radioiodide uptake in the MCF-7 breast cancer cell line. *Proceedings of the National Academy of Sciences of the United States of America*. 97:8519-8524.

Kogai, T., K. Taki, and G.A. Brent. 2006. Enhancement of sodium/iodide symporter expression in thyroid and breast cancer. *Endocr Relat Cancer*. 13:797-826.

Kuiper, G.G., E. Enmark, M. Pelto-Huikko, S. Nilsson, and J.A. Gustafsson. 1996. Cloning of a novel receptor expressed in rat prostate and ovary. *Proceedings of the National Academy of Sciences of the United States of America*. 93:5925-5930.

La Cour, T., L. Kiemer, A. Molgaard, R. Gupta, K. Skriver, and S. Brunak. 2004. Analysis and prediction of leucine-rich nuclear export signals. *Protein Engineering, Design and Selection*. 17:527-536.

Lacoste, C., J. Herve, M. Bou Nader, A. Dos Santos, N. Moniaux, Y. Valogne, R. Montjean, O. Dorseuil, D. Samuel, D. Cassio, C. Portulano, N. Carrasco, C. Brechot, and J. Faivre. 2012. Iodide transporter NIS regulates cancer cell motility and invasiveness by interacting with the Rho guanine nucleotide exchange factor LARG. *Cancer research*. 72:5505-5515.

Lahmann, P.H., K. Hoffmann, N. Allen, C.H. van Gils, K.T. Khaw, B. Tehard, F. Berrino, A. Tjonneland, J. Bigaard, A. Olsen, K. Overvad, F. Clavel-Chapelon, G. Nagel, H. Boeing, D. Trichopoulos, G. Economou, G. Bellos, D. Palli, R. Tumino, S. Panico, C. Sacerdote, V. Krogh, P.H. Peeters, H.B. Bueno-de-Mesquita, E. Lund, E. Ardanaz, P. Amiano, G. Pera, J.R. Quiros, C. Martinez, M.J. Tormo, E. Wirfalt, G. Berglund, G. Hallmans, T.J. Key, G. Reeves, S. Bingham, T. Norat, C. Biessy, R. Kaaks, and E. Riboli. 2004. Body size and breast cancer risk: findings from the European Prospective Investigation into Cancer And Nutrition (EPIC). *International journal of cancer. Journal international du cancer*. 111:762-771.

Lange, C.A., and D. Yee. 2008. Progesterone and breast cancer. *Womens Health (Lond Engl)*. 4:151-162.

Leung, A.M., and L.E. Braverman. 2014. Consequences of excess iodine. *Nat Rev Endocrinol*. 10:136-142.

Levenson, A.S., and V.C. Jordan. 1997. MCF-7: the first hormone-responsive breast cancer cell line. *Cancer research*. 57:3071-3078.

Levy, O., A. De la Vieja, C.S. Ginter, C. Riedel, G. Dai, and N. Carrasco. 1998. N-linked glycosylation of the thyroid Na+/I- symporter (NIS). Implications for its secondary structure model. *The Journal of biological chemistry*. 273:22657-22663.

Li, J., U. Rix, B. Fang, Y. Bai, A. Edwards, J. Colinge, K.L. Bennett, J. Gao, L. Song, S. Eschrich, G. Superti-Furga, J. Koomen, and E.B. Haura. 2010. A chemical and phosphoproteomic characterization of dasatinib action in lung cancer. *Nat Chem Biol*. 6:291-299.

Li, X., and B.W. O'Malley. 2003. Unfolding the action of progesterone receptors. *The Journal of biological chemistry*. 278:39261-39264.

Lim, S.J., J.C. Paeng, S.J. Kim, S.Y. Kim, H. Lee, and D.H. Moon. 2007. Enhanced expression of adenovirus-mediated sodium iodide symporter gene in MCF-7 breast cancer cells with retinoic acid treatment. *Journal of nuclear medicine : official publication, Society of Nuclear Medicine*. 48:398-404.

Lin, X., K.Y. Ryu, and S.M. Jhiang. 2004. Cloning of the 5'-flanking region of mouse sodium/iodide symporter and identification of a thyroid-specific and TSH-responsive enhancer. *Thyroid : official journal of the American Thyroid Association*. 14:19-27.

Lin, Z., S. Reierstad, C.C. Huang, and S.E. Bulun. 2007. Novel estrogen receptor-alpha binding sites and estradiol target genes identified by chromatin immunoprecipitation cloning in breast cancer. *Cancer research*. 67:5017-5024.

Liu, Y., A. Bishop, L. Witucki, B. Kraybill, E. Shimizu, J. Tsien, J. Ubersax, J. Blethrow, D.O. Morgan, and K.M. Shokat. 1999. Structural basis for selective inhibition of Src family kinases by PP1. *Chem Biol*. 6:671-678.

Liu, Y., M.O. Lee, H.G. Wang, Y. Li, Y. Hashimoto, M. Klaus, J.C. Reed, and X. Zhang. 1996. Retinoic acid receptor beta mediates the growth-inhibitory effect of retinoic acid by promoting apoptosis in human breast cancer cells. *Molecular and cellular biology*. 16:1138-1149.

Lu, Y., P. Selvakumar, K. Ali, A. Shrivastav, G. Bajaj, L. Resch, R. Griebel, D. Fourney, K. Meguro, and R.K. Sharma. 2005. Expression of N-myristoyltransferase in human brain tumors. *Neurochem Res*. 30:9-13.

Luttrell, D.K., A. Lee, T.J. Lansing, R.M. Crosby, K.D. Jung, D. Willard, M. Luther, M. Rodriguez, J. Berman, and T.M. Gilmer. 1994. Involvement of pp60c-src with two major signaling pathways in human breast cancer. *Proceedings of the National Academy of Sciences of the United States of America*. 91:83-87.

Lydon, J.P., F.J. DeMayo, C.R. Funk, S.K. Mani, A.R. Hughes, C.A. Montgomery, Jr., G. Shyamala, O.M. Conneely, and B.W. O'Malley. 1995. Mice lacking progesterone receptor exhibit pleiotropic reproductive abnormalities. *Genes & development*. 9:2266-2278.

Madrid, R., S. Le Maout, M.B. Barrault, K. Janvier, S. Benichou, and J. Merot. 2001. Polarized trafficking and surface expression of the AQP4 water channel are coordinated by serial and regulated interactions with different clathrin-adaptor complexes. *EMBO J*. 20:7008-7021.

Magnuson, B.A., R.V. Raju, T.N. Moyana, and R.K. Sharma. 1995. Increased N-myristoyltransferase activity observed in rat and human colonic tumors. *J Natl Cancer Inst*. 87:1630-1635.

Mandell, R.B., L.Z. Mandell, and C.J. Link, Jr. 1999. Radioisotope concentrator gene therapy using the sodium/iodide symporter gene. *Cancer research*. 59:661-668.

Mardones, G.A., P.V. Burgos, Y. Lin, D.P. Kloer, J.G. Magadan, J.H. Hurley, and J.S. Bonifacino. 2013. Structural basis for the recognition of tyrosine-based sorting signals by the mu3A subunit of the AP-3 adaptor complex. *The Journal of biological chemistry*. 288:9563-9571.

Marsee, D.K., A. Venkateswaran, H. Tao, D. Vadysirisack, Z. Zhang, D.D. Vandre, and S.M. Jhiang. 2004. Inhibition of heat shock protein 90, a novel RET/PTC1-associated protein, increases radioiodide accumulation in thyroid cells. *The Journal of biological chemistry*. 279:43990-43997.

Martin, G.S. 2001. The hunting of the Src. *Nat Rev Mol Cell Biol*. 2:467-475.

Martinez, A., J.A. Traverso, B. Valot, M. Ferro, C. Espagne, G. Ephritikhine, M. Zivy, C. Giglione, and T. Meinnel. 2008. Extent of N-terminal modifications in cytosolic proteins from eukaryotes. *Proteomics*. 8:2809-2831.

Maurer-Stroh, S., B. Eisenhaber, and F. Eisenhaber. 2002. N-terminal N-myristoylation of proteins: prediction of substrate proteins from amino acid sequence. *J Mol Biol*. 317:541-557.

Mayer, E.L., J.F. Baurain, J. Sparano, L. Strauss, M. Campone, P. Fumoleau, H. Rugo, A. Awada, O. Sy, and A. Llombart-Cussac. 2011. A phase 2 trial of dasatinib in patients with advanced HER2-positive and/or hormone receptor-positive breast cancer. *Clinical cancer research : an official journal of the American Association for Cancer Research*. 17:6897-6904.

McCabe, C.J., J.S. Khaira, K. Boelaert, A.P. Heaney, L.A. Tannahill, S. Hussain, R. Mitchell, J. Olliff, M.C. Sheppard, J.A. Franklyn, and N.J. Gittoes. 2003. Expression of pituitary tumour transforming gene (PTTG) and fibroblast growth factor-2 (FGF-2) in human pituitary adenomas: relationships to clinical tumour behaviour. *Clin Endocrinol (Oxf)*. 58:141-150.

McPherson, K., C.M. Steel, and J.M. Dixon. 2000. ABC of breast diseases. Breast cancer-epidemiology, risk factors, and genetics. *BMJ*. 321:624-628.

Mitri, Z., R. Nanda, K. Blackwell, C.M. Costelloe, I. Hood, C. Wei, A.M. Brewster, N.K. Ibrahim, K.B. Koenig, G.N. Hortobagyi, C. Van Poznak, M.F. Rimawi, and S. Moulder-Thompson. 2016. TBCRC-010: Phase I/II Study of Dasatinib in Combination with Zoledronic Acid for the Treatment of Breast Cancer

Bone Metastasis. *Clinical cancer research : an official journal of the American Association for Cancer Research*.

Moasser, M.M. 2007. The oncogene HER2: its signaling and transforming functions and its role in human cancer pathogenesis. *Oncogene*. 26:6469-6487.

Mohammed, H., I.A. Russell, R. Stark, O.M. Rueda, T.E. Hickey, G.A. Tarulli, A.A. Serandour, S.N. Birrell, A. Bruna, A. Saadi, S. Menon, J. Hadfield, M. Pugh, G.V. Raj, G.D. Brown, C. D'Santos, J.L. Robinson, G. Silva, R. Launchbury, C.M. Perou, J. Stingl, C. Caldas, W.D. Tilley, and J.S. Carroll. 2015. Progesterone receptor modulates ERalpha action in breast cancer. *Nature*. 523:313-317.

Molina, M.A., R. Saez, E.E. Ramsey, M.J. Garcia-Barchino, F. Rojo, A.J. Evans, J. Albanell, E.J. Keenan, A. Lluch, J. Garcia-Conde, J. Baselga, and G.M. Clinton. 2002. NH(2)-terminal truncated HER-2 protein but not full-length receptor is associated with nodal metastasis in human breast cancer. *Clinical cancer research : an official journal of the American Association for Cancer Research*. 8:347-353.

Moon, D.H., S.J. Lee, K.Y. Park, K.K. Park, S.H. Ahn, M.S. Pai, H. Chang, H.K. Lee, and I.M. Ahn. 2001. Correlation between 99mTc-pertechnetate uptakes and expressions of human sodium iodide symporter gene in breast tumor tissues. *Nucl Med Biol*. 28:829-834.

Moulder, S., and G.N. Hortobagyi. 2008. Advances in the treatment of breast cancer. *Clin Pharmacol Ther*. 83:26-36.

Mukhopadhyay, D., L. Tsiokas, X.M. Zhou, D. Foster, J.S. Brugge, and V.P. Sukhatme. 1995. Hypoxic induction of human vascular endothelial growth factor expression through c-Src activation. *Nature*. 375:577-581.

Murray, D., L. Hermida-Matsumoto, C.A. Buser, J. Tsang, C.T. Sigal, N. Ben-Tal, B. Honig, M.D. Resh, and S. McLaughlin. 1998. Electrostatics and the membrane association of Src: theory and experiment. *Biochemistry*. 37:2145-2159.

Nada, S., M. Okada, A. MacAuley, J.A. Cooper, and H. Nakagawa. 1991. Cloning of a complementary DNA for a protein-tyrosine kinase that specifically phosphorylates a negative regulatory site of p60c-src. *Nature*. 351:69-72.

Nishi, H., K. Hashimoto, and A.R. Panchenko. 2011. Phosphorylation in protein-protein binding: effect on stability and function. *Structure*. 19:1807-1815.

Ogbagabriel, S., M. Fernando, F.M. Waldman, S. Bose, and A.P. Heaney. 2005. Securin is overexpressed in breast cancer. *Mod Pathol*. 18:985-990.

Oh, H.J., J.K. Chung, J.H. Kang, W.J. Kang, D.Y. Noh, I.A. Park, J.M. Jeong, D.S. Lee, and M.C. Lee. 2005. The relationship between expression of the sodium/iodide symporter gene and the status of hormonal receptors in human breast cancer tissue. *Cancer research and treatment : official journal of Korean Cancer Association*. 37:247-250.

Ohashi, E., T. Kogai, H. Kagechika, and G.A. Brent. 2009. Activation of the PI3 kinase pathway by retinoic acid mediates sodium/iodide symporter induction and iodide transport in MCF-7 breast cancer cells. *Cancer research*. 69:3443-3450.

Ohno, M., M. Zannini, O. Levy, N. Carrasco, and R. di Lauro. 1999. The paired-domain transcription factor Pax8 binds to the upstream enhancer of the rat sodium/iodide symporter gene and participates in both thyroid-specific and cyclic-AMP-dependent transcription. *Molecular and cellular biology*. 19:2051-2060.

Olins, G.M., and R.D. Bremel. 1984. Oxytocin-stimulated myosin phosphorylation in mammary myoepithelial cells: roles of calcium ions and cyclic nucleotides. *Endocrinology*. 114:1617-1626.

Palmieri, C., G.J. Cheng, S. Saji, M. Zelada-Hedman, A. Warri, Z. Weihua, S. Van Noorden, T. Wahlstrom, R.C. Coombes, M. Warner, and J.A. Gustafsson. 2002. Estrogen receptor beta in breast cancer. *Endocr Relat Cancer*. 9:1-13.

Panethymitaki, C., P.W. Bowyer, H.P. Price, R.J. Leatherbarrow, K.A. Brown, and D.F. Smith. 2006. Characterization and selective inhibition of myristoyl-CoA:protein N-myristoyltransferase from Trypanosoma brucei and Leishmania major. *Biochem J*. 396:277-285.

Parkin, D.M. 2011. 10. Cancers attributable to exposure to hormones in the UK in 2010. *British journal of cancer*. 105 Suppl 2:S42-48.

Pasqualini, J.R. 2007. Progestins and breast cancer. *Gynecol Endocrinol*. 23 Suppl 1:32-41.

Paterson, R., and M.H. Russel. 1959. Clinical trials in malignant disease. Part II-breast cancer: value of irradiation of the ovaries. *J Fac Radiol*. 10:130-133.

Patwardhan, P., and M.D. Resh. 2010. Myristoylation and membrane binding regulate c-Src stability and kinase activity. *Molecular and cellular biology*. 30:4094-4107.

Pei, L., and S. Melmed. 1997. Isolation and characterization of a pituitary tumor-transforming gene (PTTG). *Molecular endocrinology*. 11:433-441.

Peseckis, S.M., I. Deichaite, and M.D. Resh. 1993. Iodinated fatty acids as probes for myristate processing and function. Incorporation into pp60v-src. *The Journal of biological chemistry*. 268:5107-5114.

Poleev, A., O. Okladnova, A.M. Musti, S. Schneider, B. Royer-Pokora, and D. Plachov. 1997. Determination of functional domains of the human transcription factor PAX8 responsible for its nuclear localization and transactivating potential. *European journal of biochemistry / FEBS*. 247:860-869.

Pommier, Y., E. Leo, H. Zhang, and C. Marchand. 2010. DNA topoisomerases and their poisoning by anticancer and antibacterial drugs. *Chem Biol*. 17:421-433.

Poole, V.L., and C.J. McCabe. 2015. Iodide transport and breast cancer. *The Journal of endocrinology*. 227:R1-R12.

Porter, W., B. Saville, D. Hoivik, and S. Safe. 1997. Functional synergy between the transcription factor Sp1 and the estrogen receptor. *Molecular endocrinology*. 11:1569-1580.

Prentice, R.L., B. Caan, R.T. Chlebowski, R. Patterson, L.H. Kuller, J.K. Ockene, K.L. Margolis, M.C. Limacher, J.E. Manson, L.M. Parker, E. Paskett, L. Phillips, J. Robbins, J.E. Rossouw, G.E. Sarto, J.M. Shikany, M.L. Stefanick, C.A. Thomson, L. Van Horn, M.Z. Vitolins, J. Wactawski-Wende, R.B. Wallace, S. Wassertheil-Smoller, E. Whitlock, K. Yano, L. Adams-Campbell, G.L. Anderson, A.R. Assaf, S.A. Beresford, H.R. Black, R.L. Brunner, R.G. Brzyski, L. Ford, M. Gass, J. Hays, D. Heber, G. Heiss, S.L. Hendrix, J. Hsia, F.A. Hubbell, R.D. Jackson, K.C. Johnson, J.M. Kotchen, A.Z. LaCroix, D.S. Lane, R.D. Langer, N.L. Lasser, and M.M. Henderson. 2006. Low-fat dietary pattern and risk of invasive breast cancer: the Women's Health Initiative Randomized Controlled Dietary Modification Trial. *JAMA*. 295:629-642.

Price, H.P., M.R. Menon, C. Panethymitaki, D. Goulding, P.G. McKean, and D.F. Smith. 2003. Myristoyl-CoA:protein N-myristoyltransferase, an essential enzyme and potential drug target in kinetoplastid parasites. *The Journal of biological chemistry*. 278:7206-7214.

Rad, A.M., A.S. Iskander, B. Janic, R.A. Knight, A.S. Arbab, and H. Soltanian-Zadeh. 2009. AC133+ progenitor cells as gene delivery vehicle and cellular probe in subcutaneous tumor models: a preliminary study. *BMC biotechnology*. 9:28.

Rajala, R.V., J.M. Radhi, R. Kakkar, R.S. Datla, and R.K. Sharma. 2000. Increased expression of N-myristoyltransferase in gallbladder carcinomas. *Cancer*. 88:1992-1999.

Raju, R.V., T.N. Moyana, and R.K. Sharma. 1997. N-Myristoyltransferase overexpression in human colorectal adenocarcinomas. *Exp Cell Res*. 235:145-154.

Rao, R.S., and W. Bernd. 2010. Do N-glycoproteins have preference for specific sequons? *Bioinformation*. 5:208-212.

Read, M.L., J.C. Fong, H. Fan, G. Lewy, W. Imruetaicharoenchoke, V.L. Poole, B. Modasia, G. Ryan, N. Sharma, A. Bacon, V.E. Smith, J.C. Watkinson, K. Boelaert, A.S. Turnell, and C.J. McCabe. 2016. Novel interactions between PTTG and PBF impair the DNA damage response and contribute to genetic instability. *Under Submission*.

Read, M.L., G.D. Lewy, J.C. Fong, N. Sharma, R.I. Seed, V.E. Smith, E. Gentilin, A. Warfield, M.C. Eggo, J.A. Knauf, W.E. Leadbeater, J.C. Watkinson, J.A. Franklyn, K. Boelaert, and C.J. McCabe. 2011. Proto-oncogene PBF/PTTG1IP regulates thyroid cell growth and represses radioiodide treatment. *Cancer research*. 71:6153-6164.

Read, M.L., R.I. Seed, J.C. Fong, B. Modasia, G.A. Ryan, R.J. Watkins, T. Gagliano, V.E. Smith, A.L. Stratford, P.K. Kwan, N. Sharma, O.M. Dixon, J.C. Watkinson, K. Boelaert, J.A. Franklyn, A.S. Turnell, and C.J. McCabe. 2014a. The PTTG1-binding factor (PBF/PTTG1IP) regulates p53 activity in thyroid cells. *Endocrinology*. 155:1222-1234.

Read, M.L., R.I. Seed, B. Modasia, P.P. Kwan, N. Sharma, V.E. Smith, R.J. Watkins, S. Bansal, T. Gagliano, A.L. Stratford, T. Ismail, M.J. Wakelam, D.S. Kim, S.T. Ward, K. Boelaert, J.A. Franklyn, A.S. Turnell, and C.J. McCabe. 2014b. The proto-oncogene PBF binds p53 and is associated with prognostic features in colorectal cancer. *Molecular carcinogenesis*.

Reeves, G.K., K. Pirie, V. Beral, J. Green, E. Spencer, D. Bull, and C. Million Women Study. 2007. Cancer incidence and mortality in relation to body mass index in the Million Women Study: cohort study. *BMJ*. 335:1134.

Renehan, A.G., M. Tyson, M. Egger, R.F. Heller, and M. Zwahlen. 2008. Body-mass index and incidence of cancer: a systematic review and meta-analysis of prospective observational studies. *Lancet*. 371:569-578.

Renier, C., H. Vogel, O. Offor, C. Yao, and I. Wapnir. 2010. Breast cancer brain metastases express the sodium iodide symporter. *Journal of neuro-oncology*. 96:331-336.

Resh, M.D. 1994. Myristylation and palmitylation of Src family members: the fats of the matter. *Cell*. 76:411-413.

Resh, M.D. 1999. Fatty acylation of proteins: new insights into membrane targeting of myristoylated and palmitoylated proteins. *Biochim Biophys Acta*. 1451:1-16.

Riedel, C., O. Levy, and N. Carrasco. 2001. Post-transcriptional regulation of the sodium/iodide symporter by thyrotropin. *The Journal of biological chemistry*. 276:21458-21463.

Riesco-Eizaguirre, G., A. De la Vieja, I. Rodriguez, S. Miranda, P. Martin-Duque, G. Vassaux, and P. Santisteban. 2011. Telomerase-driven expression of the sodium iodide symporter (NIS) for in vivo radioiodide treatment of cancer: a new broad-spectrum NIS-mediated antitumor approach. *The Journal of clinical endocrinology and metabolism*. 96:E1435-1443.

Ritte, R., A. Lukanova, F. Berrino, L. Dossus, A. Tjonneland, A. Olsen, T.F. Overvad, K. Overvad, F. Clavel-Chapelon, A. Fournier, G. Fagherazzi, S. Rohrmann, B. Teucher, H. Boeing, K. Aleksandrova, A. Trichopoulou, P. Lagiou, D. Trichopoulos, D. Palli, S. Sieri, S. Panico, R. Tumino, P. Vineis, J.R. Quiros, G. Buckland, M.J. Sanchez, P. Amiano, M.D. Chirlaque, E. Ardanaz, M. Sund, P. Lenner, B. Bueno-de-Mesquita, C.H. van Gils, P.H. Peeters, S. Krum-Hansen, I.T. Gram, E. Lund, K.T. Khaw, N. Wareham, N.E. Allen, T.J. Key, I. Romieu, S. Rinaldi, A. Siddiq, D. Cox, E. Riboli, and R. Kaaks. 2012. Adiposity, hormone replacement therapy use and breast cancer risk by age and hormone receptor status: a large prospective cohort study. *Breast Cancer Res*. 14:R76.

Romero, F., M.C. Multon, F. Ramos-Morales, A. Dominguez, J.A. Bernal, J.A. Pintor-Toro, and M. Tortolero. 2001. Human securin, hPTTG, is associated with Ku heterodimer, the regulatory subunit of the DNA-dependent protein kinase. *Nucleic acids research*. 29:1300-1307.

Romond, E.H., E.A. Perez, J. Bryant, V.J. Suman, C.E. Geyer, Jr., N.E. Davidson, E. Tan-Chiu, S. Martino, S. Paik, P.A. Kaufman, S.M. Swain, T.M. Pisansky, L. Fehrenbacher, L.A. Kutteh, V.G. Vogel, D.W. Visscher, G. Yothers, R.B. Jenkins, A.M. Brown, S.R. Dakhil, E.P. Mamounas, W.L. Lingle, P.M. Klein, J.N. Ingle, and N. Wolmark. 2005. Trastuzumab plus adjuvant chemotherapy for operable HER2-positive breast cancer. *The New England journal of medicine*. 353:1673-1684.

Rosen, N., J.B. Bolen, A.M. Schwartz, P. Cohen, V. DeSeau, and M.A. Israel. 1986. Analysis of pp60c-src protein kinase activity in human tumor cell lines and tissues. *The Journal of biological chemistry*. 261:13754-13759.

Roskoski, R., Jr. 2015. Src protein-tyrosine kinase structure, mechanism, and small molecule inhibitors. *Pharmacol Res*. 94:9-25.

Rossi, L., D. Stevens, J.Y. Pierga, F. Lerebours, F. Reyal, M. Robain, B. Asselain, and R. Rouzier. 2015. Impact of Adjuvant Chemotherapy on Breast Cancer Survival: A Real-World Population. *PloS one*. 10:e0132853.

Rubin, I., and Y. Yarden. 2001. The basic biology of HER2. *Ann Oncol*. 12 Suppl 1:S3-8.

Ruff, M., M. Gangloff, J.M. Wurtz, and D. Moras. 2000. Estrogen receptor transcription and transactivation: Structure-function relationship in DNA- and ligand-binding domains of estrogen receptors. *Breast Cancer Res*. 2:353-359.

Russo, J., R. Moral, G.A. Balogh, D. Mailo, and I.H. Russo. 2005. The protective role of pregnancy in breast cancer. *Breast Cancer Res*. 7:131-142.

Russo, J., and I.H. Russo. 1987. Biological and molecular bases of mammary carcinogenesis. *Lab Invest*. 57:112-137.

Ryu, K.Y., Q. Tong, and S.M. Jhiang. 1998. Promoter characterization of the human Na+/I- symporter. *The Journal of clinical endocrinology and metabolism*. 83:3247-3251.

Sapino, A., P. Cassoni, A. Stella, and G. Bussolati. 1998. Oxytocin receptor within the breast: biological function and distribution. *Anticancer research*. 18:2181-2186.

Scaltriti, M., F. Rojo, A. Ocana, J. Anido, M. Guzman, J. Cortes, S. Di Cosimo, X. Matias-Guiu, S. Ramon y Cajal, J. Arribas, and J. Baselga. 2007. Expression of p95HER2, a truncated form of the HER2 receptor, and response to anti-HER2 therapies in breast cancer. *J Natl Cancer Inst*. 99:628-638.

Schaller, M.D., J.D. Hildebrand, J.D. Shannon, J.W. Fox, R.R. Vines, and J.T. Parsons. 1994. Autophosphorylation of the focal adhesion kinase, pp125FAK, directs SH2-dependent binding of pp60src. *Molecular and cellular biology*. 14:1680-1688.

Schmitt, T.L., C.R. Espinoza, and U. Loos. 2002. Characterization of a thyroid-specific and cyclic adenosine monophosphate-responsive enhancer far upstream from the human sodium iodide symporter gene. *Thyroid : official journal of the American Thyroid Association*. 12:273-279.

Schmitz, K.J., F. Grabellus, R. Callies, F. Otterbach, J. Wohlschlaeger, B. Levkau, R. Kimmig, K.W. Schmid, and H.A. Baba. 2005. High expression of focal adhesion kinase (p125FAK) in node-negative breast cancer is related to overexpression of HER-2/neu and activated Akt kinase but does not predict outcome. *Breast Cancer Res*. 7:R194-203.

Schweppe, R.E., A.A. Kerege, J.D. French, V. Sharma, R.L. Grzywa, and B.R. Haugen. 2009. Inhibition of Src with AZD0530 reveals the Src-Focal Adhesion kinase complex as a novel therapeutic target in papillary and anaplastic thyroid cancer. *The Journal of clinical endocrinology and metabolism*. 94:2199-2203.

Scott, M.S., F.M. Boisvert, M.D. McDowall, A.I. Lamond, and G.J. Barton. 2010. Characterization and prediction of protein nucleolar localization sequences. *Nucleic acids research*. 38:7388-7399.

Seaton, K.E., and C.D. Smith. 2008. N-Myristoyltransferase isozymes exhibit differential specificity for human immunodeficiency virus type 1 Gag and Nef. *J Gen Virol*. 89:288-296.

Sefton, B.M., and J.E. Buss. 1987. The covalent modification of eukaryotic proteins with lipid. *J Cell Biol*. 104:1449-1453.

Seidlin, S.M., L.D. Marinelli, and E. Oshry. 1946. Radioactive iodine therapy; effect on functioning metastases of adenocarcinoma of the thyroid. *J Am Med Assoc*. 132:838-847.

Serrano-Nascimento, C., S. da Silva Teixeira, J.P. Nicola, R.T. Nachbar, A.M. Masini-Repiso, and M.T. Nunes. 2014. The acute inhibitory effect of iodide excess on sodium/iodide symporter expression and activity involves the PI3K/Akt signaling pathway. *Endocrinology*. 155:1145-1156.

Shalloway, D., P.M. Coussens, and P. Yaciuk. 1984. Overexpression of the c-src protein does not induce transformation of NIH 3T3 cells. *Proceedings of the National Academy of Sciences of the United States of America*. 81:7071-7075.

Shiratori, T., S. Miyatake, H. Ohno, C. Nakaseko, K. Isono, J.S. Bonifacino, and T. Saito. 1997. Tyrosine phosphorylation controls internalization of CTLA-4 by regulating its interaction with clathrin-associated adaptor complex AP-2. *Immunity*. 6:583-589.

Shrivastav, A., A.R. Sharma, G. Bajaj, C. Charavaryamath, W. Ezzat, P. Spafford, R. Gore-Hickman, B. Singh, M.A. Copete, and R.K. Sharma. 2007. Elevated N-myristoyltransferase activity and expression in oral squamous cell carcinoma. *Oncol Rep*. 18:93-97.

Sinn, H.P., and H. Kreipe. 2013. A Brief Overview of the WHO Classification of Breast Tumors, 4th Edition, Focusing on Issues and Updates from the 3rd Edition. *Breast Care (Basel)*. 8:149-154.

Slamon, D.J., G.M. Clark, S.G. Wong, W.J. Levin, A. Ullrich, and W.L. McGuire. 1987. Human breast cancer: correlation of relapse and survival with amplification of the HER-2/neu oncogene. *Science*. 235:177-182.

Smanik, P.A., K.Y. Ryu, K.S. Theil, E.L. Mazzaferri, and S.M. Jhiang. 1997. Expression, exon-intron organization, and chromosome mapping of the human sodium iodide symporter. *Endocrinology*. 138:3555-3558.

Smart, J.E., H. Oppermann, A.P. Czernilofsky, A.F. Purchio, R.L. Erikson, and J.M. Bishop. 1981. Characterization of sites for tyrosine phosphorylation in the transforming protein of Rous sarcoma virus (pp60v-src) and its normal cellular homologue (pp60c-src). *Proceedings of the National Academy of Sciences of the United States of America*. 78:6013-6017.

Smith, V.E., J.A. Franklyn, and C.J. McCabe. 2011. Expression and function of the novel proto-oncogene PBF in thyroid cancer: a new target for augmenting radioiodine uptake. *The Journal of endocrinology*. 210:157-163.

Smith, V.E., M.L. Read, A.S. Turnell, N. Sharma, G.D. Lewy, J.C. Fong, R.I. Seed, P. Kwan, G. Ryan, H. Mehanna, S.Y. Chan, V.M. Darras, K. Boelaert, J.A. Franklyn, and C.J. McCabe. 2012. PTTG-binding factor (PBF) is a novel regulator of the thyroid hormone transporter MCT8. *Endocrinology*. 153:3526-3536.

Smith, V.E., M.L. Read, A.S. Turnell, R.J. Watkins, J.C. Watkinson, G.D. Lewy, J.C. Fong, S.R. James, M.C. Eggo, K. Boelaert, J.A. Franklyn, and C.J. McCabe. 2009. A novel mechanism of sodium iodide symporter repression in differentiated thyroid cancer. *Journal of cell science*. 122:3393-3402.

Smith, V.E., N. Sharma, R.J. Watkins, M.L. Read, G.A. Ryan, P.P. Kwan, A. Martin, J.C. Watkinson, K. Boelaert, J.A. Franklyn, and C.J. McCabe. 2013. Manipulation of PBF/PTTG1IP phosphorylation status; a potential new therapeutic strategy for improving radioiodine uptake in thyroid and other tumors. *The Journal of clinical endocrinology and metabolism*. 98:2876-2886.

Solbach, C., M. Roller, C. Fellbaum, M. Nicoletti, and M. Kaufmann. 2004. PTTG mRNA expression in primary breast cancer: a prognostic marker for lymph node invasion and tumor recurrence. *Breast*. 13:80-81.

Sonnenfeld, M.R., T.H. Frenna, N. Weidner, and J.E. Meyer. 1991. Lobular carcinoma in situ: mammographic-pathologic correlation of results of needle-directed biopsy. *Radiology*. 181:363-367.

Soule, H.D., J. Vazguez, A. Long, S. Albert, and M. Brennan. 1973. A human cell line from a pleural effusion derived from a breast carcinoma. *J Natl Cancer Inst*. 51:1409-1416.

Spaeth, E., A. Klopp, J. Dembinski, M. Andreeff, and F. Marini. 2008. Inflammation and tumor microenvironments: defining the migratory itinerary of mesenchymal stem cells. *Gene Ther*. 15:730-738.

Speirs, V., G.P. Skliris, S.E. Burdall, and P.J. Carder. 2002. Distinct expression patterns of ER alpha and ER beta in normal human mammary gland. *J Clin Pathol*. 55:371-374.

Spitzweg, C., K.J. Harrington, L.A. Pinke, R.G. Vile, and J.C. Morris. 2001. Clinical review 132: The sodium iodide symporter and its potential role in cancer therapy. *The Journal of clinical endocrinology and metabolism*. 86:3327-3335.

Spitzweg, C., M.K. O'Connor, E.R. Bergert, D.J. Tindall, C.Y. Young, and J.C. Morris. 2000. Treatment of prostate cancer by radioiodine therapy after tissue-specific expression of the sodium iodide symporter. *Cancer research*. 60:6526-6530.

Stjernsward, J. 1974. Decreased survival related to irradiation postoperatively in early operable breast cancer. *Lancet*. 2:1285-1286.

Stratford, A.L., K. Boelaert, L.A. Tannahill, D.S. Kim, A. Warfield, M.C. Eggo, N.J. Gittoes, L.S. Young, J.A. Franklyn, and C.J. McCabe. 2005. Pituitary tumor transforming gene binding factor: a novel transforming gene in thyroid tumorigenesis. *The Journal of clinical endocrinology and metabolism*. 90:4341-4349.

Summy, J.M., and G.E. Gallick. 2003. Src family kinases in tumor progression and metastasis. *Cancer Metastasis Rev*. 22:337-358.

Takamune, N., K. Gota, S. Misumi, K. Tanaka, S. Okinaka, and S. Shoji. 2008. HIV-1 production is specifically associated with human NMT1 long form in human NMT isozymes. *Microbes Infect*. 10:143-150.

Taki, K., T. Kogai, Y. Kanamoto, J.M. Hershman, and G.A. Brent. 2002. A thyroid-specific far-upstream enhancer in the human sodium/iodide symporter gene requires Pax-8 binding and cyclic adenosine 3',5'-monophosphate response element-like sequence binding proteins for full activity and is differentially regulated in normal and thyroid cancer cells. *Molecular endocrinology*. 16:2266-2282.

Tallman, M.S., J.W. Andersen, C.A. Schiffer, F.R. Appelbaum, J.H. Feusner, A. Ogden, L. Shepherd, C. Willman, C.D. Bloomfield, J.M. Rowe, and P.H. Wiernik. 1997. All-trans-retinoic acid in acute promyelocytic leukemia. *The New England journal of medicine*. 337:1021-1028.

Tatton, L., G.M. Morley, R. Chopra, and A. Khwaja. 2003. The Src-selective kinase inhibitor PP1 also inhibits Kit and Bcr-Abl tyrosine kinases. *The Journal of biological chemistry*. 278:4847-4853.

Tazebay, U.H., I.L. Wapnir, O. Levy, O. Dohan, L.S. Zuckier, Q.H. Zhao, H.F. Deng, P.S. Amenta, S. Fineberg, R.G. Pestell, and N. Carrasco. 2000. The mammary gland iodide transporter is expressed during lactation and in breast cancer. *Nat Med*. 6:871-878.

TCGA. 2016. Thyroid carcinoma: Case Counts. Vol. 2016. National Cancer Institute.

Thomas, S.M., and J.S. Brugge. 1997. Cellular functions regulated by Src family kinases. *Annu Rev Cell Dev Biol*. 13:513-609.

Thompson, E.W., R. Reich, T.B. Shima, A. Albini, J. Graf, G.R. Martin, R.B. Dickson, and M.E. Lippman. 1988. Differential regulation of growth and invasiveness of MCF-7 breast cancer cells by antiestrogens. *Cancer research*. 48:6764-6768.

Thorpe, S.M. 1976. Increased uptake of iodide by hormone-responsive compared to hormone-independent mammary tumors in GR mice. *International journal of cancer. Journal international du cancer*. 18:345-350.

Thune, I., and A.S. Furberg. 2001. Physical activity and cancer risk: dose-response and cancer, all sites and site-specific. *Med Sci Sports Exerc*. 33:S530-550; discussion S609-510.

Titcomb, M.W., M.M. Gottardis, J.W. Pike, and E.A. Allegretto. 1994. Sensitive and specific detection of retinoid receptor subtype proteins in cultured cell and tumor extracts. *Molecular endocrinology*. 8:870-877.

Travis, R.C., and T.J. Key. 2003. Oestrogen exposure and breast cancer risk. *Breast Cancer Res*. 5:239-247.

Tryfonopoulos, D., S. Walsh, D.M. Collins, L. Flanagan, C. Quinn, B. Corkery, E.W. McDermott, D. Evoy, A. Pierce, N. O'Donovan, J. Crown, and M.J. Duffy. 2011. Src: a potential target for the treatment of triple-negative breast cancer. *Ann Oncol*. 22:2234-2240.

Uno, F., J. Sasaki, M. Nishizaki, G. Carboni, K. Xu, E.N. Atkinson, M. Kondo, J.D. Minna, J.A. Roth, and L. Ji. 2004. Myristoylation of the fus1 protein is required for tumor suppression in human lung cancer cells. *Cancer research*. 64:2969-2976.

Unterholzner, S., M.J. Willhauck, N. Cengic, M. Schutz, B. Goke, J.C. Morris, and C. Spitzweg. 2006. Dexamethasone stimulation of retinoic Acid-induced sodium iodide symporter expression and cytotoxicity of 131-I in breast cancer cells. *The Journal of clinical endocrinology and metabolism*. 91:69-78.

Uyttersprot, N., N. Pelgrims, N. Carrasco, C. Gervy, C. Maenhaut, J.E. Dumont, and F. Miot. 1997. Moderate doses of iodide in vivo inhibit cell proliferation and the expression of thyroperoxidase and Na+/I-symporter mRNAs in dog thyroid. *Molecular and cellular endocrinology*. 131:195-203.

Vadysirisack, D.D., E.S. Chen, Z. Zhang, M.D. Tsai, G.D. Chang, and S.M. Jhiang. 2007. Identification of in vivo phosphorylation sites and their functional significance in the sodium iodide symporter. *J Biol Chem*. 282:36820-36828.

Valabrega, G., F. Montemurro, and M. Aglietta. 2007. Trastuzumab: mechanism of action, resistance and future perspectives in HER2-overexpressing breast cancer. *Ann Oncol*. 18:977-984.

Van Cleef, A., S. Altintas, M. Huizing, K. Papadimitriou, P. Van Dam, and W. Tjalma. 2014. Current view on ductal carcinoma in situ and importance of the margin thresholds: A review. *Facts Views Vis Obgyn*. 6:210-218.

van Nimwegen, M.J., and B. van de Water. 2007. Focal adhesion kinase: a potential target in cancer therapy. *Biochem Pharmacol*. 73:597-609.

Vendrell, J.A., S. Ghayad, S. Ben-Larbi, C. Dumontet, N. Mechti, and P.A. Cohen. 2007. A20/TNFAIP3, a new estrogen-regulated gene that confers tamoxifen resistance in breast cancer cells. *Oncogene*. 26:4656-4667.

Vinh-Hung, V., and C. Verschraegen. 2004. Breast-conserving surgery with or without radiotherapy: pooled-analysis for risks of ipsilateral breast tumor recurrence and mortality. *J Natl Cancer Inst*. 96:115-121.

Vlotides, G., M. Cruz-Soto, T. Rubinek, T. Eigler, C.J. Auernhammer, and S. Melmed. 2006. Mechanisms for growth factor-induced pituitary tumor transforming gene-1 expression in pituitary folliculostellate TtT/GF cells. *Molecular endocrinology*. 20:3321-3335.

Wahed, A., J. Connelly, and T. Reese. 2002. E-cadherin expression in pleomorphic lobular carcinoma: an aid to differentiation from ductal carcinoma. *Ann Diagn Pathol*. 6:349-351.

Waksman, G., S.E. Shoelson, N. Pant, D. Cowburn, and J. Kuriyan. 1993. Binding of a high affinity phosphotyrosyl peptide to the Src SH2 domain: crystal structures of the complexed and peptide-free forms. *Cell*. 72:779-790.

Wapnir, I.L., M. Goris, A. Yudd, O. Dohan, D. Adelman, K. Nowels, and N. Carrasco. 2004. The Na+/I-symporter mediates iodide uptake in breast cancer metastases and can be selectively down-regulated in the thyroid. *Clinical cancer research : an official journal of the American Association for Cancer Research*. 10:4294-4302.

Wapnir, I.L., M. van de Rijn, K. Nowels, P.S. Amenta, K. Walton, K. Montgomery, R.S. Greco, O. Dohan, and N. Carrasco. 2003. Immunohistochemical profile of the sodium/iodide symporter in thyroid, breast, and other carcinomas using high density tissue microarrays and conventional sections. *The Journal of clinical endocrinology and metabolism*. 88:1880-1888.

Watkins, R.J., W. Imruetaicharoenchoke, N. Sharma, ML Read, VL Poole, E. Gentilin, S. Bansal, E. Bosseboeuf, R. Fletcher, HR Nieto, U Mallick, A Hacksaw, H Mehanna, K Boelaert, VE Smith and CJ McCabe. 2016. Pro-invasive Effect of Proto-oncogene PBF is Modulated by an interaction with Cortactin. *Journal of clinical endocrinology and metabolism*. 101:4551-4563

Watkins, R.J., M.L. Read, V.E. Smith, N. Sharma, G.M. Reynolds, L. Buckley, C. Doig, M.J. Campbell, G. Lewy, M.C. Eggo, L.S. Loubiere, J.A. Franklyn, K. Boelaert, and C.J. McCabe. 2010. Pituitary tumor transforming gene binding factor: a new gene in breast cancer. *Cancer research*. 70:3739-3749.

Wellings, S.R., and H.M. Jensen. 1973. On the origin and progression of ductal carcinoma in the human breast. *J Natl Cancer Inst*. 50:1111-1118.

Weston, S.A., R. Camble, J. Colls, G. Rosenbrock, I. Taylor, M. Egerton, A.D. Tucker, A. Tunnicliffe, A. Mistry, F. Mancia, E. de la Fortelle, J. Irwin, G. Bricogne, and R.A. Pauptit. 1998. Crystal structure of the anti-fungal target N-myristoyl transferase. *Nat Struct Biol*. 5:213-221.

Wilcox, C., J.S. Hu, and E.N. Olson. 1987. Acylation of proteins with myristic acid occurs cotranslationally. *Science*. 238:1275-1278.

Wilson, G.R., A. Cramer, A. Welman, F. Knox, R. Swindell, H. Kawakatsu, R.B. Clarke, C. Dive, and N.J. Bundred. 2006. Activated c-SRC in ductal carcinoma in situ correlates with high tumour grade, high proliferation and HER2 positivity. *British journal of cancer*. 95:1410-1414.

Wilson, L.K., D.K. Luttrell, J.T. Parsons, and S.J. Parsons. 1989. pp60c-src tyrosine kinase, myristylation, and modulatory domains are required for enhanced mitogenic responsiveness to epidermal growth factor seen in cells overexpressing c-src. *Molecular and cellular biology*. 9:1536-1544.

Wolff, J., I.L. Chaikoff, and et al. 1949. The temporary nature of the inhibitory action of excess iodine on organic iodine synthesis in the normal thyroid. *Endocrinology*. 45:504-513, illust.

Wong, Y.H., T.Y. Lee, H.K. Liang, C.M. Huang, T.Y. Wang, Y.H. Yang, C.H. Chu, H.D. Huang, M.T. Ko, and J.K. Hwang. 2007. KinasePhos 2.0: a web server for identifying protein kinase-specific phosphorylation sites based on sequences and coupling patterns. *Nucleic acids research*. 35:W588-594.

Wright, M.H., W.P. Heal, D.J. Mann, and E.W. Tate. 2010. Protein myristoylation in health and disease. *J Chem Biol*. 3:19-35.

Xiang, C., H. Gao, L. Meng, Z. Qin, R. Ma, Y. Liu, Y. Jiang, C. Dang, L. Jin, F. He, and H. Wang. 2012. Functional variable number of tandem repeats variation in the promoter of proto-oncogene PTTG1IP is associated with risk of estrogen receptor-positive breast cancer. *Cancer Sci*. 103:1121-1128.

Xu, W., A. Doshi, M. Lei, M.J. Eck, and S.C. Harrison. 1999. Crystal structures of c-Src reveal features of its autoinhibitory mechanism. *Mol Cell*. 3:629-638.

Xue, Y., J. Ren, X. Gao, C. Jin, L. Wen, and X. Yao. 2008. GPS 2.0, a tool to predict kinase-specific phosphorylation sites in hierarchy. *Mol Cell Proteomics*. 7:1598-1608.

Yager, J.D., and N.E. Davidson. 2006. Estrogen carcinogenesis in breast cancer. *The New England journal of medicine*. 354:270-282.

Yaspo, M.L., J. Aaltonen, N. Horelli-Kuitunen, L. Peltonen, and H. Lehrach. 1998. Cloning of a novel human putative type Ia integral membrane protein mapping to 21q22.3. *Genomics*. 49:133-136.

Yu, H., M.K. Rosen, T.B. Shin, C. Seidel-Dugan, J.S. Brugge, and S.L. Schreiber. 1992. Solution structure of the SH3 domain of Src and identification of its ligand-binding site. *Science*. 258:1665-1668.

Zha, J., S. Weiler, K.J. Oh, M.C. Wei, and S.J. Korsmeyer. 2000. Posttranslational N-myristoylation of BID as a molecular switch for targeting mitochondria and apoptosis. *Science*. 290:1761-1765.

Zhang, S., W.C. Huang, P. Li, H. Guo, S.B. Poh, S.W. Brady, Y. Xiong, L.M. Tseng, S.H. Li, Z. Ding, A.A. Sahin, F.J. Esteva, G.N. Hortobagyi, and D. Yu. 2011. Combating trastuzumab resistance by targeting SRC, a common node downstream of multiple resistance pathways. *Nature medicine*. 17:461-469.

Zhang, X., G.A. Horwitz, A.P. Heaney, M. Nakashima, T.R. Prezant, M.D. Bronstein, and S. Melmed. 1999a. Pituitary tumor transforming gene (PTTG) expression in pituitary adenomas. *The Journal of clinical endocrinology and metabolism*. 84:761-767.

Zhang, X., G.A. Horwitz, T.R. Prezant, A. Valentini, M. Nakashima, M.D. Bronstein, and S. Melmed. 1999b. Structure, expression, and function of human pituitary tumor-transforming gene (PTTG). *Molecular endocrinology*. 13:156-166.

Zhao, Q., Y. Xie, Y. Zheng, S. Jiang, W. Liu, W. Mu, Z. Liu, Y. Zhao, Y. Xue, and J. Ren. 2014. GPS-SUMO: a tool for the prediction of sumoylation sites and SUMO-interaction motifs. *Nucleic acids research*. 42:W325-330.

Zheng, J., D.R. Knighton, N.H. Xuong, S.S. Taylor, J.M. Sowadski, and L.F. Ten Eyck. 1993. Crystal structures of the myristylated catalytic subunit of cAMP-dependent protein kinase reveal open and closed conformations. *Protein Sci*. 2:1559-1573.

Zou, H., T.J. McGarry, T. Bernal, and M.W. Kirschner. 1999. Identification of a vertebrate sister-chromatid separation inhibitor involved in transformation and tumorigenesis. *Science*. 285:418-422.

List of Publications

Lewy GD, Ryan GA, Read ML, Fong JC, Poole V, Seed RI, Sharma N, Smith VE, Kwan PP, Stewart SL, Bacon A, Warfield A, Franklyn JA, McCabe CJ, Boelaert K. 2013. Regulation of pituitary tumor transforming gene (PTTG) expression and phosphorylation in thyroid cells. *Endocrinology*. 154(11):4408-22.

Poole, V.L., and C.J. McCabe. 2015. Iodide transport and breast cancer. *The Journal of endocrinology*. 227:R1-R12.

Watkins, R.J., W. Imruetaicharoenchoke, N. Sharma, ML Read, VL Poole, E. Gentilin, S. Bansal, E. Bosseboeuf, R. Fletcher, HR Nieto, U Mallick, A Hacksaw, H Mehanna, K Boelaert, VE Smith and CJ McCabe. 2016. Pro-invasive Effect of Proto-oncogene PBF is Modulated by an interaction with Cortactin. *Journal of clinical endocrinology and metabolism*. 101:4551-4563